

**The Marine Geochemistry of Rhenium, Iridium and Platinum**

by

Debra Colodner

B.S. Geology and Geophysics, Yale University

(1985)

SUBMITTED IN PARTIAL FULFILLMENT  
OF THE REQUIREMENTS FOR THE DEGREE OF  
DOCTOR OF PHILOSOPHY

at the

MASSACHUSETTS INSTITUTE OF TECHNOLOGY  
and the  
WOODS HOLE OCEANOGRAPHIC INSTITUTION

September, 1991

© Massachusetts Institute of Technology 1991

Signature of Author \_\_\_\_\_

Department of Earth, Atmospheric and Planetary Sciences,  
Massachusetts Institute of Technology and the Joint Program in  
Oceanography, Massachusetts Institute of Technology/Woods  
Hole Oceanographic Institution, September, 1991

Certified by \_\_\_\_\_

John M. Edmond, Thesis Supervisor

Edward A. Boyle, Thesis Supervisor

Accepted by \_\_\_\_\_

Philip M. Gschwend, Chairman, Joint Committee for Chemical  
Oceanography, Massachusetts Institute of Technology/Woods Hole  
Oceanographic Institution

WITHDRAWN  
FROM  
MIT LIBRARIES



THE MARINE GEOCHEMISTRY OF  
RHENIUM, IRIDIUM AND PLATINUM

by

DEBRA COLODNER

Submitted to the Department of Earth, Atmospheric and Planetary Sciences  
on September 9, 1991 in partial fulfillment of the requirements for  
the Degree of Doctor of Philosophy in Oceanography

**Abstract**

The platinum group elements occur in low concentrations in most crustal materials. Sedimentary enrichments above these low background levels are thought to arise only from very specific processes, and thus are relatively easy to interpret. The thesis describes aspects of the marine geochemistry of two of these elements, iridium and platinum, as well as a neighbor in the periodic table, rhenium. Because Pt and Ir are highly enriched in meteorites compared to the Earth's crust, variations in their concentrations have been interpreted as reflecting changes in the amount of cosmic material in sediments. Re is also scarce (<0.1 ppb) in most crustal materials, but is highly enriched in anoxic sediments, making it a very sensitive indicator of anoxic conditions. Our ability to interpret the sedimentary concentrations of these elements has been hampered by our lack of knowledge about their marine geochemistry and their behavior during sediment diagenesis. The thesis therefore attempts to answer two general questions: 1. Can Re, Ir and Pt be redistributed by the geochemical changes associated with early diagenesis of marine sediments? 2. What are the processes controlling Re enrichment in anoxic sediments?

Techniques were developed to measure Re, Ir and Pt in seawater, sediments and sediment pore waters. For all of these elements, this involves separation and preconcentration by anion exchange (Hodge et al., 1986 and Koide et al., 1987) and analysis by isotope-dilution, inductively-coupled plasma mass spectrometry, with flow injection to introduce the sample.

The distribution of Pt in the water column has been the subject of two recent studies with conflicting results (Goldberg et al., 1986 and Jacinto et al., 1989). In an attempt to resolve their differences, and to gain insight into the forms in which Pt arrives at the sediment-water interface, Pt was determined in two Atlantic and one Pacific profile. The results agree with neither of the former studies and reveal invariant concentrations with depth of  $270 \pm 60$  fM. The observed profiles indicate that Pt is relatively unreactive in the water column.

The post-depositional mobility of Re, Ir and Pt was investigated in North Atlantic abyssal sediments, where pelagic sediments are interspersed with relatively organic-rich turbidites. The emplacement of turbidite units leads to the

reduction and partial dissolution of hydrogenous minerals in the pelagic sediments directly underlying them. Pt and Ir are cycled with manganese and cobalt, during this process, indicating a hydrogenous, relatively mobile form of these elements. Following emplacement, an oxidation front gradually penetrates through the turbidites, leading to the redistribution of many transition metals. In these sediments, Pt exhibits a peak at the redox boundary similar to that found for Cu and V, suggesting an association with organic matter. These early-diagenetic processes lead to variations in the concentrations of Pt and Ir that should not be confused with changes in cosmic flux when interpreting the geologic record.

In order to constrain the oceanic Re budget, Re was determined in seawater, river waters, sediment pore waters and the Black Sea. Two detailed open ocean profiles confirm predictions of conservative behavior for the element with a concentration of  $44 \pm 1$  pmol/kg. A survey of Re in rivers of the Orinoco Basin indicates a strong black shale source for the element. A transect through the Amazon Estuary suggests a possible desorptive flux of the element near the river mouth. The Orinoco and Amazon values, combined with several measurements in the Ganges-Brahmaputra Basin, allows calculation of a residence time for Re in seawater of approximately 750 ky.

Re concentrations in pore waters were determined at one oxic (Pacific) and one anoxic (Chesapeake Bay) site. The results are consistent with previous work which suggested that Re can only be enriched in sediments under reducing conditions. Additionally, Re does not appear to cycle with manganese oxides in the upper portion of sediments. Compared to Mo, Re is removed from pore waters deeper in the sediment column. Re was also compared to Mo and U in the Black Sea. Its distribution is similar to the other elements, with enrichment in surface relative to deep waters, and removal to sediments at or below the sediment-water interface. The residence time of Re in the Black Sea appears to be intermediate between that of Mo (~100 y) and U (~1000y).

Thesis supervisors: Dr. John M. Edmond and Dr. Edward A. Boyle

Titles: Professors of Oceanography



---

## Acknowledgements

This work benefited from the aid and inspiration of folks too numerous to name them all here - but I'll try. I would especially like to thank both of my thesis advisors, Ed Boyle and John Edmond, for sharing their seemingly limitless knowledge and their scarce time, in guiding me through this process. They provided access to samples, lab space, instrumentation and opportunities that made this work possible. I would also like to thank the other members of my thesis committee, Ed Sholkovitz and Karl Turekian. Ed generously offered his expertise and scientific and moral support throughout my years in the Joint Program. Karl Turekian was the first to convince me that studying the Earth was a worthwhile pursuit, and it was from him I learned first of meteorites, dinosaurs and iridium spikes.

I learned a great deal from the students who passed through building E34 during my time here. Scott Doney and Sarah Green made my transition from geologist to "chemist" much less painful by sharing that elusive "chemical intuition" I seemed to lack. Office-mates David (but can you measure it in forams?) Lea and Yair (can you measure anything in forams?) Rosenthal were masters of the idea-toss, which was always fun, even if most of our ideas were eventually tossed away. Yair's careful reading and comments also helped to improve upon previous drafts of this thesis. Rob Sherrell was always there to answer/discuss the mundane ("How do I hang a Niskin?") and the metaphysical ("What's next?") questions. Erik Brown was a great companion through Stan's dance class and Manning's aerobics as well as role model in the art of producing a thesis. Kelly Falkner taught me all I know (and more than either of us ever wanted to know) about ICP-MS, and provided friendship, guidance and encouragement in our "noble" corner of the lab. Julian Sachs had the dubious honor of being the first student I helped to supervise. The results of his Senior Thesis are a huge contribution to our understanding of Re geochemistry and his questions always stimulated me to learn more.

Others who overlapped with me at MIT contributed their advice and insight to this study. I am lucky to have worked with Chris Measures, Martin Palmer, Chris German, Gary Klinkhammer, Teri Bowers, Andy Campbell, Kristin Orians and Didier Bourles. Patty Marcus always kept our lab groups running smoothly, even when we tried our hardest to promote chaos.

Many people extended ship time, equipment, samples and expertise toward this thesis work, including Jim Broda, Steve Calvert, Bill Curry, Greg Cutter, Steve Emerson, Brad Esser, Flip Froelich, Tim Grove, Stan Hart, Susumu Honjo, Glenn Jones, Chris Measures, Jim Moffett, Greg Ravizza, Steve Recca, Kathleen Ruttenberg, Tim Shaw, Ken Smith and John Thomson. Additionally, the crews of the research vessels Atlantis II, New Horizon and R. Warfield made the collection of samples for this work as easy as possible.

I would like to thank all of my family for supporting me through this crazy endeavor. Special thanks go to my grandmother Helen, who never imagined what she was starting by reading me dinosaur stories; to my grandfather Abe, who always forced me to think of new ways to justify and explain my esoteric pursuits, and to my grandmother Sylvia, who always wanted a doctor in the family. Finally, I would like to thank my father, for showing me at an early age

that a more natural world still existed outside of New York City, and my mother whose constant support buoyed me through all this education.

Funds for this work were provided by an Ida Green Fellowship from the Massachusetts Institute of Technology, a National Science Foundation Graduate Fellowship, an Ocean Ventures Fund grant from Woods Hole Oceanographic Institution, the Office of Naval Research (grant N00014-90-J-1759), and the National Science Foundation (grants OCE-8918633 and OCE-9018820).

To Tom  
for the perspective



---

**Table of Contents**

Title page.....	1
Abstract.....	3
Acknowledgements.....	5
Dedication.....	7
Table of contents.....	9
List of figures.....	
List of tables.....	
Chapter 1 Introduction .....	19
1.1 Goals of the thesis.....	19
1.2 Chemical Properties of Re, Ir and Pt.....	23
Rhenium .....	24
Iridium .....	25
Platinum.....	26
1.3 Geochemistry of the elements .....	27
1.4 Outline of the thesis .....	31
References for Chapter 1 .....	33
Chapter 2 Determination of Re, Ir and Pt in natural waters and sediments.....	39
2.1 Abstract.....	39
2.2 Previous work.....	39
Other methods.....	39
Method intercomparison and validation.....	40
2.3 Apparatus .....	43
2.4 Reagents and standards.....	45
2.5 Sediment dissolution.....	46
2.6 Water sample preparation.....	49
Pt measurement.....	50
Re measurement.....	50
2.7 Column preparation.....	50
2.8 Anion exchange preconcentration.....	51
Oxidation of Ir.....	51
Addition of samples to columns .....	51
Sample elution.....	53

Sample evaporation.....	53
Recoveries .....	53
2.9 ICP-MS.....	54
Isobaric interferences.....	54
Sample introduction.....	57
2.10 Isotope dilution calculations .....	57
Target spiking ratios.....	57
Calculation of sample concentration.....	58
Blank correction .....	59
A note on isotopic equilibration.....	60
References for Chapter 2 .....	62
Chapter 3 Platinum in seawater.....	65
3.1 Abstract .....	65
3.2 Introduction.....	65
3.3 Analytical methods.....	68
Seawater sample collection and storage.....	68
Hydrothermal sample preparation.....	71
Anion exchange preconcentration .....	72
ICP-MS Analysis.....	72
3.4 Results.....	72
Bermuda profile (W. Atlantic).....	73
Azores Profile (E. Atlantic).....	77
Pacific profile .....	77
Hydrothermal samples.....	82
Calculation of uncertainties .....	82
3.5 Discussion.....	83
Potential causes of the discrepancies among methods.....	83
a) Do Pt(II) and Pt(IV) behave differently on the anion exchange resin? .....	85
b) Is there an organically-complexed fraction of the Pt in seawater that is not exchanging with the tracer? .....	86
c) Was sufficient equilibration time allowed?.....	88
Thermodynamic considerations.....	91
Water column Pt behavior.....	91
Global budget considerations .....	94

3.6 Conclusions .....	96
3.7 Acknowledgements .....	97
References for Chapter 3 .....	99
 Chapter 4 Post-depositional mobility of Pt, Ir and Re in abyssal marine sediments .....	103
4.1 Abstract .....	103
4.2 Introduction.....	104
Background.....	105
General geochemistry of the elements.....	107
Post-depositional mobility of Re, Ir and Pt? .....	110
4.3 Core locations and descriptions.....	112
Cores 11334 and 11805 .....	116
Cores 10400 and 52-2.....	117
4.4 Methods .....	118
4.5 Results.....	119
4.6 Discussion.....	140
The formation of Pt peaks.....	140
Ir and Re in partially oxidized turbidites.....	150
Release of Pt and Ir by the reduction of hydrogenous minerals.....	151
4.7 Conclusions .....	153
4.8 Acknowledgements .....	155
References for Chapter 4 .....	156
 Chapter 5.....	161
5.1 Abstract .....	161
5.2 Introduction.....	162
5.3 Methods .....	163
Sample collection and storage .....	163
Orinoco .....	164
Amazon.....	164
Ganges - Brahmaputra .....	164
Chesapeake Bay. ....	164
Black Sea and Soviet rivers. ....	165
Seawater samples.....	165

Anion exchange preconcentration .....	165
Mo measurement.....	165
5.4 Results and Discussion.....	166
Sources of Re to rivers.....	166
a) Orinoco River, Venezuela.....	167
b) Amazon River.....	181
c) Ganges-Brahmaputra Rivers.....	184
Behavior of Re in the estuarine environment .....	190
Anthropogenic inputs of Re to the environment?.....	197
Re in the ocean .....	209
5.5 Summary and Conclusions.....	214
5.6 Acknowledgements .....	217
References for Chapter 5 .....	218

## Chapter 6

6.1 Abstract .....	223
6.2 Introduction.....	223
6.3 Methods .....	225
Sample collection.....	225
Analyses.....	227
6.4 Results.....	228
North Pacific sediment porewaters.....	228
Chesapeake Bay sediment porewaters .....	231
Black Sea and Sea of Marmara.....	238
6.5 Discussion.....	246
Pore waters.....	246
The Black Sea.....	249
Applications .....	17
6.6 Conclusions .....	20
6.7 Acknowledgements .....	21
References for Chapter 6 .....	22
Appendix 6.1.....	25

## Chapter 7

7.1 Platinum in seawater.....	1
-------------------------------	---



7.2 Post-depositional mobility of rhenium, iridium and platinum in abyssal sediments under changing redox conditions .....	1
7.3 The riverine source of Re to seawater.....	3
7.4 The removal of Re from seawater .....	5



---

**List of figures**

Figure 2.1	Microwave digestion system .....	44
Figure 2.2	Sediment sample preparation flow chart.....	47
Figure 2.3	Column set-up for seawater processing for Pt.....	52
Figure 2.4	Example trace of flow injection sample peak.....	56
Figure 3.1	Previous results for Pt in seawater.....	67
Figure 3.2	Pt results from this study compared to previous work.....	75
Figure 3.3	Bermuda Pt profile.....	76
Figure 3.4	Azores Pt profile.....	79
Figure 3.5	Pacific Pt profile .....	81
Figure 4.1	Histogram of average values of Re, Ir and Pt in geologic materials.....	109
Figure 4.2	Map of the North Atlantic showing locations of samples 11334, 10400 and 11805 .....	113
Figure 4.3	Map of the Southern Nares Abyssal Plain with location of core 52-2 .....	114
Figure 4.4	Pt in core 11334 compared to other transition metals.....	122
Figure 4.5	Pt in core 11805 compared to other transition metals.....	125
Figure 4.6	Pt, I, Cu and V in core 11334.....	126
Figure 4.7	Pt, I, Cu and V in core 11805.....	127
Figure 4.8	Pt and Ir in core 11334 .....	129
Figure 4.9	Pr and Ir in core 11805.....	130
Figure 4.10	Re and U profiles in core 11805.....	131
Figure 4.11	Pt and Ir in core 10400.....	136
Figure 4.12	Pt, Ir and Re in core 52-2 .....	137
Figure 4.13	Pt in core 10400 compared to other transition metals.....	138
Figure 4.14	Pt , Ir in core 52-2 compared to other transition metals.....	139
Figure 4.15	Re and Al in core 52-2.....	141
Figure 4.16	Cartoon illustrating the development of a Pt peak.....	147
Figure 4.17	Model results for core 11334 .....	148
Figure 4.18	Model results for core 11805 .....	149
Figure 5.1	Map of the Orinoco River Basin .....	168
Figure 5.2	Black shale deposits in the Venezuelan Andes .....	172
Figure 5.3	Re vs. Ca and SO <sub>4</sub> in the Orinoco Basin .....	176
Figure 5.4	Re vs. Mo and U in rivers of the Orinoco Basin.....	177

Figure 5.5	Re vs. Sr and $^{87}\text{Sr}/^{86}\text{Sr}$ in Orinoco Basin rivers .....	180
Figure 5.6	Map of the Amazon River Basin.....	182
Figure 5.7	Map of the Ganges-Brahmaputra Rivers.....	185
Figure 5.8	Re vs. U in Ganges-Brahmaputra rivers.....	188
Figure 5.9	Salt-affected soils in the Ganges-Yamuna River Basin .....	188
Figure 5.10	Re in surface waters of the Amazon Estuary.....	192
Figure 5.11	U in the Amazon Estuary .....	192
Figure 5.12	Re concentrations in bottom waters of Chesapeake Bay..	196
Figure 5.13	Seasonal study of Fe and Mn in Chesapeake Bay .....	196
Figure 5.14	Rivers draining into the Black Sea from Soviet territory ....	198
Figure 5.15	Re and Mo in Black Sea surface waters.....	200
Figure 5.16	Black Sea station locations.....	201
Figure 5.17	Black Sea surface box model.....	202
Figure 5.18	Main coal basins of the USSR.....	207
Figure 5.19	Atlantic Ocean Re profile .....	212
Figure 5.20	Pacific Ocean Re profile.....	213
Figure 6.1	Sediment core extruder.....	226
Figure 6.2	Re, Mo and $\text{NO}_3$ profiles in Pacific sediment pore waters...	230
Figure 6.3	Station locations in Chesapeake Bay .....	232
Figure 6.4	Re, Mo and $\text{H}_2\text{S}$ profiles in Chesapeake Bay pore waters .	234
Figure 6.5	Results of oxidation experiments.....	237
Figure 6.6	Map of the Black Sea.....	239
Figure 6.7	Re profile in the Black Sea .....	241
Figure 6.8	Re vs. potential density in the Black Sea.....	243
Figure 6.9	Re, $\text{O}_2$ and $\text{H}_2\text{S}$ in Black Sea surface waters.....	244
Figure 6.10	Re vs. salinity in the Black Sea.....	245
Figure 6.11	Black Sea box model .....	251
Figure 6.12	Model predictions for Re, Mo and U concentrations in the Black Sea .....	256
Figure 6.13	Re, Mo and U depletions in the Black Sea.....	260

---

**List of Tables**

Table 1.1	Biostratigraphic boundaries with reported Ir spikes.....	21
Table 1.2	Solubilities of perrhenate salts.....	24
Table 1.3	Abundances of Re, Ir and Pt in some geological materials ....	28
Table 2.1	Detection limits of some methods for the determination of the PGE's in natural materials.....	41
Table 2.2	Interlaboratory/intermethod comparison .....	42
Table 2.3	ICP-MS operating conditions .....	43
Table 2.4	Isotopic composition of spikes and standards.....	46
Table 2.5	Isobaric interferences.....	55
Table 2.6	Target spiking ratios for isotope dilution.....	58
Table 3.1	Pt seawater sample collection information .....	69
Table 3.2	Pt data for Atlantic station, Bermuda .....	74
Table 3.3	Pt data for Atlantic station, Azores .....	78
Table 3.4	Pt data for Pacific stations .....	80
Table 3.5	Pt data for Mid Atlantic Ridge hydrothermal fluids.....	82
Table 3.6	Replicate seawater Pt measurements .....	83
Table 3.7	Pt recovery experiment.....	86
Table 3.8	Pt UV experiments.....	87
Table 3.9	Seawater sample-spike equilibration times .....	89
Table 3.10	Best guess parameters used in dust input calculations.....	93
Table 3.11	Abundances of Pt and Au in some geologic materials.....	97
Table 4.1	Abundances of Re, Ir and Pt in some geologic materials.....	108
Table 4.2	Core locations and general information.....	115
Table 4.3	Pt and Ir results for core 11334 .....	120
Table 4.4	Ancillary data for core 11334.....	121
Table 4.5	Pt, Ir and Re data for core 11805 .....	123
Table 4.6	Ancillary data for core 11805.....	124
Table 4.7	Pt and Ir data for core 10400 .....	132
Table 4.8	Ancillary data for core 10400.....	133
Table 4.9	Pt, Ir and Re data for core 52-2.....	134
Table 4.10	Ancillary data for core 52-2.....	135
Table 4.11	Sediment properties used in model calculations.....	146
Table 4.12	Some stratigraphic boundaries with Ir spikes.....	155
Table 5.1	Rivers sampled in the Orinoco Basin.....	169

Table 5.2	Re, Mo, U and SO <sub>4</sub> in rivers of the Orinoco Basin.....	171
Table 5.3	Ancillary data for rivers of the Orinoco Basin.....	173
Table 5.4	Mo/Re and U/Re ratios in rivers, seawater and organic-rich sediments.....	178
Table 5.5	Amazon River Re data .....	183
Table 5.6	Re in the Ganges-Brahmaputra river system.....	189
Table 5.7	Re in surface waters of the Amazon Estuary .....	191
Table 5.8	Seasonal study of Re in Chesapeake Bay .....	195
Table 5.9	Profile of Re in Chesapeake Bay.....	194
Table 5.10	Re in rivers draining into the Black Sea.....	203
Table 5.11	Re in the Black Sea.....	199
Table 5.12	Black Sea surface water budget.....	202
Table 5.13	Mo and U in rivers draining into the Black Sea .....	205
Table 5.14	Estimates used in calculating coal-burning source of Re to Black Sea rivers.....	208
Table 5.15	Re North Atlantic data.....	210
Table 5.16	Re North Pacific data .....	211
Table 6.1	Re and Mo pore water data for an oxic Pacific site.....	229
Table 6.2	Re and Mo pore water data for Chesapeake Bay.....	233
Table 6.3	Oxidation experiments on anoxic sediments.....	236
Table 6.4	Re data for the Black Sea.....	240
Table 6.5	Re in the Sea of Marmara .....	246
Table 6.6	Parameters used in calculating the flux of Re into Chesapeake Bay sediments.....	248
Table 6.7	Sources and sinks of Re, Mo and U to the Black Sea .....	253
Table 6.8	Authigenic flux calculations for the Black Sea .....	254
Table 6.9	Residence times of Re, Mo and U in the Black Sea.....	258

## Chapter 1

---

### Introduction

#### 1.1 Goals of the thesis

The trace element content of ancient sediments has been used in numerous studies as a guide to sediment sources and depositional environments (for example, Pedersen et al. 1986; Finney et al. 1988 and Brumsack 1986). The platinum group elements, of which iridium and platinum are members, are highly enriched in meteorites compared to the Earth's crust, thus variations in their sedimentary concentrations have been interpreted as the result of changes in the flux of extraterrestrial material to the Earth (eg. Alvarez et al. 1980). Rhenium, which is a neighbor of the platinum group also occurs in very low concentrations in most crustal materials. Sedimentary Re concentrations greater than 0.1 ppb have been attributed to its accumulation from seawater under reducing conditions, leading to its use in dating ancient black shales (Ravizza and Turekian 1989), and potentially as an indicator of the oxygen content of ancient environments (Koide et al. 1986). Our understanding of the marine geochemistry of Re, Ir and Pt is rudimentary, however. The utility of these elements as geochemical probes depends on answers to fundamental questions regarding the behavior of the elements in seawater and in sediments during diagenesis.

The use of Ir (and other platinum group element (PGE)) concentrations in marine sediments as a proxy for the flux of cosmic material was initiated by Barker and Anders (1968) who noted that the concentrations of Ir and Os in sediments were roughly inversely related to sediment accumulation rates. Alvarez et al. hoped to use Ir, and what they assumed was a relatively constant flux of extraterrestrial material to the Earth, to determine the duration of the

Cretaceous-Tertiary (K-T) extinction event, 65 million years ago. Instead, they found a large enrichment of Ir in the boundary clay, and proposed that this was the result of the impact of a 10 km meteorite with the Earth (Alvarez et al. 1980). Subsequently, Ir spikes have been reported in many other locations of the K-T boundary, and at other biostratigraphic boundaries as well (see Table 1.1). Many of these Ir spikes are quite small, however, and their origin in terrestrial geochemical processes is plausible (Turekian et al., 1982; Playford et al. 1984; Orth et al. 1988; Holser et al. 1989). One goal of the thesis was therefore to elucidate the role of diagenetic processes in creating or modifying PGE spikes, and to address the related questions of the behavior of Pt in seawater and mechanisms by which it may be removed from seawater to sediments.

Ravizza and Turekian (1989) pioneered the use of the  $^{187}\text{Re}$ - $^{187}\text{Os}$  geochronometer for dating ancient black shales. Previous attempts to date ancient sediments by isotopic methods were frustrated by the fact that sediments acquire their isotopic composition from a mixture of detrital materials that may be much older than the age of the sediment, and authigenic materials added to the sediment at the time of deposition. The Re-Os system is unique in that the Re content (and to a lesser extent, the Os content) of reducing sediments is nearly exclusively acquired from seawater at the time of deposition. The more abundant isotope,  $^{187}\text{Re}$ , is radioactive and decays (by  $\beta^-$  emission) to  $^{187}\text{Os}$  with a half-life of 46 billion years. Assuming that the sediments remain a closed system with respect to Re and Os, ages may be determined using the whole-rock isochron method. Ravizza and Turekian successfully applied this technique to black shales deposited approximately 300 million years ago, although they noted some scatter in the data that might be ascribed to post-depositional mobility.



Table 1.1 Some biostratigraphic boundaries at which Ir spikes have been reported

Boundary	Age (my)	Location	Ir spike (ppb) bkgd.-peak	Notes	Ref.
Frasnian-Famennian (Late Devonian)	365	Carling Basin, Australia	0.02-0.3	stromatolite bed with iron-oxide filled filaments	1
Devonian-Carboniferous	360	Oklahoma	0.03-0.6	limest. - shale transition	2
Permo-Triassic	245	Alps, Austria	0.01-0.2	probable chemical origin	3
Cenomanian-Turonian	92	Colorado	0.01-0.1	coincides with Mn peak	4
Cretaceous-Tertiary	65	Denmark	0.3-42	pyritic clay layer in "fish clay"	5,6
		Italy	0.3-9	clay layer in limestone	5
		DSDP 465A N. Pacific	1-10	calc. ooze with pyrite	7
		LL44, GPC3 N. Pacific	2-11	abyssal clay	8
		Raton Basin, New Mexico (& 70 more sites)	0.02-15	above black shale layer	9
Eocene-Oligocene	37	DSDP149 Caribbean	bd-0.4	impact debris	10

1. Playford 1984, 2. Orth et al. 1988, 3. Holser et al. 1989, 4. Orth et al. 1988, 5. Alvarez et al. 1980, 6. Schmitz 1988, 7. Kyte et al. 1980, 8. Kyte and Wasson, 1986, 9. Izett, 1987, 10. Asaro et al. 1982, bd = below detection

The oxygen content of the ocean and atmosphere in the past is a question that arises from a number of perspectives. The most dramatic changes in oxygen levels probably occurred early in the Earth's history, due to the initial proliferation of photosynthetic organisms. The timing and magnitude of these changes is an area of long-standing debate, as summarized in Holland (1984). Another period in which relatively large changes in oceanic oxygen levels may have occurred is the Cretaceous, 135-65 million years ago, when organic rich sediments were deposited at open ocean sites which have been oxic for most of their history (Ryan and Cita 1977). In more recent Earth history, the question of the oxygen content of past oceans has become important in models of atmospheric carbon dioxide changes over the last glacial period (eg. Broecker 1982; Knox and McElroy 1984 and Sarmiento and Toggweiler 1984).

The use of Re as an indicator of the oxygen content of ancient environments might follow a number of approaches, which are quite speculative as yet. These are described in more detail in Chapters 4, 5 and 6, and will be mentioned here: 1) Koide et al. (1986) suggested that concentrations of Re in excess of 0.1 ppb in Precambrian strata could be used to indicate the first presence of an oxygenated atmosphere. This relies on the assumption that Re enrichments in anoxic sediments require high concentrations in seawater as a source. As Re is immobile under reducing conditions, the development of high concentrations in seawater is dependent on the existence of an oxidative weathering environment and reducing sediments. 2) The Re content of more recent sediments (in combination with other elements) might also yield information about the oxygen content of their depositional environment. One simple explanation for Re enrichment in reducing sediments holds that Re diffuses in from seawater to the depth at which it is reduced and fixed in the

solid phase. The concentration of Re in the sediment is then a function of the depth to the Re redox boundary, which is in turn a function of many factors, one of which is the oxygen content of bottom waters. With multiple tracers it might be possible to make some inferences about oxygen levels (see Pedersen et al. (1988) and Elderfield and Yang (1988) for similar applications of Mo and U). 3) Emerson and Huested (1991) and Russell et al. (1990) have suggested that the Mo and U contents of the oceans are sensitive to the area of the ocean floor overlain by anoxic waters, with concentrations decreasing with increasing anoxia. If this is true for Re, and if a phase could be found which recorded the Re concentration of seawater, then changes in seawater Re, or in the ratio of Re to other elements, might be indirectly related to oxygen content of the ocean as a whole.

The applications suggested above require an understanding of the processes by which Re is added to organic-rich sediments, its behavior in seawater and a basic knowledge of its geochemical cycle. Better comprehension of the extent to which Re is remobilized by oxidation, both in ancient sediments exposed on the continents, and in recent marine sediments due to changing redox conditions is also necessary. A second goal of the thesis was therefore to begin to describe the marine geochemistry of Re, in terms of its sources to and removal from seawater, its behavior and residence time in the ocean, and its post-depositional mobility in sediments.

## **1.2 Chemical Properties of Re, Ir and Pt**

Re, Ir and Pt are members of the third-row transition metals and all have partially filled 5d electron shells in the elemental state. They each have multiple oxidation states, but Re, having fewer d electrons is relatively more stable in the

higher states (Cotton and Wilkinson 1988). Numerous compounds and complexes of the elements have been isolated and are described in Cotton and Wilkinson and references therein. Only those which are relevant to their geochemistry or analytical chemistry are discussed below.

### *Rhenium*

The following discussion of the chemistry of Re is largely drawn from Colton (1965) and Cotton and Wilkinson (1988). Re chemistry shows only superficial similarities to its congener element in the first-row transition series, Mn, and is much more similar to Mo in its chemistry and geochemistry. Re is a fairly reactive metal, dissolving in oxidizing acids to give perrhenic acid ( $\text{HReO}_4$ ), but it is not dissolved by hydrochloric acid. The heptoxide ( $\text{Re}_2\text{O}_7$ ) may also be obtained by heating the metal in air, and is volatile, subliming at  $250^\circ\text{C}$ . The structure of  $\text{Re}_2\text{O}_7$  consists of an infinite array of  $\text{ReO}_4$  tetrahedra and  $\text{ReO}_6$  octahedra sharing corners, and it dissolves readily in water, yielding  $\text{ReO}_4^-$ .  $\text{ReO}_4^-$  is very stable and shows little oxidizing power, in contrast with  $\text{MnO}_4^-$ . The solubilities of perrhenate salts are quite high, as listed in Table 1.2

Table 1.2 Solubilities of some perrhenate salts

<u>Compound</u>	<u>Solubility @ <math>30^\circ\text{C}</math> (moles/L)</u>
$\text{LiReO}_4 \cdot 2\text{H}_2\text{O}$	14
$\text{NaReO}_4$	5.3
$\text{KReO}_4$	0.051
$\text{NH}_4\text{ReO}_4$	0.32
$\text{RbReO}_4$	0.047
$\text{CsReO}_4$	0.029
$\text{Mg}(\text{ReO}_4)_2$	10.3
$\text{Ca}(\text{ReO}_4)_2$	6.4

Anhydrous rhenium dioxide may be prepared by reduction of the heptaoxide with the metal or with hydrogen at 300°C. The hydrated dioxide ( $\text{ReO}_2 \cdot 2\text{H}_2\text{O}$ ) is readily formed by the action of various reducing agents on solutions of  $\text{ReO}_4^-$ . Briscoe et al. (1931) found that reduction of  $\text{ReO}_4^-$  with zinc, hydrazine and stannous chloride led to the precipitation of a colloidal phase which eventually settled out as the hydrated dioxide.

Rhenium heptasulfide ( $\text{Re}_2\text{S}_7$ ) is obtained by saturation of 2 to 6 M HCl solutions of  $\text{ReO}_4^-$  with  $\text{H}_2\text{S}$ , although the precipitation is sensitive to conditions and is often incomplete. In basic solutions the compound is precipitated more slowly. When  $\text{H}_2\text{S}$  is passed into neutral solutions containing  $\text{ReO}_4^-$ , thioperrhenates ( $\text{ReO}_3\text{S}^-$ ) are formed. The prolonged action of  $\text{H}_2\text{S}$  on perrhenate solutions is said to lead to the replacement of more of the oxygen atoms by sulfur, but there does not seem to be evidence for complete replacement. The thioperrhenates are all more soluble than their oxygen analogs, (ie. the solubility of  $\text{KReO}_3\text{S}$  is 2 M, compared to 0.05 M for  $\text{KReO}_4$ ) (Peacock 1966).  $\text{ReS}_2$  may be prepared by heating  $\text{Re}_2\text{S}_7$  in nitrogen or in a vacuum, or by direct combination of the elements at red heat.  $\text{ReS}_2$  is relatively inert chemically, and has the  $\text{MoS}_2$  structure. It is insoluble in alkaline hydroxide or sulfide solutions, in HCl and  $\text{H}_2\text{SO}_4$ , but like the heptasulfide, may be dissolved in nitric acid.

### *Iridium*

The following description of Ir chemistry is drawn largely from Griffith (1967) and Cotton and Wilkinson (1988). Ir metal is extremely unreactive. It does not dissolve in any simple acid and is only slightly attacked by aqua regia, even in a finely divided state. Its oxidation to a soluble form may be carried out in an oxidizing flux, such as  $\text{Na}_2\text{O}_2$ , or by the action of  $\text{F}_2$  or  $\text{Cl}_2$  on the metal,

and the hexachloro salts are quite soluble.  $\text{Na}_2\text{IrCl}_6$  may be formed by the action of  $\text{Cl}_2$  on a heated mixture of Ir and NaCl.  $\text{IrCl}_6^{2-}$  is unstable in basic solution, undergoing spontaneous reduction within minutes to  $\text{IrCl}_6^{3-}$ . Hydrolysis of solutions of  $\text{IrCl}_6^{3-}$  leads to precipitation of the hydrated dioxide. The iridium sesquioxide ( $\text{Ir}_2\text{O}_3$ ) is chemically not as stable as the dioxide. The Ir sulfides,  $\text{IrS}_2$  and  $\text{Ir}_2\text{S}_3$  are known, but only  $\text{Ir}_2\text{S}_3$  has been found in nature. Passing  $\text{H}_2\text{S}$  into a solution of  $\text{IrCl}_6^{2-}$  produces an impure sulfide containing both Ir(III) and Ir(IV) (Westland 1981).

### *Platinum*

The chemistry of Pt is summarized in Cotton and Wilkinson (1988) and Westland (1981), on which the following discussion is largely based. The principal oxidation states of Pt are 0, II and IV. Pt shows low affinity for oxygen ligands, and a preference for sulfur or the heavier halogen ions, as well as ligands that can  $\pi$ -bond, such as  $\text{CN}^-$ ,  $\text{NO}_2^-$ , alkenes and alkynes. Pt metal may be dissolved in aqua regia, due to the oxidizing effect of chlorine and nitrosyl chloride which are evolved from the mixture, and the complexing action of chloride ions. The dissolution of the metal in aqua regia results in a solution containing  $\text{PtCl}_6^{2-}$ . Thermodynamic data suggest that  $\text{PtCl}_6^{2-}$  should be unstable with respect to  $\text{PtCl}_4^{2-}$  at Eh conditions typical of surface environments. Pt(IV) complexes are relatively kinetically inert however (Llopis and Colom 1976), although the reduction may be catalyzed by visible light (Cotton and Wilkinson 1988). Recent experimental determinations of the hydrolysis constants of Pt suggest that hydroxide complexes may dominate chloride complexes in aqueous Pt solutions at neutral to basic pH (Wood 1991). The kinetics of ligand substitution in aqueous Pt complexes are relatively sluggish, however, so that thermodynamics may not determine the speciation of

Pt in natural waters (Elding 1978). The sulfides, PtS<sub>2</sub> and PtS are obtained when solutions of PtCl<sub>6</sub><sup>2-</sup> and PtCl<sub>4</sub><sup>2-</sup> (respectively) are bubbled with H<sub>2</sub>S. Only PtS has been observed in nature.

### 1.3 Geochemistry of the elements

Re, Ir and Pt are strongly siderophile in nature, preferring bonds with iron or nickel to those with oxygen. This is reflected in the high concentrations of these elements in iron meteorites compared to chondritic meteorites, and in metallic phases in chondrites relative to bulk chondrite (Parthe and Crocket 1978). During differentiation of the Earth, Re and the PGE's were probably partitioned strongly into the Fe-Ni core, leaving the crust and the mantle depleted relative to a chondritic bulk earth composition. The three elements are also chalcophilic, favoring bonds with sulfur over those with oxygen. This is reflected in the strong enrichments of these elements in sulfide minerals compared to host silicate rocks (Morgan 1986; Barnes et al. 1985; Naldrett 1981). Re is slightly enriched in mafic crustal rocks relative to ultramafic mantle rocks, suggesting that it may behave as an incompatible lithophile element during partial melting of mantle materials or fractional crystallization of the resulting liquids. Ir and Pt show the opposite trend, and occur in successively lower concentrations in ultramafic, mafic and sialic rocks (Table 1.3). Whether this distribution is due to substitution of the PGE's in the lattice of early-crystallizing minerals such as chromite and olivine, or the segregation of PGE alloys or sulfides from the silicate magma has not been resolved (see Esser (1991) for a succinct review of the subject).

The behavior of Re, Ir and Pt in hydrothermal processes is poorly understood, due to a paucity of relevant data. The importance of submarine

hydrothermal systems as a source or a sink of the elements in seawater is therefore unknown at this time. The occurrence of Re enrichments of up to 10% in porphyry molybdenite and copper deposits attests to its mobility in high

Table 1.3 Abundances of Re, Ir and Pt in chondrites, crustal materials and the marine environment.

	Re (ppb)	Ir (ppb)	Pt (ppb)
Chondrites	36.9 <sup>a</sup>	473 <sup>a</sup>	953 <sup>a</sup>
Ultramafic rocks	0.3 <sup>b</sup>	5 <sup>c</sup>	15 <sup>c</sup>
Mafic rocks	1 <sup>b</sup>	0.1 <sup>c</sup>	5 <sup>c</sup>
Intermediate-sialic rocks	0.3 <sup>d</sup>	0.01 <sup>c</sup>	1 <sup>ck</sup>
Pelagic sediment (carbonate poor)	0.05 <sup>ef</sup>	0.3 <sup>ghi</sup>	3 <sup>fg</sup>
Anoxic sediments	50 <sup>j</sup>	0.08 <sup>fg</sup>	1 <sup>fg</sup>
Manganese nodules	<0.1 <sup>e</sup>	1.1 <sup>g</sup>	100 <sup>g</sup>
Seawater	45 pM <sup>f</sup>	5 fM <sup>g</sup>	300 fM <sup>f</sup>

a. (Anders and Ebihara 1982), b. (Martin 1990), c. (Crocket 1981) and references therein, d. (Esser 1991), e. (Koide et al. 1986), f. This work, g. (Goldberg et al. 1986), h. (Barker and Anders 1968), i. (Crocket and Kuo 1979), j. (Ravizza 1991), k. (Wedepohl 1978)

temperature fluids, although it appears that Mo and Re are deposited close to their magmatic source. Bernard et al. (1990) suggest that Re may be carried as  $\text{HReO}_4$  in the vapor phase and that it condenses at relatively high temperatures (~600°C) with  $\text{MoS}_2$ . Ir enrichments in volcanic gases and sublimates have been measured at two hot-spot volcanoes (Kilauea (Olmez et al. 1986) and Piton de la Fournaise (Toutain and Meyer 1989)), as well as in ashes from Kamchatkan volcanoes (Felitsyn and Vaganov 1988) and in Antarctic blue ice fields (Koeberl 1989). Iridium enrichment factors, defined relative to Hawaiian basalt (and relative to Sc) range from  $10^4$  to  $10^5$ . The transport of Ir in volcanic gases has been proposed as the origin of the Cretaceous-Tertiary Ir spike, as



the boundary is nearly coincident with the extrusion of the Deccan Traps flood basalts in India.

Recent studies have suggested that hydrothermal fluids may play a role in the formation of Pt-group metal deposits (Rowell and Edgar 1986; Mihalik et al. 1974; McCallum et al. 1976; Boudreau et al. 1986). The ability of hydrothermal fluids to dissolve, transport and deposit the PGE's is an area of active experimental and theoretical investigation (Wood 1991; Wood et al. 1989). These studies have suggested that the PGE's may be transported as chloride, hydroxide, bisulfide, and/or ammonia complexes at elevated temperatures, although the relative importance of these complexing ions is debated. McKibben et al. (1990) report that Salton Sea geothermal brines carry up to 5nM Pt at temperatures near 300°C, pH ~ 5.4, and an oxidation state near aqueous SO<sub>4</sub>-H<sub>2</sub>S equilibrium.

During low temperature weathering processes Re is relatively mobile, due to the stability of the ReO<sub>4</sub><sup>-</sup> ion in oxidizing aqueous environments. Morachevskii and Necheva (1960) have suggested that Re is more easily mobilized from molybdenite deposits than Mo, based on groundwater and experimental data. The relative mobility of Re compared to Os in molybdenites was also postulated by Luck and Allegre (1982). The mobility of Pt and Ir is poorly known. Wood and Vlassopoulos (1990) failed to find detectable Pt concentrations in streams and lakes surrounding a PGE prospect in Quebec. Fuchs and Rose (1974) concluded that Pt showed little mobility in soils developed on or near PGE-enriched rocks of the Stillwater layered igneous complex. The occurrence of euhedral platinum group metal crystals in laterite deposits and associated placers suggests that Pt may be locally transported in solution and redeposited during laterite development (Bowles 1986).

Much of what is known about Re, Ir and Pt in the marine environment comes from the work of Goldberg et al. (1986), Hodge et al. (1985) and Koide et al. (1986). Their work has provided a survey of Re, Ir and Pt concentrations in a variety of marine materials and defined some of the principal features of their geochemistries. The concentrations of Re, Ir and Pt in seawater are 45, 0.3 and ~0.005 pM, respectively. The relative enrichment of Re over Ir and Pt compared to their crustal values is due to the stability of the  $\text{ReO}_4^-$  oxyanion in seawater, (and its mobility during weathering). Its high concentrations and the lack of a trend in its vertical profile led Koide et al. to suggest that Re behaves conservatively in seawater and should have a long residence time in the oceans. The principal sink for Re from seawater is reducing sediments, leading to its enrichment in anoxic vs. oxic sediments by a factor of approximately 500. The mechanism for its removal may either involve its reduction to Re(IV) and subsequent scavenging onto solid phases, or precipitation as the sulfide,  $\text{Re}_2\text{S}_7$ , without reduction. The marine geochemistry of Re bears strong resemblance to that of Mo and U, which are also relatively stable in seawater (as  $\text{MoO}_4^{2-}$  and  $\text{UO}_2(\text{CO}_3)_3^{4-}$ ), and are strongly enriched in anoxic sediments. Unlike Mo and U, however, Re does not appear to be scavenged by ferromanganese oxides, as it is not enriched in manganese nodules, and its concentrations in pelagic sediments are less than or equal to crustal abundances (Ku and Broecker, 1969; Bertine and Turekian, 1973; Koide et al. 1986).

Goldberg et al. (1986) suggested that Pt is relatively stable in seawater compared to Ir, due to the stronger stability of Pt than Ir chloro complexes, however the ratio of the elements in seawater is similar to their ratio in crustal materials, within our limited knowledge of these numbers (Table 1.2). In addition, recent studies suggest that chloro complexes may be less important

than hydroxy complexes in controlling Pt speciation in seawater (Wood 1991). The behavior of Pt in seawater was the subject of two previous studies with conflicting results. Goldberg et al. (1986) reported Pt depletion in surface waters and enrichment with depth (a "nutrient-type" profile), suggesting that Pt was involved in the cycling of biogenic matter in the water column. In contrast, the results of Jacinto and van den Berg (1989) suggested that Pt was highly reactive in the water column, with a profile typical of a "scavenged-type" element showing enrichments in surface waters and depletion with depth. The two studies utilized different analytical methods, and the different results are likely to be an artifact of analysis, as discussed further in Chapter 3. Ir has only been determined in three 100 L samples of Scripps Pier water (Goldberg et al. 1986), and thus its open ocean concentration and water column behavior are not well constrained. The relative importance of various sources of Pt and Ir to seawater (such as rivers, terrestrial and cosmic dust, and possibly high and low temperature alteration of submarine basalts and peridotites) is also unknown. Pt and Ir appear to be enriched in slowly accumulating pelagic sediments relative to their concentrations in the continental crust, due to their accommodation in authigenic ferromanganese oxy-hydroxides, and to contributions from cosmic dust (Goldberg et al. 1986; Kyte and Wasson 1986; and Barker and Anders 1968). Their concentrations are also elevated in manganese nodules compared to sediment values, with a Pt/Ir ratio similar to that of seawater.

#### **1.4 Outline of the thesis**

The thesis consists of six chapters. The next chapter describes the analytical methods utilized in this study. Chapter three addresses the behavior

of Pt in seawater and attempts to resolve contradictions between the two previous studies. Chapter four explores the question of the post-depositional mobility of Re, Ir and Pt in abyssal sediments in response to changing redox conditions. Chapters 5 and 6 focus on the geochemical cycle of Re; chapter 5 describes the riverine inputs of the element, and its distribution in seawater, and Chapter 6 examines the mechanisms by which Re is removed from seawater in anoxic sediments and in an anoxic basin (the Black Sea).

### References for Chapter 1

- Alvarez, L. W., W. Alvarez, F. Asaro and H. Michel. (1980). "Extraterrestrial cause for the Cretaceous-Tertiary extinction." Science. **208**: 1095-1108.
- Anders, E. and M. Ebihara. (1982). "Solar-system abundances of the elements." Geochim. Cosmochim. Acta. **46**: 2363-2380.
- Asaro, F., L.W. Alvarez, W. Alvarez, and H.V. Michel. (1982). "Geochemical anomalies near the Eocene-Oligocene and Permo-Triassic boundaries." Geol. Soc. Amer. Spec. Publ. **190**: 517-520.
- Barker, J. and E. Anders. (1968). "Accretion rate of cosmic matter from Ir and Os in deep sea sediments." Geochim. Cosmochim. Acta. **32**: 627-645.
- Barnes, S. J., A. J. Naldrett and M. P. Groton. (1985). "The origin of the fractionation of the platinum group elements in terrestrial magmas." Chem. Geol. **53**: 303-323.
- Bernard, A., R. B. Symonds and W. I. Rose Jr. (1990). "Volatile transport and deposition of Mo, W and Re in high temperature magmatic fluids." Appl. Geochem. **5**: 317-326.
- Bertine, K.K. and K.K. Turekian. (1973). " Molybdenum in marine deposits." Geochim. Cosmochim. Acta. **37**: 1415-1434.
- Boudreau, A. E., E. A. Mathez and I. S. McCallum. (1986). "Halogen geochemistry of the Stillwater and Bushveld complexes: evidence for transport of the platinum-group elements by Cl-rich fluids." J. Petrol. **27**(4): 967-986.
- Bowles, J. F. (1986). "The development of platinum-group minerals in laterites." Econ. Geol. **81**: 1278-1285.
- Briscoe, H. V. A., P. L. Robinson and E. M. Stoddart. (1931). "The reduction of Potassium perrhenate." J. Chem. Soc. : 666-669.
- Broecker, W. S. (1982). "Ocean chemistry during glacial time." Geochim. Cosmochim. Acta. **46**: 1689-1705.
- Brumsack, H. J. (1986). "The inorganic geochemistry of Cretaceous black shales (DSDP leg 41) in comparison to modern upwelling sediments from the Gulf of California." North Atlantic Paleoceanography. London, Geological Society Special Bulletin.
- Colton, R. (1965). The chemistry of rhenium and technetium. New York, Interscience Publishers.
- Cotton, F. A. and G. Wilkinson. (1988). Advanced Inorganic Chemistry. New York, John Wiley and Sons.

Crocket, J. H. (1981). Geochemistry of the platinum-group elements. Platinum Group Elements. Mineralogy, Geology, Recovery. Canadian Institute of Mining and Metallurgy.

Crocket, J. H. and H. Y. Kuo. (1979). "Sources for gold, palladium and iridium in deep-sea sediments." Geochim. Cosmochim. Acta. **43**: 831-842.

Elderfield, H. and Y. Yang. (1988). "Glacial/interglacial fluctuations of uranium and thorium isotope fluxes in the Panama Basin (Abstr.)." Chem. Geol. **70**(1/2): 109.

Elding, L. I. (1978). "Stabilities of platinum (II) chloro and bromo complexes and kinetics for anation of the tetraaquaplatinum (II) ion by halides and thiocyanate." Inorg. Chim. Acta. **28**: 255-262.

Emerson, S. and S. S. Husted. (1991). "Ocean anoxia and the concentration of molybdenum in seawater." in press, Marine Chem.

Esser, B. K. (1991). Osmium Isotope Geochemistry of Terrigenous and Marine Sediments. PhD thesis, Yale University.

Felitsyn, S. B. and P. A. Vaganov. (1988). "Iridium in the ash of Kamchatkan Volcanoes." Int'l. Geol. Rev. 1288-1291.

Finney, B. P., M. W. Lyle and G. R. Heath. (1988). "Sedimentation at MANOP site H (Eastern Equatorial Pacific) over the past 400,000 years: Climatically induced redox effects on transition metal cycling." Paleoceanogr. **3**: 169-189.

Fuchs, W. A. and A. W. Rose. (1974). "The geochemical behavior of platinum and palladium in the weathering cycle in the Stillwater Complex, Montana." Econ. Geol. **69**: 332-346.

Goldberg, E. D., V. Hodge, P. Kay, M. Stallard and M. Koide. (1986). "Some comparative marine chemistries of platinum and iridium." Appl. Geochem. **1**: 227-232.

Griffith, W. P. (1967). The chemistry of the rarer platinum metals (Os, Ru, Ir, and Rh). N.Y., Interscience Publ.

Hastings, D., S. Emerson, A. Mix and B. Nelson. (1990). Vanadium incorporation into planktonic foraminifera as a tracer for the extent of anoxic bottom waters. EOS, Transactions, American Geophysical Union. **71**(43): 1351.

Hodge, V. F., M. Stallard, M. Koide and E. D. Goldberg. (1985). "Platinum and the platinum anomaly in the marine environment." Earth and Plan. Sci. Lett. **72**: 158-162.

Holland, H. D. (1984). The Chemical Evolution of the Atmosphere and Oceans. Princeton, N.J., Princeton University Press.

Holser, W. T., H.-P. Schonlaub, M. Attrep, K. Boeckelmann, P. Klein, M. Magaritz, C. J. Orth, A. Fenninger, C. Jenny, M. Kralik, H. Mauritsch, E. Pak, J.-M. Schramm, K. Stattegger and R. Schmoller. (1989). "A unique geochemical record at the Permian/Triassic boundary." Nature, **337**(6202): 39-44.

Izett, G. (1987). "The Cretaceous-Tertiary boundary interval, Raton Basin, Colorado and New Mexico, and its shock-metamorphosed minerals: Implications concerning the K-T boundary impact-extinction theory." USGS Open File Report, **87-606**.

Jacinto, G. S. and C. M. G. van den Berg. (1989). "Different behavior of platinum in the Indian and Pacific Oceans." Nature, **338**: 332-334.

Knox, F. and M. B. McElroy. (1984). "Changes in atmospheric CO<sub>2</sub>: influence of marine biota at high latitudes." J. Geophys. Res., **89**: 4629-4637.

Koeberl, C. (1989). "Iridium enrichment in volcanic dust from blue ice fields, Antarctica, and possible relevance to the K/T boundary event." Earth and Plan. Sci. Lett., **92**: 317-322.

Koide, M., V. F. Hodge, J. Yang, M. Stallard, E. Goldberg, J. Calhoun and K. Bertine. (1986). "Some comparative marine chemistries of rhenium, gold, silver and molybdenum." Appl. Geochem., **1**: 705-714.

Ku, T.-L. and W.S. Broecker. (1969). "Radiochemical studies on manganese nodules of deep-sea origin." Deep Sea Res., **16**: 625.

Kyte, F.T., Z. Zhou and J.T. Wasson. (1980). "Siderophile enriched sediments from the Cretaceous-Tertiary boundary." Nature, **288**: 651-656.

Kyte, F. T. and J. T. Wasson. (1986). "Accretion rate of extraterrestrial matter: iridium deposited 33 to 67 million years ago." Science, **232**: 1225-1229.

Llopis, J. F. and F. Colom. (1976). Platinum. Encyclopedia of Electrochemistry of the Elements. New York, Marcel Dekker.

Martin, C. E. (1990). Rhenium-Osmium Isotope Geochemistry of the Mantle, PhD Thesis, Yale University.

McCallum, M. E., R. R. Loucks, R. R. Carlson, E. F. Cooley and T. A. Doerge. (1976). "Platinum metals associated with hydrothermal copper ores of the New Rambler Mine, Medicine Bow Mountains, Wyoming." Econ. Geol., **71**: 1429-1450.

- McKibben, M. A., A. E. Williams and G. E. M. Hall. (1990). "Solubility and transport of platinum group elements and Au in saline hydrothermal fluids: constraints from geothermal brine data." Econ. Geol. **85**: 1926-1934.
- Mihalik, P., J. B. E. Jacobsen and S. A. Hiemstra. (1974). "Platinum-group minerals from a hydrothermal environment." Econ. Geol. **69**: 257-262.
- Morachevskii, D. E. and A. A. Necheva. (1960). "Characteristics of migration of Re from molybdenites." Geochem. **6**: 648-649.
- Morgan, J. W. (1986). "Ultramafic xenoliths: clues to the Earth's late accretionary history." J. Geophys. Res. **91**: 12375-12387.
- Naldrett, A. J. (1981). "Nickel sulfide deposits." Econ. Geol. **75th anniversary volume**: 628-685.
- Olmez, I., D. L. Finnegan and W. H. Zoller. (1986). "Iridium emissions from Kilauea volcano." J. Geophys. Res. **91(B1)**: 653-663.
- Orth, C. J., L. R. Quintana, J. S. Gilmore, J. E. Barrick, J. N. Haywa and S. A. Spesshardt. (1988). "Pt-group metal anomalies in the Lower Mississippian of southern Oklahoma." Geol. **16**: 627-630.
- Orth, C.J., M. Attrep, X.Y. Mao, E.G. Kauffmann, R. Diner and W.P. Elder. (1988). "Iridium abundance maxima in the Upper Cenomanian Extinction Interval." Geophys. Res. Lett. **15(4)**: 346-349.
- Parthe, E. and J. H. Crocket. (1978). Platinum Group. Handbook of Geochemistry. New York, Springer-Verlag.
- Peacock, R. D. (1966). The Chemistry of Technetium and Rhenium. New York, Elsevier Publishing Co.
- Pedersen, T. F., J. S. Vogel and J. R. Southon. (1986). "Copper and manganese in hemipelagic sediments at 21N, East Pacific Rise: Diagenetic contrasts." Geochim. Cosmochim. Acta. **50**: 2019-2031.
- Pedersen, T. F., M. Pickering, J. S. Vogel, J. N. Southon and D. E. Nelson. (1988). "The response of benthic foraminifera to productivity cycles in the Eastern Equatorial Pacific: faunal and geochemical constraints on glacial bottom water oxygen levels." Paleoceanogr. **3(2)**: 157-168.
- Playford, P. E., D. J. McLaren, C. J. Orth, J. S. Gilmore and W. D. Goodfellow. (1984). "Iridium anomaly in the Upper Devonian of the Canning Basin, Western Australia." Science. **226**: 437-439.
- Ravizza, G. (1991). Rhenium and Osmium Geochemistry of Modern and Ancient Organic-Rich Sediments. PhD Thesis, Yale University.



Ravizza, G. and K. K. Turekian. (1989). "Application of the  $^{187}\text{Re}$ - $^{187}\text{Os}$  system to black shale geochronometry." Geochim. Cosmochim. Acta. **53**(12): 3257-3262.

Rowell, W. F. and A. D. Edgar. (1986). "Platinum-group element mineralization in a hydrothermal Cu-Ni sulfide occurrence, Rathburn Lake, Northeastern Ontario." Econ. Geol. **81**: 1272-1277.

Russell, A. D., S. R. Emerson, B. K. Nelson, A. Mix and J. Erez. (1990). Uranium in foraminiferal calcite as a tracer of ocean redox conditions. EOS, Transactions, American Geophysical Union. **71**(43): 1352.

Ryan, W. B. F. and M. B. Cita. (1977). "Ignorance concerning episodes of ocean-wide stagnation." Mar. Geol. **23**: 237-215.

Sarmiento, J. L. and J. R. Toggweiler. (1984). "A new model for the role of the oceans in determining atmospheric  $\text{pCO}_2$ ." Nature. **308**: 621-624.

Schmitz, B., P. Anderson and J. Dahl. (1988). "Iridium, sulfur isotopes and rare earth elements in the Cretaceous-Tertiary boundary clay at Stevns Klint, Denmark." Geochim. Cosmochim. Acta **52**: 229-236.

Toutain, J. P. and G. Meyer. (1989). "Iridium-bearing sublimates at a hot-spot volcano (Piton de la Fournaise, Indian Ocean)." Geophys. Res. Lett. **16**(12): 1391-1394.

Turekian, K.K. (1982). "Potential of  $^{187}\text{Os}/^{186}\text{Os}$  as a cosmic vs. terrestrial indicator in high Ir layers of sedimentary strata." Geol. Soc. Am. Spec. Paper **190**: 243-249.

Wedepohl. (1978). Handbook of Geochemistry, New York, Springer-Verlag.

Westland, A. D. (1981). "Inorganic chemistry of the platinum-group elements." Can. Inst. Mining and Mineral. Spec. Vol., L. Cabri ed. **23**: 7-18.

Wood, S. A. (1991). "Experimental determination of the hydrolysis constants of  $\text{Pt}^{2+}$  and  $\text{Pd}^{2+}$  at 25C from the solubility of Pt and Pd in aqueous hydroxide solutions." Geochim. Cosmochim. Acta. **55**(7): 1759-1768.

Wood, S. A., B. W. Mountain and B. J. Fenlon. (1989). "Thermodynamic constraints on the solubility of platinum and palladium in hydrothermal solutions: reassessment of hydroxide, bisulfide and ammonia complexing." Econ. Geol. **84**: 2020-2028.

Wood, S. A. and D. Vlassopoulos. (1990). "The dispersion of Pt, Pd and Au in surficial media about two PGE-Cu-Ni prospects in Quebec." Can. Miner. **28**: 649-663.



## **Chapter 2**

---

### **Determination of Rhenium, Iridium and Platinum in natural waters and sediments**

#### **2.1 Abstract**

Methods have been developed to measure Re, Ir and Pt in natural waters and sediments by isotope dilution - inductively coupled plasma mass spectrometry (ICP-MS). The techniques have been applied to the determination of Ir and Pt in sediments, Re and Pt in seawater and Re in sediment pore waters and river waters. In each case, a stable isotope-enriched spike is added to the sample before processing. Sediments are dissolved in all-teflon bombs using a modified standard kitchen microwave oven. Anion exchange of the chloro-complexes is used to separate the elements of interest from species which present potential isobaric interferences. Samples are then introduced into the ICP-MS in a small volume using flow injection. The method has detection limits (three times background) of approximately 30 fmol Ir, 70 fmol Pt and 25 fmol Re.

#### **2.2 Previous work**

##### *Other methods*

Determination of the platinum group elements (PGE's) in natural materials can be accomplished by a number of techniques. Hodge et al. (1986) and Koide et al. (1987) describe methods to separate and preconcentrate Re, Ir and Pt from marine sediments and waters, upon which the methods employed in this study are largely based. They employed graphite furnace atomic absorption spectrometry as the determinative step, necessitating laborious chemical

separations to reduce potential interferences. Additional methods by which the PGE's have been determined in natural materials include instrumental and radiochemical neutron activation, negative thermal ion mass spectrometry, resonance ion mass spectrometry, secondary ion mass spectrometry and voltammetry. The detection limits of these methods are listed in Table 2.1. ICP-MS offers several advantages over techniques available previously: 1) it requires relatively small sample sizes, 2) isotope dilution methods may be used to correct for variable recovery, 3) there are relatively few interferences in the mass range of interest, 4) extensive handling of radioactive samples is not necessary, and 5) it has multielement capabilities.

#### *Method intercomparison and validation*

Because of the lack of standard sedimentary reference materials with known PGE contents, results from this method were compared to others in the literature for which samples were available. The Re, Ir and Pt concentrations found in this work are generally consistent with previous studies, as summarized in Table 2.2. The seawater Pt concentrations reported here fall in the lower range of the published values (Jacinto and van den Berg 1989; and Goldberg et al. 1988). Re seawater values agree quite well with the graphite furnace method of Koide et al. (1987), although the ICP-MS technique yields higher precision by a factor of thirty. This technique was compared to instrumental neutron activation analysis of Ir in deep sea sediments (LL44 GPC3; Kyte and Wasson 1986) and Cretaceous-Tertiary boundary sediments (Raton Basin; Izett 1987) and the results agree within 10%. Re determinations in sediments were compared to results from nickel-sulfide fire assay/secondary-ion mass spectrometry (Ravizza 1991) and results agree within 4%.

Table 2.1 Detection limits of some methods for the determination of platinum group elements in natural materials

Elements	Technique	Detection Limits <sup>a</sup>	Ref.
Ir	INAA:HPGe-coincidence / NaI(Tl) anticoincidence spectrometry	20 fmol Ir for glass 500 fmol Ir for Mn-nodules	1
Re,Os, Ir	Negative thermal ion mass spectrometry	< 10 fmol Re < 0.05 fmol Os < 5000 fmol Ir	2,10
Re,Ir, Pt	Graphite furnace atomic absorption spectrometry	2500 fmol Re 100 fmol Ir 80 fmol Pt	3, 4
Re, Os	Resonance ion mass spectrometry	500 fmol Re or Os	5
Re, Ir	Radiochemical neutron activation analysis	5 fmol Re or Ir	6
Pt	Adsorptive cathodic stripping voltammety	0.5 fmol Pt	7
Re, Os	Secondary ion mass spectrometry	< 2000 fmol Re, Os	8, 9
Re, Ir, Pt	ID-FIA-ICP-MS at MIT	25 fmol Re <sup>b</sup> 30 fmol Ir <sup>b</sup> 70 fmol Pt <sup>b</sup>	

a. Author defined detection limits: usually two times background or three times standard deviation of the blank.

b. Three times background levels.

1. Murali et al. 1990, 2. Creaser et al. 1991, 3. Koide et al. 1987, 4. Hodge et al. 1986, 5. Walker 1988, 6. Keays et al. 1974, 7. Van Den Berg and Jacinto 1988, 8. Esser 1991, 9. Luck and Turekian 1983 10. Hauri et al. in prep.

Table 2.2 Interlaboratory / intermethod comparison

Sample	Description	Method (ref)	Concentration	This method: Concentration (#replicates)
LL44-1 GPC3 1440-1442 cm	pelagic sediment Central N. Pacific	RNAA (1)	1.9 ppb Ir*	2.1 ± 0.1 ppb Ir (3)
LL44-1 GPC3 1420-1422 cm	pelagic sediment Central N. Pacific	RNAA (1)	1.5 ppb Ir*	1.5 ± 0.1 ppb Ir (4)
Starkville South "magic layer"	K-T boundary clay, Raton Basin, CO.	INAA (2)	1.2 - 14.6 ppb Ir**	5.1 ppb Ir (1)
Seawater	Pacific Ocean Indian Ocean Atlantic & Pacific	GFAAS (3) ACSV (5)	460 - 1170 fM Pt 200 - 1600 fM Pt	260 ± 70 fM Pt (52)
	Pacific Ocean Atlantic & Pacific	GFAAS (4)	49 ± 14 pM Re	44.3±0.4 pM Re (34)
Black Sea	recent sediments	SIMS (6)	31.8 ± 0.6 ppb Re	33.1 ppb Re (1)
Peru shelf	phosphatic crust	SIMS (6)	34.6 ± 0.3 ppb Re	33.3 ppb Re (1)
Bakken shale	black shale	SIMS (6)	285 ±11 ppb Re	287 ppb Re (1)

R/I NAA = radiochemical / instrumental neutron activation analysis

GFAAS = graphite furnace atomic absorption spectrometry

ACVS = adsorptive cathodic stripping voltammetry

SIMS = secondary ion mass spectrometry

\* uncertainties not given

\*\* range for several outcrops of "magic layer"

1. Kyte and Wasson 1986, 2. Izett 1987, 3. Goldberg et al. 1986, 4. Koide et al. 1987, 5. Jacinto and van den Berg 1989, 6. Ravizza 1991

## 2.3 Apparatus

Sediment samples were dissolved in 120 mL teflon microwave digestion vessels, with pressure-release valves (CEM Corporation, Matthews, North Carolina). The dissolutions were carried out in a standard kitchen Toshiba microwave oven, model ERS 8610B, modified to allow venting of acid fumes (figure 2.1). Analyses were performed on a VG-Plasmaquad (PQ1) ICP-MS. A flow injection valve (Cheminert, 6 - port) was added to the sample introduction path between the peristaltic pump (Gilson Minipuls 2) and the nebulizer (concentric Meinhard, TR-30-A3, glass). ICP-MS operating parameters are listed in Table 2.3.

**Table 2.3. ICP-MS operating conditions:**

ICP RF power:	1350 W
Coolant Ar flow:	13.7 L/min
Auxiliary Ar flow:	0.6 L/min
Nebulizer Ar flow:	0.7 - 0.8 L/min
Peristaltic pump rate:	0.8 mL/min
Spray chamber coolant temperature:	8 °C
Quadrupole chamber pressure:	$2 \times 10^{-6}$ mbar
Interface pressure:	1.7 mbar
Quadrupole:	VG 12-12S
Detector:	continuous dynode (Galileo, 4870)
Run time per sample:	20 or 40 seconds
Run mode:	peak jumping
Points per peak:	5
Dwell time per point:	1280 $\mu$ s
Sweeps per peak:	600 for two isotopes (~20 s run) 250 for four isotopes (~20 s run) 400 for six isotopes (~40 s run)

Teflon lab-ware was cleaned between uses by soaking in aqua regia for at least 12 hours, and the digestion vessels were additionally cleaned with 50% HF for 12 hours. Teflon-ware used only for Re measurements was cleaned by

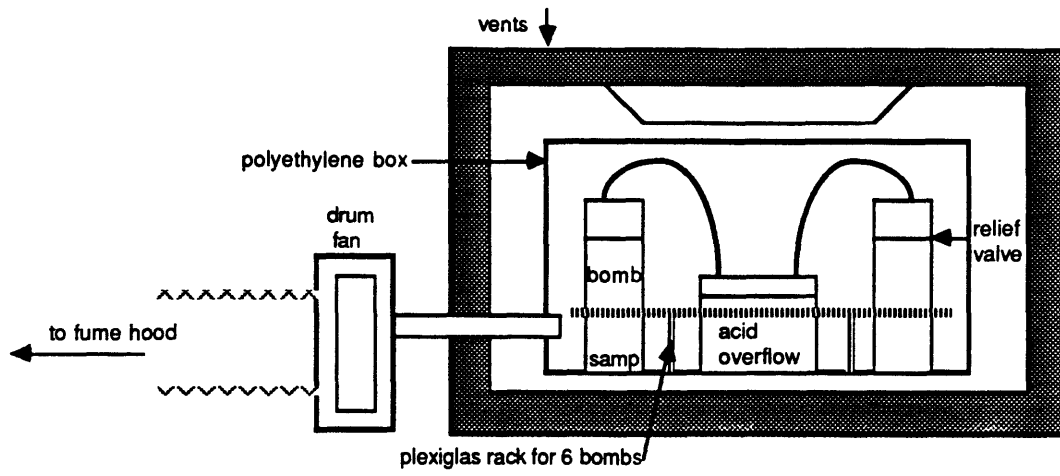


Figure 2.1. Microwave digestion system



soaking in 50% HNO<sub>3</sub>, as Re is readily soluble in HNO<sub>3</sub> (whereas Pt and Ir are not), and repeated exposure to aqua regia etched the surfaces of the teflon beakers. Polyethylene and polypropylene vessels (beakers, bottles, columns, centrifuge tubes, etc.) were leached in 10% aqua regia before and between uses, or 10% HNO<sub>3</sub> for Re-only use.

Procedures that did not involve the handling of concentrated acids, or HF at any dilution, were carried out in a laminar flow bench under filtered air. For safety purposes, concentrated acids and HF were handled in a well-ventilated fume hood with care taken to minimize exposure of the samples to unfiltered air.

## **2.4 Reagents and standards**

Reagent grade hydrochloric and nitric acids were triply distilled in a Vycor still. Reagent grade hydrofluoric acid was singly distilled in a two-bottle teflon still at sub-boiling temperatures. Sediment samples were bubbled with chlorine gas (Mattheson, ultra-high purity) in order to oxidize Ir before the anion exchange step (see below). Ir standards were made gravimetrically from K<sub>2</sub>IrCl<sub>6</sub> as well as purchased from SPEX Industries. Pt standard solution was purchased from Johnson-Matthey Aesar Corp. and a Re standard was prepared from Re metal. Stable, isotopically enriched spikes for the elements were obtained from Oak Ridge National Laboratory, TN. The isotopic compositions of the spikes as determined at Oak-Ridge are listed in Table 2.4. The spikes were supplied as metals and dissolved as follows: The Ir spike was fused with Na<sub>2</sub>O<sub>2</sub> over a bunsen burner in a zirconium crucible and dissolved in 3N HCl (Beamish and Russell 1936). The Pt spike was dissolved in a 3:1 mixture of 6N HCl and 16N HNO<sub>3</sub> and the Re spike was dissolved in 16 N HNO<sub>3</sub>. Spike

solution concentrations were calibrated against standard solutions by repeated measurement of the isotopic ratios of mixtures of the two by ICP-MS.

Table 2.4 Isotopic composition of spikes and standards			
<b>Iridium</b>	<b>Platinum</b>	<b>Rhenium</b>	<b>Molybdenum</b>
<b>SPIKES<sup>a</sup>:</b>			
191: 96.188%	190: <0.02%	185: 97.4%	92: 0.26%
193: 3.812%	192: 57.3%	187: 2.6%	94: 0.63%
	194: 26.05%		95: 96.47%
	195: 11.04%		96: 1.45%
	196: 4.74%		97: 0.46%
	198: 0.87%		98: 0.63%
			100: 0.15%
<b>NATURAL ISOTOPIC COMPOSITION:</b>			
191: 37.4%	190: 0.013%	185: 37.4%	92: 14.8%
193: 62.6%	192: 0.78%	187: 62.6%	94: 9.1%
	194: 32.9%		95: 15.9%
	195: 33.8%		96: 16.7%
	196: 25.3%		97: 9.5%
	198: 7.23%		98: 24.4 %
			100: 9.6%
a. as determined by Oak Ridge National Labs (Re, Ir, Pt ) and US Services (Mo)			

## 2.5 Sediment dissolution

Sediment digestion was accomplished with acid dissolution aided by microwave heating as outlined in figure 2.2. In order to oxidize organic matter, samples were first combusted overnight at 550-575°C in covered porcelain crucibles in a muffle furnace. (Organic material is not completely decomposed by the acid-dissolution scheme described here, and uncombusted sediments left a nearly permanent dark "bathtub ring" in the digestion vessels). Although

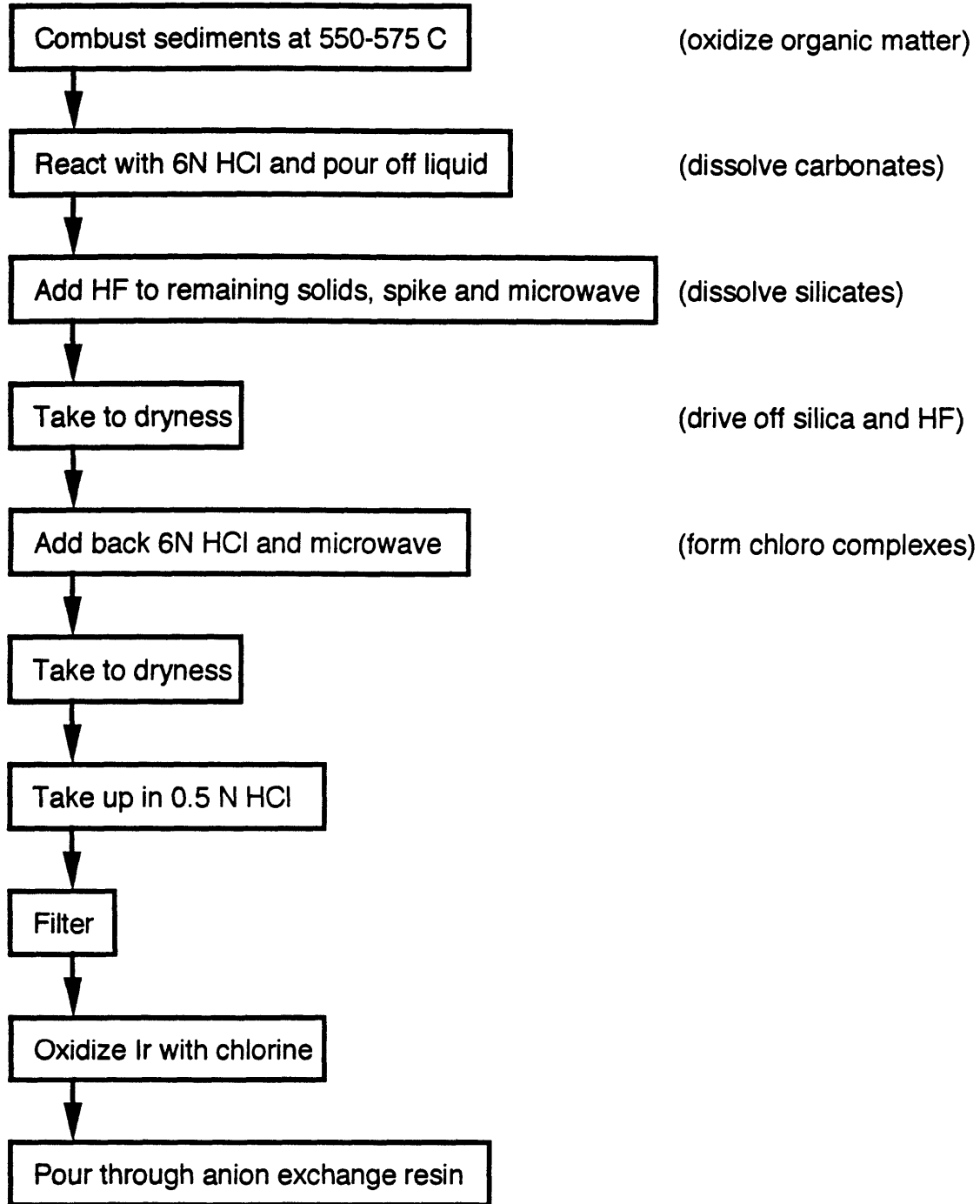


Figure 2.2 Sediment sample preparation scheme

$\text{Re}_2\text{O}_7$  is volatile at these temperatures, it was not measurably lost in this step based on comparison of results from this method with previous work (Table 2.2).

The major decomposition of the sample was performed using hydrofluoric acid; it was found, however, that the dissolution of carbonate rich sediments resulted in the formation of a large amount of insoluble calcium fluoride precipitate. It was therefore preferable to treat the samples first with hydrochloric acid in order to dissolve the carbonate and keep the Ca in solution. Between 0.5 and 1 g of sample was placed in a polypropylene centrifuge tube to which 15 mL 6N HCl was added. The initial mixture was quite effervescent, especially in carbonate rich samples. The samples were allowed to sit loosely capped overnight. After centrifuging for 10 minutes the next day, the acid was poured off into polypropylene beakers and saved for later re-addition to the sample. Duplicate samples processed with and without the HCl pretreatment yielded ~30% lower Ir concentrations without pretreatment, indicating removal of some Ir by the calcium fluoride precipitate.

Fifteen mL of a 5:1 mixture of HF (28.9 N) and  $\text{HNO}_3$  (16 N) were added to the remaining solids, and this mixture was transferred quantitatively to a teflon digestion vessel ("bomb"). The samples were allowed to sit loosely capped for at least one hour, as the initial reaction evolves heat, HF and  $\text{SiF}_4$ . The samples were then spiked with isotopically enriched Re, Ir and/or Pt, and the bombs were sealed, with pressure relief valves in place, using glass-reinforced polypropylene wrenches (Saville Corp.). The samples were microwaved for 90 minutes at 20% power (153W), as higher power levels resulted in venting through the pressure relief valves and loss of sample. After cooling to room temperature, the samples (dissolved and solid) were transferred to teflon beakers, rinsing the bombs with 0.1N HCl, for evaporation under infrared lamps.

The samples were taken to dryness and the 6N HCl solution which had been set aside previously, was poured back into the sample beakers. The resulting slurry was transferred back to the bombs for an additional 90 minutes of microwave heating (at 20%) in order to encourage the formation of Pt- and Ir-chloro complexes which could be subsequently separated by anion exchange. The samples were then poured back into teflon beakers and evaporated. Five mL 16N HNO<sub>3</sub> were added to the previously used bombs, and they were microwaved at 40% power for 10 minutes, in order to remove visible rings of material which had precipitated at the acid/vapor interface during the sample digestion. This acid was added to the samples and the evaporation continued to dryness.

Samples were redissolved in 0.5 N HCl, using ultrasonication to facilitate dissolution when necessary. The samples were filtered through 0.8 μm Nuclepore filters to remove any precipitate that did form, as well as refractory primary minerals. Characterization of the undissolved material was attempted by X-ray diffraction (at Woods Hole) and electron microprobe (at MIT). XRD did not reveal unambiguous peaks, but probe work showed incomplete dissolution of zircon in near-shore (Buzzard's Bay sediments). Since zircon is not a significant component of most off-shore marine sediments (Rothwell 1989), and since this study was primarily interested in the "mobilizable" fraction of PGE's in sediments, complete dissolution of zircon was not attempted. For sediments which were likely to contain zircon, such as the turbidites of the Madeira and Nares Abyssal Plains discussed later, care was taken to monitor Zr concentrations.

## **2.6 Water sample preparation**

*Pt measurement*

Two liter samples were acidified to pH 1 with 6N HCl in order to promote formation of the Pt - chloro complex,  $\text{PtCl}_4^{2-}$ , which is efficiently retained by the anion exchange resin. Filtered and unfiltered samples (0.45  $\mu\text{m}$ ) gave indistinguishable results. Samples were spiked at least twenty four hours before passing through columns in order to allow isotopic equilibration between sample and spike.

*Re measurement*

Pore water samples were filtered through 0.2  $\mu\text{m}$  Gelman syringe-disc filters and acidified with 0.1 mL 16N  $\text{HNO}_3$  per 10 mL sample. Other samples were acidified either with HCl or  $\text{HNO}_3$  in varying amounts since many had been collected for a variety of other purposes. All samples were spiked at least twenty four hours before passing through columns.

**2.7 Column preparation**

Approximately 1.5 mL of the resin (Biorad AG1 x-8, 100-200 mesh, Cl<sup>-</sup> form) was added to a polyethylene column (Biorad, polyprep) and a porous polyethylene frit (cut with a #5 cork borer) was fitted into the column on top of the resin bed. The frit was necessary to keep the resin from floating up during the elution step. The resin was then washed with 10 mL 12N  $\text{HNO}_3$  at 90°C, 20 mL distilled water, 10 mL 6N HCl and 20 mL 0.5N HCl, for columns to be used for Ir and Pt measurements. The resin contained very high (as high as sample) levels of Re, so the first step of the cleaning procedure was modified for Re determinations: 20 ml of 8N  $\text{HNO}_3$  for Re-only, or 10 mL hot 12N  $\text{HNO}_3$  and 10

mL 8N HNO<sub>3</sub> for Re-Ir-Pt measurements. This cleaning was adequate to reduce the Re blank introduced by the resin to below detection limits.

## 2.8 Anion exchange preconcentration

### *Oxidation of Ir*

In order to ensure efficient retention of Ir on the resin it was necessary to oxidize the element from Ir<sup>3+</sup> to Ir<sup>4+</sup>. A number of oxidants were tried, including (NH<sub>4</sub>)<sub>2</sub>Ce<sup>4+</sup>(NO<sub>3</sub>)<sub>6</sub>, H<sub>2</sub>O<sub>2</sub> and H<sub>5</sub>IO<sub>6</sub>, but these were unsatisfactory due to isobaric interferences (from CeClO) in the first case and insufficient oxidation in the latter two. Bubbling sediment solutions with Cl<sub>2</sub> for 1.5 minutes (Hodge et al. 1986) oxidized iridium and did not introduce blank problems. Care was taken to filter the gas to remove particles originating from corrosion of the gas delivery tube and valves.

### *Addition of samples to columns*

Sediment solutions were poured into funnels at the top of the columns, and allowed to drip at the unregulated drip rate of approximately one mL/min. Small (<50 mL) water samples were handled the same way. Seawater samples for Pt were collected in, or transferred to, two liter bottles with 1/4 inch "tubulation" at the base. A column was attached to the tubulation via a short length of corrugated teflon tubing (Cole Parmer) and a pipet tip (figure 2.3), and the sample was allowed to drip under atmospheric pressure (usually about 15 hours).

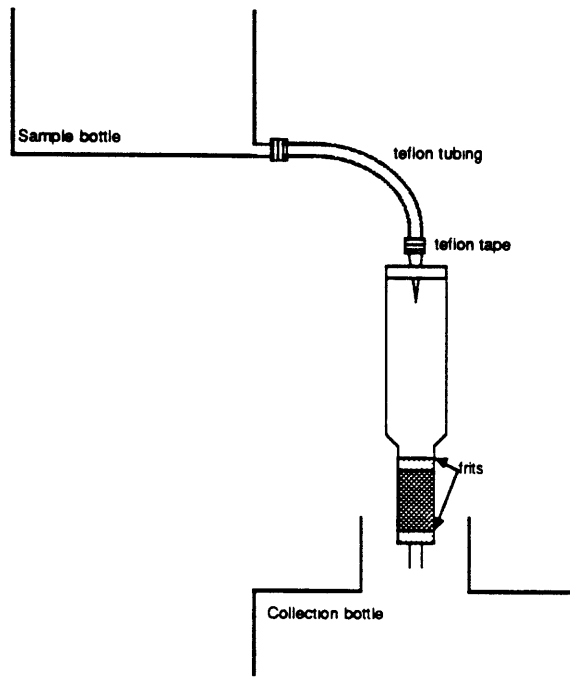


Figure 2.3 Column set-up for seawater sample processing for Pt



### *Sample elution*

After the samples had passed through, the columns were rinsed with 50 mL 0.1N HCl and 50 mL distilled water to remove sea salts and loosely-held metal ions. Because Pt and Ir were retained very strongly by the resin, their elution was accomplished with 30 mL 12N HNO<sub>3</sub> at 90 - 100 °C. Re was eluted with 30 mL 8N HNO<sub>3</sub> at room temperature. Eluted samples were collected in teflon beakers. For sediment samples in which all three elements were to be determined, Re was eluted with Pt and Ir, rather than before, since a significant fraction of the Ir was observed to come off the resin with 8N HNO<sub>3</sub>. (Separate elution of the elements would have been preferable because more time could have been spent in the measurement of each by ICP-MS, leading to an improvement in counting statistics.)

### *Sample evaporation*

The eluant (in 12N or 8N HNO<sub>3</sub> was evaporated at about 80°C under infrared lamps until sample volume was reduced to less than 5 mL. Temperatures were kept relatively low since ReO<sub>4</sub><sup>-</sup> is relatively volatile (as Re<sub>2</sub>O<sub>7</sub> which sublimates at 250°C.) Samples were then transferred to 5 mL conical teflon vials and evaporated to approximately 100 µL. For simultaneous determination of all three elements samples were diluted with 250 µL 0.8N HNO<sub>3</sub> plus 250 µL 0.5N HCl. Samples to be analyzed for Pt and Ir were diluted with 250 µL 0.5N HCl. For Re determinations, samples were diluted with 250 µL 0.8N HNO<sub>3</sub>.

### *Recoveries*

Recoveries for all three elements were calculated by comparing the amount of spike in the final solution (as determined by comparison with Re, Ir and Pt standards run on the same day) with the amount added to the samples. Recovery of the spikes was 80 - 100% for all three elements. The range in this value is due to the manner in which recoveries were calculated, and difficulty comparing samples and standards with very different matrices. An additional constraint on recoveries was gained by passing two liter seawater samples (for Pt) or 20 mL samples (for Re) through two consecutive columns. Platinum and rhenium eluted from the second column were below blank levels, indicating that Pt and Re were nearly quantitatively retained by the first column.

## 2.9 ICP-MS

### *Isobaric interferences*

Although isotope-dilution ICP-MS is relatively insensitive to matrix effects, isobaric interferences from oxides of Hf, Lu, Yb and Tm; chlorides of Tb, Gd, Sm, and Nd; and hydrides of W, Os, Ir and Pt were potential interferences for Re, Ir and Pt. The chlorides and hydrides all presented negligible interferences on the elements of interest. However, in the analysis of sediments, the oxides of the rare earth elements and Hf could potentially produce isobaric peaks of similar magnitude to those of Re, Ir and Pt, based on measurement of the MO/M ratio in elemental standard solutions. The column procedure reduced the concentrations of Hf, Lu, Yb and Tm by about a factor of 1000, which lowered their oxide levels to <6% of the Re, Ir or Pt signal. Attempts were made to minimize oxide interferences by pulling the plasma back slightly from the sampling cones, to sample it in a slightly cooler region. Some pertinent information regarding isobaric interferences is summarized in Table 2.5.

Table 2.5 Isotopes of interest and potential isobaric interferences

Isotope of interest (Iso A)	Isobar (Iso B)	Atomic abundance of isobar (%) <sup>a</sup>	Oxide peak/element peak (eg., TmO/Tm) <sup>b</sup>	(IsoB/IsoA) Typical sediment analysed	Potential interference in typical sediments
185Re	169TmO	100	0.002	27-10000	0.005 - 2 %
	184OsH	0.02	?	?	?
	184WH	30.7	<0.001	32-15000	0.003 - 2 %
187Re	171YbO	14.3	0.001	14-7000	0.001 - 1 %
	186 WH	28.6	<0.001	18-10000	0.002 - 1%
	186 OsH	1.6	?	?	?
191Ir	175Lu	97.4	0.002	13000	3 %
	190OsH	26.4	?	?	?
	190PtH	0.013	<0.001	0.35	3E-5 %
192Pt	176HfO	5.2	0.005	10000	5 %
	176LuO	2.6	0.002	1000	0.2 %
	176YbO	12.7	0.001	24000	2 %
	191IrH	37.4	<0.001	2.3	2E-4 %
193Ir	177HfO	18.5	0.005	12000	6%
	192OsH	41.0	?	?	?
	192PtH	0.78	<0.001	0.26	2E-5 %
194Pt	178HfO	27.2	0.005	1700	0.8 %
	193IrH	62.6	<0.001	0.1	1E-5 %

a. assuming 100% <sup>16</sup>O

b. as determined from measurements of standard solutions of interfering elements

? : Os occurs in extremely low concentrations in the samples, and is nearly quantitatively lost during sample processing.

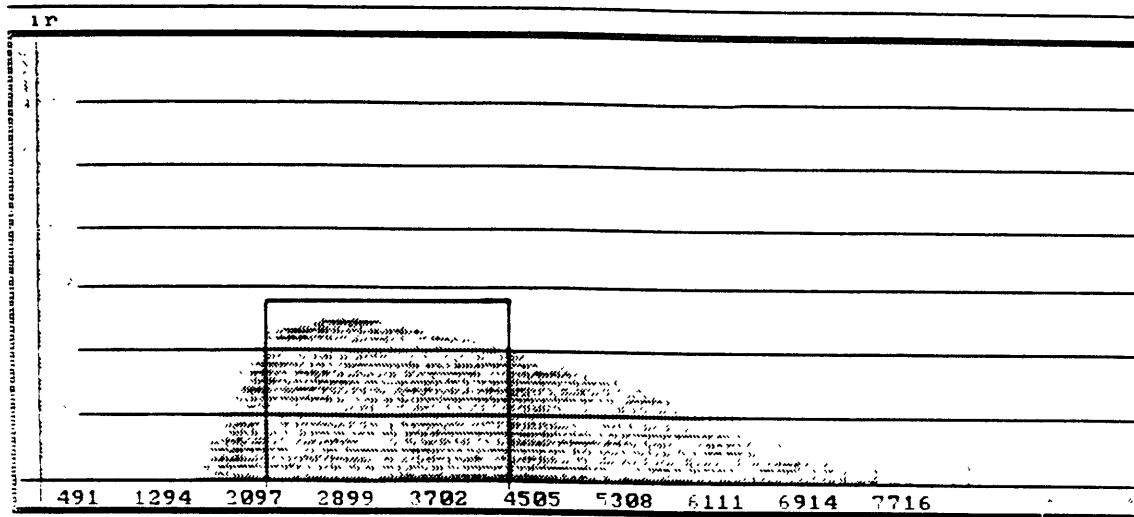


Figure 2.4 Transient signal from the injection of 250 $\mu$ L of a 15 nM Ir solution. The quadrupole was set to transmit mass 191 for 83.8 seconds. The horizontal scale is in milliseconds/10. Data for isotopic ratios was collected in the time window enclosed by the box (about 20 seconds).

### *Sample introduction*

In order to maximize the sample signal relative to background, it was beneficial to use small sample volumes. However, since at least two isotopes had to be determined for each sample, the sample volume had to be large enough so that many determinations of their ratio could be made. Additionally, the sample matrix became quite viscous if the evaporated column eluant was taken up in less than 250  $\mu\text{L}$  of acid. Based on these considerations, samples were diluted either to 250 or 500  $\mu\text{L}$  (as above). The sample was introduced via a 6-port flow injection valve downstream of a peristaltic pump, and the length of tubing the sample had to traverse was minimized. This arrangement avoided sample contact with the tygon tubing of the pump, and reduced diffusive broadening of the sample peak (Falkner and Edmond 1990). The trace of a typical injection is shown in figure 2.3. Memory effects receded to below background levels using this all-teflon introduction system and 0.2% aqua regia as an eluant.

Operating parameters for the ICP-MS are outlined in Table 2.3.

## **2.10 Isotope dilution calculations**

### *Target spiking ratios*

The precision of an isotope dilution calculation depends in part on the value of the ratio of spiked isotope to unspiked isotope (isotope "1" to isotope "2"). For Re, Ir, and Pt, these ratios were  $^{185}\text{Re}/^{187}\text{Re}$ ,  $^{191}\text{Ir}/^{193}\text{Ir}$ , and  $^{192}\text{Pt}/^{194}\text{Pt}$ , respectively. The optimal spiking ratio was established by compromise among a number of considerations. For samples with low concentrations compared to background, as was true for nearly all the samples measured in this study, a ratio of "1"/"2" = 1 minimizes the effects of variable background counts,

assuming that the background counts on the two isotopes vary in concert. However, in order to minimize the uncertainty introduced by propagation of error through the isotope dilution equation, one would like a ratio close to the geometric mean of the "1"/"2" ratios of the spike and sample (see below). Target spiking ratios were chosen to lie between these two values, as summarized in Table 2.6.

	<u>Re</u>	<u>Ir</u>	<u>Pt</u>
mass isotope 1	185	191	192
mass isotope 2	187	193	194
"1"/"2" sample ( $R_s$ )	0.5974	0.5974	0.02371
"1"/"2" spike ( $R_t$ )	37.46	25.23	2.1996
geometric mean $\sqrt{R_s \times R_t}$	4.73	3.88	0.228
target ratio	3	2	0.5

#### *Calculation of sample concentration*

The number of moles of sample present in a solution spiked with an isotopically enriched tracer was calculated as follows:

$$S = \frac{(\%2_t)}{(\%2_s)} (T) \left( \frac{R_m - R_t}{R_s - R_m} \right) \quad (1)$$

where there are at least two isotopes (1 and 2) and the spike is enriched in isotope 1. Then,

S = number of moles of sample

$\%2_t$  = the atomic abundance of isotope 2 in the tracer

$\%2_s$  = the atomic abundance of isotope 2 in the sample (same as natural abundance)

T = number of moles of tracer added

$R_m$  = measured ratio of the mixture (" $1/2$ ")

$R_t$  = ratio (" $1/2$ ") of the tracer measured by Oak Ridge National Labs

$R_s$  = ratio (" $1/2$ ") of the sample (natural abundances).

The measured ratio ( $R_m$ ) of the mixture was corrected for instrumental mass discrimination by comparing it to a "monitor" solution with a known isotopic ratio, consisting of a mixture of the tracer with a gravimetric standard. If the concentration and isotopic composition of the monitor are similar to that of the samples, multiple determinations of the monitor ratio provide an estimate of instrumental uncertainty as well as bias. Error in the measured ratio is magnified through the isotope-dilution equation (equation 1) by a factor dependent on the value of the ratio. The "magnification factor" (M) has been defined as follows:

$$M = \frac{\Delta S/S}{\Delta R_m/R_m}$$

where  $\Delta S$  is the random error in S introduced by a random error ( $\Delta R_m$ ) in  $R_m$ .

For the isotope dilution equation, above:

$$M = (R_t - R_s) * \frac{R_m}{(R_m - R_s)(R_t - R_m)}$$

The magnification factor is minimized when the ratio of the mixture is equal to the geometric mean of the ratio of the spike and the ratio of the sample, or when  $R_m = \sqrt{R_t \times R_s}$  (Heumann 1988).

*Blank correction*

Procedural blanks were run parallel to every 5 or 10 samples. Because it was difficult to calculate a meaningful blank concentration from spiked samples where the blank was small ( $R_m \sim R_t$ ), the blanks were not spiked. Count rates on the blank solutions were subtracted from those of the samples before applying isotope-dilution calculations.

*A note on isotopic equilibration*

The application of isotope dilution methods requires that sample and spike mix completely, and are not fractionated during any step in the analysis (with the exception of mass discrimination in the ICP-MS, which is corrected for by comparison with the "monitor" solution, as above). For water samples, isotopic exchange is facilitated by adding the spike in the same form as the sample, where possible. Re spike was added in the same form as the sample ( $\text{ReO}_4^-$ ), but the Pt spike was probably a mixture of  $\text{PtCl}_4^{2-}$  and  $\text{PtCl}_6^{2-}$ , whereas the sample was probably in the former state. Experiments designed to check for potential problems in equilibration of Pt sample and spike are described in Chapter 3. Exchange of  $^{192}\text{Ir}$  between  $\text{IrCl}_6^{3-}$  and  $\text{IrCl}_6^{2-}$  has been studied in 1N HCl solutions; with concentrations of the complexes between 0.1M and 0.1 mM, exchange was always complete within about one minute (at 50°C, in darkness) (Griffith 1967). Spiked samples were always allowed to sit for at least 24 hours, before addition to columns, which should have enabled isotopic exchange if the rates for Ir and Pt are at all similar.

For sediment samples, it was not possible to add the spike in the same matrix as the sediment. Spike in acid solution was added to a mixture of HF and the sample, before the sediment was completely dissolved. It is assumed that the spike and the sediment-derived element mixed completely as the sample dissolved, and that any undissolved residue remained unequilibrated.



Sufficient equilibration of sample and spike is inferred from results that are consistent with previous work.

## References for Chapter 2

- Beamish, F. E. and Russell. (1936). "The assay of the platinum metals." Ind. Eng. Chem. Anal. Ed. **8**: 141-144.
- Creaser, R.A., D.A. Papanastassiou and G.J. Wasserburg. (1991). "Negative thermal ion mass spectrometry of osmium, rhenium and iridium." Geochim. Cosmochim. Acta. **55**(1): 397-401.
- Esser, B.K. (1991). Osmium Isotope Geochemistry of Terrigenous and Marine Sediments, PhD. Thesis, Yale University
- Falkner, K. K. and J. M. Edmond. (1990). "Determination of gold at femtomolar levels in natural waters by flow injection inductively coupled plasma quadrupole mass spectrometry." Anal. Chem. **62**: 1477-1481.
- Goldberg, E. D., M. Koide, J. S. Yang and K. K. Bertine. (1988). Comparative marine chemistries of platinum group metals and their periodic table neighbors. Metal speciation, theory analysis and application. Chelsea, MI, Lewis Publishers, Inc.
- Goldberg, E.D., V. Hodge, P. Kay, M. Stallard and M. Koide. (1986). "Some comparative marine chemistries of platinum and iridium." Appl. Geochem. **1**: 227-232.
- Griffith, W. P. (1967). The chemistry of the rarer platinum metals (Os, Ru, Ir, and Rh). N.Y., Interscience Publ.
- Hauri, E., S. Hart and G. Ravizza. "The determination of Re and Os in geological samples by negative thermal ionization mass spectrometry." Anal. Chem., in prep.
- Heumann, K. G. (1988). Isotope dilution mass spectrometry. Inorganic Mass Spectrometry. New York, J. Wiley and Sons.
- Hodge, V. F., M. Stallard, M. a. Koide and E. Goldberg. (1986). "Determination of platinum and iridium in marine waters, sediments, and organisms." Anal. Chem. **58**: 616-620.
- Izett, G. A. (1987). The Cretaceous-Tertiary boundary interval, Raton Basin, Colorado and New Mexico, and its shock-metamorphosed minerals: Implications concerning the K-T boundary impact-extinction theory, USGS Open File Report No. 87-606.
- Jacinto, G. S. and C. M. G. van den Berg. (1989). "Different behavior of platinum in the Indian and Pacific Oceans." Nature. **338**: 332-334.
- Keays, R.R., R. Ganapathy, J.C. Laul, U.R.S. Krahenbuhl and J.W. Morgan. (1974). "The simultaneous determination of 20 trace elements in terrestrial,

lunar and meteoritic material by radiochemical neutron activation analysis." Anal. Chim. Acta. **72**: 1-29.

Koide, M., V. Hodge, J. S. Yang and E. D. Goldberg. (1987). "Determination of rhenium in marine waters and sediments by graphite furnace atomic absorption spectrometry." Anal. Chem. **59**: 1802-1805.

Kyte, F. T. and J. T. Wasson. (1986). "Accretion rate of extraterrestrial matter: iridium deposited 33 to 67 million years ago." Science. **232**: 1225-1229.

Luck, J.M. and K.K. Turekian. (1983). "Osmium-187/osmium-186 in manganese nodules and the Cretaceous-Tertiary boundary." Science. **232**: 1225-1229.

Murali, A.V., P.P. Parekh and J.B. Cumming. (1990). "On the determination of iridium in diverse geologic samples employing HPGe-coincidence/NaI-anticoincidence spectrometry." Geochim. Cosmochim. Acta. **54**(3): 889-894.

Ravizza, G. (1991). Rhenium and Osmium Geochemistry of Modern and Ancient Organic-Rich Sediments. PhD Thesis, Yale University.

Rothwell, R.G. (1989). Minerals and Mineraloids in Marine Sediments. Elsevier, N.Y. p109-138.

Van Den Berg, C.M.G. and G.S. Jacinto. (1988). "The determination of platinum in seawater by adsorptive cathodic stripping voltammetry." Anal. Chim. Acta. **211**: 129-139.

Walker, R.J. (1988). "Low blank chemical separation of rhenium and osmium from gram quantities of silicate rock for measurement by resonance ionization mass spectrometry." Anal. Chem. **60**: 1231-1234.



## **Chapter 3**

### **Platinum in seawater**

---

#### **3.1 Abstract**

Two previous studies of the distribution of platinum in seawater yielded conflicting results, one suggesting nutrient-type behavior for the element (Goldberg et al., 1986), and the other, scavenging-controlled behavior (Jacinto and Van den Berg, 1989). This study was therefore undertaken to help resolve the differences between the two. Pt was determined in two profiles from North Atlantic stations and one profile in the North Pacific. The results agree with neither of the previous works, and the data show no trend with depth, with a mean concentration of 260 fM and a standard deviation of the data set of 70 fM (n=54). Neither the factor of three depletion in surface compared to deep waters found by Goldberg et al., nor the factor of four enrichment in surface waters found by Jacinto and Van den Berg were observed. Some analytical possibilities for the origin of the discrepancies among the three studies are examined, but a definitive explanation is not yet possible. The new results suggest that Pt is not substantially involved in the cycling of biogenic matter in the water column. The Pt profiles observed here are similar to those observed previously for gold (Falkner and Edmond, 1990). A better understanding of Pt behavior in seawater awaits determination of its concentrations in potential sources to seawater, such as river waters and eolian dust.

#### **3.2 Introduction**

The distribution of Pt in seawater has been the subject of two recent investigations which gave contradictory results. Goldberg et al. (1986) reported "nutrient-type" Pt profiles at three Pacific sites, with low Pt values in surface waters (400 fM) and continual enrichment with depth (up to 1200 fM). In a later work, Jacinto and van den Berg (1989) determined Pt levels at two stations in the Southwest Indian Ocean. The resulting profiles showed enrichment of Pt in surface waters (1600 fM) and depletion to near-constant values at depth (to ~350 fM). Composite profiles from these studies are illustrated in figure 3.1.

Goldberg et al. concluded that Pt is taken up by biogenic material in surface waters and released at depth as this material is degraded. They calculated a long residence time for Pt in seawater of about one million years, and attributed its unreactivity to the stability of the chloro complex of the divalent metal ( $\text{PtCl}_4^{2-}$ ). Their analytical methods consisted of anion exchange preconcentration of Pt from two liters of seawater, followed by analysis by graphite furnace atomic absorption spectrometry. In the second work, the data of Jacinto and Van Den Berg indicated scavenging of Pt throughout the deep water column. They suggested that Pt is present as Pt(IV) through most of the water column, but occurs as Pt(II) in surface waters due to the possible dominance of the  $\text{O}_2/\text{H}_2\text{O}_2$  redox couple in the euphotic zone (Zika et al., 1985). Their argument relies on oxidative removal of Pt (IV) onto oxide surfaces (as suggested by Goldberg et al. to explain the marked enrichment of Pt in manganese nodules) to produce the observed profiles. Jacinto and Van Den Berg used cathodic stripping voltammetry with a hanging mercury drop electrode to determine Pt concentrations in 10 mL seawater samples.

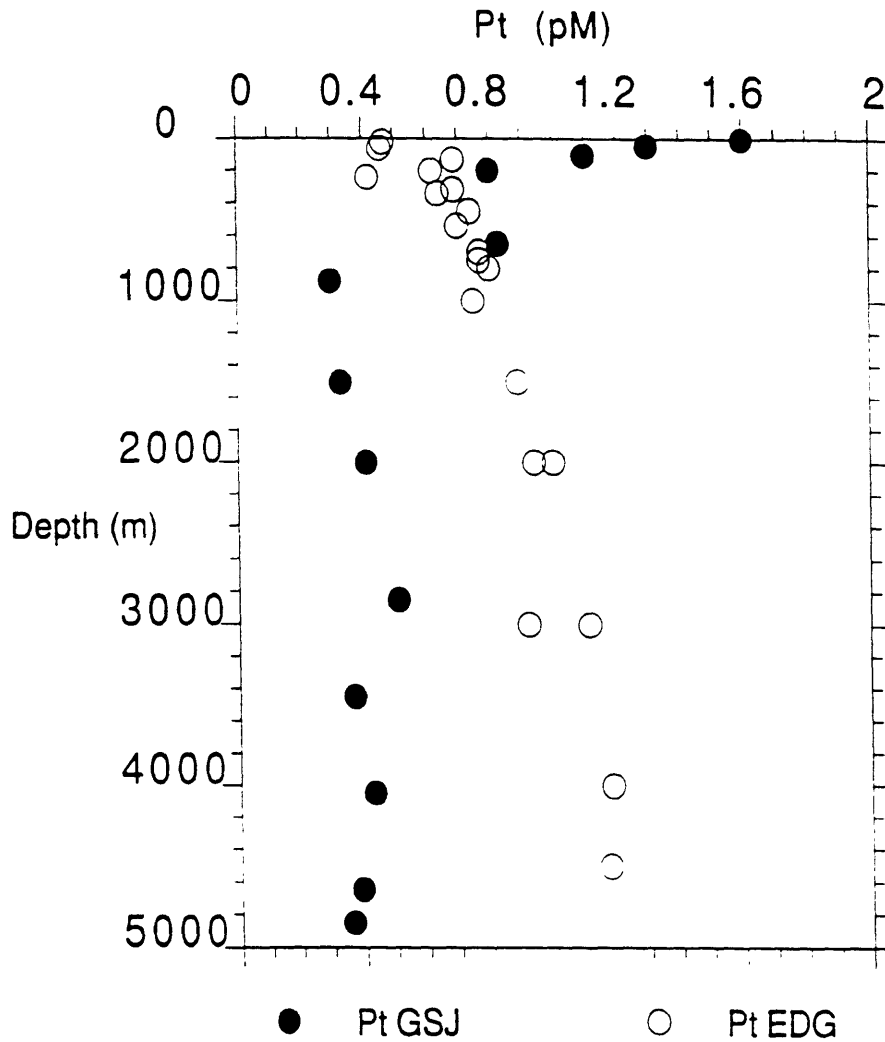


Figure 3.1 Composite profiles from previous studies of Pt in seawater.  
EDG = Goldberg, et al., 1986: results from NE Pacific.  
GSJ = Jacinto et al., 1989: results from SW Indian Ocean.

Given the discrepancy between these studies, an independent appraisal of Pt distributions is desirable. Pt was therefore measured in two profiles from the Atlantic Ocean and one from the Pacific Ocean using isotope-dilution inductively-coupled plasma mass spectrometry. An upper limit for Pt concentrations in hydrothermal solutions from the Mid-Atlantic Ridge was also determined using this technique. A preliminary attempt to identify the factors responsible for the Pt distributions reported here serves to highlight areas for future inquiry.

### **3.3 Analytical methods**

#### *Seawater sample collection and storage*

Samples were collected at five sites: western Atlantic, eastern Atlantic, western Pacific, eastern Pacific and at Woods Hole, with depth profiles from the first three locations. Atlantic samples were collected specifically for this work, whereas Pacific samples were collected either for gold determinations (by K. Falkner) or for selenium and beryllium determinations (by C. Measures). Sample collection information is summarized in Table 3.1.

The western Atlantic (Bermuda, Oct. '89) and eastern Atlantic (Azores) samples were collected with 30L Niskin bottles which had been acid-leached with 0.1N HCl prior to the cruise. The bottles were equipped with epoxy-coated internal springs and red silicone o-rings and were hung individually on a standard steel hydrowire. Samples were drawn through polyethylene tubing into 10 L polyethylene carboys with spigots. The carboys were connected to a nitrogen tank via holes in the caps, and an in-line filter cartridge was attached to the spigots using "C-flex" tubing. Samples were pressure filtered through acid-leached 0.4  $\mu\text{m}$  Nuclepore filters and collected in 2 L polyethylene bottles with



Table 3.1 Pt seawater sample collection information

Location	Lat.	Long.	Date	6N HCl added per liter	Filtered?	Vessel
Bermuda	32°10'N	64°30'W	Oct.'89 May '90	15mL 15mL	yes no	AtlantisII Weatherbird
Azores	26°20'N	33°40'W	Oct.'89	15mL	yes	AtlantisII
W. Pacific	24°15'N	164°51'E	May'85	4mL	no	Thompson
E. Pacific	42°09'N	125°45'W	Sept.'89	*	yes	Wacoma
Woods Hole, MA	41°30'N	70°40'W	various	15mL	yes	shore lab

\* 0.5 mL 0.4% KCN added upon collection

Open ocean samples were collected in acid-leached Niskin bottles with epoxy-coated internal springs and red silicone rubber o-rings, hung on a stainless steel hydrowire. Pacific samplers were rosette-mounted.

plugged spigots. All polyethylene containers used for sample storage were precleaned with 0.1 N or 1 N HCl at 60°C overnight. Within six hours of collection, samples were acidified with 30 mL 6N HCl and spiked with enriched  $^{192}\text{Pt}$  tracer in a laminar flow bench. After at least 24 hours, columns (prepared as in section 2.7) were attached to the spigots and the samples were allowed to drip in the manner described in section 2.8. The column-preconcentration step was carried out in stacked milk crates which were draped in plastic. When the sample stopped dripping, the column was removed, capped and sealed with Parafilm at the bottom and top. Columns were stored in a polyethylene bottle until they were eluted at MIT.

Bermuda (May '90) samples were collected directly into 2L bottles with plugged spigots. They were acidified and spiked at sea and shipped back to MIT for preconcentration. Western Pacific samples were collected in May, 1985 into acid-leached 1 L polyethylene bottles and acidified with 4 mL 6N HCl at sea. An additional 5 mL 6N HCl were added to the samples along with the spike for Pt measurements in August, 1990. Samples were allowed to sit for at least a week before pouring through columns. Two one liter samples were combined for Pt determinations. Eastern Pacific samples were collected in September, 1989, and filtered through 0.4  $\mu\text{m}$  Nuclepore filters into acid-cleaned 1 L polyethylene bottles and preserved using 0.5 mL 0.4% KCN. Due to the high stability of Pt-cyanide complexes ( $\log \beta_4 \text{Pt}(\text{CN})_4^{2-} = \sim 10^{78}$ ) it is expected that, platinum, like gold (Falkner and Edmond, 1990a), would remain in solution under these conditions. In a well-ventilated fume hood at MIT, these samples were acidified with 15 mL 6NHCl, and spiked for Pt. Each one liter sample was run individually. Woods Hole samples were collected at the Coastal Research Lab at WHOI, from their filtered seawater line.

*Hydrothermal sample preparation*

Samples were collected at the TAG and MARK sites on the Mid-Atlantic Ridge in January, 1990, aboard the R/V AtlantisII - DSRV Alvin. They were drawn directly from titanium-syringe samplers (Von Damm et al., 1985) into 125mL polyethylene bottles containing 2mL aqua regia (a 6:1 mixture of 6N HCl and 16N HNO<sub>3</sub>) and stored until further processing in the lab. Because Pt concentrations in hydrothermal fluids were completely unknown, the sample bottles did not contain <sup>192</sup>Pt spike, although this would be recommended if one knew the approximate level of Pt in solution. This would be preferable because a mixed amorphous-silica/sulfide precipitate forms in the bottles during storage (Von Damm et al., 1985), and the sulfides are likely to scavenge Pt from solution (Goldberg and Hepler, 1968). In this case, the samples were spiked after the precipitate had been redissolved.

For the 100 mL samples, dissolution was accomplished in a number of steps. Samples were first bubbled with Cl<sub>2</sub> for one minute and then allowed to sit overnight in order to oxidize the sulfide material. This usually resulted in formation of a white-brown precipitate to which 1mL HF was added to dissolve amorphous silica. Over about one day, a brown (mixed iron oxyhydroxide - silica - barite?) film precipitated on the inside of the sample bottles. The liquid portion of the samples was poured off into larger bottles and 5 mL 6N HCl was added to each of the original bottles. These were heated at 60°C and allowed to reflux for one hour. The oxyhydroxides dissolved after about 10 minutes in the oven, as evidenced by the disappearance of the brown film, and appearance of a bright yellow (iron chloride) color in solution. This acid was added back to the rest of the sample, rinsing the original bottle with HCl, and the samples were spiked. One larger volume sample (700 mL) was run, which was a combination of two samples from the same hydrothermal vent. These

samples were filtered through 0.45  $\mu\text{m}$  Nuclepore filters shortly after arrival at MIT. The filters were refluxed in 20 mL 16N  $\text{HNO}_3$  at 60°C for one day. The particle-digest and fluid portions of the samples were recombined and spiked. Spiked samples were allowed to sit for at least three days and then preconcentrated on the anion exchange resin.

#### *Anion exchange preconcentration*

Except for samples which had been processed at sea (Bermuda '89 and Azores), samples were added to the anion exchange resin in the lab, in the manner described in sections 2.7 and 2.8. All samples were eluted in the lab, in a fume hood, using 30 mL or 50 mL 12 N  $\text{HNO}_3$  at 90-100°C. They were collected in teflon beakers and evaporated to approximately 100 $\mu\text{L}$ , followed by dilution with 250 $\mu\text{L}$  0.5 N HCl. Samples were stored in conical teflon vials, or in 0.5 mL snap-top centrifuge tubes until analysis.

#### *ICP-MS Analysis*

Determination of Pt was accomplished with isotope dilution, flow injection, ICP-MS, as described in Chapter 2.

### **3.4 Results**

The results of this study agree with neither of the previous two in detail, although surface concentrations are similar to those reported by Goldberg et al. (1986) and deep concentrations agree with those of Jacinto and Van den Berg (1989). The profiles reported here are featureless, within the uncertainties of the method, and are compared to the previous works in figure 3.2.

*Bermuda profile (W. Atlantic)*

The measurements at this station (BDA Oct.'89) comprise the first profile collected for this work. Pt data for this station, along with ancillary analyses are presented in Table 3.2 and are plotted in figure 3.3. Pt concentrations are uniform within the uncertainties of the measurements, with a weighted mean and standard deviation for the data set of  $230 \pm 90$  fM. (To calculate the mean, samples were weighted by the inverse of their variance). The apparent minimum in surface waters was not reproduced in a second set of samples collected at this station in May of 1990, which may be due to natural variability, or sampling/analytical artifacts. The magnitude of the apparent variation ( $\pm 22\%$ ) is similar to that observed seasonally for lead in surface waters at this site ( $\pm 25\%$ ) (Boyle et al., 1986). However, the direction of the change for Pb is opposite to that for Pt, with higher Pb concentrations in October than in May. The sources for Pb and Pt and/or their removal rates from seawater may be quite different; Pb has a predominantly eolian source, and is scavenged rapidly by particles, whereas Pt sources and behavior are not well constrained. Preliminary indications are that Pt has a longer residence time in seawater than Pb (see below). Alternatively, since the October surface samples involved the first use of the Niskin bottles, carboys and filtration apparatus after acid-cleaning, the lower values may have been a result of Pt adsorption onto container walls before the samples were acidified. These first five samples were also processed as a group (the first group processed), although subsequent groups of samples did not show similar coherence. Because of the potential for analytical artifacts associated with particular sample batches, the remaining profiles were run in mixed-depth batches.

Table 3.2 Data for Atlantic stations "BDA'89" and "BDA'90": near Bermuda, 32°10'N, 64°30'W. Platinum values in fmol/L. Samples were collected in October, 1989, unless otherwise indicated

Depth(m)	Pt (SD)	Salinity	Temp.(°C)	O <sub>2</sub> (μM)	PO <sub>4</sub> (μM)	SiO <sub>2</sub> (μM)
1 (May'90)	290(40)		21.3	241.03	0.02	0.24
5	190(30)	36.624			0.01	1.03
50	140(20)	36.623	22.8	215.01	0.01	0.97
100	140(20)	36.645			0.01	0.67
150	190(30)	36.599	18.9		0.05	0.92
200	140(20)	36.574			0.1	1.08
201(May'90)	270(40)		18.8	235.49	0.08	1.05
390	320(70)	36.445	17.8	234.63	0.21	1.7
605	300(70)	36.012	15.3	187.30	0.66	3.98
735(May'90)	300(40)			175.06	1.05	7.60
740	220(70)	35.506		157.82	1.28	9.01
854	380(50)	35.188	10.6		1.7	14.07
990	280(40)	35.086	5.9	201.35	1.56	13.49
1465	200(30)	35.003	4.3	270.85	1.3	11.89
1959	240(30)	34.987	3.8	272.86	1.29	14.21
2464	390(90)	34.965		272.99	1.35	18.78
2958	360(50)	34.932		278.97	1.28	22.25
3452	350(50)	34.910		285.49	1.28	27.75
3947	290(40)	34.892	2.2	277.51	1.33	34.81

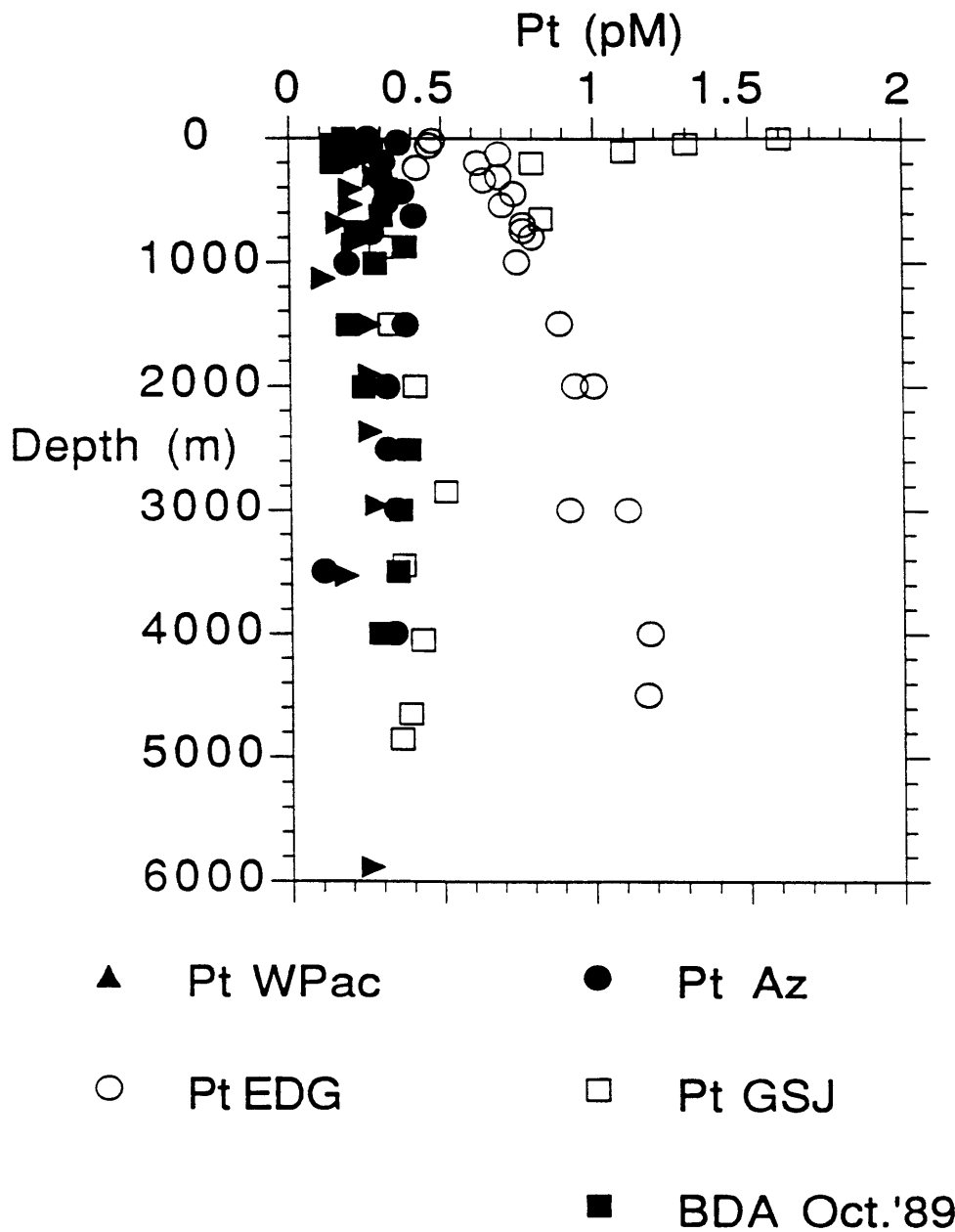


Figure 3.2 Pt results from this study compared to previous studies. WPac = west Pacific station, this study. Az = Azores station, this study. BDA = Bermuda station, this study. EDG = E.D. Goldberg, et al., 1986, Pacific Ocean. GSJ = G.S. Jacinto, et al., 1989, Indian Ocean.

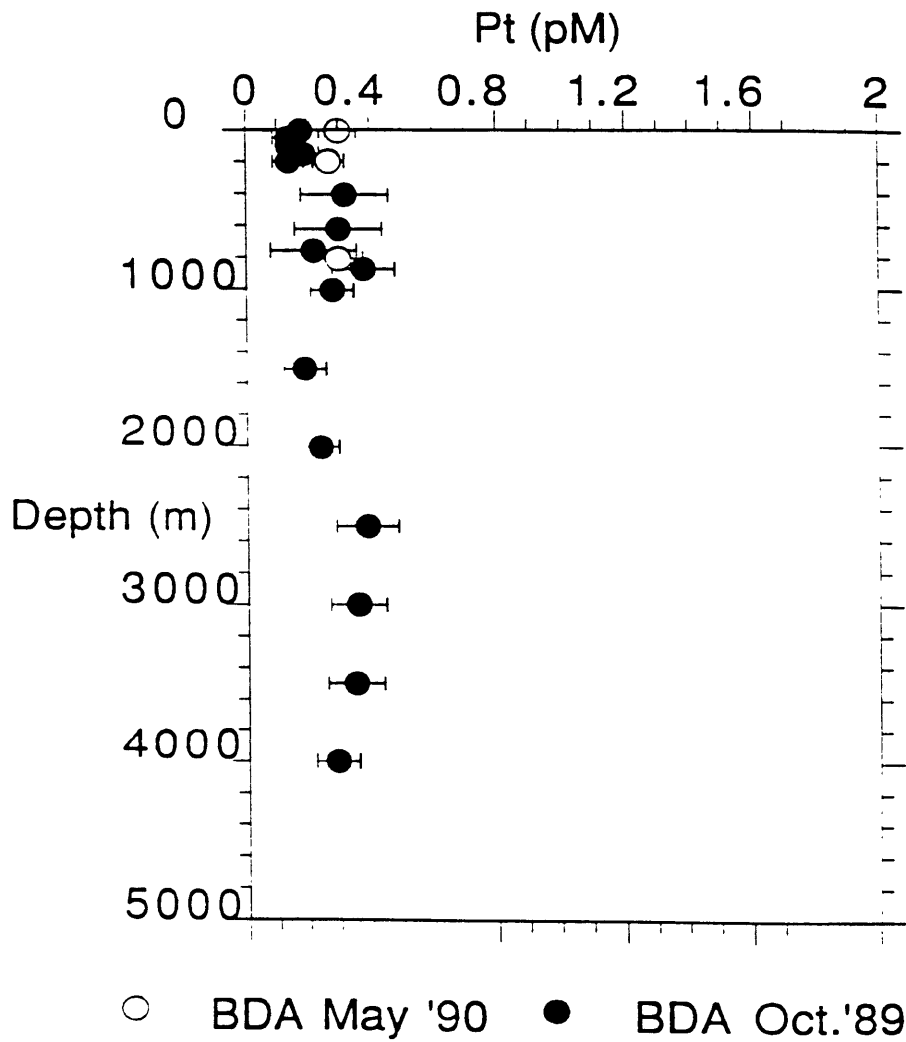


Figure 3.3 Bermuda platinum profile (32°10'E, 64°30'W). Two  $\sigma$  error bars.



*Azores Profile (E. Atlantic)*

Results for this profile taken near the Azores are presented in Table 3.3 and figure 3.4. Again, the Pt profile is featureless within errors of the data, with a weighted mean of 300 and standard deviation of  $\pm 60$  fM. This value is indistinguishable from the mean concentration of the deeper Bermuda samples, excluding the five samples above 200 m ( $280 \pm 60$  fM). If the difference ( $\sim 100$  fM) in surface water values between these two stations is real, it might be explained by more dust input to surface waters in the eastern station. Since there is no data for Pt in atmospheric aerosols, it is difficult to evaluate this possibility.

*Pacific profile*

Like the Atlantic profiles, the western Pacific Pt data show no trend with depth (Table 3.4 and figure 3.5). As this profile was collected in 1985, there was the potential for loss of Pt to bottle walls during the five-year storage period, even though the samples had been acidified on collection. Two additional samples were therefore run, from 1400 and 2000 m in the California current region, which had been stored for only six months and preserved with  $30\mu\text{M}$  KCN. The earlier data of Goldberg et al., 1986 showed no significant difference between Pt concentrations in the open Pacific vs. California Current region in this depth range. In this work as well, the recently-collected samples give the same results for Pt as the stored samples. The weighted mean concentration for the eastern Pacific profile is 230 fM with a standard deviation of  $\pm 50$  fM. Although this value is less than the mean Atlantic station concentrations (280 and 300 fM), the differences among the profiles, or between the oceans, are not significant at the 95% confidence level (based on an F-test).

Table 3.3 Data for Atlantic station "Azores", 26°20'N, 33°40'W. Platinum values in fmol/L. All samples were collected in October, 1989.

Depth (m)	Pt (SD)	Salinity	Temp.(°C)	O <sub>2</sub> (μM)	PO <sub>4</sub> (μM)	SiO <sub>2</sub> (μM)
4	260(30)	37.643		172.25	0	1.48
43	360(50)	37.649			0	1.46
72	270(40)	37.075	22.5	243.57	0	1.13
113	240(40)	37.049	20.5	199.36	0	1.35
194	310(60)	36.542	18.1		0.14	1.18
300	300(40)	36.095	15.4	161.52	0.41	4.01
415	370(50)	35.991	15.0	199.04	0.57	4.94
499	320(40)	35.725		191.43	0.80	7.03
607	410(50)	35.571	12.1		0.99	9.42
735	270(40)	35.356		162.92	0.31	14.92
981	190(50)	35.211		162.85	1.62	20.60
1478	380(50)	35.183		173.64	1.47	16.40
1972	320(40)	35.069		202.98	1.36	19.67
2466	320(40)	34.986			1.43	23.46
2950	350(50)	34.942		173.64		28.46
3444	110(20)	34.916		248.02	1.58	28.16
3938	340(40)	34.900	2.4	219.42	1.56	28.98

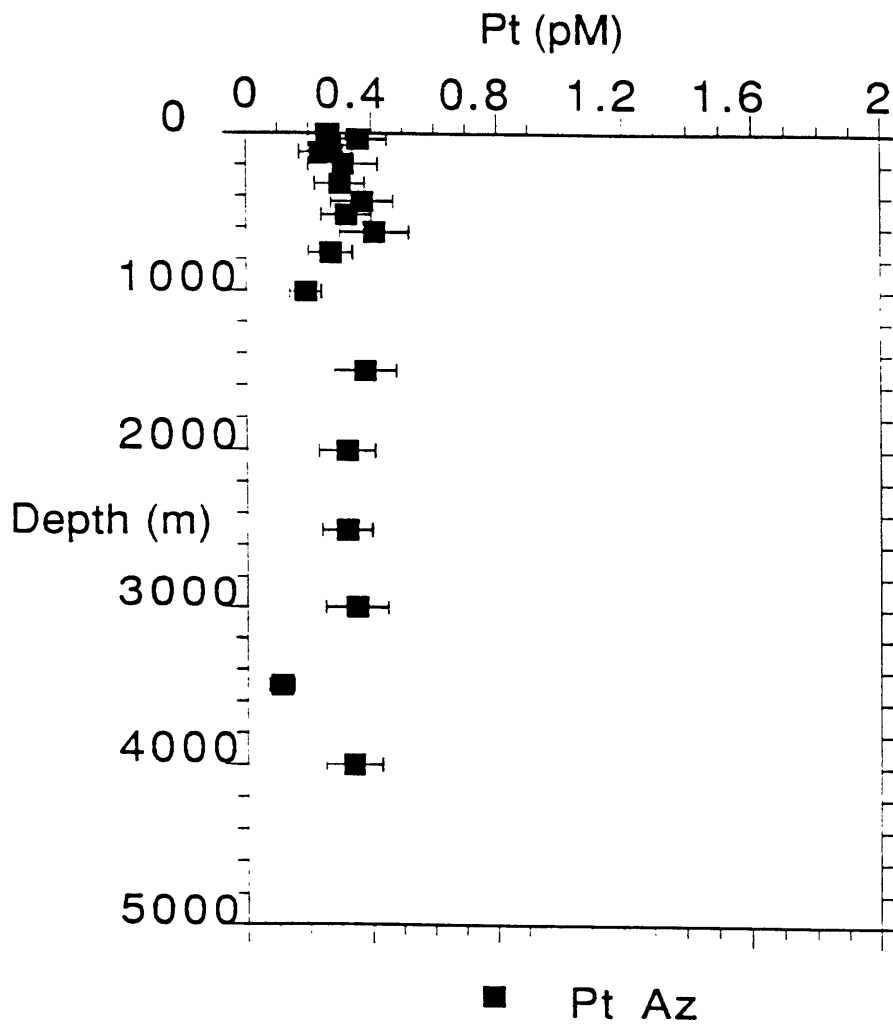


Figure 3.4 NE Atlantic platinum profile (26°20'N, 33°40'W). Two  $\sigma$  error bars.

Table 3.4 Data for Pacific stations. Pt values in fmol/L.

Station "TP" (W. Pacific): 24°15'N, 164°51'E						
Depth (m)	Pt (SD)	Salinity	PTemp. (°C)	O <sub>2</sub> (ml/L)	SiO <sub>2</sub> (μM)	PO <sub>4</sub> (μM)
14	280(40)	35.113	25.33	4.771	1.03	0.056
60	250(30)	35.136	23.88	4.951	0.80	0.050
125	250(40)	35.007	21.04	5.089	1.22	0.097
208	200(40)	34.824	17.82	4.619	2.71	0.315
308	280(50)	34.709	15.72	4.798	5.28	0.483
416	200(40)	34.508	13.47	4.752	10.64	0.756
536	200(40)	34.236	10.10	4.266	24.79	1.297
686	160(50)	34.084	6.98	3.045	51.57	2.141
857	210(50)	34.178	4.96	1.425	87.30	2.741
1134	110(40)	34.379	3.46	0.844	125.11	3.000
1511	260(50)	34.521	2.65	1.453	141.85	2.912
1915	260(40)	34.593	2.03	2.110	149.15	2.784
2367	260(40)	34.629	1.70	2.509	151.08	2.692
2963	280(40)	34.657	1.44	2.923	151.51	2.604
3538	180(40)	34.670	1.28	3.247	148.11	2.546
5888	260(50)	34.694	0.97	4.137	129.67	2.333

Station W8909A (E. Pacific) 42°08.62'N, 125°44.97'W	
Depth (m)	Pt (SD)
1400	270(40)
2000	240(30)

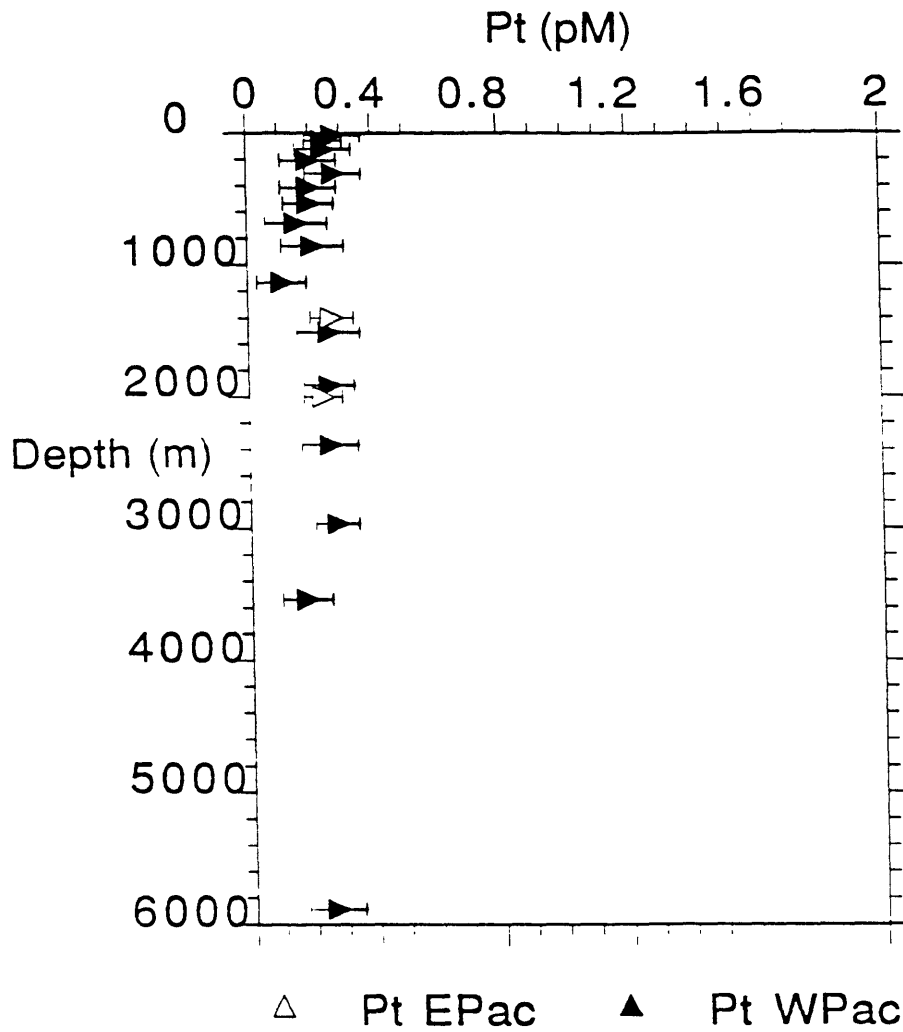


Figure 3.5 NW Pacific Pt profile (24°15'N, 164°51'E) with two samples from a NE Pacific station (42°08.62'N, 125°44.97'W). Two  $\sigma$  error bars.

*Hydrothermal samples*

The 100 mL samples collected for this work contain Pt below the limit of detection (Table 3.5). The detection limits were determined by the sensitivity of the ICP-MS on a given day, thus the values are reported as either <300 or <700 fM, depending on the day on which the sample was run. The one large volume sample that was analyzed has a Pt concentration of  $500 \pm 200$  fM, with the rather large error bar due partly to uncertainty in the isobaric interference from HfO on the Pt signal. This sample had a near-endmember hydrothermal fluid composition, as evidenced by its Mg concentration of 4.2 mM.

Dive#	Bottle#	Wt. samp. (g)	Mg (mM)	%seawater	Pt (fM)
2179T	1c&2c	704.8	4.08	7.6	500±200
2179T	1c	92.1	4.27	8.0	<700
2186T	4c	129.9	10.09	18.9	<300
2187T	2c	138.3	12.71	23.8	<700
2187T	3c	123.8	14.37	26.9	<300
2187T	6c	96.1	27.23	51.0	<300
2191T	1c	117.1	28.47	53.3	<700
2191T	6c	117.6	34.07	63.8	<300
2192M	1c	80.2	32.24	60.3	<300
2192M	6c	97.5	4.60	8.6	<700
ambient bottom water			53.44		300

T = TAG site, M = Mark site

*Calculation of uncertainties*

Uncertainties for each measurement were computed in two ways. 1) In the first case, a theoretical minimum error in the ratio measured was computed based on counting statistics and uncertainty in the blank. Count rates for these samples ranged from 500 - 2000 total counts, or 70 - 500 counts per second.

Error in the measured ratio was propagated through the isotope dilution equation by multiplying it by a "magnification factor" which was dependent on the value of the ratio for each sample (see section 2.10). The errors calculated ranged from 9 to 38 %, with a mean of 16%. 2) A second estimate of uncertainties was taken to be the pooled standard deviation ( $\pm 13\%$ ) of the four sets of replicate samples listed in Table 3.6. The uncertainty quoted in Tables 3.2-3.4 is the larger of the two for each sample.

	<u>Pt (fmol/L)</u>	<u>SD ,or difference from mean</u>
Azores 100m	280 320	20 (7%)
BDA surface	210 370	80 (27%)
Woods Hole water Run 1	240 280 280 270	20 (7%)
Woods Hole water Run 2	320 270 250 250	30 (11%)
Pooled standard deviation = 13%		

### 3.5 Discussion

#### *Potential causes of the discrepancies among methods*

It is highly unlikely that Pt exhibits the widely varying behaviors suggested by the three studies, and the differences are probably analytical. Jacinto and Van Den Berg (1989) measured Pt by cathodic stripping voltammetry, in which

a Pt-formazone complex is adsorbed on a hanging mercury drop electrode over five minutes, and then the electrode potential is scanned in the negative direction. The Pt-formazone complex catalyzes the production of hydrogen and the reduction current associated with this reaction is said to be linearly related to the combined Pt(II) and Pt (IV) concentration (Van Den Berg and Jacinto, 1988). This technique is subject to interferences from surface-active compounds, such as the organic matter present in seawater. Jacinto and Van Den Berg therefore irradiated their samples with ultraviolet light for 6-8 hours to destroy dissolved organic matter. Since it is known that this process does not oxidize all of the organic carbon in seawater (Sugimura and Suzuki, 1986), it is possible that enough remained in surface waters to produce a positive interference, giving the maximum in surface waters which is observed in their data, but not in profiles reported here. Their experiments, however, showed that organic material (Triton X-100) added to UV-irradiated seawater tended to decrease, rather than increase the Pt peak.

The preconcentration and purification methods used here are based on those developed by Goldberg et al., and so the two techniques are necessarily very similar; it is therefore surprising that they yield such different results. The principal differences between their method and that employed here are that Goldberg et al. used a radiotracer ( $^{191}\text{Pt}$ ,  $t_{1/2} = 3.0$  days) to monitor recoveries, and used graphite furnace atomic absorption spectrometry as the determinative step. In both methods equilibration between sample and spike must be assumed. If tracer recovery is more efficient than sample recovery, then both techniques underestimate the amount of Pt in seawater. For example, this would be the case if organic Pt complexes in seawater did not exchange with the tracer Pt, and were less efficiently retained by or eluted from the anion exchange resin than the tracer Pt. If sample recovery is more efficient than



tracer recovery, then the techniques overestimate the concentration, with upper limits imposed by the known tracer recoveries (80-100% for this technique and 50-90% for Goldberg et al.'s technique), and the fact that sample recoveries cannot be greater than 100%. This would be the case if Pt(II) was more efficiently preconcentrated than Pt(IV), since in both cases the sample is likely to be mostly divalent, whereas the tracer (prepared by dissolving Pt metal in aqua regia) is probably quadrivalent (Goldberg and Hepler, 1968). Tests of some of these possibilities were devised and are described below:

*a) Do Pt(II) and Pt(IV) behave differently on the anion exchange resin?*

PtCl<sub>4</sub> and PtCl<sub>2</sub> (Johnson-Matthey Aesar) were dissolved in 0.5N HCl and 6N HCl, respectively. PtCl<sub>4</sub> dissolves to form PtCl<sub>6</sub><sup>2-</sup> or PtCl<sub>4</sub>(OH)<sub>2</sub><sup>2-</sup>, whereas PtCl<sub>2</sub> forms PtCl<sub>4</sub><sup>2-</sup> along with some PtCl<sub>6</sub><sup>2-</sup> (Goldberg and Hepler, 1968). These were diluted to 2.92 nM Pt (IV) and 1.52 nM Pt (II (+IV?)) with 0.5N HCl and poured through a column. Recoveries were calculated by spiking the solutions after elution from the columns, and were found to be 90±5% in both cases. This confirms the results of Goldberg et al. (1986), who reported that Pt(II) and Pt(IV) were equally retained by the resin in preliminary experiments.

Additionally, since the tracer was likely to be Pt(IV) and the sample Pt(II), retention efficiency for both could be evaluated by measuring Pt in spiked seawater that had already passed through a column. Seawater was poured through two successive columns, and Pt eluted from the second column was found to be indistinguishable from blank levels. Therefore, within uncertainties in the blank and sample signals, Pt (II) and Pt(IV) appear to be equally retained by the resin (as in Table 3.7). In a final experiment, a spiked 2L seawater sample (TP:1915m) was bubbled with chlorine for 2 minutes in order to force all

the Pt to Pt(IV). The concentration measured was indistinguishable from other samples in the same profile.

Table 3.7. Recovery experiment. Two liters of spiked seawater were passed through two columns sequentially, and each was eluted with hot 12N HNO<sub>3</sub>. Samples were evaporated to a drop and taken up in 250 µL to be run:

Sample eluted from...	<u>Counts per second</u>	
	first column	634(±4%)
second column	14(±14%)	35(±8%)
blank	13(±14%)	30(±9%)
retention by first column	<u>99-100%</u>	<u>97-100%</u>

*b) Is there an organically-complexed fraction of the Pt in seawater that is not exchanging with the tracer?*

In order to address this question, seawater was UV-irradiated in a number of batches, as summarized in Table 3.8. In the first case, 8L unacidified Woods Hole seawater was divided into four 2L samples, and two of these were UV-irradiated in quartz tubes overnight for approximately 12 hours. The other two were allowed to sit in the quartz tubes overnight without irradiation. The UV-irradiated samples gave lower Pt concentrations, presumably because of enhanced adsorption of Pt onto the quartz tubes under conditions in the UV reactor. Van Den Berg and Jacinto (1988) also noted loss of Pt from unacidified samples during UV-oxidation. Thus, subsequent experiments were run with acidified samples. In the second set of experiments, acidified Pacific deep water samples that sat in quartz tubes overnight were found to have higher Pt concentrations than samples that did not sit in quartz tubes, whether or not the quartz tubes were UV-oxidized. Thus although the tubes had been leached

Table 3.8 Summary of Pt - UV experiments

<u>Experiment 1:</u>			Pt meas. (pM)
E1-1	WHSW, uac	UV-oxidize in quartz tubes overnight	0.44
E1-2	WHSW, uac	UV-oxidize in quartz tubes overnight	0.25
E1-3	WHSW, uac	let sit in quartz tubes overnight (no UV)	0.54
E1-4	WHSW, uac	let sit in quartz tubes overnight (no UV)	0.56
<u>Experiment 2:</u>			
E2-1	PacDW, ac	UV-oxidize in quartz tubes overnight	0.80
E2-2	PacDW, ac	let sit in quartz tubes overnight (no UV)	0.62
E2-3	PacDW, ac	no quartz tubes, no UV	0.25
E2-4	PacDW, ac	no quartz tubes, no UV	0.28
<u>Experiment 3:</u>			
E3-1	AtlDW, ac ("Pt-free")	Seawater that's been through a column, let sit in quartz tubes overnight (no UV)	0.03
E3-2	AtlDW, ac ("Pt-free")	Seawater that's been through a column, do not pour into quartz tubes (no UV)	<0.01

WHSW = Woods Hole seawater

uac = unacidified

ac = acidified

PacDW = Pacific deep water (4000-5000 m)

AtlDW = Atlantic deep water (2500 and 3000 m)

with concentrated aqua regia for several days prior to contact with seawater, there appeared to be Pt that could be desorbed from the walls (remaining from previous seawater samples) or leached from the quartz itself by contact with acidified seawater. In order to confirm this, Pt-free seawater (ie., seawater that had been passed through a column) was allowed to sit in the quartz tubes without UV-oxidation overnight. The Pt concentration measured in this seawater was at least a factor of three greater than that in similar Pt-free seawater that had not been exposed to the quartz tubes.

To summarize, the effects of UV-oxidation on recovery of Pt from seawater, or on exchange with tracer Pt, were largely masked by the sorption and desorption of Pt from the quartz tubes. Nevertheless, there is no evidence that the large (factor of five) difference in Pt deep water concentrations between this study and that of Goldberg et al. can be explained by the existence of "nonexchangeable" organic-Pt. If such a species exists, it is not broken down by UV-irradiation under acidic conditions. With regard to Jacinto and Van Den Berg's work, they found that there were no adsorptive losses to quartz tubes if samples had been acidified to pH 2, but did not note whether acidification might have resulted in desorptive addition of Pt to solutions.

*c) Was sufficient equilibration time allowed?*

Spiked and acidified seawater samples sat for varying amounts of time before they were poured through the anion exchange resin. Given the tracer equilibration times allowed (24hrs - few months), at the pH conditions of the acidified samples (pH1), it is unlikely that equilibration would not take place. As expected, Pt concentrations measured do not correlate with tracer-equilibration times of greater than one day. Equilibration times of less than one day were not investigated. These results are summarized in Table 3.9.

Table 3.9 Seawater sample spike-equilibration times. Pt concentrations are not dependent on the amount of time the sample and spike were allowed to equilibrate before the anion exchange step.

Station	Depth (m)	Pt (pM)	Equilibration time (days)
BDA	0	0.29	32
	5	0.19	1
	50	0.14	1
	100	0.14	1
	150	0.19	1
	200	0.14	1
	201	0.27	32
	390	0.32	1
	605	0.30	1.6
	735	0.30	32
	740	0.22	1.6
	854	0.38	1.8
	990	0.28	2
	1465	0.20	2
	1959	0.24	2
	2464	0.39	2.8
	2958	0.36	2.8
	3452	0.35	2.8
	3947	0.29	2.8
	AZ	4	0.26
43		0.36	2
72		0.27	2
113		0.24	2
194		0.31	2
300		0.30	2
415		0.37	2
499		0.32	2
607		0.41	3
735		0.27	3
981		0.19	3
1478		0.38	2
1972		0.32	2
2466		0.32	2
2950		0.35	2
3444		0.11	2
3938		0.34	4

Table 3.9 continued

WPac	14	0.28	8
	60	0.25	93
	125	0.25	8
	208	0.20	193
	308	0.28	8
	416	0.20	193
	536	0.20	8
	686	0.16	193
	857	0.21	8
	1134	0.11	193
	1511	0.26	8
	1915	0.26	93
	2367	0.26	8
	2963	0.28	93
	3538	0.18	8
	5888	0.26	8

### *Thermodynamic considerations*

It is generally agreed that Pt(II) is the dominant oxidation state in seawater although using different literature values for  $E^{\circ}$  of the  $\text{PtCl}_4/\text{PtCl}_6$  redox couple, one can predict otherwise (Jacinto and van den Berg, 1989; Wood et al., 1989; Goldberg et al., 1986; Goldberg and Hepler, 1968 and Westland, 1981). Goldberg et al., 1986 and Jacinto and VanDen Berg, 1989 both assume that chloro- complexes control the solubility of Pt, and Goldberg et al. use this to argue for the relative stability of Pt in seawater and its long residence time. However, recent thermodynamic calculations and experimental work predict the predominance of Pt and Pd hydroxy-complexes in seawater (Wood, 1991 and references therein; and Tait et al., 1991). Wood conclude that  $\text{Pt}(\text{OH})_2^0$  governs the inorganic speciation of Pt in seawater. In a separate experimental study Wood (1990) reports that dissolved organic matter (as represented by phthalic and soil-derived fulvic acid) either stabilizes Pt colloids or complexes Pt in distilled water. Li and Byrne (1990) suggest that the high affinity of Pt for nitrogenous ligands may lead to significant formation of Pt-amino acid complexes, even at seawater amino acid concentrations and salinities. The kinetics of ligand substitution in aqueous Pt complexes are quite sluggish ( a factor of  $10^4$ - $10^6$  slower than for Pd complexes (Elding, 1978), and slower than those of other transition metals (Fe, Mn, Co, Ni, Cu, (Sutin, 1966)) by an even greater factor), so metastable complexes are likely to be important components of the speciation of Pt in seawater.

### *Water column Pt behavior*

If neutral hydroxide complexes dominate the seawater chemistry of Pt, one would expect Pt to be fairly particle-reactive, and to exhibit profiles with maxima dominated by external inputs, such as dust or sediments, much like other

particle-reactive, hydrolysis dominated, elements such as Al, Th, Fe and Mn (Bruland, 1983). This description would be consistent with the profiles reported by Jacinto and Van Den Berg if enough Pt could be delivered to ocean surface waters by atmospheric aerosols to produce the maximum they observed. A rough calculation reveals that this could only be the case if Pt were highly enriched in atmospheric dust compared to Al or Mn. This scenario is summarized in Table 3.10, using the Mn values for surface waters at these stations reported by Jacinto and Van Den Berg. If Pt is enriched in dust by a factor of 500 (ie.,  $(Pt/Mn)_{dust} / (Pt/Mn)_{crust} = 500$ ), and if Pt and Mn are equally dissolved on contact with seawater, then perhaps half of the observed surface enrichment may be accounted for. For comparison, reported enrichment factors for gold in aerosols range from 10 (Rahn, 1970) to 500 (Buat-Menard and Chesselet, 1979) and enrichments for other transition metals (Co, Ni and Cu) range from 2 to 7 (Buat-Menard and Chesselet, 1979). In the absence of information about Pt concentrations in atmospheric aerosols, it appears unlikely that dust input can explain the high surface concentrations, unless Pt is unusually enriched in these aerosols. The featureless Pt distributions observed in the present study indicate that Pt is less reactive than many of the hydroxide-dominated elements, and that chloro complexing may be more important than suggested by Wood, 1991.

There is some evidence that Pt is accumulated by organic matter under certain sedimentary conditions, as in the turbidite units from abyssal plains described in Chapter 4, and in peat, algal mats and some coal deposits (Dissanayake and Kritsotakis, 1984; and Van Der Flier-Keller, 1990). In contrast with the results of Goldberg et al., however, the profiles presented here suggest that Pt is not notably involved in the production and mineralization of organic matter within the water column.



Table 3.10 "Best guess" parameters used in terrestrial and cosmic dust flux calculations

		<u>Reference</u>
Mn in J&VdB surface waters	1.1 nM	1
(Pt) <sub>avg. crust</sub>	1 ppb	2,3,4,5,6
(Mn) <sub>avg. shale</sub>	500 ppm	7
(Pt/Mn) <sub>crust</sub>	1 x 10 <sup>-6</sup> mol/mol	
(Pt/Al) <sub>dust</sub> / (Pt/Al) <sub>crust</sub>	500 (upper limit?)	8
(Mn/Al) <sub>dust</sub> / (Mn/Al) <sub>crust</sub>	1	9
% dissolution of Pt from terrestrial dust	same as Mn	
Seawater Pt conc. resulting from above	500 fM (+background values ~ total of 800 fM)	
Surface water Pt conc. observed	1600 pM	
.....		
Chondritic Os flux	3.5 ng/cm <sup>2</sup> ·Myr	10
(Pt/Os) <sub>chond</sub>	1.36	11
Water column depth	5000 m	
Pt flux to sediments	100 pg/cm <sup>2</sup> ·ky	12
Pt residence time w.r.t. removal to sed.	100 ky	
% dissolution of Pt from cosmic dust	100% (extreme upper limit)	
Seawater Pt conc. resulting from above	0.005 pM	

1. Jacinto and Van den Berg 1989; 2. Govindaraju 1989; 3. Parthe and Crocket 1978; 4. Crocket 1981; 5. Goldberg et al. 1986; 6. Goldberg et al. 1988; 7. Wedepohl, 1978; 8. An upper limit guess based on enrichment factor for Au of 500 (Buat-Menard and Chesselet, 1979); 9. Buat-Menard and Chesselet, 1979; 10. (Esser and Turekian 1988); 11. (Anders and Ebihara 1982); 12. based on hydrogenous Pt = 2ppb in pelagic sediments, in situ dry density of sediment = 0.4 g dry/cm<sup>3</sup> wet, accumulation rate = 0.1 cm/ky

Within uncertainties in the data, it is impossible to say whether or not there is any interocean-basin fractionation of Pt. With a mean Atlantic concentration of  $280 \pm 10$  fM and a mean Pacific concentration of  $230 \pm 10$  fM, the Atlantic appears to be slightly enriched over the Pacific, however, potential biases in the data sets, as suggested by the lower values obtained for the first set of Bermuda samples, are not well constrained. In any case the difference is relatively small, consistent with the observed lack of variation in Pt concentrations with depth.

#### *Global budget considerations*

The lack of information about the global distribution of Pt is nearly absolute. Its low concentrations in surficial materials, coupled with the relatively poor sensitivity of neutron activation techniques for the element have resulted in a paucity of data that might allow informed consideration of an oceanic Pt budget. There appears to be no published data for Pt in fresh waters, except those draining mine tailings (Pogrebnyak et al., 1984). Two attempts to determine Pt concentrations in river and lake waters of the Transbaikal region, and near a PGE-Cu-Ni prospect in Quebec both found Pt to be less than their detection limits of 10 pM and 130 pM, respectively (Pogrebnyak and Tat'yankina, 1979; and Wood and Vlassopoulos, 1990). There are very few measurements of Pt in felsic rocks, so its crustal abundance is poorly known. There are no data for Pt in atmospheric aerosols of which I am aware. Very preliminary data for Pt concentrations in submarine hydrothermal solutions which are reported here (Table 3.5) give an order of magnitude estimate for this number, and McKibben et al. (1990) present data for Pt in Salton Sea hydrothermal fluids. The best known component of the marine geochemical cycle of Pt is probably its concentration in marine sediments, and based on this

number, Goldberg et al. (1986) calculated a residence time in seawater of around one million years.

Given these constraints, some preliminary attempts can be made to reassess the marine geochemical cycle of Pt. The ratio of Pt to other reactive elements in seawater, such as Al or Fe, is greater than that in the continental crust by a factor of  $10^4$ - $10^5$  suggesting that either Pt is preferentially mobile, that there is an extra source of Pt to seawater, and/or that Pt is more stable in seawater than either of these elements. Previous studies of Pt mobility have focused on areas around Pt-ore deposits and soils developed on Pt- enriched ultramafic rocks. They suggest that Pt is relatively immobile in weathering processes, as it is known to be enriched in laterites (although local mobility is indicated) (Bowles, 1986) and is commonly present in highly resistant minerals, notably chromite (either in solid solution or as inclusions) (Fuchs and Rose, 1974). Pt is also enriched in sulfide minerals, however, which degrade relatively rapidly, and may release Pt to weathering solutions. Additionally, Pt is probably present in the dispersed state in most crustal rocks, from which it might be mobilized, especially at high Eh, low pH conditions. The preliminary data presented here suggest that high temperature submarine fluids are not an important source (or sink) of Pt to seawater, although the effect of low temperature weathering of submarine basalts and peridotites is not yet known. The contribution of cosmic dust to the Pt content of seawater is negligible, and an extreme upper limit of 1.7% may be calculated based on the flux of chondritic Os to sediments (Table 3.10). The major sources of Pt to seawater are therefore probably eolian and riverine, although neither of these have been quantified as yet.

The most important sink for Pt is probably Mn-Fe oxyhydroxides, although it is possible that some Pt is removed from seawater in organic-rich

sediments as well (Chapter 4). Pt is known to be highly enriched in manganese nodules, with concentrations of 6-900 ppb and a mean of 245 ppb for 15 nodules (Goldberg et al., 1986), compared with an average pelagic sediment concentration of approximately 3 ppb. In turn, slowly accumulating, non biogenic pelagic sediments appear to be somewhat enriched compared to crustal values (although the latter are poorly known). This is most likely due to the inclusion of Pt precipitated from seawater in a hydrogenous Fe-Mn phase, as discussed in Chapter 4. Even given the lower water column Pt concentrations measured here and by Jacinto and Van Den Berg (that is, lower than those of Goldberg et al.), the calculated residence time for Pt in seawater with respect to removal in pelagic sediments is relatively long (on the order of 100 ky: hydrogenous Pt = 2ppb, *in situ* dry density of sediment = 0.4g dry/cm<sup>3</sup> wet, Pt concentration in seawater = 300 fM, sediment accumulation rate = 0.1cm/ky, water column = 4000m).

### 3.6 Conclusions

The platinum distributions observed in this study are very similar to those observed by Falkner and Edmond (1990b) for gold in seawater. A comparison of Pt and Au concentrations in various geologic materials is shown in Table 3.11. Pt concentrations in seawater are a factor of five higher than those of Au in spite of their similar crustal abundances, requiring either the greater stability of Pt in seawater, or the fractionation of the elements during weathering processes. As is the case for gold, it appears that Pt is not significantly cycled with biogenic matter in the water column, in contrast with previous work (Goldberg et al., 1986). The residence time for Pt calculated with respect to removal to sediments is approximately 100 ky, a factor of 100 greater than that calculated for Au (Falkner and Edmond, 1990b). This relatively long calculated

Table 3.11 Abundances of Pt and Au in some geologic materials

	<u>Pt (ppb)</u>	<u>Au (ppb)</u>
C1 chondrite	953 <sup>a</sup>	145 <sup>a</sup>
crustal rocks	1-5 <sup>b</sup>	0.5-5 <sup>c</sup>
pelagic sediments	3 <sup>d</sup>	1.5 <sup>e</sup>
anoxic sediments	1 <sup>d</sup>	2.4 <sup>f</sup>
manganese nodules	100 <sup>d</sup>	2 <sup>e</sup>
	<u>(fM)</u>	<u>(fM)</u>
seawater	300 <sup>g</sup>	50 <sup>h</sup>

a. Anders and Ebihara, 1982; b. Crocket, 1981 and references therein, and Parthe and Crocket, 1978; c. Crocket, 1974 and Crocket and Kuo, 1979; d. Goldberg et al., 1986; e. Crocket and Kuo, 1979 and Koide et al., 1986; f. Koide et al., 1986; g. This work; h. Falkner and Edmond, 1990b

residence time and the featureless Pt profiles suggest that Pt is relatively unreactive in seawater.

The Pt levels measured here agree with the deep water Pt values of Jacinto and van den Berg (1989), although their data suggest a strong surface water enrichment which is not observed in the profiles reported here. It is unlikely that eolian inputs could have produced this enrichment, although they may provide a significant source of Pt to seawater. The absence of data for Pt in rivers, estuaries and aerosols makes it impossible to evaluate the relative importance of these sources to seawater, and further work will be necessary to address these issues.

### 3.7 Acknowledgements

This study benefitted from the sample collection efforts of many people: May'90 Bermuda samples were collected by I. Ellis and E. Boyle. Western Pacific samples were collected by C. Measures in May, 1985. Eastern Pacific

samples were collected by K. Falkner in September, 1989. Hydrothermal samples were collected by J. Edmond, A. Campbell and C. German, in January 1990. Ancillary data was provided by I. Ellis, E. Boyle, C. Measures and A. Campbell.

### References for Chapter 3

Anders, E. and M. Ebihara. (1982). "Solar system abundances of the elements." Geochim. Cosmochim. Acta. **46**: 2363-2380.

Bowles, J. F. (1986). "The development of platinum-group minerals in laterites." Econ. Geol. **81**: 1278-1285.

Boyle, E. A., S. D. Chapnick, G. T. Shen and M. P. Bacon. (1986). "Temporal variability of lead in the western North Atlantic." J. Geophys. Res. **91**(c7): 8573-8593.

Bruland, K. W. (1983). Trace Elements in Sea-water. Chemical Oceanography. New York, Academic Press.

Buat-Menard, P. and R. Chesselet. (1979). "Variable influence of the atmospheric flux on the trace metal chemistry of oceanic suspended matter." Earth and Plan. Sci. Lett. **42**: 399-411.

Crocket, J.H. (1974). Gold; in the Handbook of Geochemistry II-5, K.H. Wedepohl, ed., Springer-Verlag, N.Y. pp79(B-O).

Crocket, J.H. (1981). Geochemistry of the platinum group elements. Platinum Group Elements. Mineralogy, Geology and Recovery. Canadian Institute of Mining and Metallurgy.

Crocket, J.H. and H.Y. Kuo. (1979). "Sources for gold, palladium and iridium in deep-sea sediments." Geochim. Cosmochim. Acta **43**:831-842.

Dissanayake, C. B. and K. Kritsotakis. (1984). "The geochemistry of Au and Pt in peat and algal mats - a case study from Sri Lanka." Chem. Geol. **42**: 61-76.

Elding, L. I. (1978). "Stabilities of platinum (II) chloro and bromo complexes and kinetics for anation fo the tetraaquaplatinum (II) ion by halides and thiocyanate." Inorg. Chim. Acta. **28**: 255-262.

Esser, B.K. and K.K. Turekian (1988). "Accretion rate of extraterrestrial particles determined from osmium isotope systematics of Pacific pelagic clay and manganese nodules." Geochim. Cosmochim. Acta. **52**: 1383-1388.

Falkner, K. K. and J. M. Edmond. (1990a). "Determination of gold at femtomolar levels in natural waters by flow injection inductively coupled plasma quadrupole mass spectrometry." Anal. Chem. **62**: 1477-1481.

Falkner, K. K. and J. M. Edmond. (1990b). "Gold in seawater." Earth and Plan. Sci. Lett. **98**: 208-221.

Fuchs, W. A. and A. W. Rose. (1974). "The geochemical behavior of platinum and palladium in the weathering cycle in the Stillwater Complex, Montana." Econ. Geol. **69**: 332-346.

Goldberg, E.D., M. Koide, J.S. Yang and K.K. Bertine. (1988) Comparative marine chemistries of platinum group metals and their periodic table neighbors. Metal Speciation, theory, analysis and application. Chelsea, MI, Lewis Publishers, Inc.

Goldberg, E. D., V. Hodge, P. Kay, M. Stallard and M. Koide. (1986). "Some comparative marine chemistries of platinum and iridium." Appl. Geochem. **1**: 227-232.

Goldberg, R. N. and L. G. Hepler. (1968). "Thermochemistry and oxidation potentials of the platinum group metals and their compounds." Chem. Rev. **68**: 229-252.

Govindaraju, K. (1989) Geostand. Newslt. **XIII** (Special Issue): 1-113

Jacinto, G. S. and C. M. G. van den Berg. (1989). "Different behavior of platinum in the Indian and Pacific Oceans." Nature. **338**: 332-334.

Koide, M., V.F. Hodge, J.S. Yang, M. Stallard and E.D. Goldberg. (1986). "Some comparative marine chemistries of rhenium, gold, silver and molybdenum." Appl. Geochem. **1**:705-714.

Li, J.-H. and R. H. Byrne. (1990). "Amino acid complexation of palladium in seawater." Environ. Sci. Tech. **24**: 1038-1041.

McKibben, M. A., A. E. Williams and G. E. M. Hall. (1990). "Solubility and transport of platinum group elements and Au in saline hydrothermal fluids: constraints from geothermal brine data." Econ. Geol. **85**: 1926-1934.

Mountain, B. W. and S. A. Wood. (1988). "Chemical controls on the solubility, transport and deposition of platinum and palladium in hydrothermal solutions: a thermodynamic approach." Econ. Geol. **83**: 492-510.

Orians, K. J., E. A. Boyle and K. W. Bruland. (1990). "Dissolved titanium in the open ocean." Nature. **348**: 322-324.

Orians, K. J. and K. W. Bruland. (1988). "The marine geochemistry of dissolved gallium: a comparison with dissolved aluminum." Geochim. Cosmochim. Acta. **52**: 2955-2962.

Parthe, E. and J.H. Crocket. (1978). Platinum Group. Handbook of Geochemistry. New York, Springer Verlag.



- Pogrebnyak, Y. F., L. A. Kondratenko and E. M. Tat'yankina. (1984). "Forms of platinum and palladium migration in water of dispersion trains." Dokl. Akad. Nauk. SSSR. **279**(2): 203-205.
- Pogrebnyak, Y. F. and E. M. Tat'yankina. (1979). "Palladium content of natural land water, as illustrated by data on Transbaikal." Dokl. Akad. Nauk. SSSR. **247**: 211-213.
- Rahn, K.A., R.D. Borys, G.E. Shaw, L. Shutz and R. Jaenicke. (1970). "Long range impact of desert aerosol on atmospheric chemistry: Two examples." in Saharan Dust, C. Morales, ed., John Wiley and Sons, N.Y. p. 243-266.
- Sugimura, Y. and Y. Suzuki. (1988). "A high temperature catalytic oxidation method of non-volatile dissolved organic carbon in seawater by direct injection of liquid sample." Mar. Chem. **24**:105-131.
- Sutin, N. (1966). Ann. Rev. Phys. Chem. **17**: 119-172.
- Tait, C. D., D. R. Janecky and P. S. Z. Rogers. (1991). "Speciation of aqueous palladium (II) chloride solutions using optical spectroscopies." Geochim. Cosmochim. Acta. **55**(5): 1253-1264.
- Van Den Berg, C. M. G. and G. S. Jacinto. (1988). "The determination of platinum in sea water by adsorptive cathodic stripping voltametry." Anal. Chim. Acta. **211**: 129-139.
- Van Der Flier-Keller, E. (1990). "Platinum group elements in Canadian coal." Energy Sources. **12**: 225-238.
- Von Damm, K. L., J. M. Edmond, B. Grant, C. I. Measures, B. Walden and R. F. Weiss. (1985). "Chemistry of submarine hydrothermal solutions at 21N, East Pacific Rise." Geochim. Cosmochim. Acta. **49**: 2197-2220.
- Westland, A. D. (1981). "Inorganic chemistry of the platinum-group elements." Can. Inst. Mining and Mineral. Spec. Vol., L. Cabri ed. **23**: 7-18.
- Wood, S.A. (1991). "Experimental determination of the hydrolysis constants of  $Pt^{2+}$  and  $Pd^{2+}$  at 25°C from the solubility of Pt and Pd in aqueous hydroxide solutions." Geochim. Cosmochim. Acta. **55**: 1759-1768.
- Wood, S. A. (1990). "The interaction of dissolved platinum with fulvic acid and simple organic acid analogues in aqueous solutions." Can. Mineral. **28**: 665-673.
- Wood, S. A., B. W. Mountain and B. J. Fenlon. (1989). "Thermodynamic constraints on the solubility of platinum and palladium in hydrothermal solutions: reassessment of hydroxide, bisulfide and ammonia complexing." Econ. Geol. **84**: 2020-2028.

Wood, S. A. and D. Vlassopoulos. (1990). "The dispersion of Pt, Pd and Au in surficial media about two PGE-Cu-Ni prospects in Quebec." Can. Miner. **28**: 649-663.

Zika, R. G., E. S. Saltzman and W. J. Cooper. (1985). Mar. Chem. **17**: 265-275.

## Chapter 4

### Post-depositional mobility of Pt, Ir and Re in abyssal marine sediments

---

#### 4.1 Abstract

Abyssal sediments in the North Atlantic are interrupted sporadically by relatively organic-rich turbidite units which originate on the continental margins. The contrasting redox character of the pelagic and the turbidite units, and the abrupt change in accumulation rate lead to redistribution of many trace elements, as previously documented in sediments of the Madeira, Cape Verde and Nares Abyssal Plains (Buckley and Cranston, 1988; Colley et al., 1984; Thomson et al., 1989, etc.). These sediments represent ideal natural laboratories in which to study the redox behavior of trace metals, due to the long times available for element partitioning along established Eh gradients.

The behavior of the platinum group elements during early diagenesis in marine sediments is relevant to their use as indicators of the flux of cosmic material to the Earth. The role of redox changes in producing platinum-group element spikes, such as those found at extinction boundaries, was therefore investigated. Rhenium (a neighbor of the Pt-group) has been suggested as a sensitive indicator of the oxygen content of past environments, and its radioactive isotope,  $^{187}\text{Re}$ , has been utilized as a geochronometer in ancient black shales through its production of  $^{187}\text{Os}$ . Its post-depositional mobility is pertinent to these studies, and was examined here as well. Platinum, iridium and rhenium were measured in four cores from the abyssal plains named above. Like other transition metals, these elements are mobilized as redox conditions readjust.

In the cores studied here, pelagic sections are initially oxic and have low organic carbon concentrations (<0.1%) compared to the turbidites which initially

contain higher organic carbon (0.7-1.5%). The pelagic sections were also found to have higher levels of Pt and Ir than the turbidites, partly due to the incorporation of these elements in hydrogenous phases which make up a greater proportion of pelagic sediments. Subsequent to the emplacement of a turbidite, hydrogenous iron and manganese oxyhydroxides in the underlying pelagic unit are reduced, accompanied by the partial loss of Pt and Ir from the reduced section. Re occurs in higher concentrations in turbidite sediments due to its accumulation in the relatively organic-rich shelf deposits from which the turbidites arise. As oxygen and other oxidants penetrate the turbidite unit, Re is released. A fraction (10-20%) of the Pt initially present in the turbidite is also mobilized by this process and becomes concentrated in a peak below the redox front.

The consequences of these observations are as follows: 1. A fraction of the Ir and Pt in sediments is mobile, and may be redistributed by changing redox conditions. Initial peaks in elemental concentrations are therefore subject to diffusive broadening, assuming the elements are present in a form which is mobile. Early diagenetic processes may also produce Pt peaks, although Ir peaks were not observed in these sediments. Re/Ir and Pt/Ir ratios in sediments may be altered by redox changes, and therefore may not be indicative of sediment sources. 2. Re is removed from organic-rich sediments on exposure to oxygen. Oxidic weathering of Re-enriched black shales is therefore likely to mobilize Re from the rock. In addition, potential changes in the Re concentration of seawater due to changes in the area of anoxic sedimentation should be reversible.

## **4.2 Introduction**

### *Background*

Interest in the geochemistry of the platinum group elements (PGE's), particularly in the element iridium, was stimulated by the discovery of its enrichment in sediments from the Cretaceous-Tertiary boundary, 65 million years ago. This led Alvarez et al. (1980) to propose that the mass extinction which occurred at that time was the result of the Earth's collision with a 10 km meteorite. Iridium and platinum are at least one thousand times more concentrated in chondritic meteorites than in average crustal materials (Table 4.1), and thus have been used as proxies for the flux of cosmic matter to the Earth (Barker and Anders, 1968). Since the discovery of the Cretaceous-Tertiary (K-T) boundary spike, Ir enrichments have been reported at several other biostratigraphic boundaries, including the Devonian-Carboniferous (360 my, Orth et al., 1988b), Permo-Triassic (245 my, Holser et al., 1989), the Cenomanian-Turonian (92 my, Orth et al., 1988a) and the Eocene-Oligocene (38 my, Asaro et al., 1982). These spikes are quite low compared to many examples of the K-T boundary spike (all less than 0.5 ppb), and are not significantly higher than typical non-biogenic marine sediment (~0.3 ppb Ir, Table 4.1). Recent studies have suggested that terrestrial geochemical processes were responsible for these smaller enrichments (Holser et al., 1989; Orth et al., 1988a; Orth et al., 1988b; Schmitz, 1985; Turekian, 1982). Proposed mechanisms include reduction and removal of Ir from seawater into anoxic sediments (Schmitz, 1985 and Holser et al., 1989) and scavenging of Ir by iron-oxides of bacterial origin (Orth et al., 1988b and Playford et al., 1984).

The distribution of Ir at the K-T transition itself has also been the subject of further scrutiny. Crocket et al. (1988) reported broad shoulders in the Ir profile at Gubbio, interrupted by several subsidiary Ir peaks within  $\pm 2\text{m}$  ( $\pm 600\text{ ky}$ ) of the K-T boundary. Various origins have been proposed for this distribution,

including a long period of enhanced, episodic volcanism (Crocket et al., 1988), or Ir diffusion away from the K-T boundary (Rocchia et al., 1990; Alvarez et al., 1990). Similar observations have been made at the site of the Acraman meteorite impact event in Australia (Late Proterozoic). Wallace et al. (1990) and Gostin et al. (1989) report that Ir and Pt are enriched not only in the ejecta horizon, but also in the green shales which flank it. Thin green beds which occur in the predominantly red shales surrounding the impact layer are all relatively enriched in Ir and Pt, regardless of their stratigraphic position. These results strongly suggest that low-temperature diagenetic processes play a significant role in the formation and/or alteration of PGE spikes, although the mechanisms and timing of elemental redistribution remain to be elucidated.

Interest in the sediment geochemistry of Re arises from different perspectives: Ravizza and Turekian (1989) pioneered the use of the  $^{187}\text{Re}$ - $^{187}\text{Os}$  geochronometer for dating ancient black shales and Koide et al. (1986) suggested the utility of Re concentrations in studies of the oxygen content of past environments. Both of these applications take advantage of the strong enrichment of Re in anoxic sediments. Reducing sediments accumulate Re from seawater at the time of deposition, and the more abundant of the two isotopes,  $^{187}\text{Re}$ , decays to  $^{187}\text{Os}$  with a half-life of 46 billion years. Assuming that the sediments remain a closed system with respect to Re and Os, ages may be determined using the whole-rock isochron method. Ravizza and Turekian (1989) successfully applied this technique to black shales deposited approximately 300 million years ago, although they noted some scatter in the data that might be ascribed to post-depositional mobility.

The development of Re enrichments in anoxic sediments requires that Re be mobilized from crustal rocks in which it occurs in low concentrations (~0.3 ppb), and transferred to an anoxic depositional environment. As Re is immobile

under reducing conditions, its mobilization is dependent on the existence of an oxidative weathering environment. Koide et al. (1986) suggested that concentrations of Re in excess of 0.1 ppb (their estimate of Re concentrations in oxic pelagic sediments) in Archean strata could be used to indicate the presence of an oxygenated atmosphere. The Re concentration of more recent sediments (in combination with other elements) might also yield information about the oxygen content of their depositional environment, as discussed further in Chapter 6. Interpretation of Re concentrations in the sedimentary record will require a better understanding of the extent to which it is remobilized by oxidation, both in ancient sediments exposed on the continents, and in recent marine sediments due to changing redox conditions.

#### *General geochemistry of the elements*

Ir and Pt are members of the platinum group elements, which includes the second row transition metals, Ru, Rh and Pd and the third row metal, Os, in addition to Ir and Pt (all members of Group VIII B). These elements are grouped due to their siderophilic and chalcophilic tendencies which lead to their coherence in many geologic environments. They are also known as the noble metals, due to their resistance to oxidation, although none is as resistant as gold in this regard. The nobility of Pt approaches that of Au most closely (Westland, 1981). Re is a neighbor of the platinum group in the periodic table and also exhibits siderophilic and chalcophilic preferences. During differentiation of the Earth, Re, Ir and Pt were presumably partitioned strongly into the metallic core, leading to their depletion in crustal materials relative to a chondritic bulk earth composition. Determinations of the elements in sulfur-poor silicate rocks are sparse, so that their distribution in crustal materials is poorly

known. Rough estimates of their average concentrations in ultramafic, mafic and felsic rock types are presented in Table 4.1.

Table 4.1 Abundances of Re, Ir and Pt in chondrites, crustal materials and the marine environment, compared to Mo and U.

	Re (ppb)	Ir (ppb)	Pt (ppb)	Mo (ppm)	U (ppm)
Chondrites	36.9 <sup>a</sup>	473 <sup>a</sup>	953 <sup>a</sup>	920 <sup>a</sup>	8.1 <sup>a</sup>
Ultramafic rocks	0.3 <sup>b</sup>	5 <sup>c</sup>	15 <sup>c</sup>	0.1 <sup>m</sup>	0.05 <sup>k</sup>
Mafic rocks	1 <sup>b</sup>	0.1 <sup>c</sup>	5 <sup>c</sup>	0.9 <sup>m</sup>	0.5 <sup>k</sup>
Intermediate-sialic rocks	0.3 <sup>d</sup>	0.01 <sup>c</sup>	1 <sup>ck</sup>	4 <sup>m</sup>	2.5 <sup>l</sup>
Pelagic sediment (carbonate poor)	0.05 <sup>ef</sup>	0.3 <sup>ghi</sup>	3 <sup>fg</sup>	8 <sup>m</sup>	3 <sup>m</sup>
Anoxic sediments	50 <sup>j</sup>	0.08 <sup>fg</sup>	1 <sup>fg</sup>	50 <sup>n</sup>	25 <sup>n</sup>
Manganese nodules	<0.1 <sup>e</sup>	1.1 <sup>g</sup>	100 <sup>g</sup>	400 <sup>k</sup>	9 <sup>q</sup>
Seawater	45 pM <sup>f</sup>	5 fM <sup>g</sup>	300 fM <sup>f</sup>	105 nM <sup>o</sup>	14 nM <sup>p</sup>

a. Anders and Ebihara, 1982, b. Martin, 1990, c. Crocket, 1981 and references therein, d. Esser, 1991, e. Koide et al., 1986, f. This work, g. Goldberg et al., 1986, h. Barker and Anders, 1968, i. Crocket and Kuo, 1979, j. Ravizza, 1991, k. Wedepohl, 1978, l. Taylor et al., 1983, m. Bertine and Turekian, 1973, n. Emerson and Husted, 1991, o. Collier, 1985, p. Ku et al., 1977, q. Ku and Broecker, 1969.

In the marine environment, oxidized forms of the elements dominate their geochemistry and their behavior as a group is much less apparent. For example, Hodge et al. (1985) found that Pt is highly enriched in manganese nodules relative to Pd, and suggested that this was due to the stability of both the divalent and tetravalent states for Pt, whereas only the divalent state of Pd is stable in natural waters. The concentrations of Re, Ir and Pt in marine sediments and seawater are summarized in Table 4.1 and figure 4.1. Pt and Ir are enriched in pelagic sediments relative to their crustal values, due to their accommodation (adsorption/coprecipitation?) in authigenic ferromanganese oxy-hydroxides, and to a lesser extent, due to contributions from cosmic dust



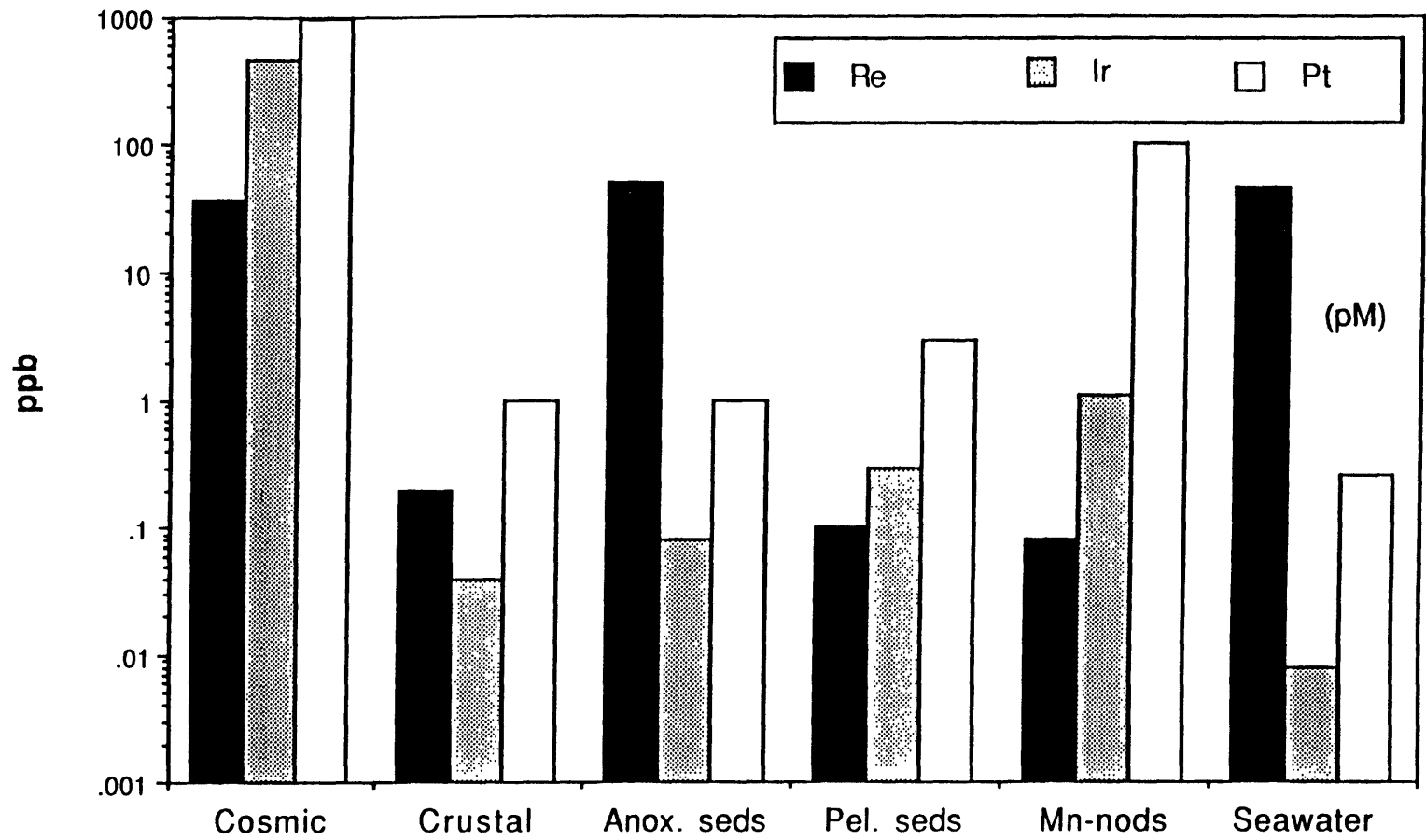


Figure 4.1 Estimates of average values of Re, Ir and Pt in meteorites, continental crust, marine sediments and seawater.

(Goldberg et al., 1986; Kyte and Wasson, 1986; and Barker and Anders, 1968). Their concentrations are also elevated in manganese nodules compared to sediment values, with a Pt/Ir ratio similar to that of seawater. Thus, if there is a single, most important phase in marine sediments which controls the distribution of Ir and Pt, Fe-Mn oxy-hydroxides are a likely candidate for this role.

Re occurs in high concentrations in seawater compared to both Pt and Ir due to the relative stability of its dissolved form,  $\text{ReO}_4^-$  under the oxidizing conditions of most of the oceans. It is removed from seawater into reducing sediments, leading to its enrichment in anoxic vs. oxic sediments by a factor of approximately 500. The mechanism for Re removal from seawater may either involve its reduction to Re(IV) which does not form soluble complexes, or precipitation as the sulfide,  $\text{Re}_2\text{S}_7$ , without reduction. The marine geochemistry of Re bears strong resemblance to that of Mo and U, which are also relatively stable in seawater (as  $\text{MoO}_4^{2-}$  and  $\text{UO}_2(\text{CO}_3)_3^{4-}$ ), and are removed primarily by diffusion into anoxic sediments. Re abundances in some common geological materials are compared to those of Mo and U in Table 4.1. Given current estimates of the crustal abundance of Re (which may be revised as more data becomes available), the Re/Mo ratio in seawater is enriched over the Re/Mo ratio in crustal materials by a factor of ten, requiring the higher stability of Re in seawater or preferential mobility of Re during weathering processes. Unlike Mo, Re does not appear to be scavenged by ferromanganese oxides, as Re is not enriched in manganese nodules, and its concentrations in pelagic sediments are less than or equal to crustal abundances (Koide et al., 1986) (also see Chapter 6).

*Post-depositional mobility of Re, Ir and Pt?*

The redistribution of many transition metals in marine sediments in response to changing redox conditions is well documented in numerous studies (see Shaw et al., 1990 for a review). As biogenic material decomposes in the sediments, it consumes a well established series of oxidants (Froelich et al., 1979). After oxygen is depleted,  $\text{NO}_3^-$ ,  $\text{MnO}_2$ ,  $\text{Fe}_2\text{O}_3$  or  $\text{FeOOH}$ , and finally  $\text{SO}_4^{2-}$  will be utilized. Trace metals experience changes in their partitioning between pore waters and solid phases as a result of these redox transitions. Some elements, such as Co and Ni (type 1), respond primarily to the manganese cycle in the upper sediment column, and thus will be largely lost from the manganese-reducing zone and fixed under more oxic conditions in the zone of  $\text{MnO}_2$  precipitation. Other elements, such as Cr, V, Mo and U, (type 2) possess stable soluble forms under oxic conditions and are scavenged or precipitated under more reducing conditions.

This description of transition metal behavior is a gross oversimplification, as most metals display aspects of both types of behavior. For example, Mo and Cu are both taken up by manganese oxides in the oxic zone, and precipitated or scavenged in the reducing zone (by reduction to a less soluble form and/or by sulfide formation). Re appears to behave exclusively like the second group of elements described above, as it is removed to sediments under anoxic conditions, and shows no obvious affinity for Mn-oxides. The strong enrichment of Ir and Pt in manganese nodules suggests that these elements may be more akin to element-type 1 described above, and should be involved in the manganese cycle in marine sediments.

The sediments of the abyssal plains of the North Atlantic are ideal natural laboratories in which to study the redox behavior of trace elements in sediments. Pelagic sediments which accumulate at rates between 0.2 and 1 cm/ky are interspersed with turbidite units which arise on the continental

shelves. The turbidite units generally contain higher levels of organic carbon, and their emplacement in the lower sedimentation rate areas leads to a sequence of redox reactions in both the turbidite and the underlying sediment. The positions of redox boundaries in the sediments change relatively slowly, allowing trace element migration to preferred levels in the  $E_h$  gradient, or to host mineral phases. Wilson et al. (1985), Jarvis and Higgs (1987), Buckley and Cranston (1988), Colley et al. (1984), and others have extensively documented the behavior of many transition elements under these conditions. Insight into the redox behavior of Pt and Ir may be gained by comparison to other, better understood elements in these sediments.

#### **4.3 Core locations and descriptions**

The cores analyzed in this study come from the Madeira Abyssal Plain (core 11334), the Nares Abyssal Plain (core 52-2), and west of the Cape Verde Abyssal Plain, in a deep basin within the foothills of the Mid-Atlantic Ridge (cores 11805 and 10400). Core locations are summarized in Table 4.2 and shown in figures 4.2 and 4.3. The turbidites studied here are extremely distal, and thus size and density grading is minor to negligible (Jarvis and Higgs, 1987). Since the PGE's may be concentrated in the heavy mineral fraction of crustal detritus, the concentration of heavy minerals at the base of some turbidites might lead to primary variation in PGE concentrations which are not related to diagenetic processes. The Zr content of the turbidites was taken to be representative of the distribution of the heavy mineral fraction (specifically the mineral zircon) and was compared to the Re, Ir and Pt data to check for any covariation. All data other than that for Re, Ir and Pt were provided by the

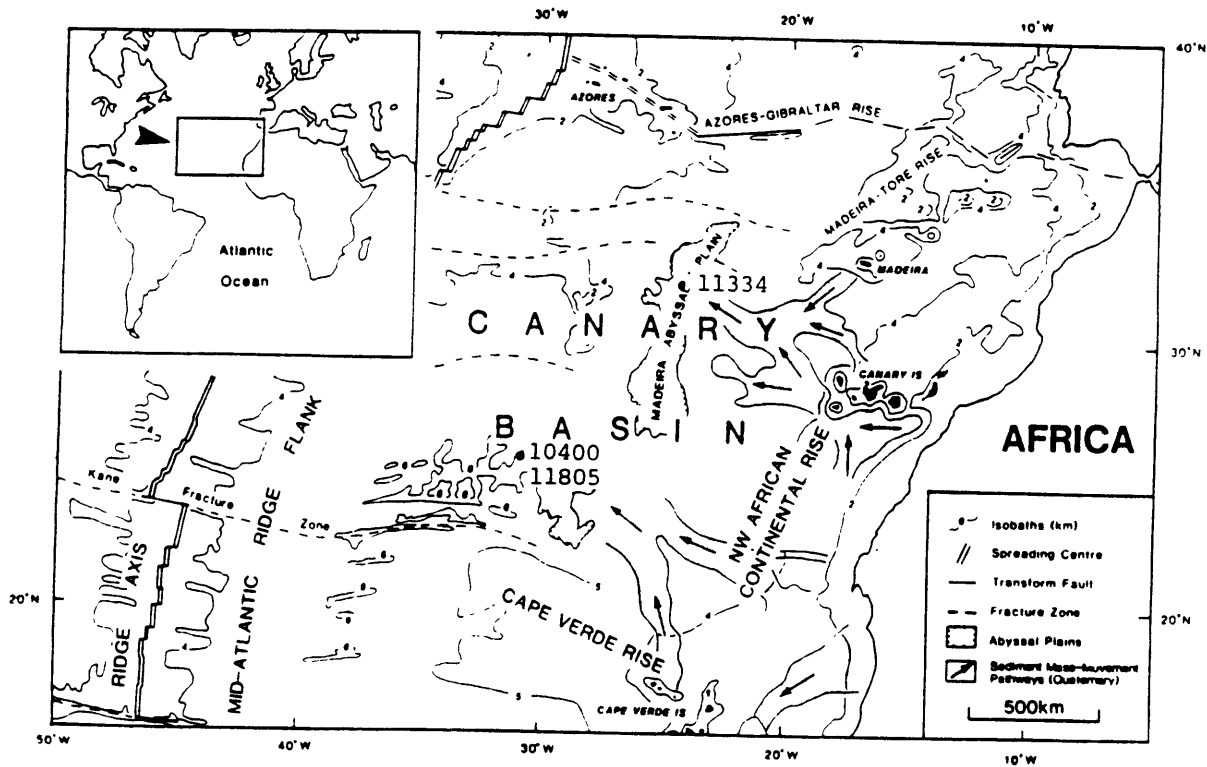


Figure 4.2 Map of the eastern North Atlantic showing the locations of the Madeira and Cape Verde Abyssal Plains, and core sites 11334, 10400 and 11805. Arrows indicate dominant sediment mass-movement pathways during the Quaternary (from Jarvis and Higgs 1987).

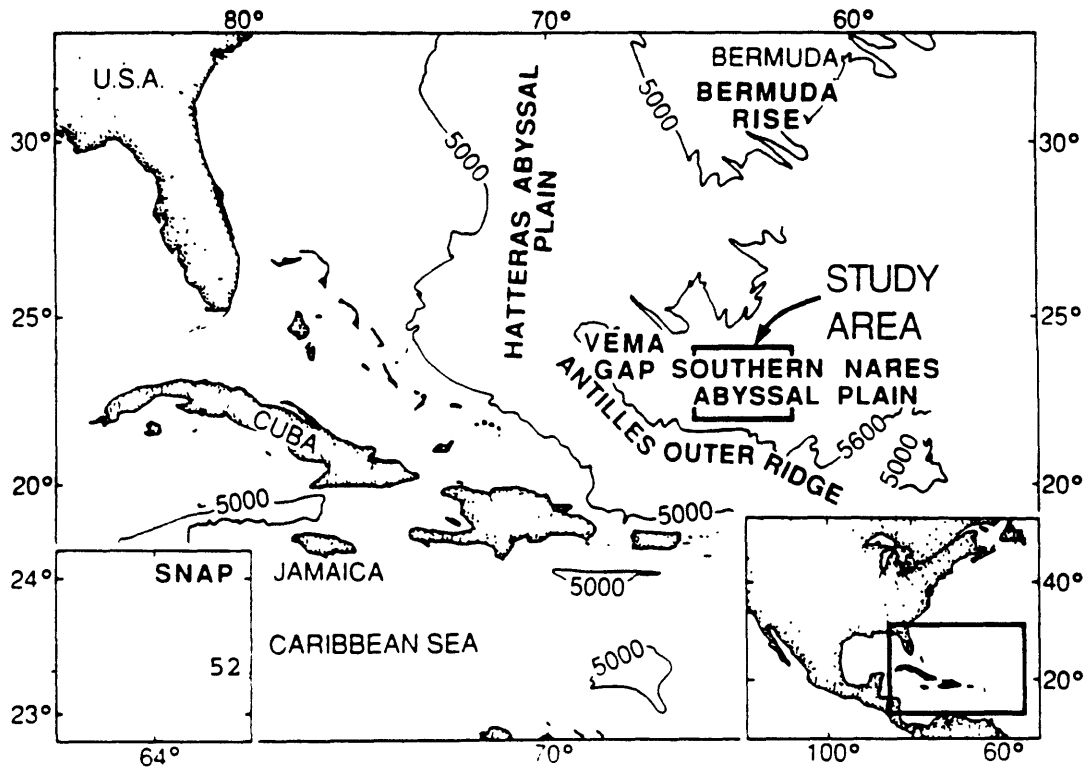


Figure 4.3 Southern Nares Abyssal Plain with location of core 52 shown in inset (from Buckley and Cranston 1988).

geochemistry group at IOS, Surrey, U.K. The data for cores 52-2 and 10400 are published in Thomson et al. (1989) and Colley et al. (1984), respectively.

Two types of diagenetic changes are encompassed by these samples. In the first, a relatively organic-rich turbidite from the continental shelf is deposited in an area of low sediment accumulation rate. Seawater oxygen (and nitrate) diffuse into the turbidite, and are consumed by the oxidation of labile organic matter. The depth to which oxygen penetrates gradually increases as organic carbon above the oxidation front is "burned away". The boundary between the

Table 4.2 Core locations and general information

Core No.	Latitude (°N)	Longitude (°W)	Water depth (m)	Core length (m)	Sampled depths (cm)	Region
11334 #4B	31°30.8'	24°25.2'	5375	0.6	25-57	Madeira A.P.
11805 #1K	25°39'	30°57'	6050	2	105-151	M.A.R. foothills
10400 #8K	25°42.4'	30°57.7'	6044	2	16-115	M.A.R. foothills
52-2	23°22.3'	63°00.7'	5878	17.4	1580-1609	Nares A.P.

upper oxidized and lower unoxidized portions is generally marked by a color change from more brown-grey to more green-grey sediments. The second process investigated was the alteration of pelagic sediment due to burial by a turbidite unit. Colley et al. (1984) and Thomson et al. (1989) have shown that reduction of Mn oxides in pelagic sediments directly underlying the turbidite leads to a bleached section referred to as the "halo" region. They suggest that in this region, Mn(IV) and Fe (III) were reduced by labile organic matter which

was present at the former sediment-water interface. Fe(II) subsequently reacted with MnO<sub>2</sub> and became fixed in the sediment as Fe(III), releasing additional Mn(II) to solution. It is also possible that dissolved organic carbon from the overlying turbidite diffuses down into the pelagic sediment (Heggie et al., 1987), but this is not necessary to produce the observed Mn and Fe redistribution, if the organic carbon levels at the buried pelagic surface were similar to those in this area today (Thomson et al., 1991).

### *Cores 11334 and 11805*

The two types of post-depositional alteration have been referred to as "oxidative burn-down" and "reductive bleaching"/"halo" formation. Cores 11334 and 11805 were studied as examples of the former type. The turbidite sediments are believed to originate on the North West African Shelf, and to follow turbidity current channel systems established by major late Quaternary submarine slides (Jarvis and Higgs, 1987). Core 11334 is a 60 cm box core which consists of a surficial turbidite (turbidite a in the terminology of Jarvis and Higgs, 1987), overlying 5 cm of pelagic sediment which in turn overlies a second turbidite (a<sub>1</sub>). The samples for this study all come from the lower turbidite (a<sub>1</sub>), which extends from 25 cm below the core top to the base of the core. The pelagic sedimentation rate in this area is estimated to be 0.5 cm/ky from <sup>230</sup>Th data (Wilson et al., 1985), although the overall sedimentation rate is closer to 10 cm/ky. The surficial turbidite is thought to be quite recent since there is no visible veneer of pelagic sediment, and surficial bioturbation is minimal (Jarvis and Higgs, 1987). The time of emplacement of turbidite a<sub>1</sub> may therefore be estimated from the overlying thickness of pelagic sediment as approximately 10 ky. The organic carbon content of the lower, unoxidized portion of the turbidite (below 44cm) is 1.5%, and is depleted to 0.3% in the



upper oxidized portion. Pore water data for a nearby core indicate that sulfate reduction is not active in the lower turbidite (Wilson et al., 1985). The  $\text{CaCO}_3$  content of the turbidite varies from 18% to 34%, having been partially dissolved in the oxidized section. The turbidite has a relatively uniform major element composition when recalculated on a carbonate-free basis (CFB):  $\text{SiO}_2 = 49 \pm 1 \text{ wt.}\%$ ,  $\text{Al}_2\text{O}_3 = 22.4 \pm 0.6 \text{ wt.}\%$  (for 12 contiguous samples, IOS, unpublished data). Zr data does not exist for this particular core, but a nearby sampling of turbidite a<sub>1</sub> reveals invariant Zr concentrations (Jarvis and Higgs, 1987). The turbidite unit is distinguished from pelagic sediment by its lower  $\text{CaCO}_3$  content (and lack of foraminifera), higher  $\text{SiO}_2$  and  $\text{Al}_2\text{O}_3$  contents, and lower  $^{230}\text{Th}$ .

Core 11805 is another calcareous, organic-rich turbidite from an area south of core site 11334 (figure 4.2). The turbidite sampled is at least 11 m thick and is overlain by 52 cm of pelagic brown clay. Nearby pore water data indicates that  $\text{O}_2$  is present in the pore waters 70 cm into the turbidite (120 cm from the core top), and that  $\text{SO}_4$  reduction is negligible above 200 cm (Thomson et al., 1991).  $\text{CaCO}_3$  has again been partly dissolved in the oxic section. The pelagic sedimentation rate is approximately 0.16 cm/ky in this area ( $^{230}\text{Th}$  data), and the turbidite is believed to have been emplaced 330 ky ago. Organic carbon increases from 0.3% in the oxidized part of the turbidite to 0.7% in the lower, unoxidized portion through a transition zone from 113 - 120 cm. Zr concentrations in a nearby core show little variation and no trend:  $\text{Zr} = 103 \pm 4 \text{ ppm}$  (7 non-contiguous samples within the top 100 cm of the turbidite). The oxidation front has been active in this turbidite longer than any other turbidite studied (Thomson et al., 1991).

*Cores 10400 and 52-2*

Examples of the other type of diagenetic process, "reductive bleaching", are contained in cores 10400 and 52-2. Core 10400 consists of brown pelagic clay interrupted by a thin greenish turbidite emplaced 170 ky ago at 47-55 cm. The turbidite is underlain by a reddish reduced halo from 55-71 cm. The lower contact of the green band is sharp, whereas its top is mottled as the result of bioturbation. Interpretation of the green band as a turbidite unit is supported by its lower  $^{230}\text{Th}$  content, and higher  $\text{SiO}_2$ ,  $\text{CaCO}_3$  and Zr than the surrounding pelagites (Colley et al., 1984).  $\text{CaCO}_3$  gets up to 5% in the turbidite unit, and is <0.5% in the underlying pelagic section. Except for a difference in Mn, Fe and other transition metal concentrations, the red band is compositionally indistinguishable from the brown clay below it.  $^{230}\text{Th}$  within the red band falls on the same decreasing trend with depth as in the rest of the pelagic section, and contents of  $\text{SiO}_2$ ,  $\text{Al}_2\text{O}_3$ , CaO, Zr, Rb, and  $\text{TiO}_2$  are very similar (Colley et al., 1984).

Similarly, core 52-2 contains a turbidite unit which extends from 1585-1595 cm, with an age of 1.5-2 my (Thomson et al., 1989). The base of the turbidite unit has higher  $\text{SiO}_2$  and lower  $\text{Al}_2\text{O}_3$  than the upper turbidite due to primary grading. This is seen in the uppermost samples from the halo section (1595-1604 cm), which otherwise have  $\text{SiO}_2$  and  $\text{Al}_2\text{O}_3$  contents identical to pelagic sediments. CaO is negligible in all of these samples (<0.5%) (Thomson et al., 1989).

#### **4.4 Methods**

Analytical procedures are described in Chapter 2. In 3 out of 4 cores, uncertainties in the data were estimated from a number of samples run in duplicate or triplicate. Duplicates were not run for core 52-2, and uncertainties were estimated based on other cores.

## 4.5 Results

Results for cores 11334 and 11805 are presented in Tables 4.3 and 4.5, with ancillary data included in Tables 4.4 and 4.6. (Note that data for these two cores are listed on a whole sediment basis in the tables, but plotted on a carbonate free basis.) In both cores, Pt forms a peak just below the oxidation front, in the region where organic carbon is still high, but is beginning to decrease (figures 4.4 and 4.5). In neither case does Pt follow Mn; in both cores MnO is enriched in the oxic compared to the post-oxic (anoxic and nonsulfidic) section of the turbidite, and in core 11805 MnO forms a peak just above the redox front. The Pt distributions more closely resemble those of Cu or V, which are thought to be released to pore waters by oxidation and continually reconcentrated just below the redox boundary as it moves through the sediment (Thomson et al., 1991). The peaks in Cu, and V are similar to those seen in uranium roll-front deposits, which are formed in porous sandstones by the flow of metal-carrying oxic groundwaters through a redox boundary which gradually migrates down-stream with the flow (Maynard, 1983). The enrichments seen in U-roll front deposits are much greater, however, and the transport in the turbidite units is diffusive rather than advective. In both cores 11334 and 11805, the Pt peak occurs above the peak in Cu, and below that of I, so that the sequence of peaks from higher to lower  $E_h$  is I, Pt, Cu, V (figures 4.6 and 4.7). In contrast with Cu and V,  $I^-$  diffuses out of the unoxidized portion of the sediment, and the origin of its peak is somewhat more complicated. On crossing the boundary, some of the  $I^-$  is thought to be oxidized to  $I_2$  which may be hydrolysed and removed by reactive organic matter (Kennedy and Elderfield, 1987). The other part is oxidized to  $IO_3^-$  which is free to diffuse in the oxic portion of the sediment column. A fraction of the  $IO_3^-$  diffuses downward through the redox front and is re-reduced to  $I^-$  or to  $I_2$ . Recycling of I at the redox

Table 4.3 Pt and Ir results for core 11334#4B, Madeira Abyssal Plain, NE Atlantic. This box core was raised from a water depth of 5375 m at 31°30.8'N, 24°25.2'W.

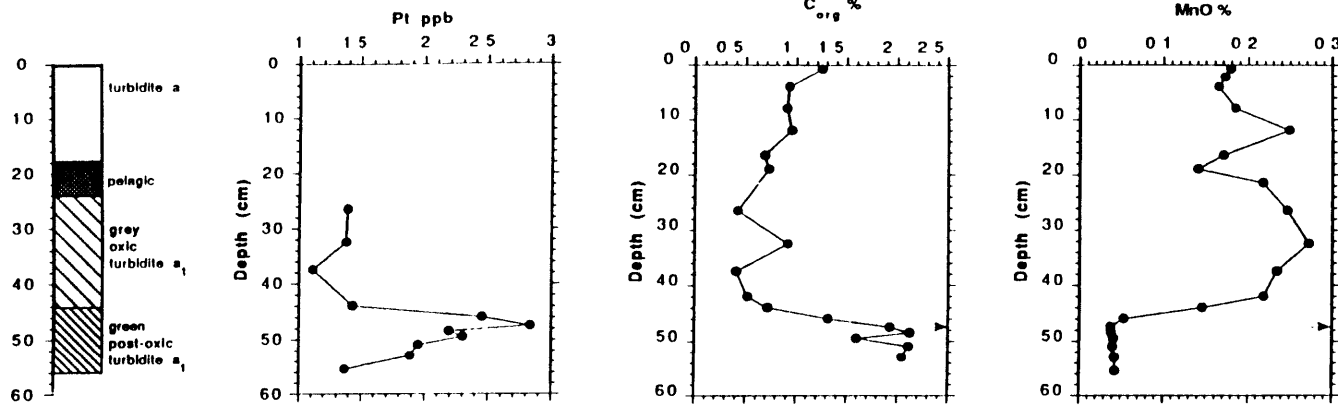
Depth (cm)	Pt ppb	Mean	SD*	Ir ppb	Mean	SD*
25-28	0.90	0.90		0.08	0.08	
31-34	0.92	0.92		0.06	0.06	
36-39	0.91	0.91		0.06	0.06	
41-43				0.10	0.10	
43-45	1.1	1.1		0.05	0.05	
45-47	2.0 1.8	1.9	0.1	0.08 0.07	0.08	0.01
47-48	2.2	2.2		0.06	0.06	
48-49	1.6	1.6		0.08	0.08	
49-50	1.7 1.7	1.7	0.01	0.09	0.09	
50-52	1.4	1.4		0.08	0.08	
52-54	1.4	1.4		0.05	0.05	
54-57	1.0	1.0		0.07	0.07	

SD\* = difference from the mean.

Data in tables are not on a carbonate free basis.

Table 4.4 Ancillary data for core 11334 (IOS, unpublished data)

Depth (cm)	C <sub>org</sub> %	CaO %	MnO %	Co ppm	Cu ppm	I ppm	V ppm
0.75	0.51	32.81	0.073	10	56	78	78
2.25		34.07	0.067	12	52	60	69
4	0.36	34.20	0.064	10	52	57	71
8	0.34	34.94	0.070	11	50	59	64
12	0.35	35.09	0.092	8	54	59	67
16.5	0.29	32.10	0.073	8	53	58	76
19	0.31	31.87	0.060	10	51	50	73
21.5		28.83	0.104	20	47	37	71
26.5	0.27	19.34	0.160	17	47	36	91
32.5		18.58	0.182	15	46	43	91
37.5	0.33	10.34	0.192	17	44	57	108
42	0.42	9.83	0.179	18	40	95	106
44	0.57	11.29	0.116	16	45	163	106
46	1.02	12.21	0.041	11	62	303	104
47.5	1.46	13.34	0.028	11	72	168	110
48.5	1.59	14.01	0.028	13	77	155	147
49.5		14.28	0.030	15	61	147	139
51	1.56	14.39	0.029	15	49	149	118
53	1.51	14.82	0.031	16	45	145	98
55.5		14.11	0.032	14	43	144	94



11334

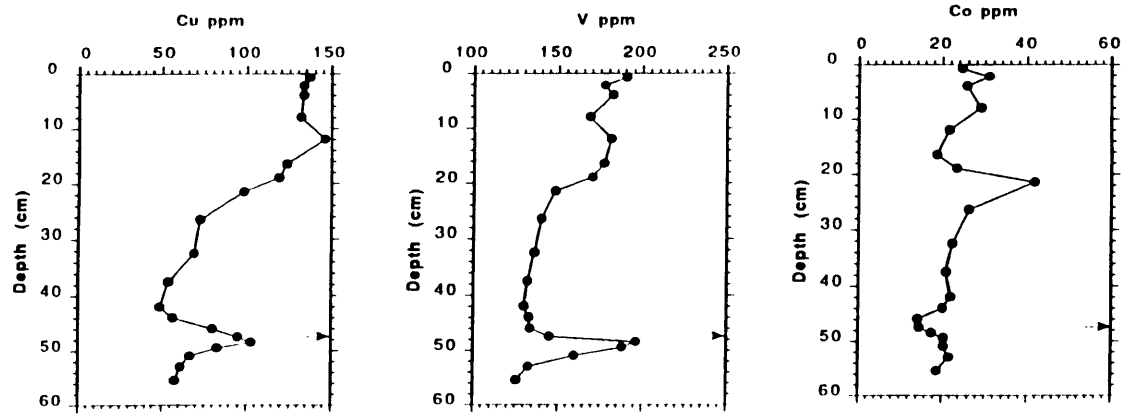


Figure 4.4 Pt results for core 11334 compared to organic carbon, MnO, Cu, V and Co. All data are plotted on a carbonate free basis. The depth of the Pt peak is indicated by an arrow. (All data except Pt data are from J. Thomson, IOS, unpublished).

Table 4.5. Pt, Ir and Re results for core 11805, Eastern North Atlantic. This Kastenlot core was raised from a water depth of 6050 m at 25°39'N, 30°57'W.

Depth (cm)	Pt ppb	Mean	SD*	Ir ppb	Mean	SD*	Re ppb	Mean (±5%)
105-106	1.0	1		0.03	0.03		0.3	
110-111	1.2	1.2		0.02	0.02		0.7	
111-112	1.2	1.2		0.02	0.02		0.4	
112-113	0.9	0.9		0.05	0.05		0.3	
113-114	1.5	1.5		0.03	0.03		1.0	
114-115	2.1 2.0	2.0	0.1	0.04 0.02	0.03	0.01	6.6 6.1	6.4
115-116	2.5	2.5		0.04	0.04		4.8	
116-117	2.8	2.8		0.03	0.03		6.6	
117-118	2.5 (4.0)	2.5		0.03 0.04	0.04	0.01	11.5	
118-119	2.4	2.4	0.1	0.04 0.05	0.04	0.01	10.5	2.5
119-120	2.6	2.6		0.04	0.04		11.0	
120-121	1.6 1.8	1.7	0.1	0.06 0.04	0.05	0.01	15.4	
121-122	1.6	1.6		0.05	0.05		10.6	
130-131	1.0 1.0	1.0	0.03	0.04 (0.2)	0.04		14.1	
140-141	0.8 1.1	0.9	0.1	0.04 0.06	0.05	0.01	14.0	
150-151	1.1	1.1		0.04	0.04			

() not included in mean

SD\* = difference from the mean

Duplicates for Re not included because first set of samples were overspiked, with the exception of one pair. Uncertainty estimated to be ± 5% based on intercalibration of three samples with G. Ravizza (see Chapter 2).

Table 4.6 Ancillary data for core 11805 (Thomson et al. in prep.)

Depth (cm)	C <sub>org</sub> %	CaCO <sub>3</sub> %	MnO %	Cu ppm	I ppm	V ppm	U ppm
105.5	0.22	43	0.074	30	80	91	1.4
110.5	0.31	43	0.080	33	134	88	1.1
111.5	0.28	43	0.114	26	137	83	0.9
112.5	0.24	42	0.180	26	165	87	0.3
113.5	0.32	41	0.148	32	224	88	1.2
114.5	0.63	41	0.032	59	268	97	1.5
115.5	0.58	42	0.081	52	215	88	1.7
116.5	0.66	44	0.087	59	182	101	1.1
117.5	0.70	45	0.028	52	41	96	1.3
118.5	0.71	45	0.028	58	82	104	0.6
119.5	0.74	45	0.028	150	28	151	4.4
120.5	0.72	46	0.028	40	32	178	13
121.5	0.69	46	0.028	35	31	96	15
130.5	0.70	47	0.032	33	26	80	12
140.5	0.70	47	0.032	33	26	80	11
150.5	0.70	47	0.034	34	26	78	6.4



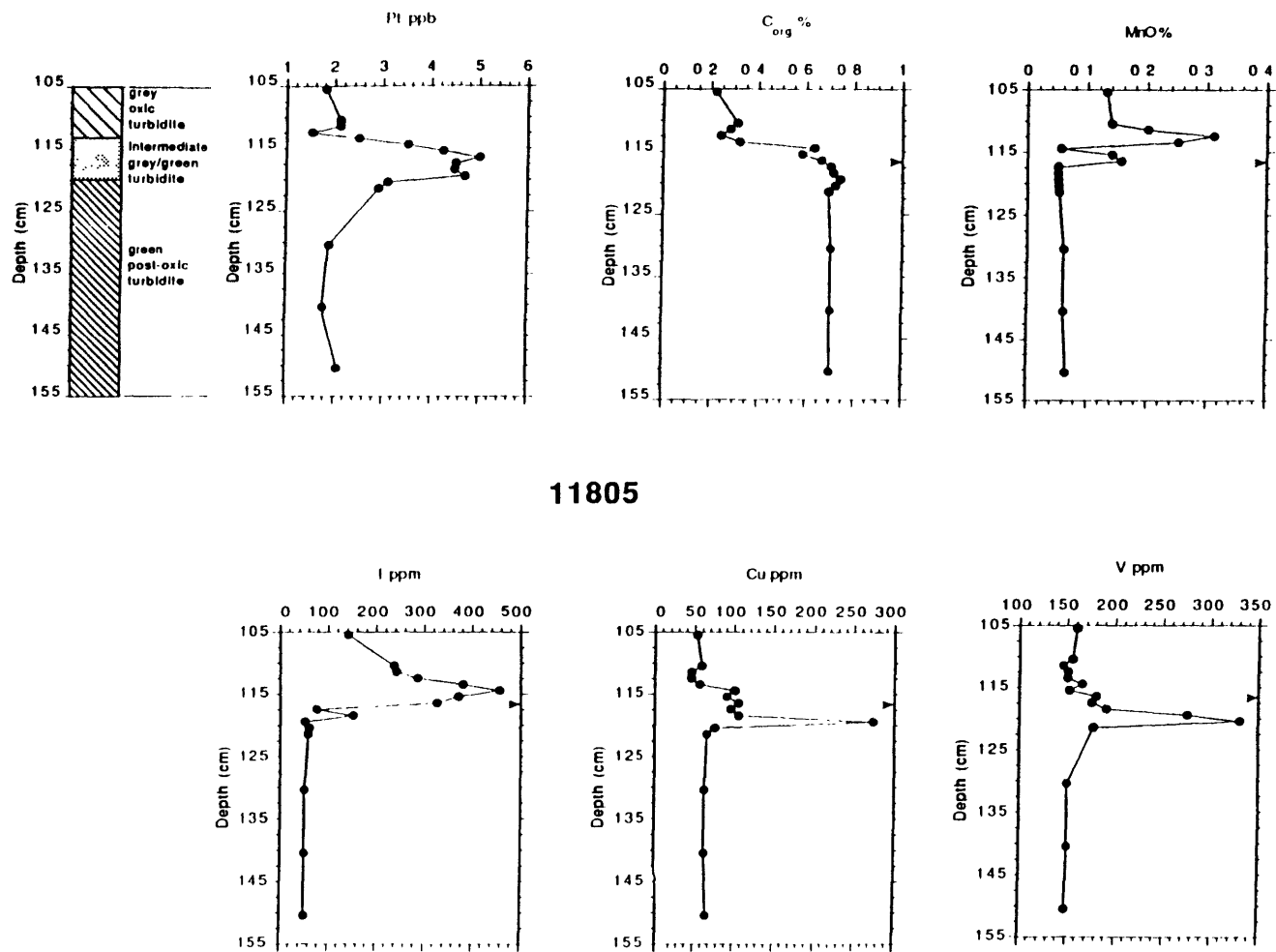


Figure 4.5 Pt results for core 11805 compared with organic carbon, MnO, I, Cu and V. All data (excluding organic carbon) are plotted on a carbonate free basis. The depth of the Pt peak is indicated by an arrow. (All data except Pt data are from Thomson et al., in prep.)

11805

125

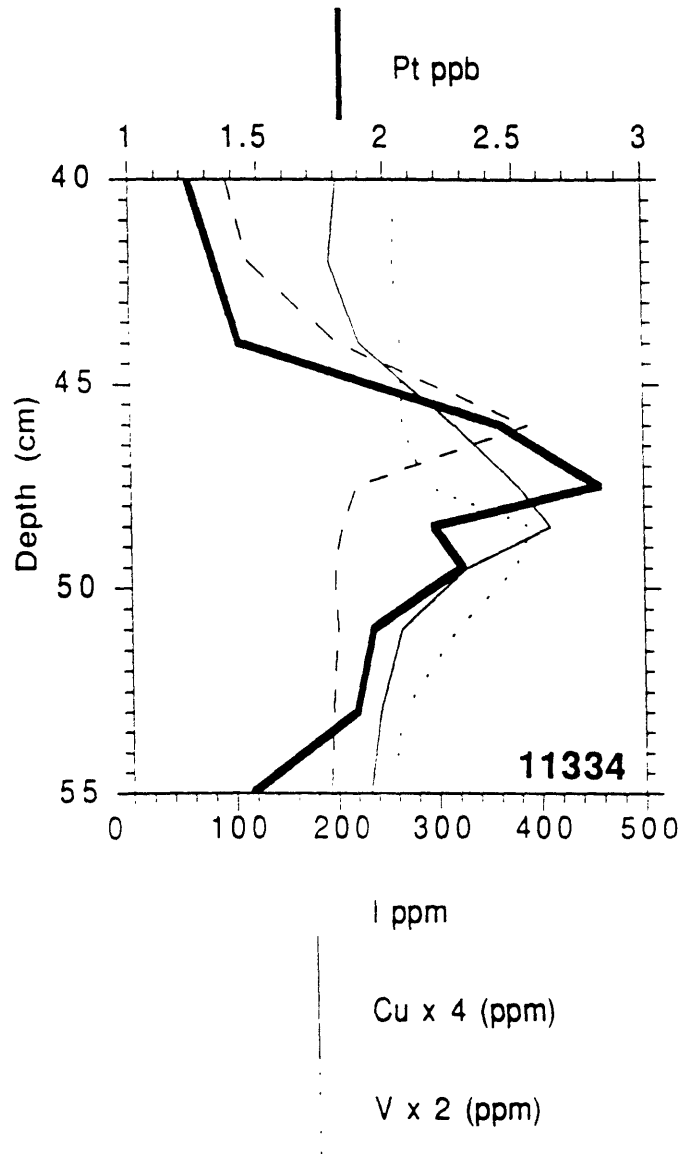


Figure 4.6 Core 11334: an expanded view of the redox boundary shows the location of the Pt peak between those of I and Cu. Data are plotted on a carbonate-free basis.

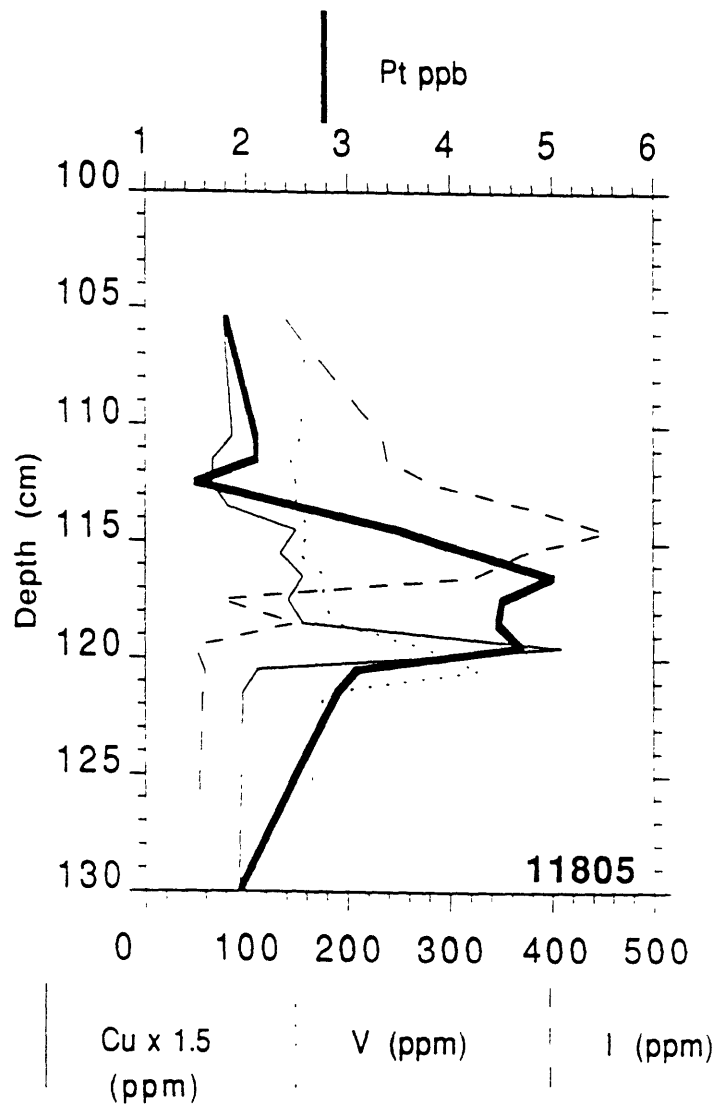


Figure 4.7 Core 11805: Pt concentrations are elevated throughout the oxic/post-oxic transition zone in this core (113-120 cm, intermediate grey-green turbidite in figure 4.5). As in core 11334 (figure 4.6), the Pt peak falls between those of I and Cu.

boundary as it moves through the sediments leads to an increase of I throughout the oxic section, with a maximum at the front, as discussed in detail in Kennedy and Elderfield (1987).

Within the resolution of the data, Ir concentrations do not show any trend in these sediments (figures 4.8 and 4.9). Ir values are consistently low, with a mean concentration of  $0.07 \pm 0.02$  ppb in core 11334 and  $0.04 \pm 0.01$  ppb in core 11805, with the difference between the two due to the difference in carbonate contents.

Re concentrations in core 11805 (it was not measured in 11334) are much lower in the oxidized portion of the turbidite (0.4 ppb) than in the unoxidized section (14 ppb). Re results are plotted in figure 4.10 on a carbonate-free basis. Re is similar to U in its distribution, but appears to be less easily remobilized, as its concentrations decrease upward throughout the zone of intermediate redox conditions in the turbidite. U concentrations, on the other hand are low throughout the transition zone (113-120 cm).

Results for cores 10400 and 52-2 (containing examples of reductive "halos") are presented in Tables 4.7 and 4.9, with ancillary data in Tables 4.8 and 4.10, respectively. In both cores Pt and Ir are depleted in the halo portion of the sediment relative to the underlying, unaltered pelagic clay (figures 4.11 and 4.12). The Pt and Ir data are compared to other transition metal results in figures 4.13 and 4.14. In core 10400, it appears that Pt is trapped at the top of the turbidite and at the bottom of the halo. It bears some similarity to Co in that regard, as Co is trapped in a peak at the base of the halo. The depth of the Pt peak in the middle of the turbidite corresponds to a local minimum in the manganese profile and may be due to the trapping of Pt by a refractory reduced phase within the turbidite as well. Duplication of this point and of adjacent data indicates that the enrichment is a real feature of the sediment (Table 4.7).

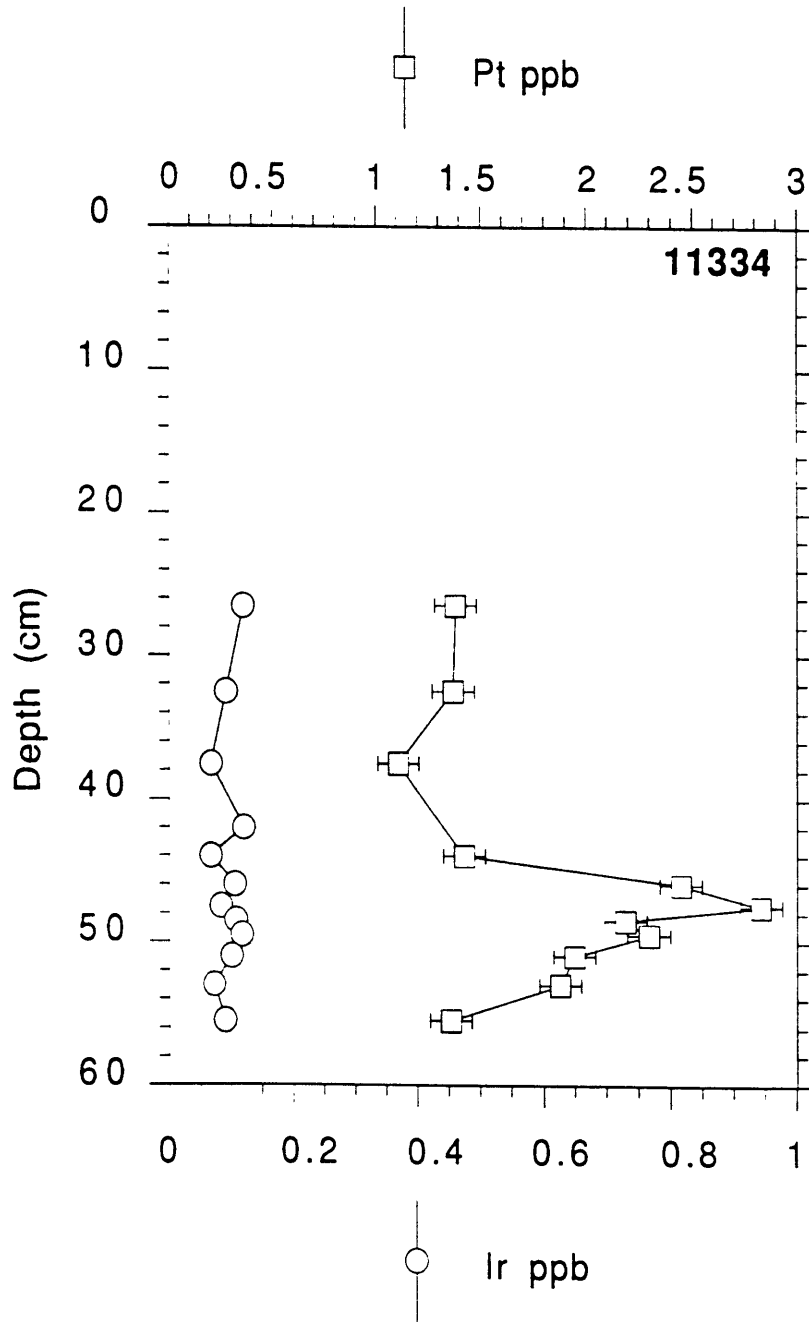


Figure 4.8 Pt and Ir results for core 11334. Error bars ( $1\sigma$ ) are  $\pm 0.1$  ppb for Pt and  $\pm 0.01$  ppb for Ir.

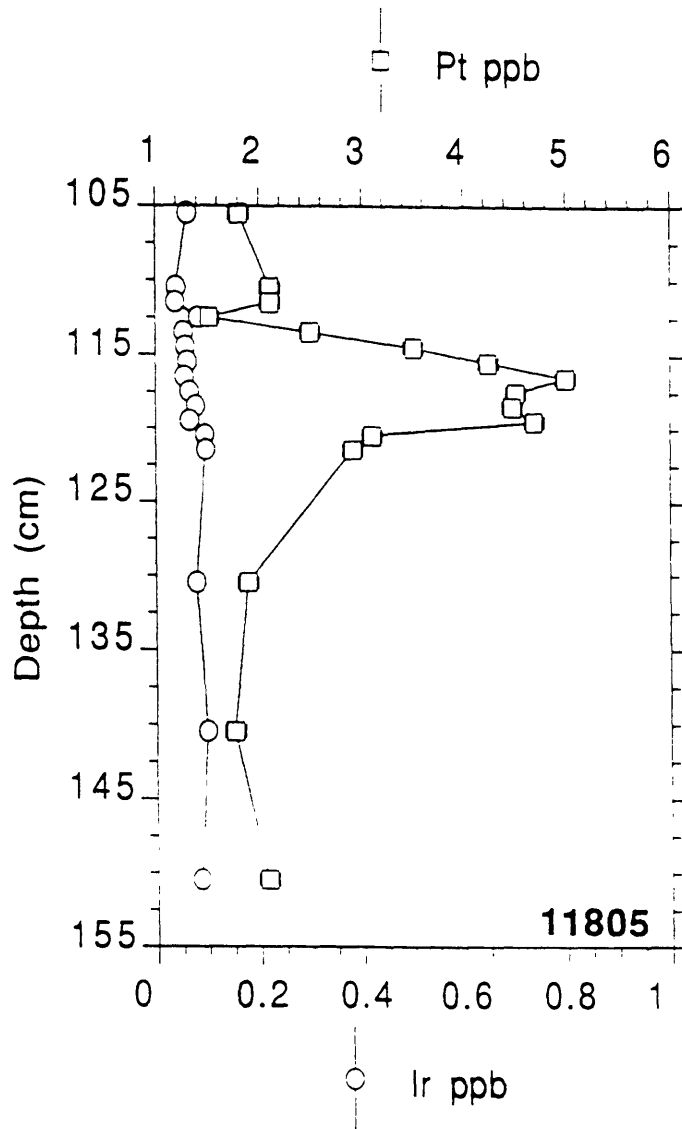


Figure 4.9 Pt and Ir results for core 11805. Error bars ( $1\sigma$ ) are  $\pm 0.1$  ppb for Pt and  $\pm 0.01$  ppb for Ir.

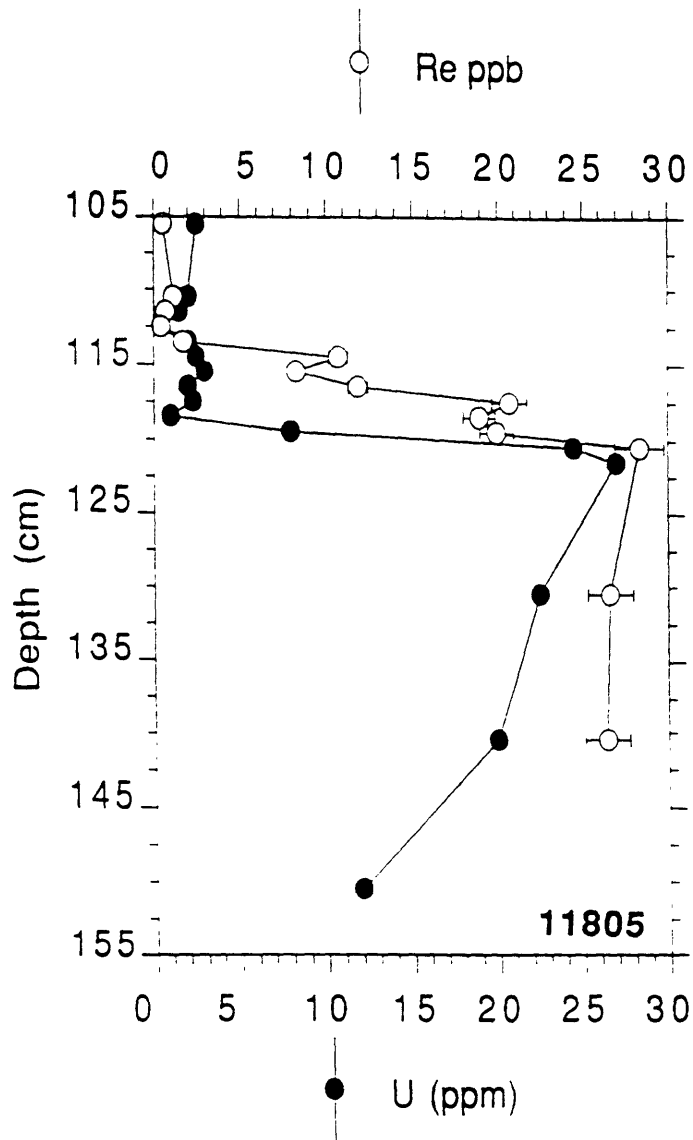


Figure 4.10 Re and U profiles in core 11805. U is low throughout the oxic/post-oxic transition zone (113-120 cm), whereas Re increases with depth through this zone. U data from Thomson et al., in prep.

Table 4.7. Pt and Ir results for core 10400#8K, Mid-Atlantic Ridge foothills, NE Atlantic. This core was raised from a water depth of 6044 m at 25°42.4'N, 30°57.7'W using a Kastenlot gravity corer.

Depth (cm)	Pt ppb	Mean	SD*	Ir ppb	Mean	SD*
16-18	4.5	4.5		0.14	0.14	
24-26	4.5	4.5		0.13	0.13	
44-46	6.5 5.1	5.8	0.7	0.17 0.11	0.14	0.03
47-49	2.5	2.5		0.06	0.06	
49-51	1.7	1.7				
51-53	3.9 3.6	3.8	0.2	0.07 0.11	0.09	0.02
53-55	1.6 1.3	1.4	0.2	0.07	0.07	
69-71	2.1 2.0 (6.6)	2.0	0.1	0.13 0.12 0.14	0.12	0.01
73-75	6.2 5.6 5.7 5.7	5.8	0.3	0.16 0.17 0.24	0.18	0.04
83-85	4.3 4.4 (6.2)	4.4	0.1	0.18 0.16 0.23	0.19	0.03
113-115	4.3	4.3				

SD\* = the standard deviation, or the difference from the mean when n=2  
 () not included in mean



Table 4.8 Ancillary data for core 10400 (Colley, et al. 1984)

Depth (cm)	C <sub>org</sub> %	CaCO <sub>3</sub> %	MnO %	Co ppm	Ni ppm	Cu ppm
11	0.01	3.42	0.41	60	117	146
17			0.39	54	123	141
25	0.11	0.83	0.39	48	121	155
45	0.03	1.75	0.28	45	121	120
48	0.09	3.50	0.19	28	77	77
50	0.10	4.25	0.18	28	74	74
52	0.05	4.92	0.12	23	68	72
54			0.17	24	64	85
62	0.15	0.50	0.05	20	74	105
70			0.06	21	70	130
72		0.33	0.28	106	105	138
74	0.10	0.42	0.37	89	115	147
84			0.47	62	120	137
114			0.47	64	115	123
134		1.25	0.49	66	117	131
164			0.46	60	120	142
174			0.50	61	123	145
184	0.08	0.50	0.48	136	57	183

Table 4.9 Pt, Ir and Re data for core 52-2, Mid-Atlantic Ridge foothills, NE Atlantic. This piston core was raised from a water depth of approximately 5878 m at 23°22.3'N, 63°00.7'W.

Depth (cm)	Pt ppb	Ir ppb	Re ppb
1580	3.7	0.11	0.05
1582	2.7	0.11	0.05
1583	3.4	0.17	0.05
1594	1.7	0.07	0.04
1595	1.9	0.06	0.03
1596	1.2	0.06	0.04
1597	2.5	0.03	0.07
1599	3.1	0.07	0.07
1600	2.0	0.08	0.07
1602	1.9	0.10	0.06
1603	4.2	0.09	0.07
1604	4.6	0.16	0.06
1605	5.1	0.15	0.06
1606	5.2	0.17	0.07
1607	5.2	0.17	0.08
1609	3.9	0.16	0.07

Approximate SD 5% 10% 20%  
(based on counting statistics and replicate samples from other cores)

Table 4.10 Ancillary data for core 52-2 (Thomson, et al. 1989)

Depth (cm)	Al <sub>2</sub> O <sub>3</sub> %	Mn %	Co ppm	Ni ppm	Cu ppm
1580	21.8	0.41	44	85	90
1582	22.2	0.36	44	86	85
1583	22.0	0.38	44	84	86
1594	20.6	0.25	41	91	68
1595	18.0	0.25	37	100	72
1596	21.5	0.28	21	95	75
1597	22.3	0.12	20	89	83
1599	22.4	0.07	18	70	80
1600	22.1	0.07	21	60	84
1602	22.1	0.07	18	70	106
1603	22.4	0.15	25	80	106
1604	22.3	0.30	42	90	100
1605	22.2	0.32	48	92	105
1606	22.3	0.40	56	96	106
1607	22.0	0.42	57	95	101
1609	22.5	0.41	48	92	101

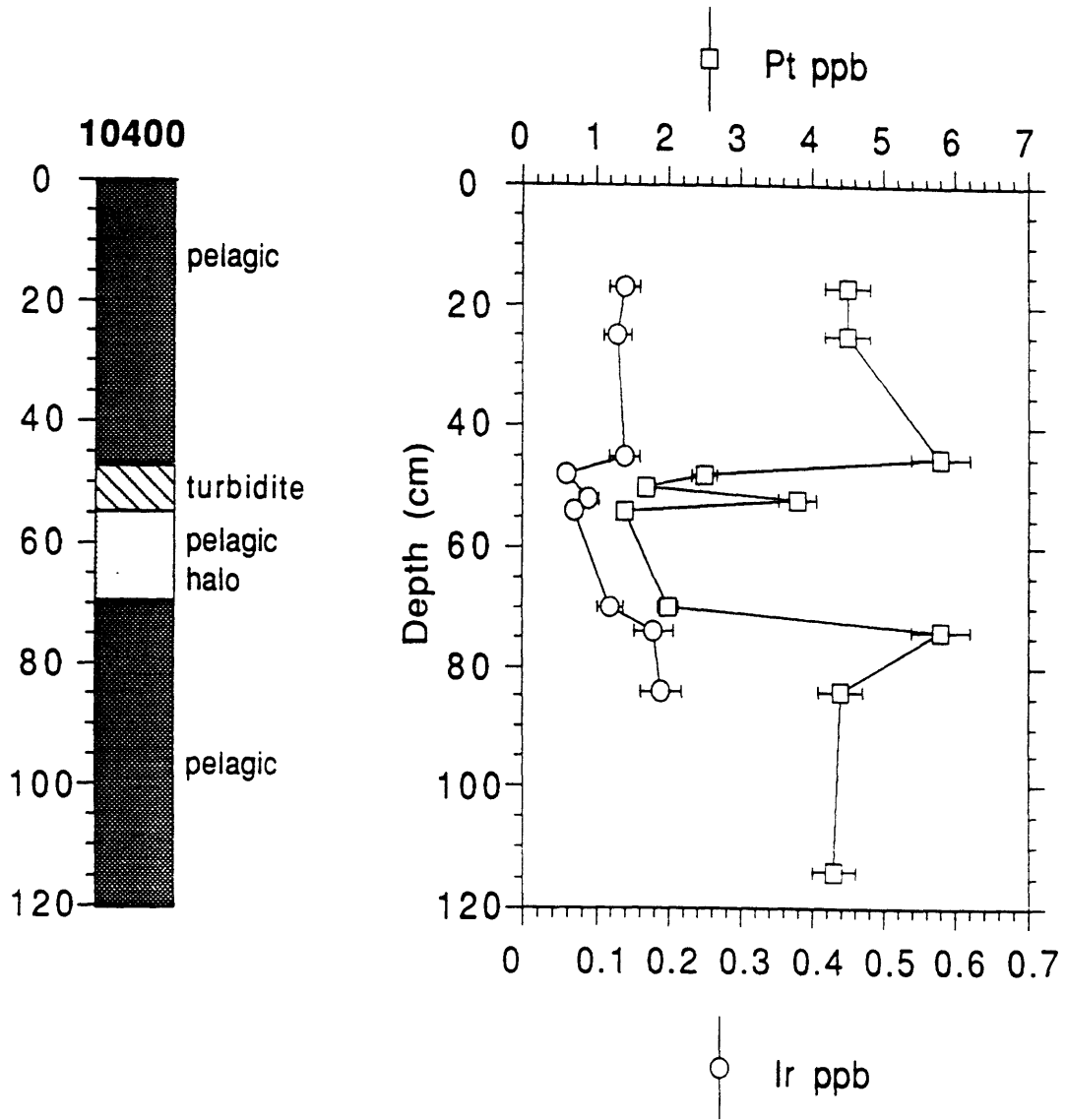


Figure 4.11 Pt and Ir results for one example of a reductive halo: core 10400. Error bars ( $1\sigma$ ) are  $\pm 7\%$  for Pt and  $\pm 15\%$  for Ir.

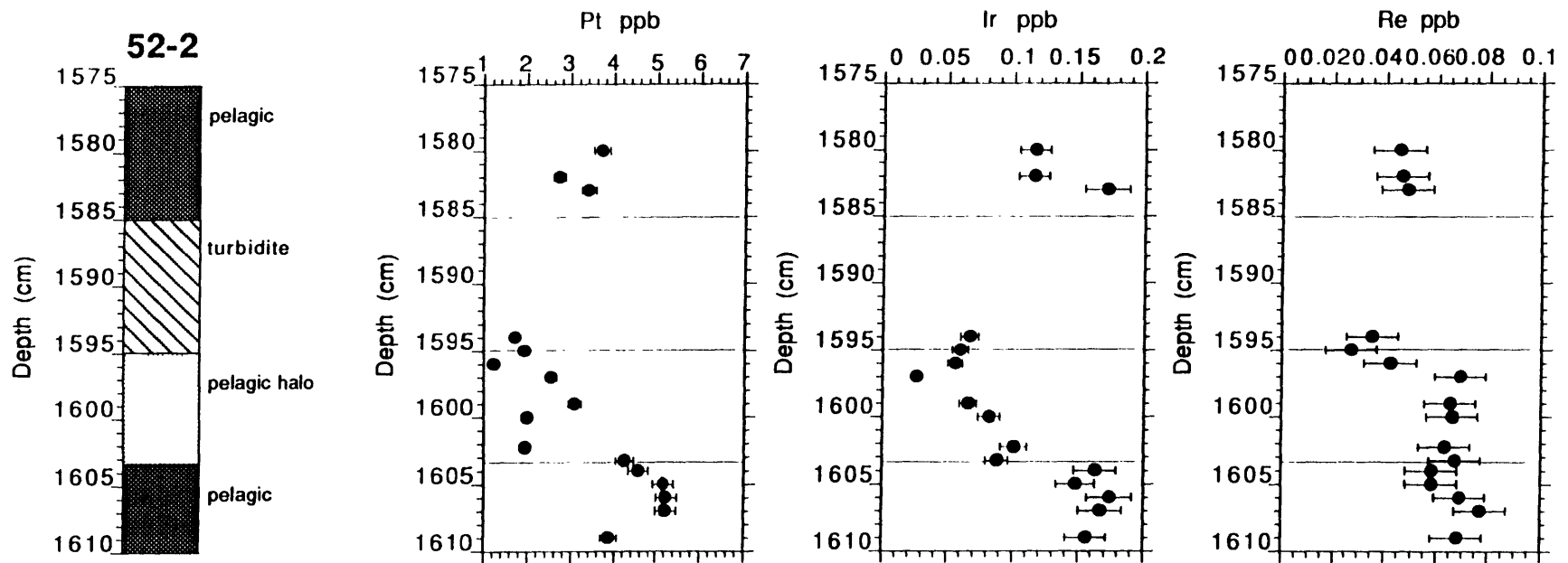
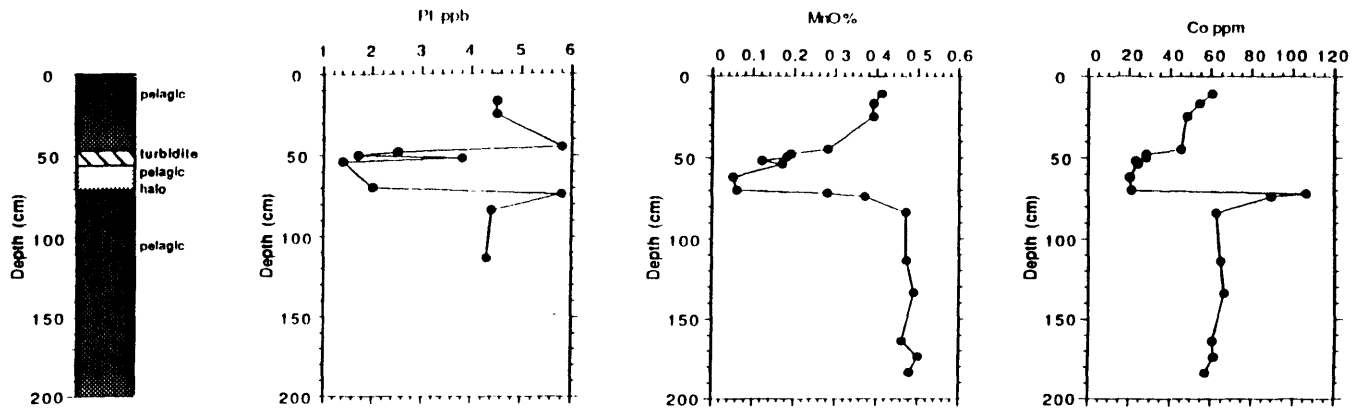


Figure 4.12 Pt, Ir and Re results for core 52-2, with another example of a reductive halo.  $1\sigma$  error bars are  $\pm 5\%$  for Pt and  $\pm 10\%$  for Ir.



10400

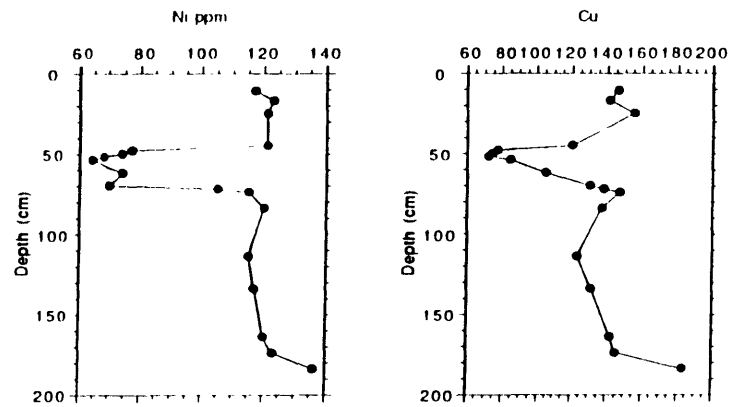
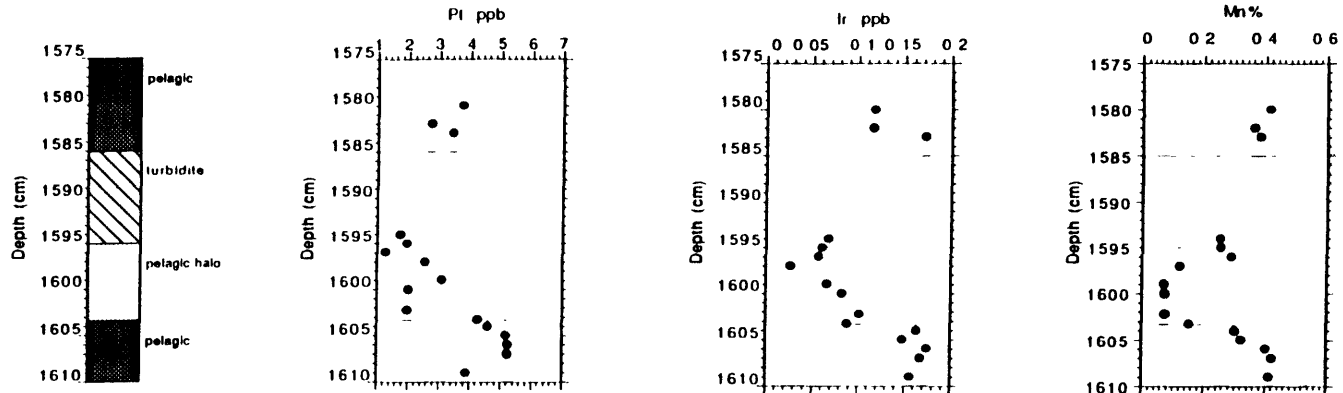


Figure 4.13 Pt results for core 10400 compared with MnO, Co, Ni and Cu data (Colley et al. 1984)



52-2

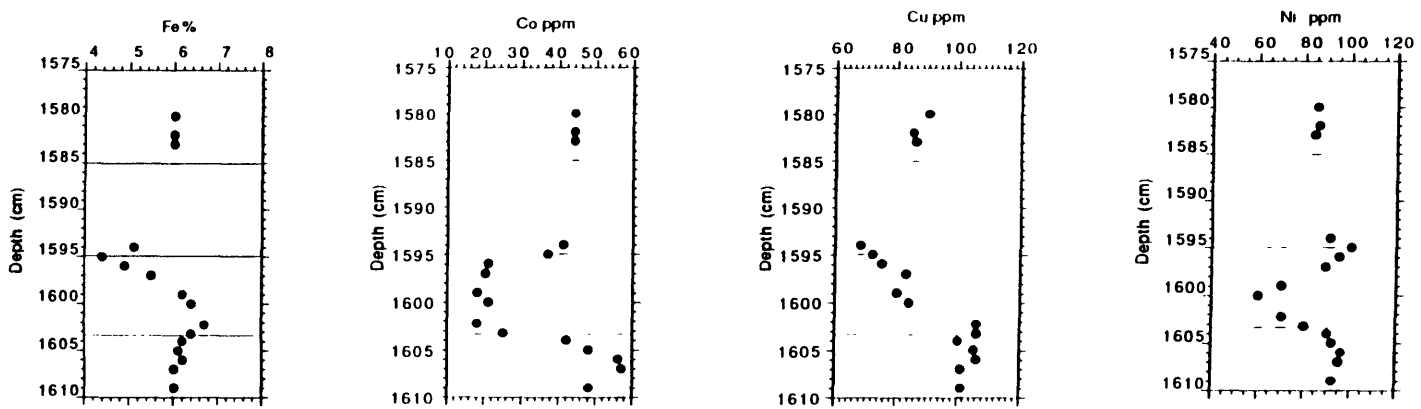


Figure 4.14 Pt and Ir results for core 52-2 compared to those for Mn, Fe, Co, Cu and Ni (Thomson et al. 1989).

The Ir results are clearer in core 52-2 where there were more available samples. The mean concentrations ( $\pm 1\sigma$ ) in the halo of core 52-2 are  $2.4 \pm 1$  ppb Pt and  $0.07 \pm 0.02$  ppb Ir ( $n=7$ ). The corresponding means in the pelagic section are  $4.8 \pm 0.6$  ppb Pt and  $0.16 \pm 0.01$  ppb Ir ( $n=5$ ). Some of the mobilized Pt and Ir may be trapped below the bleached section in this core as well, similar to Co, whose concentrations begin to decrease toward the bottom of the sampled section. Unlike Co or Mn, which have been depleted to a uniformly low value throughout the halo, Ir (and Pt?) increases with depth in the halo section. In this respect it is more like Cu, which shows intermediate behavior between that of Fe and Mn (Thomson et al., 1989).

Re occurs in very low concentrations throughout this core ( $<0.1$  ppb, figure 4.15). The decrease at the top of the halo is similar to the trend in Al, which is due to primary grading at the base of the turbidite and some mixing between the turbidite unit and the underlying pelagic sediments (Thomson et al., 1989). The comparable Re and Al profiles suggest that Re is not concentrated in the heavy mineral fraction of the detritus. There is no significant hydrogenous fraction of Re which is mobilized by Mn and Fe reduction in these sediments, as no depletion is seen in the halo region.

## 4.6 Discussion

### *The formation of Pt peaks*

The Pt peaks seen in cores 11334 and 11805 were formed by one of two possible mechanisms: 1. Pt is mobile in the unoxidized portion of the turbidite, and diffuses upwards to be fixed when it crosses the redox boundary into more oxic conditions, or 2. Pt is mobilized by the passage of the oxidation front through the turbidite, and is fixed when it crosses into the reduced section.



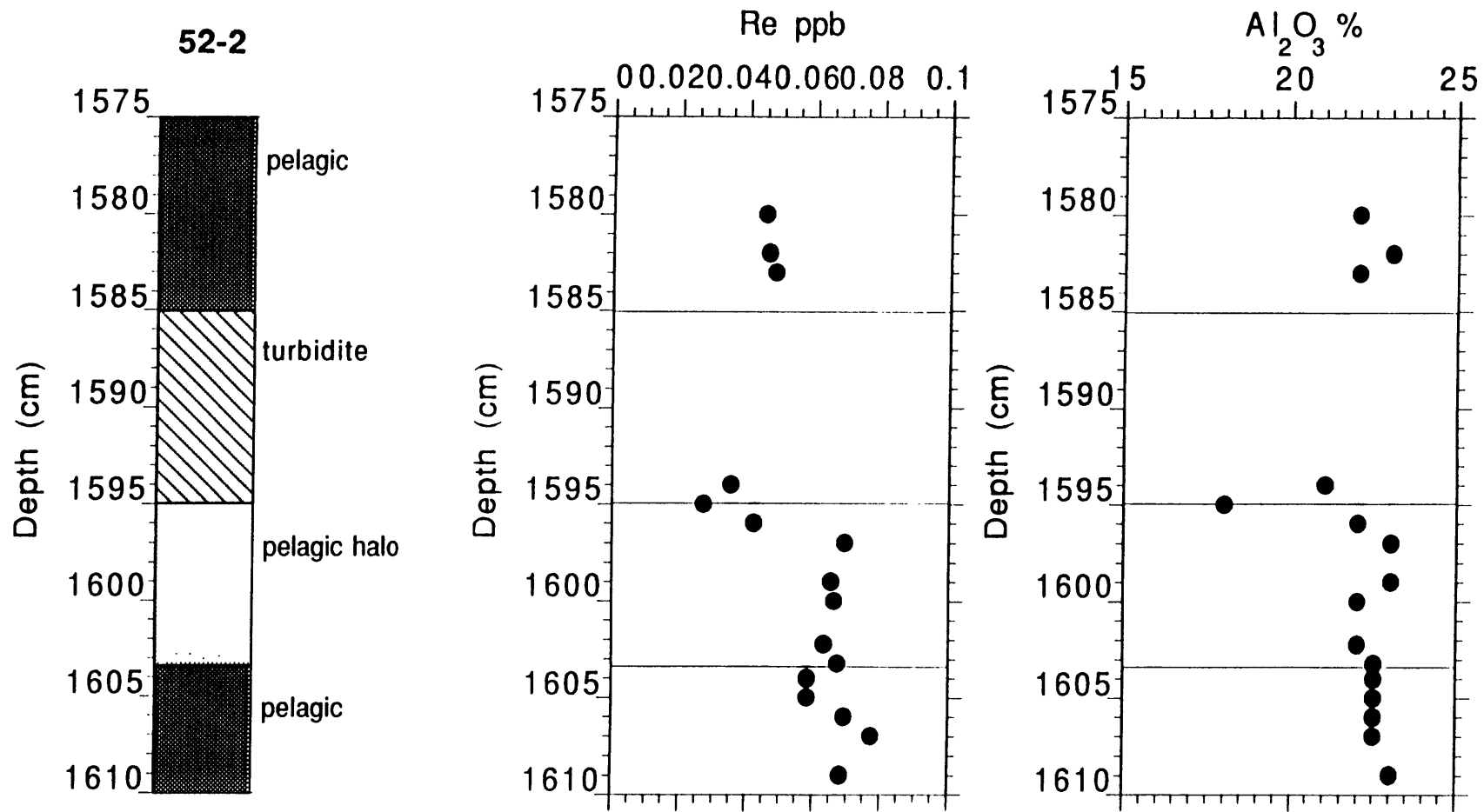


Figure 4.15 Re results for core 52-2 compared to  $Al_2O_3$ . Lower Al at the base of the turbidite is the result of primary size and density grading. Al data from Thomson et al. 1989).

Mechanism 1 describes the behavior of Mn and I in these cores, whereas mechanism 2 describes Cu, V and U. In the first case, concentrations of the element should be lower in the reduced than in the oxidized turbidite, and in case 2, the opposite should be true. The Pt data on either side of the peaks are ambiguous in this regard however. In fact, the depletion required from the upper section to produce the Pt peaks is only about 0.2 ppb. This is the same as  $2\sigma$  of the data (Tables 4.3 and 4.5), so that even with more data this change might not be observed.

The size of the Pt peaks and the thickness of the turbidites may be examined for qualitative evidence supporting one or the other of the above mechanisms. In core 11334, the thickness of the turbidite is uncertain since it extends beyond the bottom of the core. However by inference from other cores in the immediate area, turbidite  $a_1$  is relatively thin: 40 cm at site 10554 (Wilson et al., 1985) and 16 cm at site 10688 (Jarvis and Higgs, 1987). Oxygen has penetrated approximately 23 cm into the top of this turbidite over 10 ky since emplacement. The turbidite in core 11805, on the other hand is at least 11 m thick (Thomson et al., 1991), and the upper 70 cm is oxic. It was emplaced approximately 330 ky ago. The amount of Pt concentrated in the Pt peaks is 3.1 and 7.2 ng/cm<sup>2</sup> for cores 11334 and 11805, respectively. This amount corresponds to a deficit in the upper oxidized sections of these turbidites of approximately 0.2 ppb over 25 cm in core 11334 and 60 cm in core 11805. If Pt were diffusing upward, out of the post-oxic section of the turbidite, one might expect a larger enrichment in core 11805, as the anoxic portion of the turbidite is thicker (>10m vs. ~20cm), and it has been in place 30 times longer than the turbidite in core 11334. The deficits in the unoxidized turbidite necessary to produce the observed peaks would be 0.3 ppb in core 11334 but only 0.01 ppb

in core 11805. Thus the sizes of the peaks are more consistent with derivation of the excess Pt from the overlying oxidized section.

This conclusion is somewhat surprising in light of the strong enrichment of Pt in hydrogenous manganese oxides. However other elements, such as Co and Cu, which are congeners of Mn in hydrogenous phases (Calvert and Price, 1977) also show little resemblance to Mn in these cores. Co concentrations (carbonate-free basis) are the same in the oxic and post-oxic sections of the turbidite in core 11334 (figure 4.4), with a minimum at the the redox front. Cu is enriched in a peak just below that of Pt, at the point where organic carbon starts to decrease. It is unlikely that the proposed redistribution of Pt is related to changes in the oxidation state of Pt itself. Pt is probably initially present as  $Pt^{2+}$ , and oxidation to  $Pt^{4+}$  is likely to lead to its uptake by ferromanganese oxides in the oxic section of the core (as proposed by Goldberg et al., 1986, for its uptake into manganese nodules), rather than fixation at or below the redox boundary. If  $Pt^{2+}$  were reduced to  $Pt^0$  below the boundary, it is unlikely that a peak could form at a moving redox front, since the reoxidation (and remobilization) of elemental Pt is kinetically hindered (ref. the noble character of the metal). The profiles suggest that Pt is released from a carrier phase in the oxidized section of the turbidites. Since pore water data from other cores indicate that there is no sulfide formation in these turbidites, the carrier phase is probably organic matter. Other evidence for the accumulation of Pt by sedimentary organic matter is its enrichment (50-8000 ppb) in peat and algal mats from Sri Lanka (Dissanayake and Kritsotakis, 1984). A portion of the metal released by oxidation diffuses across the redox boundary and is removed from the pore waters in the post-oxic section. As the front progresses downward, the solid phase peak moves with it, growing continuously. This scenario has been

invoked to explain the distributions of Cu, V and U in these cores as well (Thomson et al., 1991 and Wilson et al., 1985).

The magnitude of the peaks, combined with the lack of an obvious concentration difference between the sediments above and below them, suggests that most of the Pt released from the upper section is fixed within the peak. In order to preserve the peak as the oxidation front deepens, the flux downward must be greater than the flux upward, requiring that the concentration gradient in the pore waters must be greater in the downward than in the upward direction. The shapes of the Pt peaks suggest that Pt continues to diffuse more slowly in the post-oxic section, spending more time on solid surfaces. A higher distribution coefficient ( $Pt_{solid}/Pt_{solution}$ ) in this section would lower the Pt pore water concentration and therefore increase the concentration gradient downward, as called for above.

Two other possibilities for the source of the Pt peak should be mentioned. One of them is that some of the Pt in the peak diffused in from seawater. The mass balance calculation that would reveal if an extra Pt source was necessary is not possible with the uncertainties of the data here. For the other transition metals, with the exception of V, a seawater source is not required. In either case, Pt is fixed when it reaches the post-oxic sediments, and the requirements for preservation of the peak are the same. The second possibility is that Pt was released from the pelagic sediments below these turbidites during the development of a reductive halo, and then diffused upward until it reached the oxic portion of the turbidite. Using the diffusion coefficients for Pt calculated below however, the length of the turbidite in 11805 (11 m) prohibits this from being a viable explanation.

A maximum estimate of the effective diffusion coefficient of Pt in the unoxidized portion of the turbidite can be made by assuming that all the Pt originated in a plane source at the top of the peak. In this case,

$$C_x = \frac{M \exp(-x^2/4Dt)}{2\sqrt{\pi Dt}} \quad \text{Crank, 1970 p.10}$$

where M is the quantity in the peak, D is the effective diffusion coefficient and  $C_x$  is the concentration at a given distance from the plane source, x. A maximum value of the diffusion coefficient (D) of  $10^{-10}$  cm<sup>2</sup>/s is derived from the Pt distribution in core 11334 using this method.

The value of D calculated above is an effective diffusion coefficient for the bulk sediment, which is orders of magnitude lower than the free solution diffusion coefficient, due to the adsorption of Pt by solid surfaces. The distribution coefficient between Pt adsorbed on solids and Pt in solution in the pore waters ( $K_d$ , dimensionless) may be estimated from:

$$D_{\text{eff}} = \frac{D_{\text{sol'n}}}{1+K_d} \quad \text{Berner, 1980 p. 76}$$

$$\text{where } K_d = \frac{\rho_s(1-\phi)}{\phi} K_d'$$

$\rho_s$  = average density of total solids (~2g/cm<sup>3</sup>, Table 4.11)

$\phi$  = porosity (0.7, Table 4.11)

$$\text{and } K_d' = \frac{\text{mass Pt adsorbed} / \text{mass solids}}{\text{mass Pt dissolved} / \text{volume pore water}}$$

The development of the peak can also be modelled as a plane source whose concentration increases with time, as illustrated in figure 4.16. The plane is taken to be  $x=0$ , which is fixed at the redox front and moves with it

through the sediments. As the peak grows, the amount of Pt released by a fixed deepening of the front increases. With the boundary conditions:

$$C_{x=0} = kt, \text{ and}$$

at  $t=0$ ,  $C_x = 0$  throughout the core,

$$M_t = \frac{4}{3} kt \sqrt{\frac{Dt}{\pi}} \quad \text{and}$$

$$C_x = 4kti^2 \operatorname{erfc} \frac{x}{2\sqrt{Dt}} \quad \text{Crank, 1970 p.34}$$

where  $M_t$  is the quantity of diffusing substance in the peak at time,  $t$ ,  $k$  is the rate at which the peak grows (concentration/time), and values of the function  $4i^2 \operatorname{erfc}(x)$  were taken from table 2.1 in Crank, 1970. Properties of the sediments used in these calculations are listed in Table 4.11. In this case, diffusion coefficients between  $5 \times 10^{-12}$  and  $1 \times 10^{-10}$   $\text{cm}^2/\text{sec}$  fit the data most closely as shown in figures 4.17 and 4.18. Again, these are only rough estimates, as the concentration at the source ( $x=0$ ) does not really increase linearly with time. An effective diffusion coefficient of  $1 \times 10^{-11}$  is consistent with that estimated from pore water and solids data for U in these sediments ( $< 2 \times 10^{-11}$ ) (Colley et al., 1989).

---

Table 4.11 Sediment characteristics used in model calculations

	<u>Core 11334</u>	<u>Core 11805</u>
Time since emplacement of turbidite (ky)	10 <sup>a</sup>	330 <sup>b</sup>
Total amount of Pt in peak (ng/cm <sup>2</sup> )	3.12	7.2
Porosity ( $\phi$ )	0.7 <sup>ac</sup>	0.7 <sup>ac</sup>
Dry density (g dry/cm <sup>3</sup> dry)	2 <sup>ad</sup>	2 <sup>ad</sup>
Background Pt concentration (ppb)	0.9	1.0

---

a. Wilson, et al. 1985; b. Thomson, et al. 1991, in prep.; c. Colley, et al. 1984; d. Buckley and Cranston 1988

---

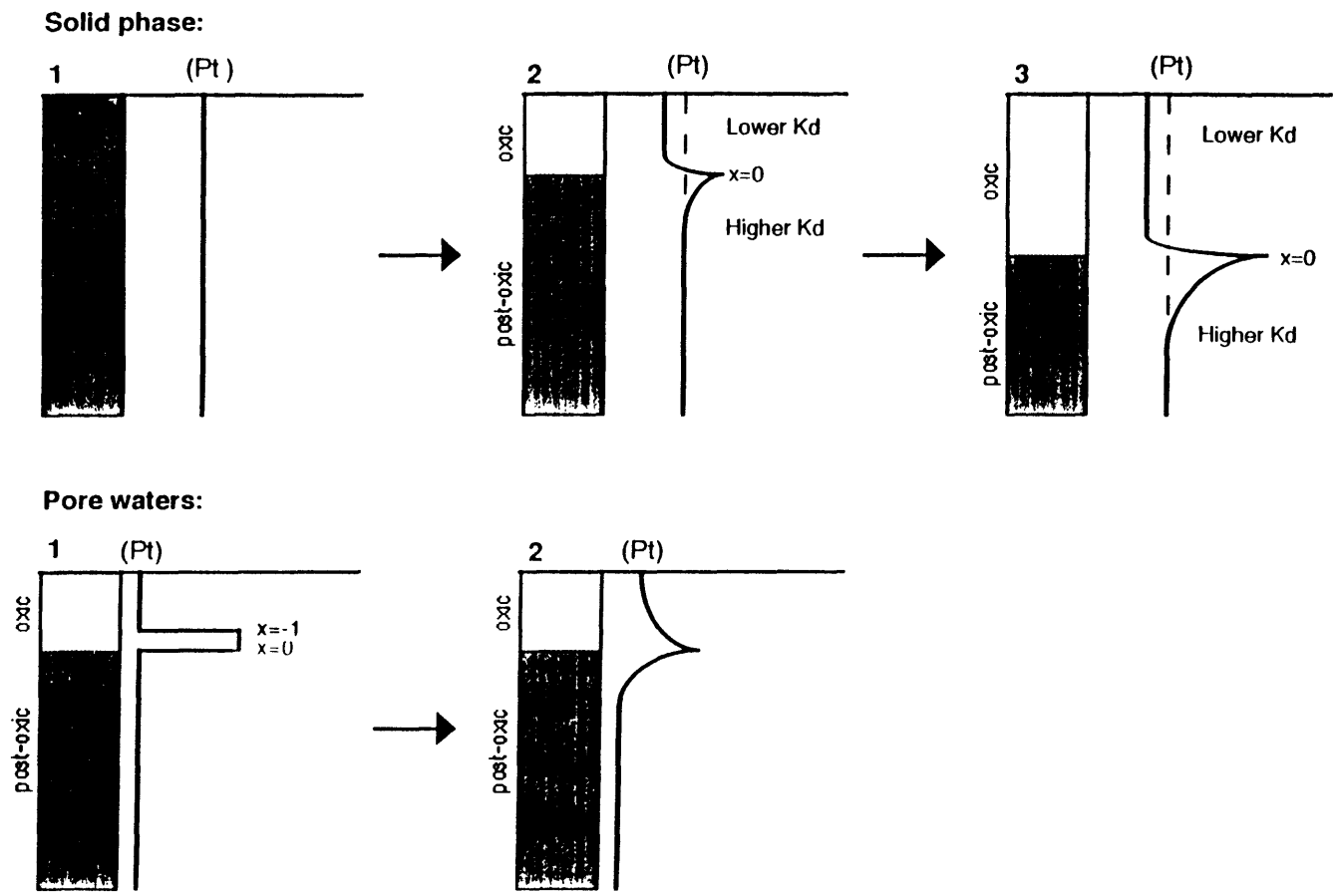


Figure 4.16 Illustration of the development of a Pt peak below the redox front in a partially oxidized turbidite. **Solid phase:** 1) Pt concentrations are initially uniform in the turbidite. 2) As the sediment is oxidized, Pt is released to pore waters (lower  $K_d$ ) and may diffuse both up and down. A higher  $K_d$  below the oxidation front ( $x=0$ ), removes Pt from pore waters and concentrates it in a peak just below the front. 3) This peak is augmented with time as the front deepens. **Pore waters:** 1) Deepening of the redox front from  $x=-1$  to  $x=0$  releases some Pt from the solid phase peak into pore waters. 2) A higher  $K_d$  in the unoxidized portion of the turbidite maintains a steeper gradient in the pore waters downward than upward.

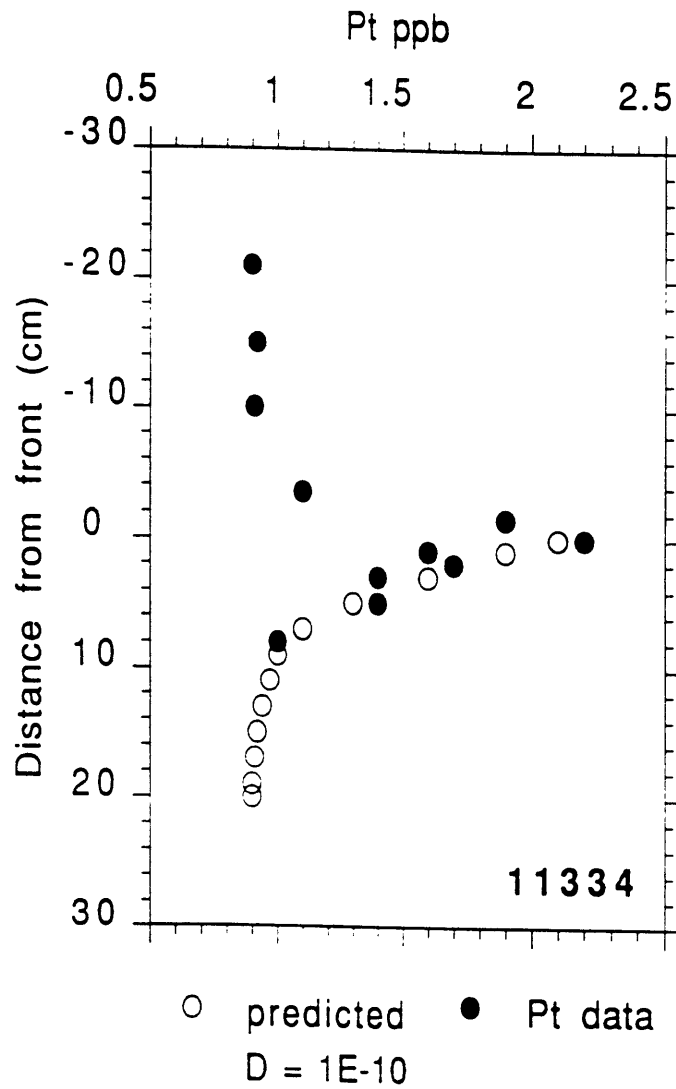


Figure 4.17 Core 11334: Pt profile observed (filled circles) compared to that predicted for the unoxidized portion of the turbidite, assuming an effective diffusion coefficient of  $1 \times 10^{-10}$  cm<sup>2</sup>/sec and a source at the redox front which increases with time (open circles).



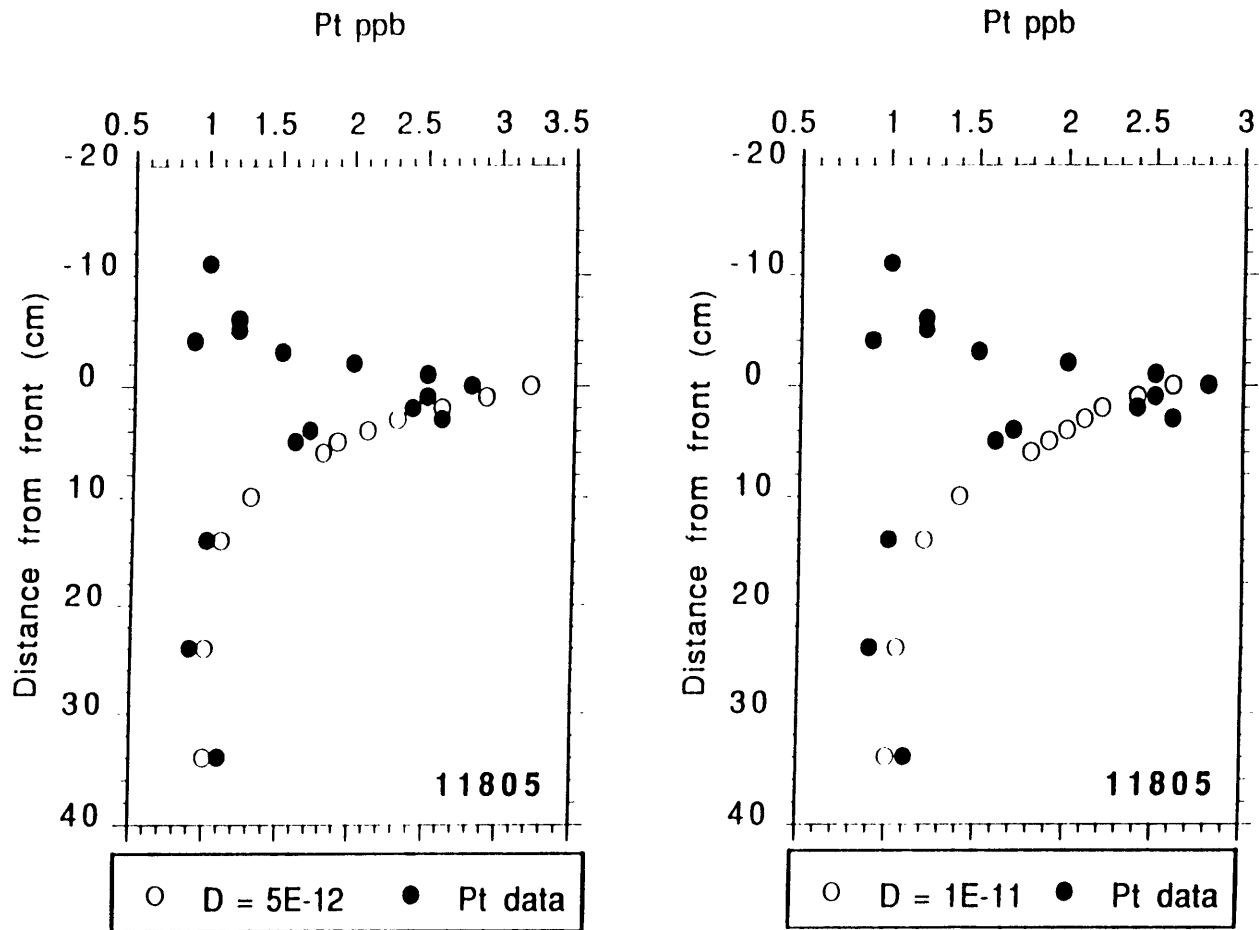


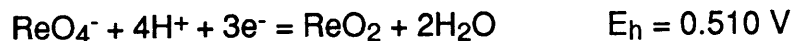
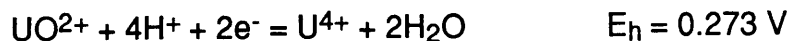
Figure 4.18 Core 11805: Pt profile observed (filled circles) compared to that predicted for the unoxidized portion of the turbidite, assuming an effective diffusion coefficient of  $5 \times 10^{-12}$  or  $1 \times 10^{-11}$   $\text{cm}^2/\text{sec}$  and a source at the redox front which increases with time (open circles).

Taking  $D_{\text{eff}} = 1 \times 10^{-11}$  cm<sup>2</sup>/sec, and  $D_{\text{sol'n}} = 1 \times 10^{-6}$  (approximate value for many trace ions in seawater (Li and Gregory, 1974)),  $K_d$  is  $1 \times 10^5$ . This value is similar to those derived experimentally for <sup>54</sup>Mn and <sup>144</sup>Ce (Duursma and Bosch, 1970), and for Au in a mixture of sediments and waters from the Cariaco Trench (Li et al., 1984).

#### *Ir and Re in partially oxidized turbidites*

Unlike Pt, Ir does not show a peak in either core. The Ir concentration in seawater is not well known, and the only measurements which exist were of three 100 L samples of Scripps Pier water (Goldberg et al., 1986). Assuming this value (5 fM) is correct, the Pt/Ir ratio in seawater is approximately 60. If Ir and Pt behaved congruently throughout the history of the turbidite sediment, from its original deposition on the shelf to its displacement and subsequent oxidation, the peak one should expect to see in the Ir profile in core 11805 would be about 0.08 ppb above background levels (0.02-0.06 ppb). A change of this magnitude should be visible above the noise in the data, if such a peak existed. The lack of evidence for Ir redistribution in these cores could be due to a number of reasons, including its weaker accumulation in organic rich sediments (on the continental shelves, or at the redox boundary in the turbidite), its immobility in response to oxidation, or an overestimation of the amount of Ir in seawater.

From the limited data presented here, Re appears to be mobilized less easily than U, as the decrease in its solid phase concentration is more gradual, and it persists at a greater distance behind the oxidation front. If there is a redox transformation involved (from Re(IV) to the soluble Re(VII)O<sub>4</sub><sup>-</sup>), it appears that Re is less easily oxidized than U. This is consistent with the redox potentials of the following reactions:



(Langmuir, 1978 and Weast, 1988 p. D154).

Similar conclusions were drawn from residence time calculations for the elements in the Black Sea, where it appears that Re is more easily reduced than U in Black Sea sediments. However, thermodynamics may be less important than kinetics in controlling the rate of release of these elements, or they may be controlled by different host phases more than by their own redox chemistries.

Whatever the mechanism for Re liberation from the sediments, it is clear that oxidation mobilizes almost all of the Re originally present. The implications for studies of Re in ancient anoxic sediments are clear: exposure to oxic waters is likely to remove Re from the rock. In addition, potential changes in the Re concentration of seawater caused by changes in the area of anoxic sedimentation (Chapter 6) should be reversible.

#### *Release of Pt and Ir by the reduction of hydrogenous minerals*

The Pt and Ir profiles in cores 10400 and 52-2 (figures 4.11 and 4.12) provide evidence for a significant hydrogenous component in sediments which may be mobilized under reducing conditions. The higher concentrations in these pelagites than in the turbidites discussed above is the result of the inclusion of this hydrogenous phase. In both cores the residual levels of Pt and Ir in the reductive halos are similar (~2ppb Pt and ~0.07 ppb Ir), and represent about half of the initial pelagic concentrations. The residual levels of the elements are similar to the background levels seen in the turbidites (CFB).

The minimum effective diffusion coefficient necessary to have produced these depletions may be calculated from core 10400, which has the thicker halo

section and the younger age. A rule of thumb estimate ( $D = x^2/t$ ) suggests  $D > 10^{-11} \text{ cm}^2/\text{sec}$ , similar to that estimated above for Pt in more organic-rich turbidites. In core 10400, the mobilized Pt appears to have been trapped below the halo and above the turbidite where the sediment becomes oxic again. The excess Pt in these peaks is less than that mobilized from the halo section, although it is difficult to quantify this further since the peak shapes are poorly defined. In core 52-2, the evidence for retention of any of the mobilized fraction is less clear, but there is some suggestion that Pt, like Co, is enhanced in the section just below the halo, compared to background pelagic levels.

Evidence that Ir can be mobilized from these particular sediments invites speculation about the role of diagenetic processes in the creation of Ir boundary spikes. For example, Alvarez et al. (1990) describe a 30 cm bleached zone below the K-T boundary in the Bottacione Gorge section in Gubbio, Italy, from which Fe has been reduced and removed, calling to mind the halo sections above. However, the rocks are limestones, not pelagic clays, and simple mass balance calculations show that the Ir enrichment could not have been derived by diffusion from this section. In order to produce an Ir excess typical of many K-T boundary clays ( $\sim 20 \text{ ng/cm}^2$ ) in pelagic sediments similar to those described above, a halo at least 100 cm thick is required. Rocchia et al. (1990) and Crocket et al. (1988) note that Ir is enriched in several shale layers on both sides of the K-T boundary in the Bottacione Gorge section, but that except for those layers immediately surrounding the boundary, the Ir concentrations are similar to that in carbonate-free limestone. The concentrations they measure in the shales ( $\sim 0.1 \text{ ppb}$ ) are similar to those reported here for pelagic sediments. Thus diffusion may help to determine the shape and dispersion of the K-T peak, but an extraordinary source appears to be necessary for its creation.

Many of the smaller Ir spikes reported in the literature may be the result of early or later diagenetic processes, however. If the Ir lost from the halo sections studied here were trapped in a peak 1cm wide the resulting peak concentrations would be 0.8-1.6 ppb. Many of the reported enrichments listed in Table 4.12 are less than this.

Wide use of platinum-group element ratios, as well as the ratios of PGE's to other siderophile and chalcophile elements, has been made in arguments about the source of noble metal enrichment at the K-T and other boundaries, as reviewed by Cisowski (1990). The ability of diagenetic processes to fractionate the elements suggests that these ratios may be misleading. For example, Hildebrand et al. (1984) suggest that the 10-20 fold enrichment in the Re/Ir ratio in the Danish K-T boundary section relative to chondrites (Kyte et al., 1980; Ganapathy, 1980) is evidence for a volcanic, rather than meteoritic, source for these elements. It is more likely, however, that the Re excess arises from accumulation of the element from seawater into these reducing sediments.

#### **4.7 Conclusions**

The utility of trace elements as indicators of sediment sources or depositional environments requires an understanding of the behavior of the elements during early diagenesis. In the case of the Pt group elements and Re, this understanding was inadequate, due to their very low concentrations in sediments and the lack of suitable analytical techniques. In the absence of information about Ir and Pt geochemistry it was commonly assumed that these elements were immobile in sediments, and hence, that changes in their concentrations, or their ratio, reflected changes in sediment sources. The data reported here show that early diagenetic processes can alter both absolute and

relative Pt, Ir and Re concentrations. Thus, Ir spikes at extinction boundaries, which have been interpreted as the result of meteorite impacts, may instead be the result of Ir redistribution in sediments due to changing redox conditions. Ir enrichments must therefore be evaluated in the context of other data, such as the presence of shocked minerals, the Os isotopic composition, and mass balance considerations of the possible source of the excess Ir within the surrounding sediment. Pt/Ir and Re/Ir ratios are not good indicators of the origin of Ir spikes, due to the ability of geochemical processes to fractionate these elements. The observations made here, regarding the behavior of Pt, Ir and Re during early diagenesis, can be summarized as follows:

1. Pt occurs in association with both organic matter and hydrogenous ferromanganese oxides in sediments. Pt affiliated with both of these phases may be mobilized by changing redox conditions. In organic-rich turbidites through which oxygen gradually penetrates, Pt becomes fixed in a peak immediately below the redox front. In pelagic sediments which are buried under turbidite units, Pt is lost from hydrogenous phases as these are reduced, and in some cases may be redeposited at surrounding redox boundaries.

2. There is no evidence for authigenic Ir enrichment in organic-rich turbidites or for any mobile behavior in this environment. However, Ir is enriched in Fe-Mn oxides in pelagic sediments and may be remobilized as these are reduced. Many small variations in Ir content seen at bio-stratigraphic boundaries are probably diagenetic in origin.

3. Oxidation of organic rich sediments mobilizes almost all of the Re initially present. The implications for studies of Re in ancient anoxic sediments are that exposure to oxic waters is likely to remove Re from the rock. Additionally, potential changes in the Re concentration of seawater caused by changes in the area of anoxic sedimentation (Chapter 6) should be reversible.

## 4.8 Acknowledgements

Samples for this study, as well as ancillary data, were generously provided by J. Thomson at the Institute of Oceanographic Sciences, Surrey, U.K.

Table 4.12 Some biostratigraphic boundaries at which Ir spikes have been reported

Boundary	Age (my)	Location	Ir spike (ppb) bkgd.-peak	Notes	Probably diagenetic?	Ref.
Frasnian-Famennian (Late Devonian)	365	Caning Basin, Australia	0.02-0.3	stromatolite bed with iron-oxide filled filaments	yes	1
Devonian-Carboniferous	360	Oklahoma	0.03-0.6	limest. - shale transition	yes	2
Permo-Triassic	245	Alps, Austria	0.01-0.2	probable chemical origin	yes	3
Cenomanian-Turonian	92	Colorado	0.01-0.1	coincides with Mn peak	yes	4
Cretaceous-Tertiary	65	Denmark	0.3-42	pyntic clay layer in "fish clay"	no	5,6
		Italy	0.3-9	clay layer in limestone		5
		DSDP 465A N. Pacific	1-10	calc. ooze with pynte		7
		LL44, GPC3 N. Pacific	2-11	abyssal clay		8
		Raton Basin, New Mexico (& 70 more sites)	0.02-15	above black shale layer		9
Eocene-Oligocene	37	DSDP149 Caribbean	bd-0.4	impact debris	?	10

1. Playford 1984, 2. Orth et al. 1988, 3. Holser et al. 1989, 4. Orth et al. 1988, 5. Alvarez et al. 1980, 6. Schmitz 1988, 7. Kyte et al. 1980, 8. Kyte and Wasson, 1986, 9. Izett, 1987, 10. Asaro et al. 1982, bd = below detection

References for Chapter 4

- Alvarez, L. W., W. Alvarez, F. Asaro and H. Michel. (1980). "Extraterrestrial cause for the Cretaceous-Tertiary extinction." Science. **208**: 1095-1108.
- Alvarez, W., F. Asaro and A. Montanari. (1990). "Iridium profile for 10 million years across the Cretaceous-Tertiary boundary at Gubbio (Italy)." Science. **250**: 1700-1702.
- Anders, E. and M. Ebihara. (1982). "Solar-system abundances of the elements." Geochim. Cosmochim. Acta. **46**: 2363-2380.
- Asaro, F., L. W. Alvarez, W. Alvarez and H. V. Michel. (1982). "Geochemical anomalies near the Eocene/Oligocene and Permo/Triassic boundaries." Geol. Soc. of Amer. Spec. Pap. **190**: 517-528.
- Barker, J. and E. Anders. (1968). "Accretion rate of cosmic matter from Ir and Os in deep sea sediments." Geochim. Cosmochim. Acta. **32**: 627-645.
- Berner, R. A. (1980). Early Diagenesis. Princeton, N.J., Princeton University Press.
- Bertine, K.K and K.K. Turekian. (1973). "Molybdenum in marine deposits." Geochim et Cosmochim. Acta. **37**: 1415-1434.
- Buckley, D. E. and R. E. Cranston. (1988). "Early diagenesis in deep sea turbidites: The imprint of paleo-oxidation zones." Geochim. Cosmochim. Acta. **52**: 2925-2939.
- Calvert, S. E. and N. B. Price. (1977). "Geochemical variation in ferromanganese nodules and associated sediments from the Pacific Ocean." Mar. Chem. **5**: 43-74.
- Cisowski, S.M. (1990). "A critical review of the case for and against extraterrestrial impact at the Cretaceous-Tertiary boundary." Surv. Geophys. **11**(1): 55-131.
- Colley, S., J. Thomson and J. Toole. (1989). "Uranium relocations and derivation of quasi-isochrons for a turbidite/pelagic sequence in the north east Atlantic." Geochim. Cosmochim. Acta. **53**: 1223-1234.
- Colley, S., J. Thomson, T. R. S. Wilson and N. C. Higgs. (1984). "Post-depositional migration of elements during diagenesis in brown clay and turbidite sequences in the North East Atlantic." Geochim. Cosmochim. Acta. **48**: 1223-1235.
- Collier, R.W. (1985). "Molybdenum in the Northeast Pacific Ocean." Limnol. Oceanogr. **30**:1351-1353.



Crank, J. (1970). The Mathematics of Diffusion. Oxford, Oxford University Press.

Crocket, J. H. (1981). Geochemistry of the platinum-group elements. Platinum Group Elements. Mineralogy, Geology, Recovery. Canadian Institute of Mining and Metallurgy.

Crocket, J. H. and H. Y. Kuo. (1979). "Sources for gold, palladium and iridium in deep-sea sediments." Geochim. Cosmochim. Acta. **43**: 831-842.

Crocket, J. H., C. B. Officer, F. C. Wezel and G. D. Johnson. (1988). "Distribution of noble metals across the K/T boundary at Gubbio, Italy; Ir variations as a constraint on the duration and nature of K/T boundary events." Geology. **16**(1): 77-80.

Dissanayake, C.B. and K. Kritsotakis. (1984). "The geochemistry of Au and Pt in peat and algal mats - a case study from Sri Lanka" Chem. Geol. **42**: 61-76.

Duursma, E. K. and C. J. Bosch. (1970). "Theoretical, experimental and field studies concerning diffusion of radioisotopes in sediments and suspended particles of the sea." Neth. J. Sea Res. **4**(4): 395-469.

Emerson, S. and S. Husted. (1991). "Ocean anoxia and the concentration of molybdenum and vanadium in seawater." Mar. Chem., in press.

Esser, B. K. (1991). Osmium Isotope Geochemistry of Terrigenous and Marine Sediments. PhD, Yale University.

Froelich, P. N., G. P. Klinkhammer, M. L. Bender, N. A. Luedtke, G. R. Heath, D. Cullen, P. Dauphin, D. Hammond, B. Hartman and V. Maynard. (1979). "Early oxidation of organic matter in pelagic sediments of the eastern equatorial Atlantic: suboxic diagenesis." Geochim. Cosmochim. Acta. **43**: 1075-1090.

Ganapathy, R. (1980). "A major meteorite impact on the Earth 65 million years ago: evidence from the Cretaceous-Tertiary boundary clay." Science **209**:921-923.

Goldberg, E. D., V. Hodge, P. Kay, M. Stallard and M. Koide. (1986). "Some comparative marine chemistries of platinum and iridium." Appl. Geochem. **1**: 227-232.

Gostin, V. A., R. R. Keays and M. W. Wallace. (1989). "Iridium anomaly from the Acraman impact ejecta horizon: impacts can produce sedimentary iridium peaks." Nature. **340**: 542-544.

Heggie, K., C. Maris, A. Hudson, J. Dymond, R. Beach and J. Cullen. (1987). Organic carbon oxidation and preservation in North West Atlantic continental margin sediments. Geology and Geochemistry of Abyssal Plains. London, Geological Society of London Special Publication.

- Hildebrand, A.R., W.V. Boynton, and W.H. Zoller. (1984). "Kilauea volcano aerosols: evidence in siderophile element abundances for impact-induced oceanic volcanism at the Cretaceous-Tertiary boundary." Meteoritics **19**: 239.
- Hodge, V. F., M. Stallard, M. Koide and E. D. Goldberg. (1985). "Platinum and the platinum anomaly in the marine environment." Earth and Plan.Sci.Lett. **72**: 158-162.
- Holser, W. T., H.-P. Schonlaub, M. Attrep, K. Boeckelmann, P. Klein, M. Magaritz, C. J. Orth, A. Fenninger, C. Jenny, M. Kralik, H. Mauritsch, E. Pak, J.-M. Schramm, K. Statterger and R. Schmoller. (1989). "A unique geochemical record at the Permian/Triassic boundary." Nature. **337**(6202): 39-44.
- Izett, G. (1987). "The Cretaceous-Tertiary boundary interval, Raton Basin, Colorado and New Mexico, and its shock-metamorphosed minerals: Implications concerning the K-T boundary impact-extinction theory." USGS Open File Report. **87-606**.
- Jarvis, I. and N. Higgs. (1987). Trace element mobility during early diagenesis in distal turbidites: late Quaternary of the Madeira Abyssal Plain, N. Atlantic. Geology and Geochemistry of Abyssal Plains. Geological Society Special Publication.
- Kennedy, H. A. and H. Elderfield. (1987). "Iodine diagenesis in non-pelagic deep sea sediments." Geochim. Cosmochim. Acta. **51**: 2505-2514.
- Koide, M., V. F. Hodge, J. Yang, M. Stallard, E. Goldberg, J. Calhoun and K. Bertine. (1986). "Some comparative marine chemistries of rhenium, gold, silver and molybdenum." Appl. Geochem. **1**: 705-714.
- Ku, T-L. and W.S. Broecker. (1969). "Radiochemical studies on manganese nodules of deep sea origin." Deep Sea Res. **16**: 625-638.
- Ku, T-L., K.G. Knauss and G.G. Mathieu. (1977). "Uranium in the open ocean: concentration and isotopic composition." Deep Sea Res. **24**: 1005-1018.
- Kyte, F.T., Z. Zhou and J.T. Wasson. (1980). "Siderophile-enriched sediments from the Cretaceous-Tertiary boundary." Nature. **288**: 651-656.
- Kyte, F. T. and J. T. Wasson. (1986). "Accretion rate of extraterrestrial matter: iridium deposited 33 to 67 million years ago." Science. **232**: 1225-1229.
- Langmuir, D. (1978). "Uranium solution-mineral equilibria at low temperatures with applications to sedimentary ore deposits." Geochim. Cosmochim. Acta. **42**: 547-569.
- Li, Y.-H., L. Burkhardt, M. Buchholtz, P. O'Hara and P. H. Santschi. (1984). "Partition of radiotracers between suspended particles and seawater." Geochim. Cosmochim. Acta. **48**: 2011-2019.

Li, Y.-H. and S. Gregory. (1974). "Diffusion of ions in seawater and in deep sea sediments." Geochim. Cosmochim. Acta. **38**: 703-714.

Martin, C. E. (1990). Rhenium-Osmium Isotope Geochemistry of the Mantle. PhD, Yale University.

Maynard, J. B. (1983). Geochemistry of Sedimentary Ore Deposits. Springer-Verlag.

Orth, C. J., M. Attrep, X. Y. Mao, E. G. Kauffmann, R. Diner and W. P. Elder. (1988a). "Iridium abundance maxima in the Upper Cenomanian extinction interval." Geophys. Res. Lett. **15**(4): 346-349.

Orth, C. J., L. R. Quintana, J. S. Gilmore, J. E. Barrick, J. N. Hayward and S. A. Spesshardt. (1988b). "Pt-group metal anomalies in the Lower Mississippian of southern Oklahoma." Geology. **16**: 627-630.

Playford, P. E., D. J. McLaren, C. J. Orth, J. S. Gilmore and W. D. Goodfellow. (1984). "Iridium anomaly in the Upper Devonian of the Canning Basin, Western Australia." Science. **226**: 437-439.

Ravizza, G. (1991). Rhenium and Osmium Geochemistry of Modern and Ancient Organic-Rich Sediments. PhD, Yale University.

Ravizza, G. and K. K. Turekian. (1989). "Application of the  $^{187}\text{Re}$ - $^{187}\text{Os}$  system to black shale geochronometry." Geochim. Cosmochim. Acta. **53**: 3257-3262.

Rocchia, R., D. Boclet, P. Bonte, C. Jehanno, Y. Chen, V. Courtillot, C. Mary and F. Wezel. (1990). "The Cretaceous-Tertiary boundary at Gubbio revisited: vertical extent of the Ir anomaly." Earth and Plan. Sci. Lett. **99**: 206-219.

Schmitz, B. (1985). "Metal precipitation in the Cretaceous-Tertiary boundary clay at Stevns Klint, Denmark." Geochim. Cosmochim. Acta. **49**: 2361-2370.

Schmitz, B., P. Anderson and J. Dahl. (1988). "Iridium, sulfur isotopes and rare earth elements in the Cretaceous-Tertiary boundary clay at Stevns Klint, Denmark." Geochim. Cosmochim. Acta. **52**: 229-236.

Shaw, T. J., J. M. Gieskes and R. A. Jahnke. (1990). "Early diagenesis in differing depositional environments: The response of transition metals in pore water." Geochim. Cosmochim. Acta. **54**: 1233-1246.

Taylor, S.R., S.M. McLennan and M.T. McCulloch. (1983). "Geochemistry of loess, continental crustal composition and crustal model ages." Geochim. et Cosmochim. Acta. **47**: 1897-1905.

Thomson, J., N. C. Higgs and S. Colley. (1989). "A geochemical investigation of reduction haloes developed under turbidites in brown clay." Mar. Geol. **89**: 315-330.

Thomson, J., N. C. Higgs and I. W. Croudace. (1991). "Zonation of redox-sensitive elements at the oxic/post-oxic interface in deep-sea sediments." in prep.

Turekian, K.K. (1982). "The potential of  $^{187}\text{Os}/^{186}\text{Os}$  as a cosmic vs. a terrestrial indicator in high Ir layers of sedimentary strata." Geol. Soc. Amer. Spec. Paper **190**: 243-249.

Wallace, M. W., V. A. Gostin and R. R. Keays. (1990). "Acraman impact ejecta and host shales: Evidence for low-temperature mobilization of iridium and other platinoids." Geology. **18**: 132-135.

Weast, R. C. (1988). CRC Handbook of Chemistry and Physics.

Wedepohl. (1978). "The Platinum Group" Handbook of Geochemistry. Springer-Verlag.

Westland, A. D. (1981). "Inorganic chemistry of the platinum-group elements." Can. Inst. Mining and Mineral. Spec. Vol., L. Cabri ed. **23**: 7-18.

Wilson, T. R. S., J. Thomson, S. Colley, D. J. Hydes, N. C. Higgs and J. Sorenson. (1985). "Early organic diagenesis: the significance of progressive subsurface oxidation fronts in pelagic sediments." Geochim. Cosmochim. Acta. **49**: 811-822.

## Chapter 5

---

### The marine geochemistry of Re: 1. Sources

Note: The determination of Re in the Orinoco and Amazon Rivers and in seawater was carried out by Julian Sachs, who did his Senior Thesis on this subject, under my supervision. His results will be included here for ease of reference.

#### 5.1 Abstract

Recent work has suggested that Re may be a sensitive indicator of anoxic conditions in ancient sediments, and that its concentrations might reflect the oxygen content of past oceans and atmospheres (Koide et al, 1986). The utility of Re as a paleoredox tracer hinges on its strong enrichment in anoxic relative to oxic sediments (by a factor of ~500) however, virtually nothing was known about the rest of its geochemical cycle. The magnitude and controls of the riverine source of Re to the ocean, as well as its distribution in seawater were therefore explored here.

Mainstream Re concentrations for the Orinoco, Amazon and Ganges-Brahmaputra Rivers lie between 1 and 10 pM, with a water flux-weighted average of approximately 2.5 pM. This leads to a calculated residence time for the element of approximately 750 ky, in agreement with conservative Re profiles in the Atlantic and Pacific Oceans determined in this study. The highest riverine Re contents were observed in the Andean tributaries of the Orinoco River, and appear to be related to the weathering of black shales. Re correlates strongly with  $\text{SO}_4$  in these rivers, with a Re/S ratio similar to that in black shales, suggesting congruent weathering of Re and sulfide from these rocks. High concentrations (up to 120 pM) were also observed in rivers draining into the Black Sea. It is proposed that the origin of the Re enrichment in these rivers is anthropogenic.

## 5.2 Introduction

The marine geochemistry of rhenium is characterized by a number of features which suggest its utility in studies of ancient anoxic environments. Despite its low crustal abundance (~0.4 ppb, Esser, 1991), Re occurs in relatively high concentrations in seawater (45 pM), due to the solubility of the perrhenate anion ( $\text{ReO}_4^-$ ) in oxidizing aqueous environments. Based on parallels between Mo and Re chemistry, Koide et al. (1987) predicted that Re should have a long residence time in seawater, and thus behave conservatively in the ocean (ie., covary with salinity). They could not demonstrate this, however, because of large uncertainties in their data and the complete absence of information about Re concentrations in major rivers.

Re is removed from solution under anoxic conditions leading to concentrations in marine organic-rich sediments of approximately 50 ppb (Koide et al., 1986 and Ravizza, 1991). In organic-poor pelagic sediments, Re concentrations appear to be depleted compared to crustal values (0.4 ppb), with concentrations less than 0.1 ppb (Koide et al., 1986). The enrichment factor of Re in anoxic sediments compared to pelagic sediments is greater than that for other elements, such as uranium and molybdenum which, like Re, are relatively enriched in anoxic marine deposits. This factor (ppb anoxic sediment / ppb oxic sediment) is approximately 500 for Re and 50 for U and Mo.

The general similarities between the geochemistries of these three elements suggest that they may be used together to help reconstruct aspects of the environment of deposition of organic-rich sediments. A better understanding of the details of their behaviors in surficial environments may reveal differences among the three that can be exploited in paleoenvironmental studies. For example, although all three elements behave conservatively in

seawater, and are enriched in anoxic sediments, there are significant differences in their relative concentrations among modern and ancient organic rich sediments. These differences may provide insight into the redox state of the sediments, sedimentary sources or diagenetic processes. Our present comprehension of the geochemistry of these elements is insufficient to warrant their use in this manner, however, with our knowledge of Re geochemistry lagging furthest behind.

This chapter begins to fill some of the gaps in our knowledge of Re geochemistry by presenting data for the Orinoco, Amazon and Ganges-Brahmaputra Rivers, as well as two detailed open ocean profiles. A survey of Re in tributaries of these major rivers, especially in the Orinoco basin, enables an assessment of the continental sources of the element. Measurements of Re in an Amazon estuarine transect and in time-series samples from Chesapeake Bay allow initial evaluation of Re behavior in the estuarine environment. These results, coupled with the anoxic sediment data of Ravizza (1991) and Koide et al. (1986) make it possible to construct a rough ocean budget for Re.

### **5.3 Methods**

#### *Sample collection and storage*

Sampling protocols for the waters included in this study varied widely, as most of the samples analyzed were collected for other purposes. Pole sampling, Niskin bottles and Go-Flo bottles were used to collect different samples with no discernible biases among the methods. A comparison of acidified and unacidified samples from the Orinoco River showed that Re values were unaffected by storage at different pH's (compare TE and MA samples for the same rivers in Table 5.2). All acid added to samples was triply distilled.

Samples collected for this work were spiked with  $^{187}\text{Re}$  tracer upon collection, whereas others were spiked at least 24 hours before pouring through anion exchange columns. The variety of sampling procedures used, and the consistency among results regardless of procedure, suggests that Re is very stable in solution during storage in polyethylene and that it is relatively unsusceptible to contamination in the field.

Orinoco: Samples were collected during seven expeditions between March, 1983 and February, 1988 at the locations listed in Table 5.1, and illustrated in figure 5.1. Trace element (TE) samples were filtered through 0.4  $\mu\text{m}$  Nuclepore filters into acid-leached 500 mL high density polyethylene (HDPE) bottles and acidified with 2 mL triply distilled 6N HCl. Major element samples (MA) were filtered through 0.45  $\mu\text{m}$  Millipore filters into hot-water leached 500 mL HDPE bottles.

Amazon: Estuary samples were collected during the AMASEDS Expedition in the summer of 1989. 500 mL samples were filtered through 0.22  $\mu\text{m}$  Millipore Millipack filter cartridges and acidified with 2 mL 6N HCl. River samples were collected between 1976 and 1978 and stored in low density polyethylene bottles (figure 5.6).

Ganges - Brahmaputra: Samples were processed in the same manner as the Orinoco samples. Locations are shown in figure 5.7.

Chesapeake Bay: Time series samples from the North Basin of Chesapeake Bay were collected during 1988 and 1989 and filtered through 0.22  $\mu\text{m}$  Millipore Millipak filter cartridges, and acidified in the field. The water column profile was collected in July of 1990, aboard the RV Warfield, filtered through 0.4  $\mu\text{m}$  Nuclepore filters and acidified with 1 mL 16N  $\text{HNO}_3$  per 100 mL. Samples were stored in acid-leached HDPE bottles.



Black Sea and Soviet rivers: Black Sea profiles were collected at two stations (Stns. 2 and 6) in the summer of 1989. They were filtered through 0.4  $\mu\text{m}$  filters and acidified at sea. Soviet river samples were collected during the summer of 1990. Samples were filtered through 0.1  $\mu\text{m}$  Nuclepore filters into acid-leached HDPE bottles and acidified with 2 mL 6N HCl per 500 mL. Station locations are shown in figures 5.14 and 5.16.

Seawater samples: North Atlantic (32°10'N; 64°30'W) samples were collected in May 1990. Unfiltered samples were acidified with 12.5 mL 6N HCl per liter. North Pacific (24°16'N; 169°32'E) samples were collected on May 10, 1985. One liter samples were acidified with 4 mL 6N HCl. All samples were collected and stored in acid-leached HDPE bottles.

#### *Anion exchange preconcentration*

Samples were purified and preconcentrated using anion exchange of  $\text{ReO}_4^-$ , as described in Chapter 2. Initial experiments demonstrated that standards acidified to pH's of 3.1, 1.8 and 0.5 (the approximate pH's of spiked unacidified and acidified samples) were recovered with the same efficiency from the anion exchange step (Sachs 1991). Sample volumes varied depending on sample availability and Re concentration, but were typically 50 mL for Orinoco, Amazon and seawater samples, and 10-30 mL for samples from other areas. Eluted samples were evaporated to a small drop, taken up in 250  $\mu\text{L}$  0.8 N  $\text{HNO}_3$  and stored in conical teflon vials or in snap-top polypropylene centrifuge vials until analysis.

#### *Mo measurement*

Mo was determined in several of the river samples using isotope dilution-ICP-MS.  $^{95}\text{Mo}$  spike was obtained from US Services, Inc. (via G. Ravizza). The

$^{95}\text{Mo}/^{98}\text{Mo}$  ratio was measured for isotope dilution calculations,  $^{98}\text{Mo}$  being the most abundant isotope of the element. The  $^{95}\text{Mo}/^{98}\text{Mo}$  of natural waters (0.652) is assumed to be dictated by the natural abundance of the isotopes, whereas this ratio in the spike is 153 (US Services). The "ideal" spiking ratio (determined from the geometric mean of spike and sample 95/98 ratios) is 10, and samples were spiked to a ratio of 8. Mass 95 is subject to isobaric interference from  $^{79}\text{BrO}$ , but this was not a problem in river waters. River water samples were run directly, without dilution or preconcentration. 0.5 - 1 mL samples were spiked with an appropriate amount of  $^{95}\text{Mo}$  and run in 250  $\mu\text{L}$  aliquots by flow-injection ICP-MS.

#### **5.4 Results and Discussion**

##### *Sources of Re to rivers*

Re was determined in the Orinoco, Amazon and Ganges-Brahmaputra river basins, with the most detailed coverage in the Orinoco basin. In order to identify important sources of the element, Re concentrations were determined in rivers draining a variety of lithologies. Re is known to be concentrated in organic-rich sediments and sedimentary rocks (Koide et al., 1986 and Ravizza and Turekian, 1989) as well as in molybdenite deposits and some copper sulfide and uraninite occurrences (Morris and Short, 1978). Of these, only organic rich sedimentary rocks (black shales) are probably of great enough extent to be of more than local importance. Because river waters integrate a relatively large land area in their chemistries, and since Re is relatively mobile in oxic waters, the rivers can be used to prospect for unaccounted-for repositories of the element.

In cases where the source of elevated riverine Re concentrations is not clear from geologic maps, Re may be compared to other chemical species whose sources are better constrained. For example, high  $\text{SO}_4$  and  $\text{SO}_4/\text{Cl}$  ratios in rivers are generally indicative of black shale weathering. Re may also be compared to U and Mo concentrations, as these elements are also relatively mobile and are enriched in organic-rich sediments. In the next sections, the major lithological features of each drainage basin will be summarized, as well as those aspects of the riverine chemistry relating to Re sources.

*a) Orinoco River, Venezuela*

The Orinoco River is the third largest in the world in terms of water discharge, and its basin occupies 830,000 km<sup>2</sup> in Venezuela and Colombia. The Venezuelan portion of the basin can be divided into four lithologically distinct regions. The river forms the northern and western boundaries of the Precambrian Guyana Shield (region 1 in figure 5.1). The terrain here is deeply weathered and is covered by thick jungle, with savannah in the higher elevations, hence the geology is only known in outline (Gibbs and Barron, 1983; and Palmer and Edmond in prep.). The basement consists largely of Proterozoic rocks, including greenstone belts in the eastern part of the Shield and the Parguazan rapakivi granitic batholith in the western portion. Mafic intrusions, hosted by quartzites and conglomerates which mantle the basement rocks (the Roraima Formation), are exposed in the eastern Shield. Weathering of the Shield region occurs slowly in the sub-surface, with river chemistries indicating nearly complete alteration of basement rocks to gibbsite, quartz and kaolinite (Palmer and Edmond, 1991; Edmond et al., in prep.)

The northwestern left bank tributaries of the Orinoco arise in the Venezuelan Andes (region 3 on map). The origin of this mountain range is

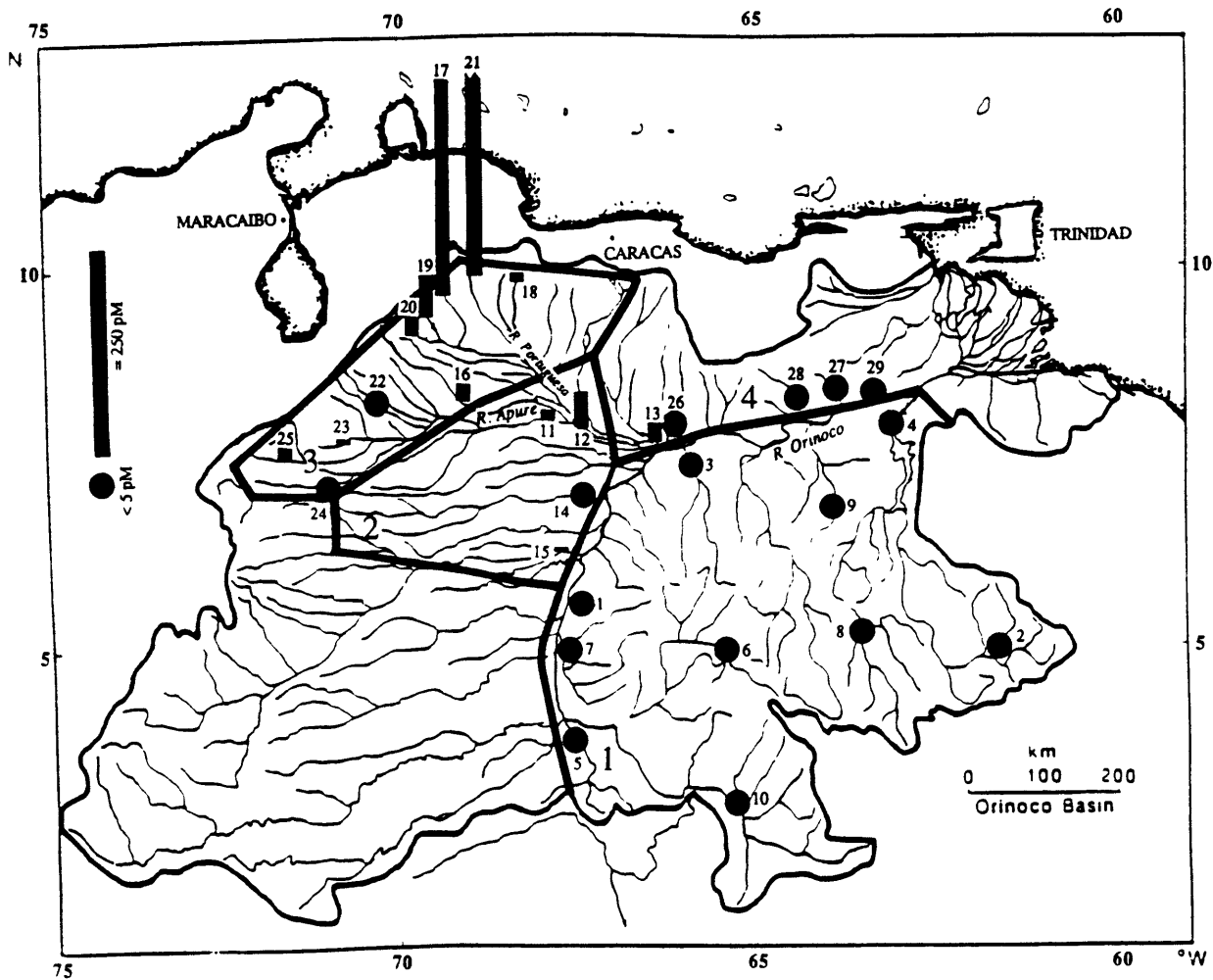


Figure 5.1 Map of the Orinoco River Basin. The basin has been divided into four regions based on drainage lithology. Re concentrations in various tributaries are indicated by the height of the bar at sampling locations. Concentrations less than 5 pM are indicated by a filled circle. Symbol key is at the left, within the map. The small number next to each symbol is the river number, as in Tables 5.1, 5.2 and 5.3.

Table 5.1 Rivers in the Orinoco Basin in which Re was measured

Region	Map Number	River	Date collected	Water Level
1	1	Cataniapo	Oct-84	Median: falling
1	2	Yuruman @ S. Ignacio	Oct-84	Median: falling
1	3	Cuchivero	Jun-87	Median-high: rising
1	4	Caroni @ Ordaz	Mar-83	Low
1	5	Atabapo	Oct-84	Median: falling
1	6	Ventuari @ Cacuri	Oct-84	Median: falling
1	7	Sipapo @ mouth	Oct-84	Median: falling
1	8	Paragua ab Karun	Oct-84	Median: falling
1	9	Aro ab falls	Oct-84	Median: falling
1	10	Padamo	Oct-84	Median: falling
2	11	Apure @ Portuguesa	Jun-87	Median-high: rising
2	12	Apure @ S. Fernando	Feb-88	Low
2	13	Apure @ el Perro	Oct-84	Median: falling
2	14	Capanaparo	Oct-84	Median: falling
2	15	Meta	Oct-84	Median: falling
3	16	Masparro @ Apure conf.	Feb-88	Low
3	17	Acariguau @ Rt. 5	Jun-87	Median-high: rising
3	18	Tamanaco near Macapa	Feb-88	Low
3	19	Ospino	Jun-87	Median-high: rising
3	20	Morador Rt. 5	Jun-87	Median-high: rising
3	21	Cojedes @ S. Rafael Rt. 5	Feb-88	Low
3	22	Canagua	Feb-88	Low
3	23	Caparo	Feb-88	Low
3	24	Flood plain Arauca	Oct-84	Median: falling
3	25	Uribante	Jun-86	Median: rising
4	26	Manapire	Oct-84	Median: falling
4	27	Caris	Oct-84	Median: falling
4	28	Pao	Oct-84	Median: falling
Mainstream	29	Orinoco @ C. Bolivar	Mar-86	Low

distinct from the subduction-related volcanism along western South America which produces the rest of the Andes chain. The shales and impure limestones which dominate the northern Andes were uplifted during the Neogene, probably as the result of the convergence of the Nazca and Caribbean plates (Case et al. 1990). The Andean rivers traverse a broad floodplain (region 2) before joining the main stream Orinoco. Further to the east and down river along the left bank lies the Eastern Venezuela Basin (region 4), which is made up of Oligocene to Pleistocene shales, reef limestones and sandstones, and is the location of petroleum wells and coal workings. The major ion chemistry of the left bank rivers is dominated by carbonate weathering, with a lesser influence from silicates, black shales and evaporites.

Re concentrations were found to span four orders of magnitude, from values below detection limits ( $<0.02$  pM) to 400 pM (Table 5.2). The lowest values were found in the Guayana shield region, as expected from the slow weathering of crystalline basement rocks which are most likely low in Re. The highest values were measured in rivers originating in the Venezuelan Andes, particularly in the drainage of the Portuguesa River. The headwaters of these rivers are distinguished by widely distributed exposures of Cretaceous black shales and bituminous limestones as well as Paleozoic evaporite deposits (Macellari and DeVries, 1987; and Tribovillard et al., 1991)(figure 5.2). This is reflected in the major ion chemistry of these rivers which have high calcium, sulfate and chloride (Edmond, 1991). Yee et al. (1987) reported that rivers in this region were highly enriched in selenium, which they related to a black shale source. Black shales are known to be enriched in Re (Poplavko et al., 1977; Ravizza and Turekian, 1989), and thus are a likely source of the high concentrations of Re in these rivers.

Table 5.2 Re, Mo, U and SO<sub>4</sub> in the Orinoco basin.

Map #	Sample#	Region#	Re (pmol/kg)	SD	Mo nmol/kg	SO <sub>4</sub> μmol/kg	U pmol/kg
1	549 MA	1	0.24			4.10	150
2	507 TE	1	0.40				37
3	826 TE	1	0.09			3.00	229
4	450 TE	1	0.03			1.20	89
5	545 MA	1	0.01				39
6	544 MA	1	0.06			4.10	83
7	580 MA	1	<0.02				199
8	506 TE	1	0.34				63
9	556 TE	1	0.02				59
10	584 MA	1	<0.02				156
11	822 TE	2	7.9				
	822 TE	2	9.1	0.6	6.4	78.14	297
12	924 TE	2	39.4				
	924 TE	2	38.4				
	924 MA	2	37.5	0.9	16.0	223.0	1589
13	523 TE	2	21.6		8.7	62.0	206
14	527 TE	2	0.8			4.60	52
15	532 TE	2	5.0		4.4	66.63	40
16	919 TE	3	21.9		10.9	264.0	3256
17	801 MA	3	253.2				
	801 MA	3	252.6				
	801 TE	3	256.6	2.2	102.5	1230.0	6333
18	901 TE	3	8.3				
	901 TE	3	8.2	0.03		45.0	258
19	802 TE	3	50.4			345.17	928
20	803 TE	3	21.9				
	803 MA	3	22.2	0.15		392.21	472
21	903 TE	3	411.8		24.6	1885.0	5787
22	912 MA	3	2.2				
	912 TE	3	2.0	0.1		30.0	95
23	914 TE	3	5.7			51.0	227
24	561 MA	3	3.4		1.8	73.7	46
25	788 MA	3	16.3		19.7	192.41	1140
26	522 TE	4	1.3			58.6	140
27	515 MA	4	0.3			4.2	153
28	517 TE	4	1.0			24.0	120
29	721 MA	Mainstream				71.61	
	736 MA		440			75.33	

Pooled standard deviation = 3.5%

where pooled standard deviation =  $\sqrt{\frac{\sum n_i (sd)_i^2}{\sum n_i}}$  and sd given in per cent

The mainstream Re measurement was made on 200 ml of water (100 ml from each sample), all other analyses were made on 50 ml of sample.

Re analyses from Sachs, 1991; SO<sub>4</sub> from Edmond et al., 1991 in prep.; U analyses from Palmer and Edmond, 1991, in prep.; Mo analyses this work.

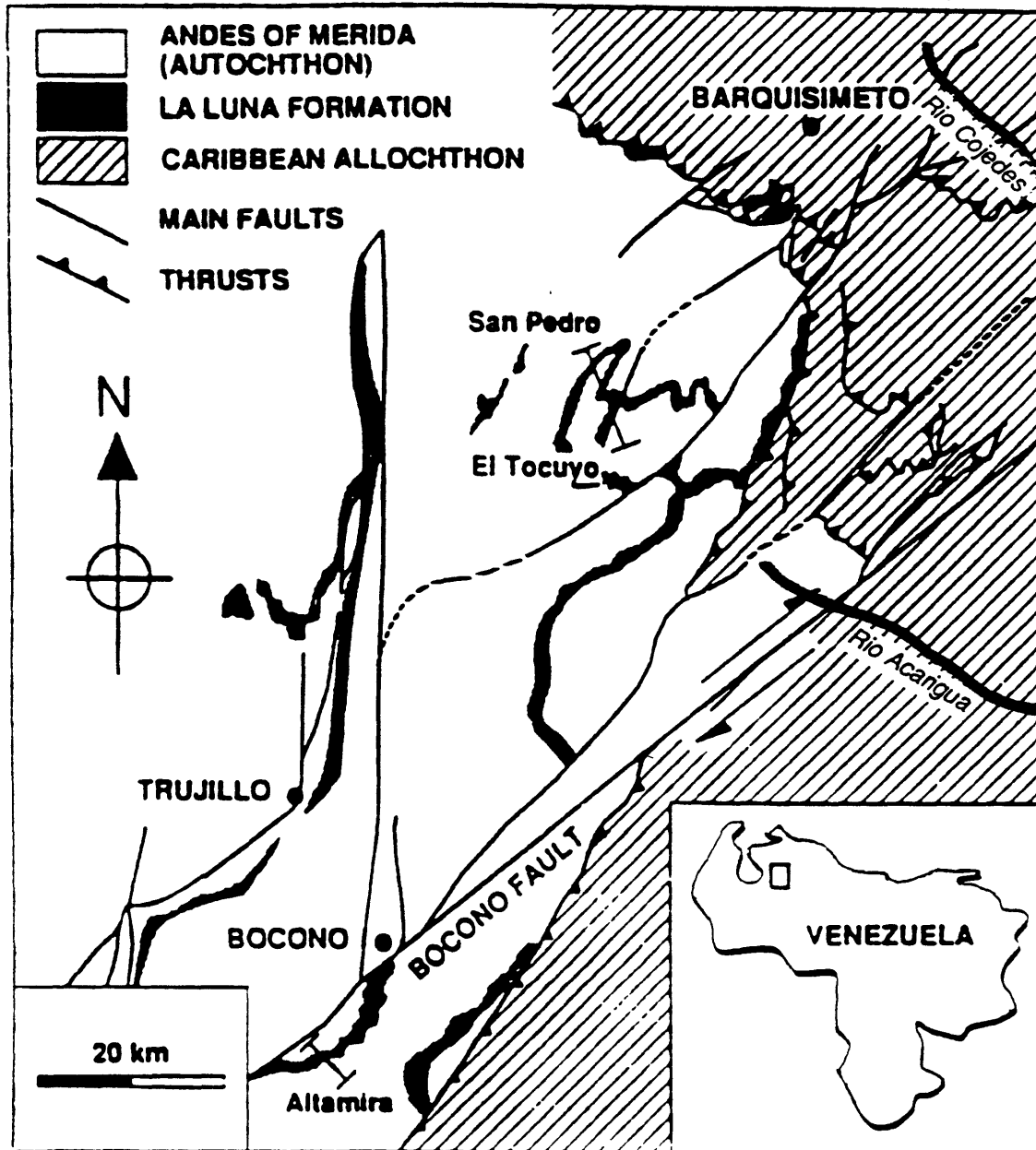


Figure 5.2 Location of Black Shale deposits (La Luna Formation) in the Venezuelan Andes. Approximate locations of high- $Re$  rivers shown.



Table 5.3 Re and ancillary data for Orinoco left bank rivers (regions 2,3,4)

Map #	River name	Samp.#	River#	Re pM	Na uM	K uM	Mg uM	Ca uM	Cl uM	SO4 uM
11	Apure @ Portuguesa	822	1110	8.5	102.21	37.74	89.15	335.21	19.73	78.14
12	Apure @ S.Fernando	924	1102	38.0	259.00	46.31	185.70	598.60	63.02	223.30
13	Apure @ el Perro	523	1101	21.6	108.90	49.70	110.00	366.00	18.40	62.00
14	Capanaparo	527	1031	0.8	27.30	9.00	22.04	31.40	9.00	4.60
15	Meta	532	1011	5.0	53.40	15.80	44.30	128.80	40.75	66.63
16	Masparro @ Apure conf.	919	1431	21.9	382.40	58.77	252.90	816.19	36.65	263.50
17	Acarigua @ Acarigua	801	1341	253.0	118.96	12.20	108.38	2008.80	9.55	1230.00
18	Tamanaco near Macapo	901	1233	8.2	327.20	90.50	953.70	433.27	108.60	44.74
19	Ospino	802	1321	50.4	213.43	13.73	129.70	1010.00	16.05	345.17
20	Morador Rt. 5	803	1331	22.0	191.97	14.21	238.26	789.06	13.88	392.21
21	Cojedes @ S.Rafael Rt.5	903	1201	411.8	1593.40	66.90	637.60	2855.48	887.58	1885.05
22	Canagua	912	1501	2.1	144.46	25.60	43.80	96.42	16.57	29.70
23	Caparo	914	1531	5.7	121.84	19.60	102.60	322.96	24.60	50.50
24	Flood plain Arauca	561	1051	3.4	72.10	18.50	70.00	148.00	11.70	73.70
25	Uribante	788	1561	16.3	197.78	23.74	168.86	702.93	33.44	192.41
26	Manapire	522	1611	1.3	97.20	25.50	43.18	36.10	3.70	58.60
27	Caris	515	1641	0.3	248.00	77.70	34.40	12.50	226.00	4.20
28	Pao	517	1631	1.0	217.00	85.90	61.60	22.70	154.00	24.00
29	Orinoco @ C. Bolivar	721	2000	4.4	84.30	20.93	49.20	131.25	38.31	71.61
29	Orinoco @ C. Bolivar	736	2000	4.4	84.70	20.41	48.93	128.82	34.37	75.33

Table 5.3 continued

River name	At ueq/L	Si uM	pH	87/86	Sr nM	Se pM	U pM	Mo nM
Apure @ Portuguesa	780	142.45	6.70	0.7148	561.0		297	6.4
Apure @ S.Fernando	1319	166.93	7.26	0.7136	734.0		1589	16.0
Apure @ el Perro	943	191.00	7.11	0.7128	753.0	1378	206	8.7
Capanaparo	104	97.00	6.38	0.7196	77.9	400	52	
Meta	206	102.00		0.7159	207.0	798	40	4.4
Masparro @ Apure conf.	1981	192.19	7.70	0.7142	708.0		3256	10.9
Acarigua @ Acarigua	1783	142.14	6.70	0.7101	4130.0	5000	6333	102.5
Tamanaco near Macapo	2733	611.29	8.28				258	
Ospino	1857	178.52	6.90	0.7100	2074.0		928	
Morador Rt. 5	1495	149.01	6.80	0.7109	1779.0	5000	472	
Cojedes @ S.Rafael Rt.5	3707	237.24	7.63	0.7098	9000.0		5787	24.6
Canagua	366	270.74	8.35	0.7239	159.0	200	95	
Caparo	836	191.10	7.48	0.7154	330.0	400	227	
Flood plain Arauca	348	105.00		0.7175	326.0		46	1.8
Uribante	1525	152.67		0.7135	907.0	700	1140	19.7
Manapire	173	240.00	6.54	0.7114	138.0	900	140	
Caris	163	489.42	5.78	0.7178	131.0		153	
Pao	249	421.01	7.24	0.7164	171.0		120	
Orinoco @ C. Bolivar	264	125.35		0.7180	200.0	500	100	
Orinoco @ C. Bolivar	251	124.89				500		

All data except Re and Mo from Palmer and Edmond, 1991 and Edmond et al. in prep.

Re concentrations correlate with both Ca and SO<sub>4</sub> in the rivers of regions 2, 3, and 4, as illustrated in figure 5.3 (data in Table 5.3). This covariation would be consistent with either an evaporite (gypsum) or black shale source for the element, however the Re/S molar ratio in the high-Re rivers ( $3 \times 10^{-7}$ ) is more like that of black shales ( $\sim 5 \times 10^{-7}$ ) than of seawater ( $2 \times 10^{-9}$ ) (using the black shale data of Ravizza, 1989). Moreover, the solubilities of the common salts of the perrhenate ion are all quite high. For example Ca(ReO<sub>4</sub>)<sub>2</sub>·2H<sub>2</sub>O is approximately 1000 times more soluble than CaSO<sub>4</sub>·2H<sub>2</sub>O (gypsum), and hence it is unlikely that Re would be concentrated in evaporites relative to sulfur, compared to their seawater values. The high SO<sub>4</sub>/Cl ratios of these rivers is additional evidence for the influence of black shale weathering.

Other elements which are enriched in black shales, such as U and Mo, roughly correlate with Re in the left bank rivers (figure 5.4). The Mo/Re and U/Re ratios in these rivers are lower than the corresponding ratios in modern organic-rich sediments or in seawater, indicating either that the shales being weathered have Mo/Re and U/Re ratios which are lower than modern sediments, or that Re is more easily dissolved than U and Mo. Given the range in these elemental ratios in some ancient black shales, and the lack of relevant data for the Venezuelan shales, either of these explanations is possible (Table 5.4). Enhanced mobility of Re over Mo was observed by Morachevskii and Necheva (1960) in the groundwaters abutting molybdenite deposits and in laboratory leachates of molybdenite powders. Their results showed 10 - 100 fold enrichments of Re over Mo in groundwaters compared to the molybdenite ore. Similar results for Re and Mo in coals were obtained by Kuznetsova and Saukov (1961). Since all of the Orinoco samples were filtered, it is also possible that U and/or Mo are being transported adsorbed to the iron hydroxide

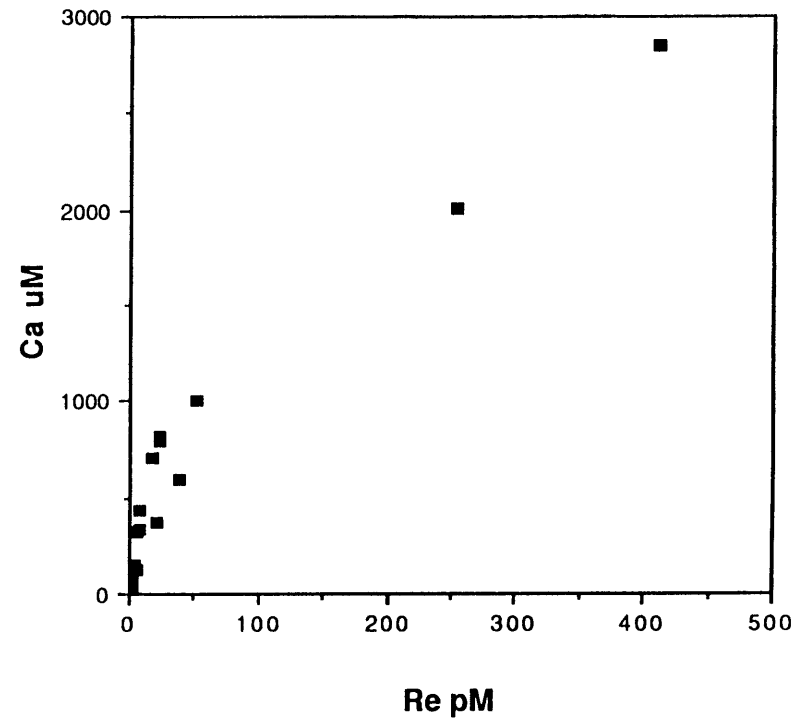
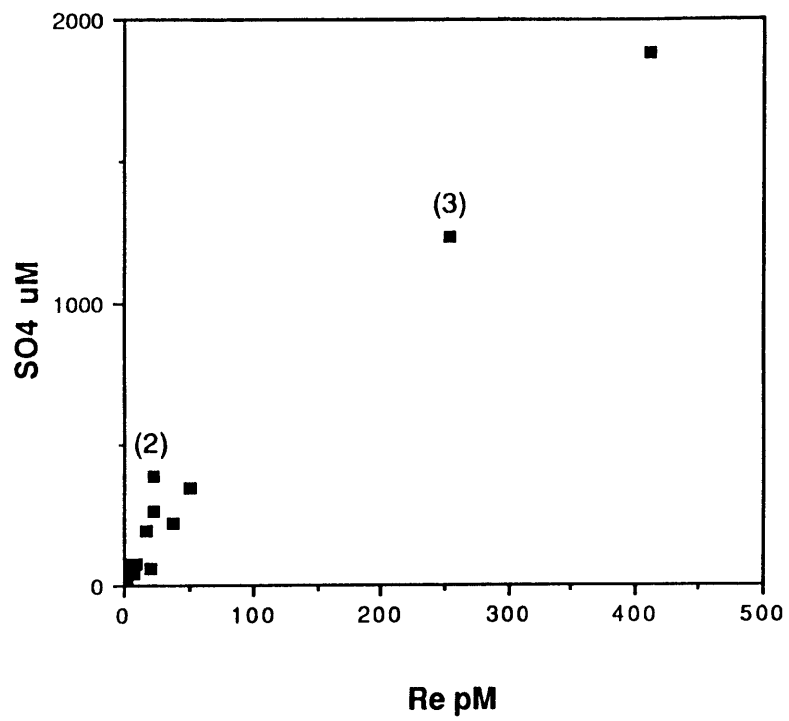


Figure 5.3 Re vs. Ca and SO<sub>4</sub> in left bank tributaries of the Orinoco River, after Sachs, 1991.

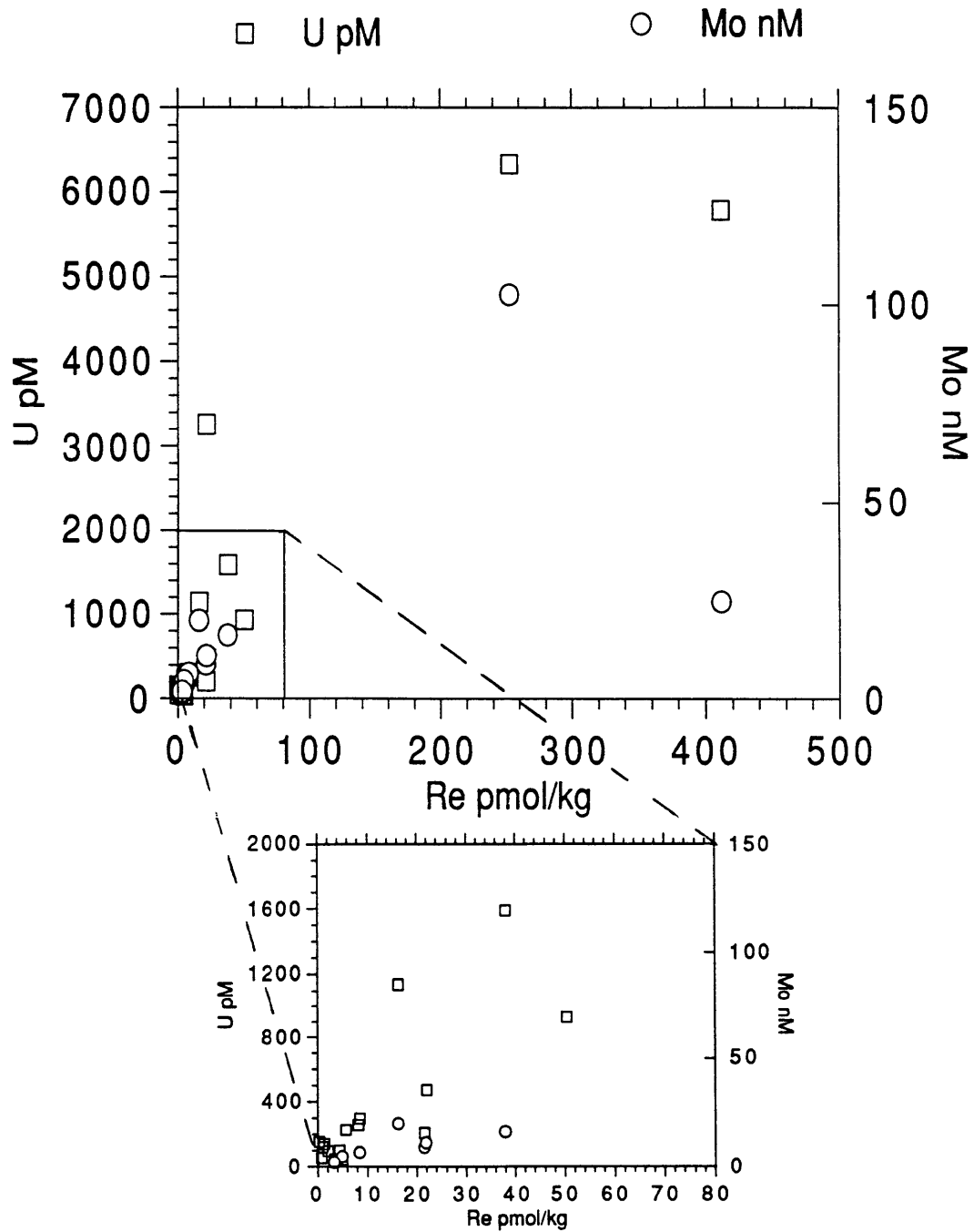


Figure 5.4 Re vs. Mo and U in the left bank tributaries of the Orinoco River.

Re:U;  $r^2 = 0.795$

Re:Mo;  $r^2 = 0.984$ , without the point at very high (411pM) Re

Table 5.4 Mo/Re and U/Re molar ratios for river waters, seawater and some ancient and modern organic-rich sediments

	Mo/Re	U/Re	Re	Mo	U
seawater	2000	300	45 pM	105 nM	14 nM
modern anoxic sed.	2000	400	50 ppb	50 ppm	25 ppm
<u>black shales:</u>					
Chattanooga Shale	700		100-300 ppb <sup>a</sup>	70 ppm <sup>b</sup>	
New Albany Shale	1500-20,000		70-900 ppb <sup>a</sup>	700 ppm <sup>c</sup>	
Devonian blk. sh.		10-150	70-900 ppb		5-15 ppm
<u>rivers:</u>					
Orinoco high Re rivers	60-400	10-30	250-400 pM		6 nM
Orinoco at C. Bolivar		25	4.4 pM		0.1 nM
Amazon endmember	4000	150	1.1 pM	4 nM <sup>d</sup>	0.15 nM <sup>e</sup>
Ganges highland rivers	1500	2000	10-15 pM	15-20 nM	20-30 nM

- a. Re data from Ravizza, 1991.
- b. Mo data from Vine and Tourtelot, 1970.
- c. Mo data from Holland, 1984 and references therein
- d. Bertine and Turekian, 1973
- e. McKee et al., 1987

coatings of suspended particles  $>0.4 \mu\text{m}$  in diameter to a greater degree than Re. Ferric oxyhydroxides are known to efficiently adsorb U from solution at pH's between 5 and 8 and to adsorb Mo to a lesser extent from pH 4-7 (Langmuir, 1978 and Kim and Zeitlin, 1969). Morachevskii and Novikov (1958) found that only 2% of a  $10^{-7}$  M solution of  $\text{ReO}_4^-$  was coprecipitated with  $\text{Fe}(\text{OH})_3$  at neutral pH. This lack of adsorption to Fe-oxides was also seen for Tc, which occurs above Re in the periodic table and is very similar in its chemistry to Re (Lieser and Bauscher, 1987; Huie et al., 1988; Brookins, 1986).

There is also a good correlation between Re and Sr (figure 5.5) in these rivers, similar to the Re/Ca relationship, which is likely due to the association of black shales with carbonate/evaporite sequences. Most of the left bank rivers have quite radiogenic Sr isotopic ratios,  $>0.71$  (Palmer and Edmond, in prep.). This ratio is higher than that of seawater at any time in the last 500 million years, and thus cannot derive from a purely seawater (carbonate, evaporite or scavenged component of black shale) source. Rivers with the lowest Sr (and lowest Re) have the highest  $^{87}\text{Sr}/^{86}\text{Sr}$  ratios (figure 5.5) due to a relatively small influence from marine sources and a stronger influence from radiogenic silicate rocks. The lowest 87/86 ratios in the entire Orinoco Basin are found in the Portugueza sub-basin where marine sources are relatively abundant. Within this sub-basin the most radiogenic rivers (the Cojedes and the Acarigua) are also those with extremely high Re concentrations. The higher 87/86 ratios in these two rivers compared to others in the sub-basin may be due to weathering of radiogenic silicate material within sulfidic black shales, as suggested by the high Re and high  $\text{SO}_4$  in these rivers.

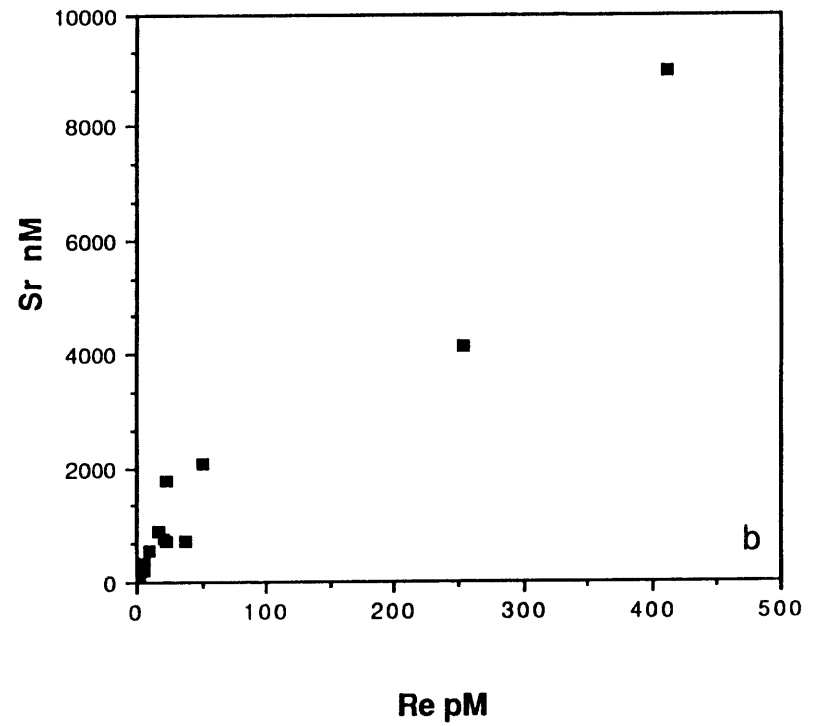
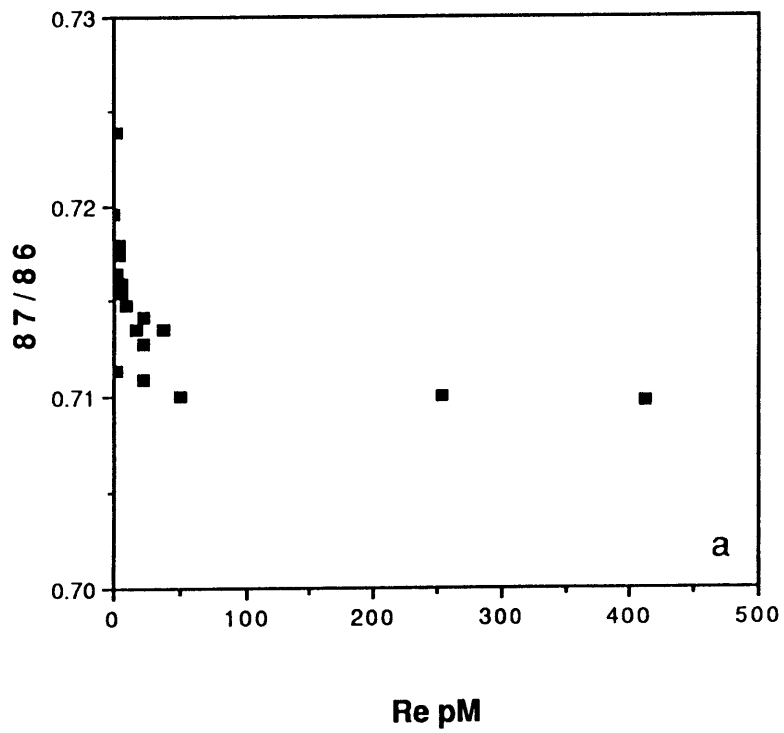


Figure 5.5 a. Re vs.  $^{87}\text{Sr}/^{86}\text{Sr}$  in Orinoco left bank tributaries b. Re vs. Sr concentrations in Orinoco left bank tributaries.



*b) Amazon River*

The Amazon River is the largest in the world in terms of water discharge and drainage area. Re was measured in a smaller set of samples from the western and southern edges of the Amazon basin (figure 5.6). The western samples (1-6) fall within the Marañon sub-basin, with headwaters lying in the Peruvian Andes. It is an area of complex geology, including metamorphosed Precambrian basement, Paleozoic shales and red beds and Mesozoic carbonates. Evaporite outcrops are common throughout the southern part of the basin (Huallaga River drainage) (Palmer and Edmond in prep; and Stallard 1980). The southern rivers sampled are within the Madeira sub-basin, with headwaters in the Bolivian Andes. The east-facing Andes here are dominated by Paleozoic sandstones, conglomerates and marine shales, with minor limestones and dolomites. Minor exposures of Cretaceous red beds, limestones and evaporites occur in the foothills, with igneous outcrops limited to Mesozoic granites in the high Andes (Palmer and Edmond in prep.). The major lithologies in the drainage area of each river sampled were summarized by Stallard and Edmond, 1983, and are listed in Table 5.5, along with the Re data.

Re concentrations vary between 2 and 46 pM in the 9 rivers analyzed. The relationship between Re and the presence of black shales is not as clear as in the Orinoco basin, nor is the correlation between Re and sulfate concentrations. Where high concentrations of Re are measured, the drainage areas contain black shales, although the converse is not true. Low Re levels in a saline spring (sample 4) draining evaporite deposits support the conclusion that evaporites are not an important source of Re. The highest Re concentration was measured in the headwaters of the Madeira sub-basin, where the major ion and Sr isotope composition is indicative of black shale weathering: high  $\text{Cl}+\text{SO}_4$ , high  $\text{SO}_4/\text{Cl}$ ,

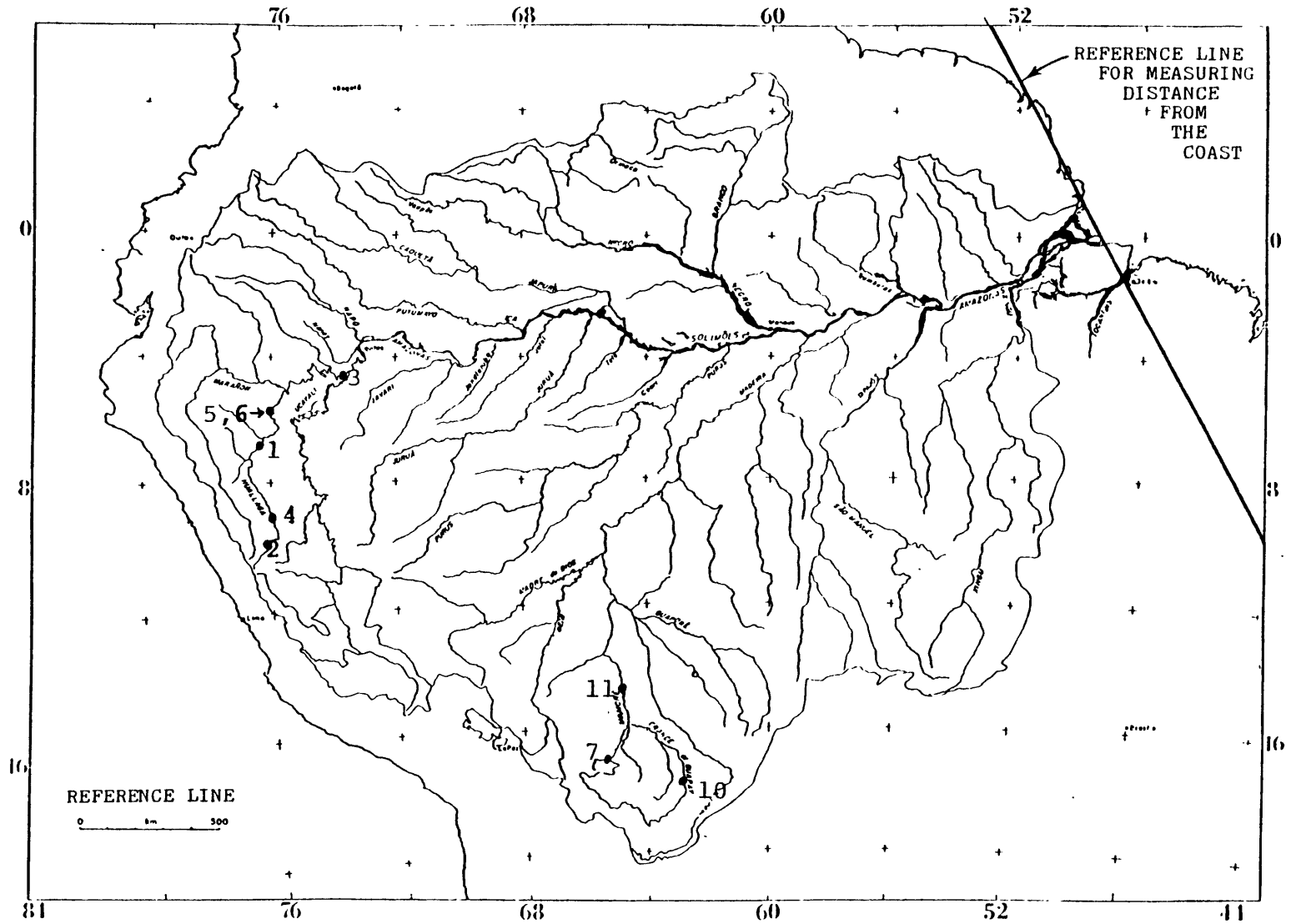


Figure 5.6 Map of the Amazon River Basin with sample locations shown.

Table 5.5 Amazon river Re data

Sample	Station	River	Re (pmol/kg)	Drainage lithology	SO <sub>4</sub> (μM)
1	BPA16	Cana	16.2	sst, drk sh, red beds, evap	2080
2	A2	Huallaga	19.9	metac, gg-blk sh, dark lst	246
3	BPA10	Maranon	3.5	metac, lst, gg-blk sh	52
4	A5	Salt spring Tingo Maria	2.9	evap	9300
5	BPA14	Shanusi	2.1	red beds, sh	37
6	BPA15	Paranapura	3.5	red beds, sh/sst	82
7	BPA02	Espiritu Santo	3.2	gg-blk sh/sst, lst, dolost	200
10	BPA05	Guapay/Grande	46.0	gg-blk sh, red-blk mudst, meta blk sh	2190
11	BPA04	Mamore	9.0	gg-blk sh, flu-lac, red beds, shield	306

relatively high silica, and radiogenic Sr (Stallard and Edmond 1983; and Palmer and Edmond, in press).

*c) Ganges-Brahmaputra Rivers*

The Ganges-Brahmaputra river system delivers the largest sediment load of any world river, and is the fourth largest in the world in terms of water discharge. The source of the Ganges is in the Kumaun Himalayas, from which it descends through the Siwalik range to alluvial plains (figure 5.7). The tributaries measured here include the Gomati, which joins the Ganges from the north, and the Yamuna and the Son which come in from the south. The Brahmaputra originates farther north, in the Tibetan Himalayas and flows parallel to the main Himalayan range until it descends to meet the Ganges through the Assam valley. The geology of the drainage area was reviewed by Sarin et al. (1989), and can be summarized as follows. The northern Kumaun Himalayas are composed of Cenozoic detrital rocks, consisting of coarsely bedded sandstones, conglomerates and clays. The central - lower Himalayas can be divided into three zones: an outer belt of carbonate rocks and sandstones of late Carboniferous age (Krol belt); an inner sedimentary belt of limestones, shales and quartzites of early Paleozoic age (Deoban-Tejam zone); and a belt of metamorphic and igneous rocks separating the two. On the right bank of the Ganges, the watershed consists of crystalline rocks of the Bundekhand Archean shield and Precambrian schists, gneisses, quartzites and marbles of the Vindhyan system. The geology of the high Tibetan Himalayas is poorly known, but the lithology of the southern slopes along the Brahmaputra river is dominated by reduced shales, gneisses and volcanic rocks.

The major ion composition of the Ganges indicates that river chemistry is controlled mainly by carbonate weathering, with Ca+Mg and HCO<sub>3</sub> making up

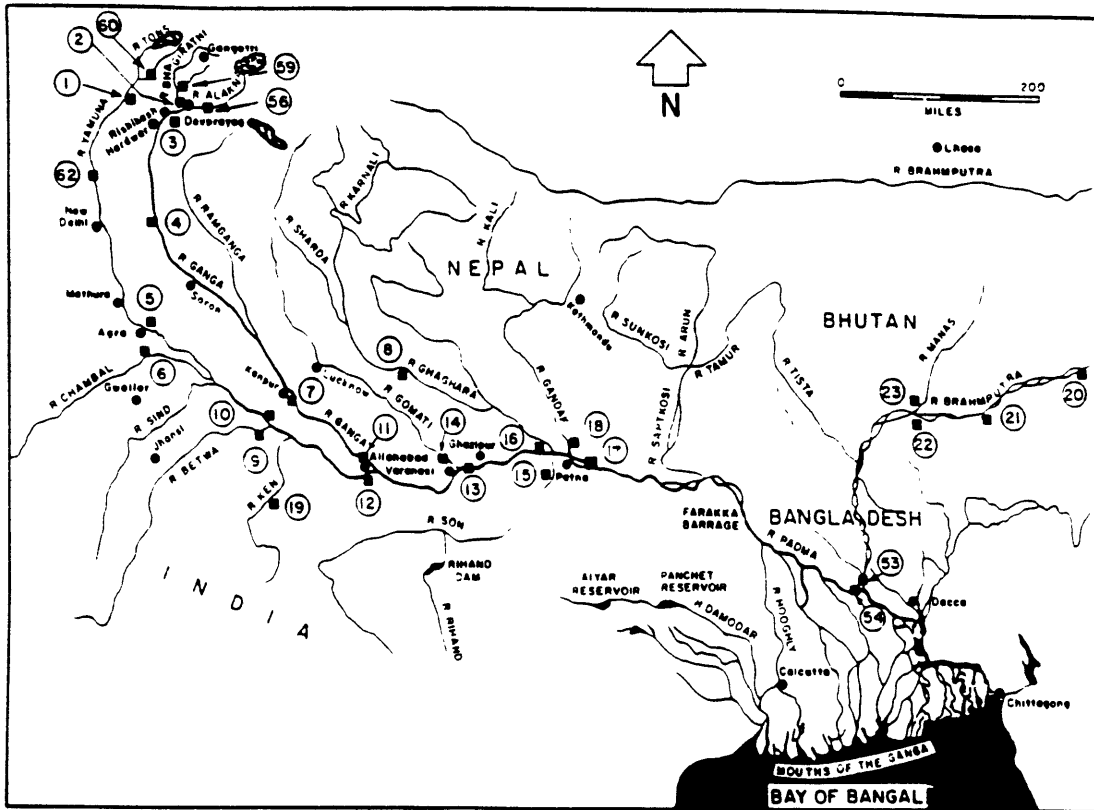



Figure 5.7 Sample location map in the Ganges-Brahmaputra River system. Numbers correspond to map numbers in Table 5.6.

 Approximate locations of black shale outcrops of the Lower Deoban Formation (early Paleozoic).

80-90% of the total dissolved cation and anion content of the river and its left-bank tributaries. Sarin et al. (1990) reported high uranium concentrations in some of these highland tributaries, especially in the Gomati River (up to 33 nM, compared to a seawater concentration of 14 nM and average river water concentrations between 1.2 and 2.5 nM). Due to the similarity of the ratio of uranium to total cations between the dissolved and suspended phases in the rivers they concluded that congruent weathering of U and major cations was taking place, although the source of this high uranium material was unclear. The average uranium content of suspended sediments they reported ( $50\mu\text{gU/g}\Sigma\text{Ca+Mg}$ ) is substantially higher than that of typical carbonate rocks ( $\sim 5\mu\text{gU/g}\Sigma\text{Ca+Mg}$ ).

Stratigraphic maps of the Kumaun Lesser Himalayas prepared by Rupke (1974) reveal that black shales of the lower Deoban formation crop out in the headwaters of some of the major tributaries, including the Gomati, the Sharda, the Alaknanda and the Tons. A black shale source for high uranium in these rivers is consistent with the location of these outcrops. Rupke maps a northwest-southeast trending exposure of the limestones and black shales of the lower Deoban following the course of the Gomati River, which contained the highest U in Sarin et al.'s study. The U content of the Alaknanda is slightly greater than that of neighboring rivers (8.4 nM vs. 6.7-7.4 nM) and the U concentration of the Yamuna increases from 7.1 to 10.5 nM after its confluence with the Tons. If it is the case that the only source of elevated ( $>\sim 5\text{pM}$ ) Re to rivers is black shales, as it appears to be in the South American rivers, then comparison of Re and U values in the Ganges-Brahmaputra rivers may provide a test of whether the high U in these rivers is black-shale derived.

Re values in the Ganges River and in a few of its major tributaries near their confluence with the main channel follow the same trend as uranium, with

higher levels in the highland rivers (Ganges and Gomati) and lower levels in a lowland river (Son) (figure 5.8 and Table 5.6). Ground waters from within the alluvial plain have elevated levels of both U and Re, which may be related to impregnation of the soils with alkaline and saline salts (Sarin, 1989). Although U concentrations reach values five times higher than any seen in the Orinoco, the highest Re value, in the Gomati river, is only 5% of the highest Orinoco levels. The  $U/SO_4$  ratios in the Ganges basin rivers are much higher than that in the high-U Orinoco tributaries as well (100 vs. 5), whereas the  $Re/SO_4$  ratios appear to be more similar (0.1 vs. 0.2). (Note however the small number of Re measurements within the Ganges basin.) Table 5.4 compares the U/Re ratio in Ganges rivers to that in the Orinoco and organic-rich sediments. Somewhat higher U/Re in the Ganges might be supported by the greater alkalinity of the Ganges rivers, and the ability of the carbonate ion to stabilize U in solution, however U concentration differences of a factor of five cannot be explained by this mechanism. It is also possible that the riverine loads of the elements are strongly influenced by alkaline soils, and that the elements are fractionated from each other during passage through these soils. According to Sarin (1989) all the rivers included here were sampled within areas affected by alkaline soils (figure 5.9). Alternatively, the different U/Re ratios may be evidence that the sources of the elements in the Orinoco and Ganges River basins are not analogous, and that there is an additional source of U in the Himalayan region, such as the gneisses and granites of the Kumaun Himalayas. Further analysis of rivers upstream from the salt-enriched alluvium, and of the black shales and crystalline rocks of this region would help to clarify the sources of these elements.

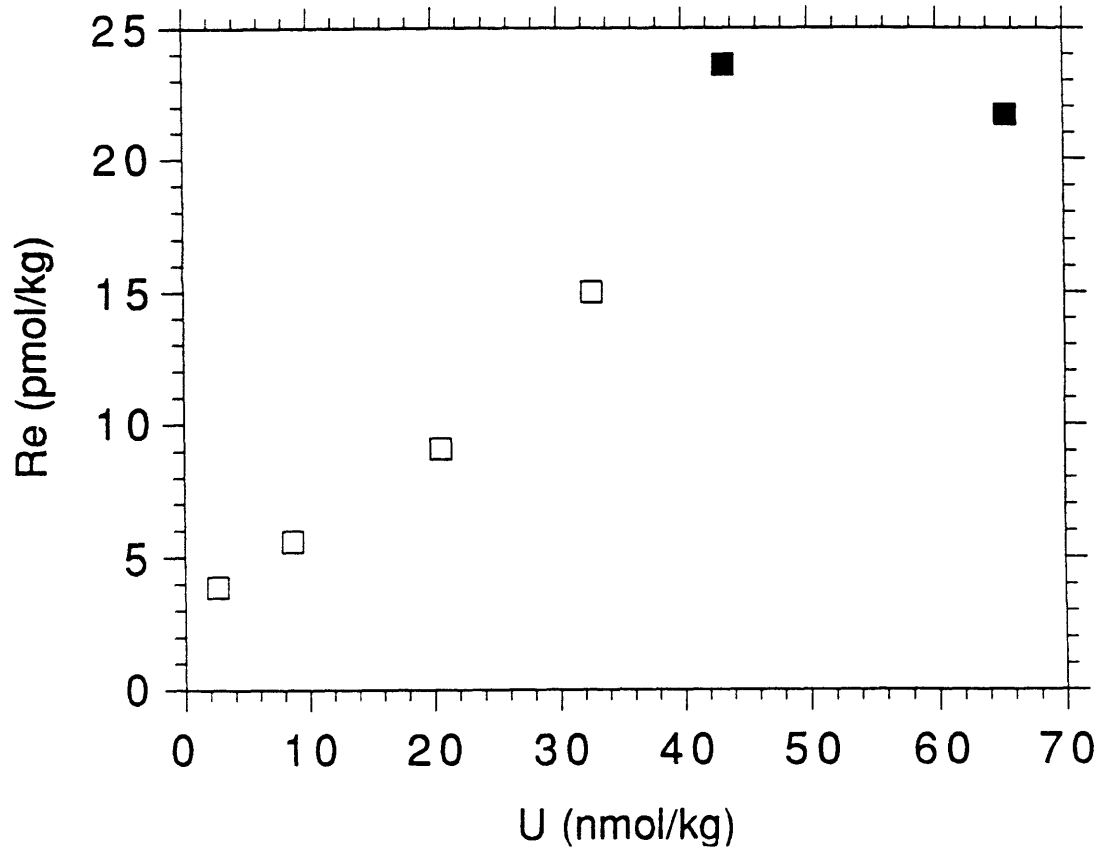


Figure 5.8 Re and U in rivers and ground waters of the Ganges-Bramaputra River systems. Darkened squares are groundwater samples

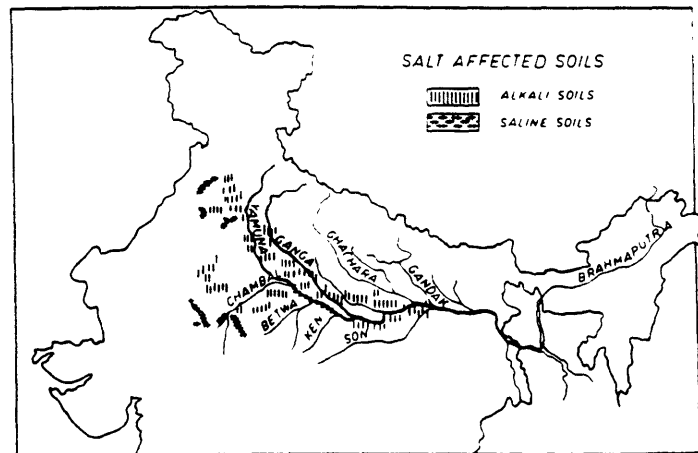


Figure 5.9 Salt affected soils in the Ganges-Yamuna River Basin. All the samples in this study, excluding the samples at the Ganges-Brahmaputra confluence (53 and 54) come from rivers or groundwaters in regions with alkaline soils.



Table 5.6 Re in the Ganges-Brahmaputra river system

Samp.#	Map#	River	Re pmol/kg	Mo nmol/kg	U pmol/kg	HCO <sub>3</sub> μM	SO <sub>4</sub> μM	Collection date
1	15	Son (Patna)	3.9		2605	1971	37	3/82 or 11/83
5	14	Gomati (Dobni)	15.0	22.1	32668	3939	250	11/83
12 <sup>G</sup>	5	Yamuna (Agra)	23.6	22.9	43403	4104		11/83
15 <sup>G</sup>	4	Ganges (Garhmukteshwar)	21.7		65420	6372		11/83
2	17	Ganges (Patna)		14.6	12080	2802	150	3/82
14	54	Ganges (Aricha Ghat)	9.1		20588	2851		11/83
13	53	Brahmaputra (Aricha Ghat)	5.6		8698	1642		

G = ground water

Uranium and carbonate and sulfate data from Sarin et al., 1990 and Sarin et al., 1989

*Behavior of Re in the estuarine environment*

The riverine contribution of trace elements to the oceans can be modified substantially by chemical and physical processes within estuaries (Boyle, et al., 1982; Sholkovitz, 1976; Honor and Chan, 1977). Even elements which display conservative behavior in seawater and are fairly mobile under fresh water conditions, such as U, can be added to or removed from the dissolved phase within estuarine systems. These effects can be very sensitive to the conditions in a particular estuary. For example, McKee et al. (1987) showed that dissolved U concentrations are enhanced in the Amazon Estuary due to mobilization of U from reducing shelf sediments, whereas Butts and Moore (1988) demonstrated that U was removed from the dissolved phase into sediments within the Ganges-Brahmaputra mixing zone.

Re was measured in 13 surface samples from the Amazon Estuary, covering a range of salinity from 0 to 36.4 ppt. If there are no sources or sinks of Re within the estuary, Re concentrations will vary linearly with salinity, forming a straight mixing line between river water and open ocean concentrations. The results (reported in Table 5.7 and illustrated in figure 5.10) show that Re is nearly conservative through the outer portion of the mixing zone. However, three points at low salinity show a positive departure from the linear mixing line, suggesting a source of Re to the dissolved (<0.22  $\mu\text{m}$ ) phase within the inner Amazon shelf. This could be due to desorption of Re from suspended sediments within the water column, or could represent a flux of Re out of shelf sediments. If these samples are generally representative of the Amazon, the desorptive flux is approximately four times the dissolved flux in the endmember sample (intercept of 4.7 vs 1.2 pM in figure 5.10). Compared with U in this system, the Re source is localized near the river mouth. McKee et al. (1987)

Table 5.7 Re concentrations of surface samples from the Amazon Estuary.

Sample	Salinity (ppt)	Re pmol/kg	Re avg. pmol/kg	SD	SD%
Am1a	0.00	1.06			
Am1b	0.00	1.17	1.11	0.07	6.4
A7	0.30	9.1			
A1	2.60	10.6			
A8	2.61	10.4			
A2	4.90	10.2			
A2	4.90	9.6	9.9	0.4	4.3
AmE2	14.78	19.5			
A3	16.40	22.9			
A9	17.60	24.7			
A4	21.60	28.9			
A10	26.50	31.7			
A5	27.30	41.2			
A5	27.30	41.3			
A5	27.30	40.8	41.12	0.3	0.7
AmE6	34.45	44.5			
AmE4	36.36	44.1			
PSD					4.2

Samples Am1a and Am1b are replicates of the fresh water end-member.

Sample AmE4 is the seawater endmember.

n = number of replicates

PSD = pooled standard deviation as defined in Table 5.15

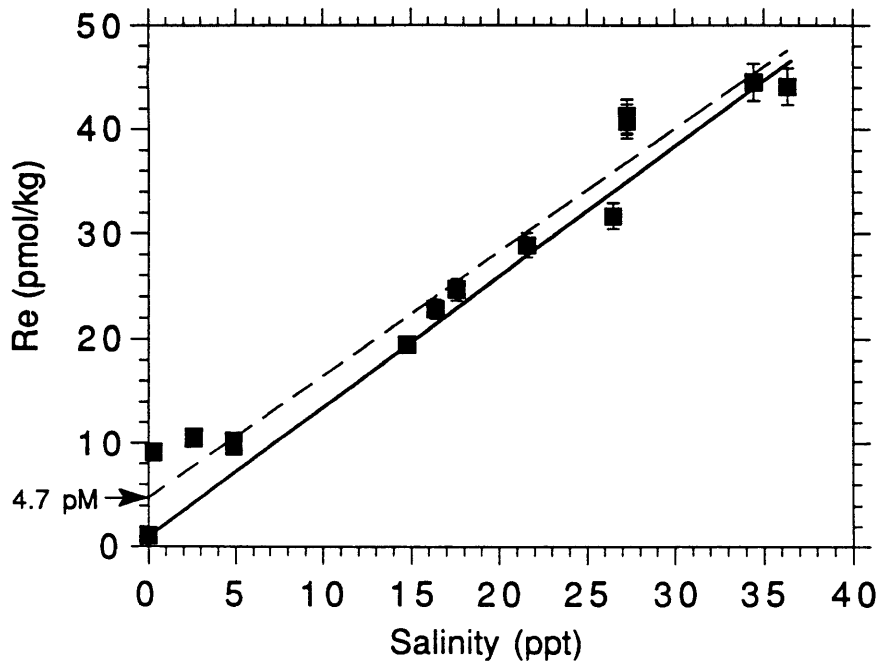


Figure 5.10 Re vs. salinity in surface waters of the Amazon Estuary. The solid line is the conservative mixing line between Amazon River waters (1.1 pmol/kg Re, 0 ppt salinity) and seawater (46.6 pmol/kg Re, 36.5 ppt salinity). The dashed line is the best fit line through the data, with a zero-salinity intercept at 4.7 pmol/kg Re. Error bars are  $\pm 1$  pooled standard deviation (4%).

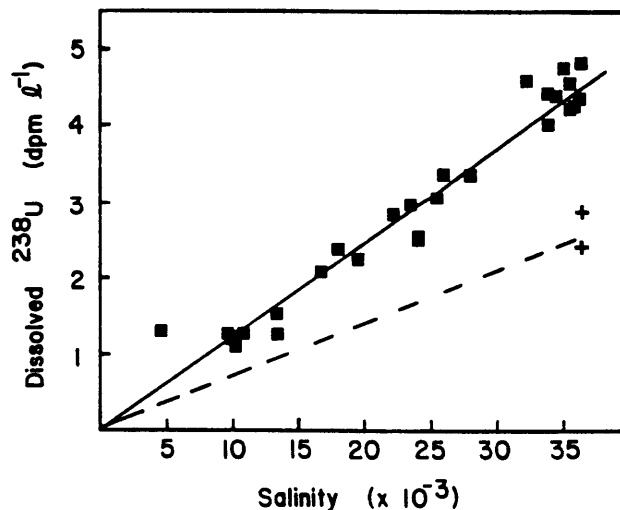


Figure 5.11  $^{238}\text{U}$  vs. salinity in the Amazon Estuary. The dashed line represents the U/sal. relationship for ideal mixing with open ocean waters. Crosses mark concentrations in two surface samples from the Amazon shelf break. After McKee et al., 1987.

showed that U concentrations are higher than expected from conservative mixing of seawater and river water throughout the Amazon Shelf, indicating a substantial flux out of reducing bottom sediments on the outer shelf (figure 5.11). Whereas U concentrations are nearly double that of open-ocean water in the outer Amazon plume, Re concentrations there are indistinguishable from open Atlantic seawater. Selective leaching experiments on high-U sediments from near the river mouth and low-U sediments from the distal portion of the cone showed that the major difference in U concentrations between sites was the U in the ferric-oxyhydroxide sediment phase (McKee et al.). This observation, and preliminary pore water data, led McKee et al. to suggest that the source of the excess U in the outer Amazon mixing zone is the ferric-oxyhydroxide coating on particles, which is solubilized within reducing sediments. Further study will be necessary to determine if this is the case for Re as well. If true, it contradicts the experimental work cited above which suggested that relatively little Re is adsorbed by ferric-oxyhydroxides (Morachevski and Novikov).

Evidence for the flux of Re out of estuarine sediments was sought in Chesapeake Bay, where Sholkovitz et al., 1991 have demonstrated large seasonal changes in bottom water concentrations of Fe and Mn. The sediment geochemistry here differs from that on the Amazon Shelf, in that the large amount of iron in Amazon sediments creates redox conditions which are dominated by iron-reduction, and sulfate reduction is not significant (Aller et al. 1986). Sulfate reduction is active in Chesapeake Bay sediments, however, especially during summer months. Monthly water column samples were collected over 1988-89, and the deepest samples analyzed for Re. Re concentrations were found to be invariant in bottom waters over the year, when corrected for changes in salinity (Table 5.8 and figure 5.12). Additionally, a

water column profile was collected in July, 1990 (Table 5.9). The release of Fe from the sediments which occurs in the summer months (figure 5.13) is not accompanied by any release of Re or U (Sholkovitz et al. 1991; Shaw and Klinkhammer 1989), due to the strongly reducing nature of the sediments which immobilizes both elements (see Chapter 6 for Re pore water profiles). In the fall, when the bottom waters become oxic, the oxidation of surface sediments and pore waters is encouraged by sediment resuspension. U in surface sediments is oxidized and remobilized, diffusing out of pore waters and into bottom waters (Shaw and Klinkhammer 1989). This is probably true for Re as well, although the magnitude of the flux is not large enough to be detectable above ambient bottom water concentrations.

Table 5.9 Profile of Re in Chesapeake Bay - Sta. 6 - July 19, 1990

Depth (m)	Re (pmol/kg)	Salinity
4	19.8	8.0
5	22.2	8.1
10	21.9	11.5
20	26.6	14.0
25	25.0	15.0
(Re $\pm$ 4%)		
bottom ~30m		

Table 5.8 Seasonal study of Re in the bottom waters of the North Basin, Chesapeake Bay

Sample	Month	Depth (m)	Re pmol/kg	Salinity ppt	Re* corr. to 18ppt
1-10	Feb88	27	32.1	20.857	27.7
2-3	Apr88	32	30.8	17.456	31.8
3-5	May88	28.5	25.5	15.526	29.6
4-8	Jun88	29	28.4	17.342	29.5
4-12	Jun88	29	26.1	17.342	27.1
5-11	6Jul88	28	29.4	15.848	33.4
6-7	26Jul88	29	28.5	16.487	31.1
7-8	Aug88	28	30.9	17.716	31.4
7-11	Aug88	28	31.1	17.716	31.6
8-6	Sep88	28	32.8	20.337	29.0
9-8	Oct88	29	34.5	21.696	28.6
9-12	Oct88	29	33.0	21.696	27.4
11-1	Dec88	28	31.8	19.212	29.8
11-5	Dec88	28	33.8	19.212	31.7
12-3	Feb89	31	31.7	21.782	26.2
12-8	Feb89	31	35.0	21.782	28.9

Pooled standard deviation =  $\pm 1\text{pM Re}$

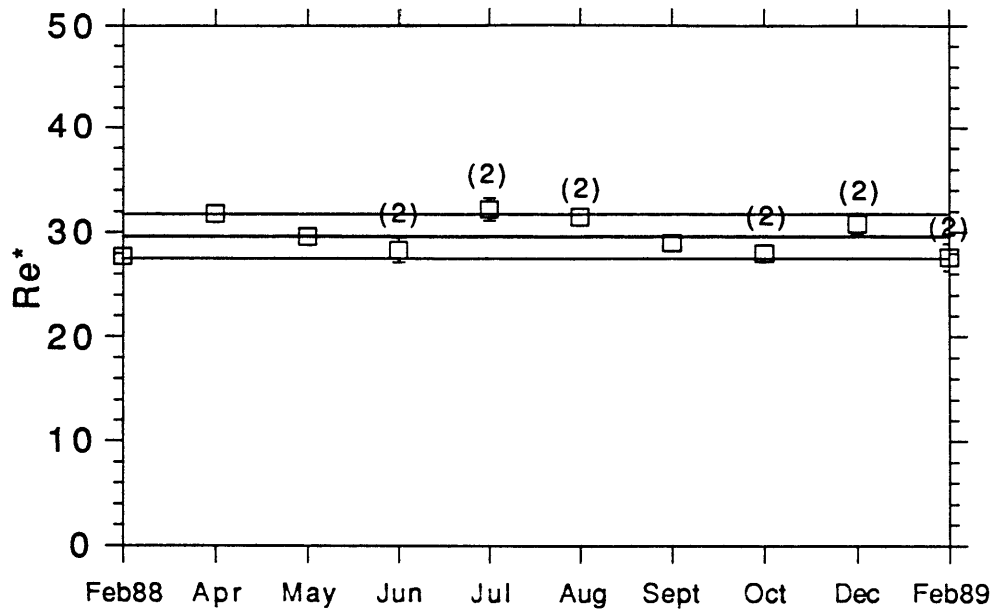


Figure 5.12 Re concentrations in the bottom waters of Chesapeake Bay throughout the year from February, 1988 to February, 1989. Re has been normalized to 18 ppt salinity. The mean of the data set is 30 pM Re, with a pooled standard deviation from the six duplicated points of  $\pm 1$  pM Re. Duplicates, indicated by (2), are from separate sample bottles.

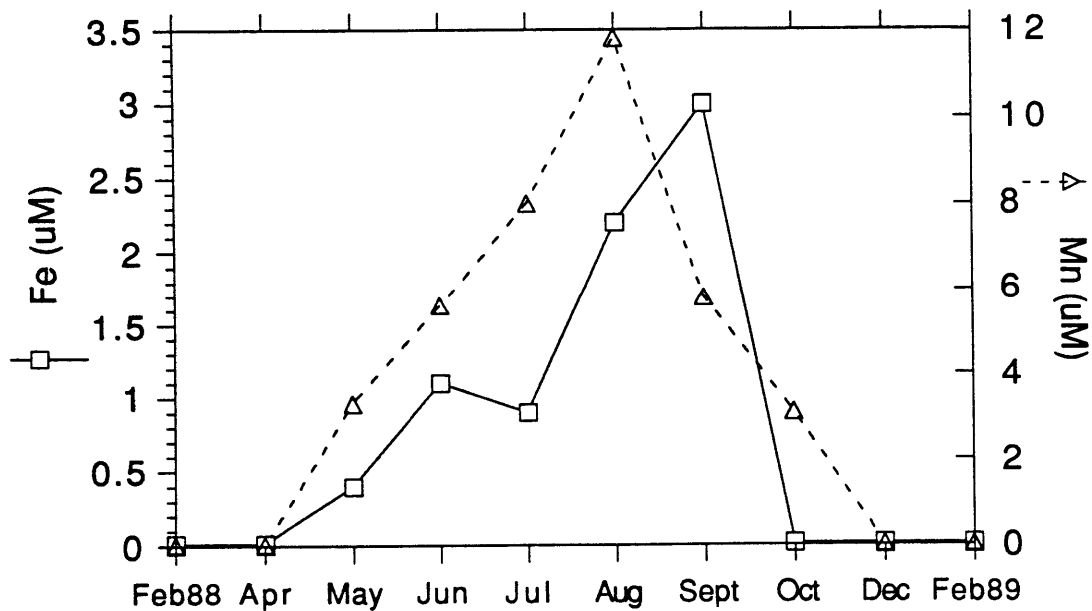


Figure 5.13 A seasonal study of Fe and Mn in the bottom waters of Chesapeake Bay, from Sholkovitz, et al., 1991.



*Anthropogenic inputs of Re to the environment?*

Rivers draining into the northern Black Sea all have Re concentrations equal to or greater than that of seawater (seawater = 45 pM, see map, figure 5.14). Re concentrations in the summer of 1990 ranged between 45 and 120 pM (Table 5.10). This high Re is reflected in Black Sea surface waters (Table 5.11), whose composition is principally the result of mixing of river waters and exchange with the deep Black Sea. Due to removal of Re into Black Sea sediments, and the stable density stratification of the Black Sea water column, Re concentrations in the deep Black Sea are depleted relative to surface waters. (The Re budget of the Black Sea will be discussed more fully in the next chapter.) Even if there were no removal of Re from the deep Black Sea, the concentrations measured in surface waters could not be produced by a simple mixture of Bosphorus overflow water (Mediterranean Sea water) and low-Re river waters. The concentrations predicted by dilution of seawater with zero-Re river water to the salinities at various depths in the Black Sea are shown by the lines in figure 5.15 (station locations in figure 5.16). The measured Re concentrations are illustrated by the squares, and show an excess in surface waters. In contrast, Mo concentrations show a deficit in surface waters compared to the concentration predicted from a mixture of Bosphorus water and zero-Mo rivers. A simple steady-state one-box model for the surface Black Sea predicts that the average river water concentration necessary to maintain the observed Re levels is about 50 pM (Table 5.12). This is at the lower end of the range of concentrations measured in the rivers.

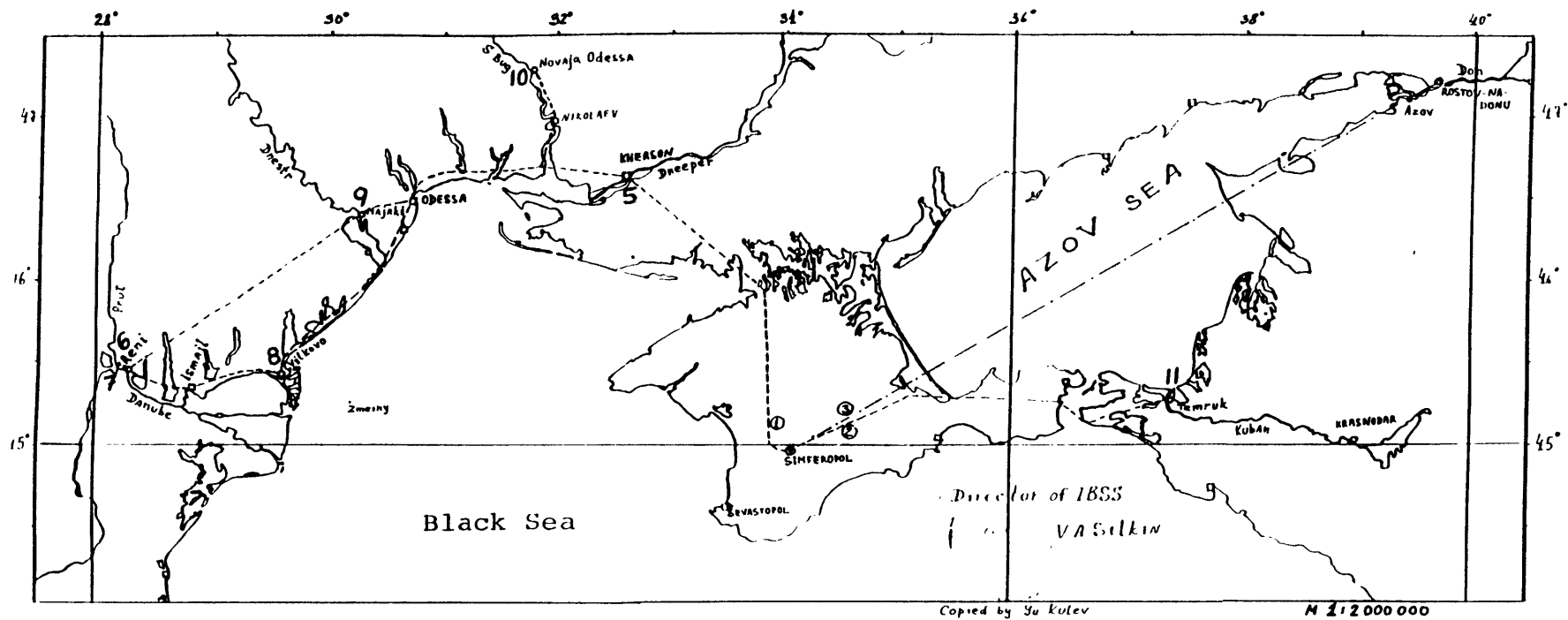


Figure 5.14 Rivers draining into the Black Sea from Soviet territory and sampling locations.

Table 5.11 Re in the Black Sea, June 1988

Sta.	Sample	Depth (m)	$\sigma_t$	Re (SD) (pmol/kg)	Salinity (ppt)	O <sub>2</sub> ( $\mu$ M)	H <sub>2</sub> S ( $\mu$ M)
2	DH2	20	13.752	29.2	18.465	309	
2	DH1	30	14.348	30.7	18.675	285	
2	DH4	40	14.671	30.3	19.189	253	
2	DH6	50	14.912	28.7	19.992	111	
2	DH8	60	15.452	27.9	20.479	3.4	
2	DH7	70	15.880	27.6 (0.2)	20.727	2.1	
2	DH11	80	16.030	22.5 (0.4)	20.887	1.4	
2	DH13	90	16.108	25.9	21.031		0.6
2	DH15	100	16.257	25.3	21.130		4.9
2	DH16	105	16.281	25.0 (0.04)	21.164		9.8
2	DH17	110	16.276	23.9	21.200		12.9
2	DH18	115	16.355	23.6	21.248		14.4
2	DH19	120	16.391	24.9	21.290		16.9
2	DH20	130	16.440	23.2	21.384		21.0
2	DH21	140	16.490	21.7	21.422		25.4
2	DH22	170	16.598	20.3	21.556		49.1
2	DH23	200	16.690	18.0	21.652		71.0
2	DH24	400	16.972	13.1	22.003		
2	DH25	600	17.104	9.0	22.162		
2	DH26	800	17.171	8.8	22.250		
2	DH27	1200	17.212	8.5	22.310		
2	DH28	1600	17.222	(17.6)	22.318		
2	DH29	2100	17.223	(18.1)	22.330		
2	G1115	2086	17.223	8.4	22.330		
6	DH35	150	16.432	23.4	21.321		
6	DH36	180	16.546	23.8	21.416		
6	DH32	500	17.023	13.0	21.962		
6	DH33	800	17.157	10.0	22.222		
6	G1092	800	17.157	12.3	22.222		
6	DH34	1500	17.219	9.9	22.313		
6	G1093	1500	17.219	9.0	22.313		
6	DH30	2153	17.221	9.1	22.320		
6	G1116	2153	17.221	9.7	22.320		
6	DH31	2174	17.221	9.1	22.320		
6	G1089	2174	17.221	10.1	22.320		
6	G1090	2185	17.221	9.6	22.320		

DH samples were collected by Bill Landing

G samples were collected by P. Froelich and R. Mortlock

SD = difference from the mean of duplicate samples

() = not included in plots

Pooled standard deviation = 1.1% from three duplicate samples, or 4.5% from different samples from the same depths

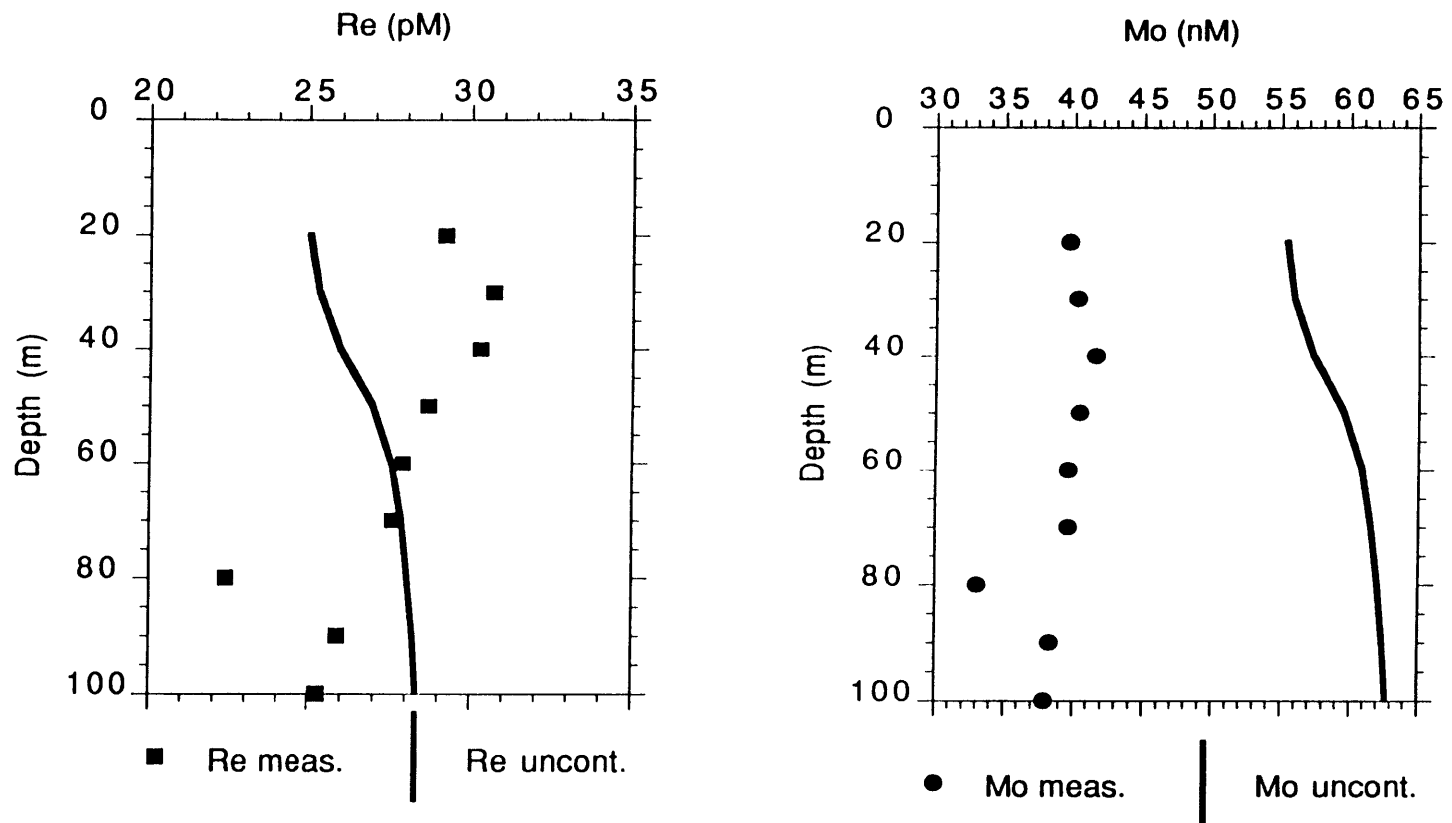


Figure 5.15 Re and Mo concentrations in Black Sea surface waters. Filled symbols are the measured concentrations. Solid lines represent the concentrations of Re and Mo predicted from a mixture of average river waters with seawater in the correct proportions to give the salinity at each depth. Average river concentrations as in Table 5.13. Black Sea Mo data from Emerson and Husted, 1991.

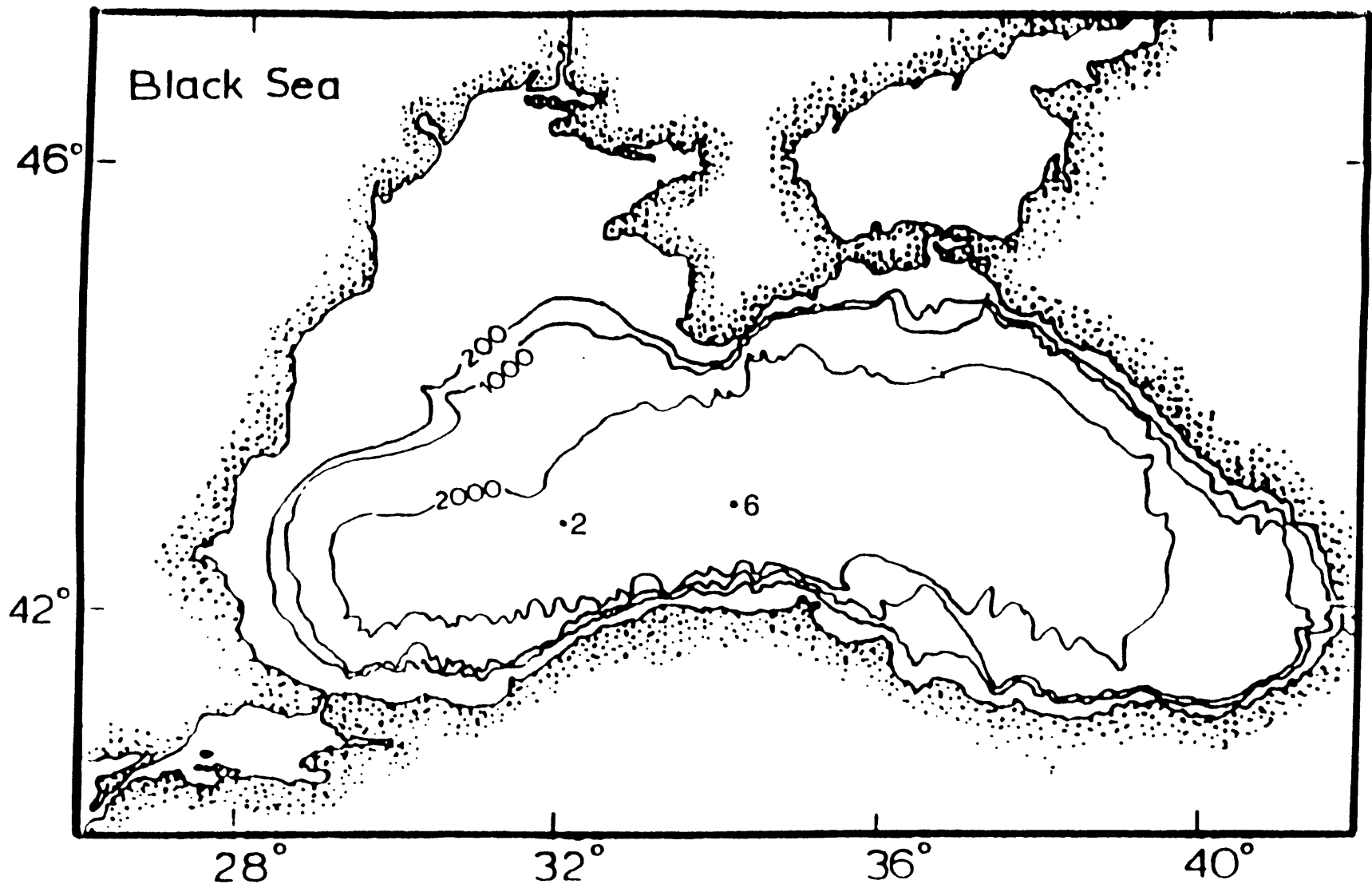


Figure 5.16 Map of the Black Sea with station locations.

Table 5.12 Black Sea surface water budget

River water flux ( $F_r$ )	346 km <sup>3</sup> /yr
Flux in at Kerch Straits ( $F_{ki}$ )	53 km <sup>3</sup> /yr
Flux out at Kerch Straits ( $F_{ko}$ )	32 km <sup>3</sup> /yr
Flux from up from deep Black Sea ( $F_u$ )	700 km <sup>3</sup> /yr
Flux down to deep Black Sea ( $F_d$ )	524 km <sup>3</sup> /yr
Flux out at Bosphorus ( $F_{bo}$ )	340 km <sup>3</sup> /yr

Re concentration in... surface waters ( $Re_s$ )	29 pM
deep waters ( $Re_d$ )	9 pM

Predicted river water concentration ( $Re_r$ )	49 pM
---	-------

$$\text{where } Re_r = \frac{Re_s(F_{ko} + F_{bo} + F_d) - F_u Re_d}{F_r + F_{ki}}$$

Figure 5.17 Black Sea surface box model. Water flux parameters from Falkner 1991:

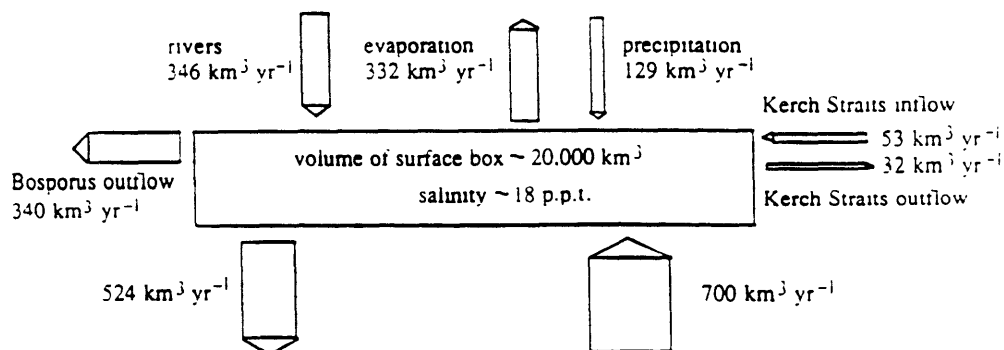


Table 5.10 Re in rivers draining into the Black Sea from the USSR

<u>Station</u>	<u>River</u>	<u>Re</u> <u>(<math>\mu\text{mol/kg}</math>)</u>	<u>U</u> <u>(nM)</u>	<u><math>\Sigma+</math> (<math>\mu\text{eq}</math>)</u> <u>(Na+K+2Mg+2Ca)</u>
5	Dnepr @ Kherson	45.4	3.19	4579
6	Prut @ Reni	122.2	5.38	5627
7	Danube @ Reni	81.9	3.63	3559
8	Danube @ Vilково	74.9	4.08	3448
9	Dnestr @ Majaki	121.0	4.97	5218
10	Bug @ Novaja Odessa	80.4	13.5	5985
11	Kuban @ Temruk	70.6	4.17	3440
Estimated uncertainty		$\pm 3\%$	$\pm 5\%$	

Uranium and major ion measurements by K. K. Falkner, unpublished data

The geology of the northern Black Sea drainage consists largely of the low-relief Russian platform: chalk, marl and argillaceous and sandy sedimentary units (Muller and Stoffers 1974). On the east, the Kuban River drains the Caucasus Mountains which are marked by Precambrian crystalline rocks, large areas of Pliocene and Quaternary volcanics and Cretaceous flysch facies (Muller and Stoffers 1974). The western drainage is dominated by the Danube River, which crosses the granitic and metamorphic rocks of the Bohemian Massif, the complex eastern Alps, and Quaternary sediments in the Hungarian lowlands. Cretaceous flysch deposits of the Carpathians influence the rivers joining the Danube from the north, and granites and crystalline schists of the Balkans are present in the south. It is unlikely that consistently high Re river values throughout this region could derive from the natural terrain, hence an anthropogenic source is indicated. Water quality is monitored along the Dneiper River, however the results of these findings are largely classified (Tolmazin 1985). Tolmazin indicates that review of these materials shows that

the Dneiper flow contains a large variety of "dangerous substances", including trace metals, radionuclides, pesticides, cyanides, PCB's etc.

Because Re, U and Mo behave coherently in many geologic settings, most potential sources of Re should furnish the other elements to the environment as well. U and Mo are elevated in Black Sea rivers compared to "average river water" by a factor of two to ten, however neither element shows the factor of 20 - 50 enrichment seen for Re. U and Mo concentrations do not appear to have changed significantly in the last 10-20 years; I am not aware of any historical data for Re (Table 5.13).

The relative enrichment of Re compared to Mo and U suggests that the proposed anthropogenic source fractionates the elements. Any high temperature process with oxygen present could have this effect, as the heptoxide,  $\text{Re}_2\text{O}_7$ , is volatile above  $360^\circ\text{C}$  (Colton 1965). Although Re is volatilized by the roasting of molybdenite and copper porphyry ores (Sutulov 1965), these sources are probably not large enough to contaminate the entire region with Re. In addition, Re can be collected from the flue dusts of molybdenite and copper smelters in economic quantities, so that efforts are made to prevent loss to the environment. Among the potential anthropogenic sources of Re, coal burning may be a dominant contributor to the widespread contamination found in the northern Black Sea region. Transport of anthropogenic Re to the Black Sea may be accomplished by direct deposition from the atmosphere to Black Sea surface waters, as well as by rivers.

There are very little data available for Re in coals; however, some guesses can be made about the importance of this source based on the wider body of knowledge available for Mo. According to Kaakinen (1977), coal combustion is the largest source of Mo to the atmosphere in the US, even though the volatilization temperature of  $\text{MoO}_3$  ( $\sim 1200^\circ\text{C}$ ) is substantially higher than that of



Table 5.13 Mo and U data for rivers draining into the Black Sea, 1960's, 1970's, 1990.

River	Mo 1990 (nM)	Mo 1960's (nM)	U 1990 (nM)	U 1977 (nM)
Dnepr	18	17	3.19	7.14
Prut	29		5.38	
Danube	19		3.63	2.7-9.2
Danube	20		4.08	
Dnestr	29	21	4.97	4.2
Bug	30	36	13.5	
Kuban	22	26	4.17	13.9
Average river water	5 (a)		1.2-2.5 (b)	
Seawater	105 (c)		14 (d)	

1990 Mo data = this work

1990 U data from K. Falkner, unpublished

1960's Mo data from Shimkus, 1974

1977 U data from Nikolayev, et al. 1977

(a) = Martin and Meybeck 1979

(b) = Bertine et al., 1970 and Sackett et al. 1973

(c) = Collier 1985

(d) = Turekian and Chan, 1971 and Ku, et al. 1977

Re<sub>2</sub>O<sub>7</sub> and most coal burning plants in the US are equipped with scrubbers and/or precipitators which will collect Mo in the ash. Most US coal-fired facilities also use hard coal, which generally has lower trace element contents than the brown coal, or lignite, which makes up a sizeable proportion (~30%) of the coal burned in the USSR (Report 1989) (figure 5.18). In a study of one power plant (burning bituminous coal), approximately 85% of the molybdenum originally present in the coal was found in ashes retained by the plant, with 15% left in particulate emissions (Kaakinen 1977). This study also showed that Mo in ash is relatively soluble in water leaches, so that Mo on emitted particles, or on fly ash which is applied to fields as a soil amendment, can end up in water supplies or in vegetation.

Using the data for US Mo emissions due to coal burning, and a series of assumptions relating Mo to Re, the magnitude of the coal source for Re may be estimated. Few measurements of Re in coal are available; Martin and Garcia Rossell (1971) and Elejade and Martin (1968) report that Re is higher in lignite than in bituminous or anthracite coal, and Re concentrations in lignite in the Spanish Ebro Basin range between 30 and 2400 ppb (69 samples). Morris and Short (1978) and Kuznetsova and Saukov (1961) report determinations of Re in Russian brown coals of between 95 and 325 ppb. The Mo concentration in US coals is 5-10 ppm, and given a Mo/Re weight ratio in modern organic rich sediments of ~1000, the Re concentration one might expect in average coals is 5 ppb. This was the value used in the calculations contained in Table 5.14. It is substantially lower than literature values for Re in coal in order to err conservatively, and since the quality of the literature data is not known. Assuming that the USSR and Eastern Europe burn approximately the same amount of coal as the US, and therefore that Mo emissions are approximately equal, Re emissions in the USSR due to coal burning would be about one ton/y

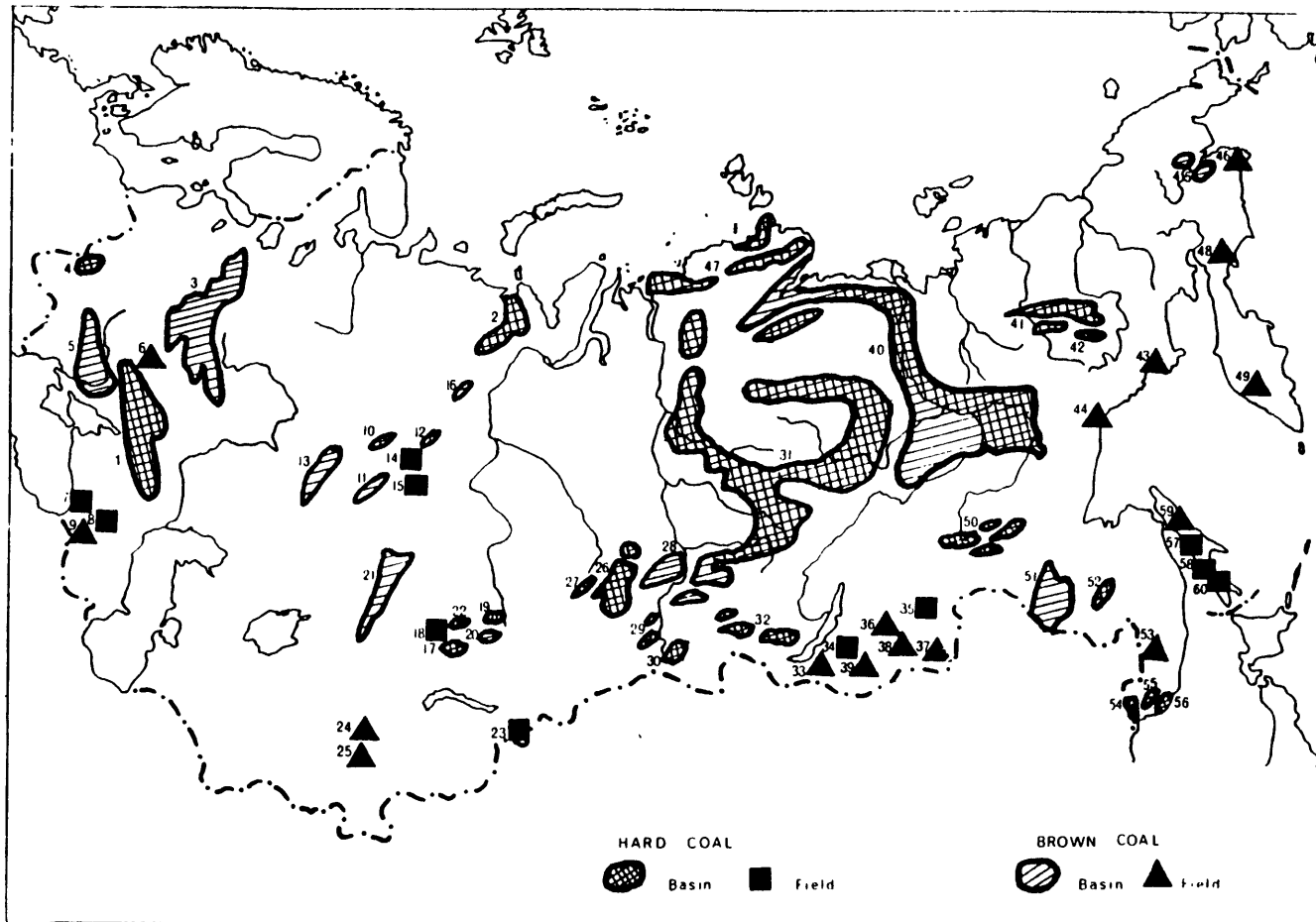


Figure 5.18 Main coal basins and fields of the USSR. The Black Sea is in the far western side of the map 1. Donets hard coal basin, 3. Moscow brown coal basin, 5. Dneipr brown coal basin (from Elliot 1974)

Table 5.14 Estimates used in calculating the contribution of coal combustion to Re concentrations in Soviet rivers.

Mo concentration in US coals: 5 - 10 ppm	(Kaakinen, 1977)
Re concentration in USSR brown coals: 95-325 ppb	(Morris, 1978)
Mo/Re in modern organic-rich sediments: 1000	(Ravizza, 1991)
	(Koide, 1986)
Mo/Re ratio used in calculations : 1000	
US Mo emissions due to coal burning: 610 tons/y (1970)	(Kaakinen, 1977)
3000 tons/y	(Torrey, 1978)
US coal burned 1988: $8.6 \times 10^8$ tons	(Report, 1989)
USSR coal burned 1988: $7.7 \times 10^8$ tons	(Report, 1989)
US coal burned ~ USSR + some E. Europe coal burned	
If USSR emissions = US emissions: (ie. same collector efficiencies)	
USSR Mo emissions due to coal burning: 1000 tons/y (1990)	
USSR Re emissions due to coal burning: 1 ton/yr	
Percentage of industrialized USSR (+E Europe) included in Black Sea drainage: ~50%	
USSR Re emissions delivered to Black Sea region: $5 \times 10^5$ g/yr	
River discharge to the Black sea = 300 km <sup>3</sup> /yr	(Shimkus, 1974)
(Dnepr + Bug + Dnestr + Don + Danube + Kuban)	
Assuming 50% of Re emitted ends up in rivers,	
Assuming no fractionation between Re and Mo during combustion and weathering:	
Average Re concentration in Black Sea rivers: <u>4.5 pM</u>	
Assuming Re enrichment over Mo by a factor of 10 during combustion and weathering:	
Average Re concentration in Black Sea rivers: <u>45 pM</u>	
Assuming fractionation Re from Mo and USSR Re emissions ten times higher than US emissions:	
Average Re concentration in Black Sea rivers: <u>450 pM</u>	

(Table 5.14). If there is no fractionation between Mo and Re during combustion, the excess Re concentration in rivers draining into the Black Sea might reach 5 pM. If Re is enriched in emissions due to its higher volatility, or is more mobile during weathering of ashes, this number would increase. If USSR scrubbers are less efficient than US scrubbers, and if higher Re coals are burned, the concentrations will increase further. It thus appears feasible that the high Re in these rivers originates from coal combustion sources (Table 5.14).

#### *Re in the ocean*

Based on the predicted speciation of Re in seawater ( $\text{ReO}_4^-$ ) and the behavior of other oxyanions, such as  $\text{MoO}_4^{2-}$ , in the oceans, it was expected that Re would behave conservatively in seawater. The data of Koide et al. (1987) are consistent with this hypothesis, but the uncertainties in the analytical methods available precluded a definitive demonstration of conservative behavior. Re was therefore determined in two profiles from the Atlantic and Pacific oceans, and the results are presented in Tables 5.15 and 5.16 and figures 5.19 and 5.20. Re shows constant concentrations relative to salinity in the Atlantic profile, within analytical uncertainties ( $\pm 2\%$ ). There is more variability in the surface waters of the Pacific profile, but the overall distribution is essentially conservative. Whether the surface variability reflects nature or analytical/sampling artifacts will hopefully become clear with further work. The mean Re concentrations in the two profiles are  $44.6 \pm 0.2$  pmol/kg and  $43.9 \pm 0.3$  pmol/kg. These agree within  $2\sigma$  of the mean, thus no inter-ocean fractionation is discerned from the data.

Table 5.15 Re North Atlantic depth profile: Bermuda Station S (32°10'N, 64°30'W)

Depth (m)	Salinity (ppt)	Re (pmol/kg)	Re* (corr. 35 ppt)	SD (n)
101	36.685	46.6	45.0	1.7 (3)
366	36.567	46.3	44.3	
551	36.308	46.8	45.1	
920	35.169	44.5	44.3	
1053	35.083	44.6	44.5	
1323	35.066	43.9	43.8	
1593	35.043	44.8	44.8	0.4 (3)
2119	35.003	44.7	44.7	
2597	34.953	45.4	45.5	
3075	34.924	44.3	44.4	
3553	34.899	44.0	44.4	0.7 (3)
Average of 17 analyses		45.1	44.6	
standard deviation		1.0	0.5	
pooled sd of 3 sets of triplicates (pmol/kg)				1.1
pooled sd (%)				2.4

where pooled standard deviation =  $\sqrt{\frac{\sum n_i (sd)_i^2}{\sum n_i}}$

(after Sachs 1991)

Table 5.16 Re North Pacific depth profile (24°16'N, 169°32'E)

Depth (m)	Salinity (ppt)	Re (pmol/kg)	Re* (corr. 35 ppt)	SD (n)	
27	35.25	43.7	43.4	0.73 (3)	
287	34.696	42.2	42.5		
566	34.136	45.2	46.3	1.18 (3)	
880	34.254	43.7	44.6		
1142	34.453	43.4	44.1		
1730	34.579	43.0	43.5		
2436	34.64	44.0	44.4		
3354	34.667	43.4	43.8		
4495	34.684	43.0	43.3		
5310	34.692	43.5	43.9		
6180	34.695	43.2	43.6		0.32 (3)

Average of 17 analyses	43.5	43.9	
standard deviation	0.8	1.0	
pooled sd of 3 sets of triplicates (pmol/kg)			0.8
pooled sd (%)			1.9

where pooled standard deviation =  $\sqrt{\frac{\sum n_i (sd)_i^2}{\sum n_i}}$

(after Sachs 1991)

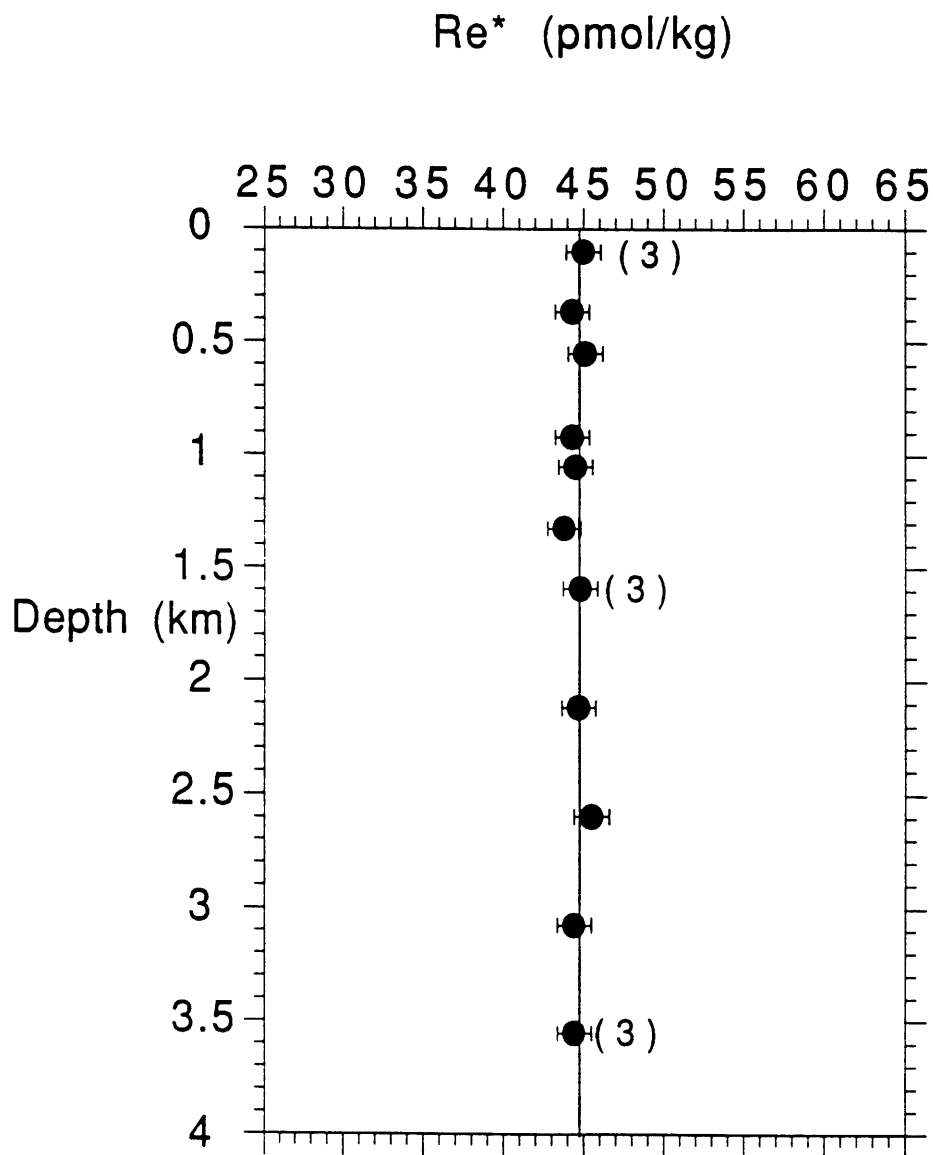


Figure 5.19 Atlantic Ocean  $Re$  profile, off Bermuda (Station S). Numbers in parentheses indicate number of replicates. Plotted  $Re$  concentrations are corrected to 35 ppt salinity. Error bars are  $\pm 2.4\%$ , which is the pooled standard deviation of the three triplicate measurements. Vertical line shows mean of the data set. (from Sachs, 1991)



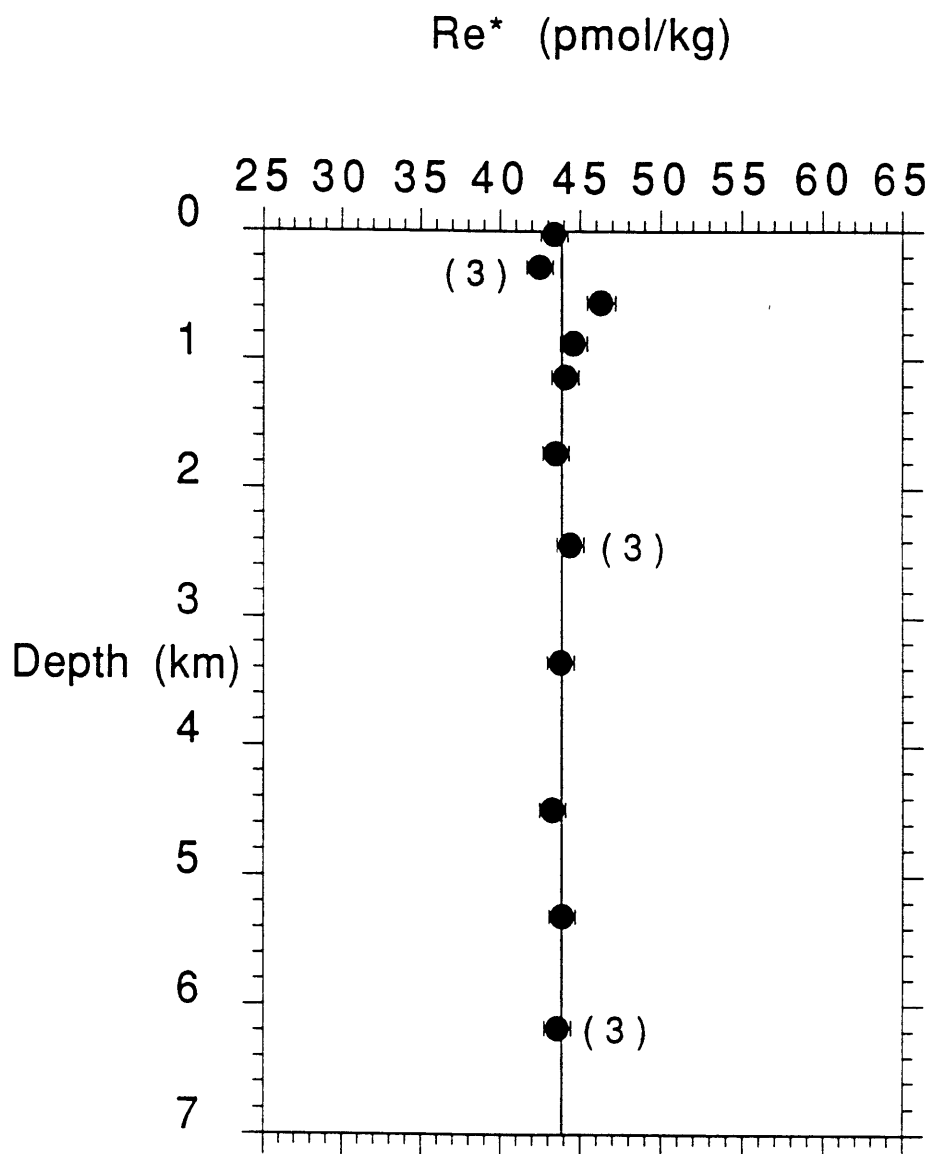


Figure 5.20 Pacific Ocean  $\text{Re}^*$  profile, 24N, 170W. Numbers in parentheses indicate number of replicates. Plotted  $\text{Re}^*$  concentrations are corrected to 35 ppt salinity. Error bars are  $\pm 1.9\%$ , which is the pooled standard deviation of the three triplicate measurements. Vertical line shows mean of the data set. (from Sachs, 1991)

## 5.5 Summary and Conclusions

The rivers analyzed in this study represent a variety of weathering environments, in terms of both weathering processes and basin lithologies. These include the Precambrian Guayana Shield of the Orinoco Basin, where slow, transport-limited weathering takes place in the sub-surface, the active tectonic regions of the Andes and the Himalayas, as well as the developed northern Black Sea drainage. The most important natural determinant of Re concentrations in the river waters appears to be the presence or absence of black shales. The highest riverine values were measured in the Venezuelan Andes in a region containing outcrops of Cretaceous black shales, and the lowest values were found in the relatively dilute rivers of the Guyana Shield. Within the Andean floodplain of the Orinoco basin, high Re values are successively diluted, maintaining a nearly constant relationship to U, Mo and SO<sub>4</sub>. The distribution of Re concentrations in rivers of the Amazon and Ganges basins is consistent with a black shale source for the element, although the data sets for these regions are more limited.

Re, U and Mo tend to follow similar trends within river basins, but the limited data available suggest that interelemental ratios vary substantially between basins. The Ganges river and its highland tributaries contain more U relative to Re and Mo than the other rivers analyzed, suggesting a non-black shale source for U, and perhaps for Re and Mo as well. The identity of this source is as yet unknown, but the high grade rocks of the Himalayas are known to contain abundant uranium minerals, and it is postulated that radioactive heating is partly responsible for the thermal evolution of the mountain range (A. MacFarlane, personal communication). Recent measurements of granites and gneisses from this region indicate U concentrations between 1 and 8 ppm

(MacFarlane 1991). These concentrations are not large enough to account for the very high U in these rivers, however.

Results from the Amazon estuary suggest that there may be a significant desorptive flux of Re in the inner mixing zone. The origin of this excess could be due release of Re from particles within the water column and/or during early diagenesis of shelf sediments. Re concentrations in the bottom waters of Chesapeake Bay showed no significant source or sink in the sediments, and did not show any seasonal fluctuation as the sediments were cycled through oxic and anoxic conditions.

Very high Re concentrations in six of the major rivers draining into the Black Sea (1-3 times seawater levels) indicate that Re is being added to the environment by anthropogenic processes. Lantzy and Mackenzie (1979) estimate that 40 times more Mo is released to the atmosphere by industrial and fossil fuel emissions than by natural processes. A similar or greater figure may apply for Re, since the elements have similar sources, and Re volatilizes at lower temperatures. Re introduced into the environment in ash particles is likely to be mobile in oxygenated waters, and should eventually be washed into rivers. It is not known to what extent Re is accumulated by vegetation.

Based on the riverine data reported here, an average value for Re in rivers can be calculated based on the water flux-weighted concentrations of the Amazon, Orinoco and Ganges-Brahmaputra Rivers. (The Amazon River concentration is taken to be its endmember value until further confirmation of a desorptive flux is available. True endmember values of the Orinoco and Ganges-Brahmaputra are not known, nor is the behavior of Re in their estuaries.) This concentration is approximately 2.3 pM Re. Using a global river flux of  $3.6 \times 10^{16}$  L/y, the annual riverine input of Re to the oceans is 82,800 moles. With an average ocean concentration of 45 pM Re, the residence time of

Re with respect to river inflow is estimated to be 750,000 years (~400 ky - 1.5 my). This is similar to the oceanic residence times for Mo and U of 780,000 and 250,000-500,000 y, respectively (Bertine and Turekian, 1973; Turekian and Chan, 1971; Ku et al., 1977). The long residence time calculated is consistent with the invariant profiles observed in the Atlantic and Pacific Oceans.

The calculated riverine flux of Re agrees to within a factor of two with the Re burial flux estimate of Ravizza (1991) of 44,500 moles/year. This burial flux is based only on Re accumulating in major anoxic basins and coastal upwelling zones (Black Sea, Gulf of California, Baltic Sea, Peru-Chile Shelf, Southwest African Shelf, and Western North American Shelf). The total burial is probably higher and should include the Re flux into reducing near-shore sediments, as well as sediments underlying the equatorial Pacific upwelling zone. Given the uncertainties inherent in estimating global sources and sinks based on a very limited data set, the ocean budget for Re appears to be very close to balanced.

## **5.6 Acknowledgements**

The samples for this study were painstakingly collected by a number of people over several years. Orinoco samples were collected by J. Edmond and E. Brown. Amazon Estuary samples were collected by E. Brook, and Amazon River samples by B. Stallard. Ganges-Brahmaputra samples were collected by Dr. M. M. Sarin of the Physical Research Laboratory, India. Chesapeake Bay time-series samples were provided by T. Shaw and E. Sholkovitz. Black Sea profiles were collected by F. Froelich and B. Landing and samples were provided for this work by F. Froelich, R. Mortlock and S. Emerson. Soviet river samples were collected by K. Falkner and J. Edmond with logistical and scientific support from the Institute of Biology of the Southern Seas at Sevastopol. North Atlantic seawater samples were collected by E. Boyle and I. Ellis. Pacific samples were collected by C. Measures.

### References for Chapter 5

- Aller, R. C., J. E. Mackin and R.T. Cox. (1986). "Diagenesis of Fe and S in Amazon inner shelf muds: apparent dominance of Fe reduction and implications for the genesis of ironstones." Cont'l. Shelf Res. 6(1/2): 263-289.
- Bertine, K.K. and K.K. Turekian. (1973). "Molybdenum in marine deposits." Geochim. Cosmochim. Acta. 37: 1415-1434.
- Bertine, K.K., L.H. Chan and K.K. Turekian. (1970). "Uranium determinations in deep sea sediments and natural waters using fission tracks." Geochim. Cosomochim. Acta. 34:641-648.
- Boyle E.A., S. Husteded and B. Grant. (1982). " The chemical mass balance of the Amazon plume II. Cu, Ni and Cd." Deep Sea Res. 29(11A): 1355-1364.
- Brookins, D.G. (1986). " Re as an analog for fissiogenic Tc; Eh-pH diagram (25°C, 1bar) constraints." Appl. Geochem. 1:513-517.
- Butts, J. L. and W. S. Moore (1988). Uranium removal in the Ganges-Brahmaputra mixing zone. EOS. American Geophysical Union, San Francisco,
- Case, J. E., R. Shagram and R.F. Giegengack (1990). Geology of the northern Andes. The Caribbean Region. The Geological Society of America. 177-199.
- Cochran, J.K. (1982). The oceanic chemistry of U and Th series nuclides. Uranium Series Disequilibrium: Application to Environmental Problems. Oxford, Clarendon Press.
- Collier, R.W. (1985). "Molybdenum in the Northeast Pacific Ocean." Limnology and Oceanogr. 30: 1351-1353.
- Colton, R. (1965). The chemistry of rhenium and technecium. New York, Interscience Publishers.
- Edmond, J. M., M.R. Palmer, C.I. Measures, B. Grant, R.F. Stallard, C.F. Nordin and R.H. Meade (1991in prep.). "Fluvial geochemistry and denudation rate of the Guyana Shield."
- Elliot, I.F. (1974). The Soviet Energy Balance. Praeger Publ., N.Y. p. 141
- Emerson, S. and S. S. Husteded (1991). "Ocean anoxia and the concentrations of molybdenum and vanadium in seawater." in press, Mar. Chem.
- Esser, B. K. (1991). Osmium Isotope Geochemistry of Terrigenous and Marine Sediments. Yale University.

Falkner, K.K., D.J. O'Neill, J.F. Todd, W.S. Moore and J.M. Edmond. (1991) "Depletion of barium and radium-226 in Black Sea surface waters over the past thirty years." Nature. **350** (6318): 491-494.

Gibbs, A. K. and C. N. Barron (1983). "The Guiana Shield reviewed." Episodes : 7-14.

Hanor J.S. and L.H. Chan (1977). "Nonconservative behavior of Ba during mixing of the Mississippi River and Gulf of Mexico waters." Earth and Plan. Sci Lett. **37**:242-250.

Holland, H.D. (1984). *The Chemical Evolution of the Atmosphere and the Oceans*. Princeton University Press, N.J., 582p.

Huie, Z., Z. Jishu, and Z. Lanying. (1988). "Sorption of radionuclides Tc and I on minerals." Radiochim. Acta. **44/45**: 143-145.

Kaakinen, J. W. (1977). Estimating the potential for molybdenum enrichment in flora due to fallout from a nearby coal-fired power plant. Molybdenum in the Environment. New York, Marcel Dekker. 685-703.

Kim, Y.S., and H. Zeitlin. (1969). "The role of Iron(III) hydroxide as a collector of Mo from seawater." Anal. Chim. Acta. **46**: 1-8.

Koide, M., V. Hodge, J.S. Yang and E.D. Goldberg (1987). "Determination of rhenium in marine waters and sediments by graphite furnace atomic absorption spectrometry." Anal. Chem. **59**: 1802-1805.

Koide, M., V. F. Hodge, J. Yang, M. Stallard, E. Goldberg, J. Calhoun and K. Bertine. (1986). "Some comparative marine chemistries of rhenium, gold, silver and molybdenum." Appl. Geochem. **1**: 705-714.

Ku, T-L, K.G. Knauss and G.G. Mathieu. (1977). "Uranium in open ocean: concentration and isotopic composition." Deep Sea Res. **24**: 1005-1017.

Kuznetsova, V.V. and A.A. Saukov. (1961). "Possible forms of occurrence of molybdenum and rhenium in the coals of middle Asia." Geochemistry **9**: 822-829. (Eng. transl.)

Langmuir, D. (1978). "Uranium solution-mineral equilibria at low temperatures with application to sedimentary ore deposits. Geochim. Cosmochim. Acta. **42**: 547-569.

Lantzy, R. J. and F. T. Mackenzie (1979). "Atmospheric trace metals: global cycles and assessment of man's impact." Geochim. Cosmochim. Acta **43**: 511-525.

Lieser, K.H. and C.H. Bauscher. (1987). "Tc in the hydrosphere and geosphere." Radiochim. Acta. **42**:205-213.

- Macellari, C. E. and T. J. DeVries (1987). "Late Cretaceous upwelling and anoxic sedimentation in Northwest South America." Paleogeog., Paleoclim., Paleoecol. **59**: 279-292.
- MacFarlane, A. (1991). Massachusetts Institute of Technology. Pers. comm.
- Martin, J.M. and M. Meybeck. (1979). "Elemental mass-balance of material carried by major world rivers." Mar. Chem. **7** : 173-206.
- McKee, B. A., D. J. DeMaster and C.A. Nittrouer (1987). "Uranium geochemistry on the Amazon Shelf: Evidence for uranium release from bottom sediments." Geochim. Cosmochim. Acta **51**: 2779-2786.
- Morachevski, Y.V. and A.I. Novikov. (1958). "Coprecipitation of some elements from dilute solutions by hydroxides." Trudy Komissii Anal. Khim. Acad. Nauk. SSSR., Anal. Khim. **9**:121-134.
- Morachevskii, D. E. and A. A. Necheva (1960). "Characteristics of migration of Re from molybdenites." Geochem. **6**: 648-649.
- Morris, D.F.C. and E.L. Short. (1978) Rhenium, in Handbook of Geochemistry K.H. Wedepohl, ed., Springer-Verlag, N.Y. II-5, 75-1 - 75-0-1.
- Muller, G. and P. Stoffers (1974). Mineralogy and petrology of Black Sea basin sediments. The Black Sea. Geology, Chemistry and Biology. Tulsa, OK, American Association of Petroleum Geologists. 200-248.
- Nikolayev, D.S., K.F. Lazarev and V.M. Drozhzhin. (1977). "Trends in the distribution of U, Io, and Th in the Black and Azov Seas." Geochem. Int'l. **14**: 141-146.
- Palmer, M. R. and J. M. Edmond (in press, 1991). "Controls over the Sr isotope composition of river water: examples from the Ganges, Orinoco, Amazon, Chinese and East African Rift Valley Basins." Chem. Geol.
- Poplavko, Y., V. Ivanov, L Longinova, V. Orekhov, A. Miller, I. Nazarenko, R Nishankhodzhayev, N. Razenkova and Y. Tarkhov. (1977). "Behavior of rhenium and other metals in combustible central Asian shales." Geochimiya **2**: 273-283.
- Ravizza, G. (1991). Rhenium and Osmium Geochemistry of Modern and Ancient Organic-Rich Sediments. PhD Thesis. Yale University.
- Ravizza, G. and K. K. Turekian (1989). "Application of the  $^{187}\text{Re}$ - $^{187}\text{Os}$  system to black shale geochronometry." Geochim. Cosmochim. Acta : **53**(12): 3257-3263.



Rupke, J. (1974). "Stratigraphic and structural evolution of the Kumaon Lesser Himalaya." Sed. Geol. Spec. Issue 11(Part1: Text, Part 2: Maps): 81-265.

Sachs, J. P. (1991). The Geochemistry of Rhenium. Massachusetts Institute of Technology. Senior Thesis.

Sackett, W.M., T. Mo, R. Spalding and M. Exner. (1972). A reevaluation of the marine geochemistry of uranium. In: Symp. Interact. Radioact. Contam. Const. Mar. Env., Seattle, WA. IAEA, Vienna.

Sarin, M. M., S. Krishnaswami, K.Dilli, B.L.K. Somayajulu and W.S. Moore (1989). "Major ion chemistry of the Ganga-Brahmaputra river system: weathering processes and fluxes to the Bay of Bengal." Geochim. Cosmochim. Acta **53**(5): 997-1009.

Sarin, M. M., S. Krishnaswami, B.L.K. Somayajulu and W.S. Moore (1990). "Chemistry of uranium, thorium and radium isotopes in the Ganga-Brahmaputra river system: weathering processes and fluxes to the Bay of Bengal." Geochim. Cosmochim. Acta **54**(5): 1387-1396.

Shaffer, N.R., R. Leininger, E. Ripley, and M. Gilstrap. (1981). "Heavy metals in organic-rich New Albany Shale of Indiana (abstr.) Abstr. w. Prog., Geol. Soc. Amer. **13**(7):551.

Shaw, T. J. and G. Klinkhammer (1989). A time series study of uranium cycling in the Chesapeake Bay. EOS, Transactions of the American Geophysical Union, San Francisco, American Geophysical Union.

Shimkus, K.M. and E.S. Trimonis (1974) Modern sedimentation in the Black Sea, in The Black Sea. Geology. Chemistry. Biology, E.T. Degens and D.A. Ross, eds., Amer. Assn. Petrol. Geol, **Memoir 20**, 249-278.

Sholkovitz, E., T. Shaw, and D. Schneider (1991). "The response of rare earth elements to seasonal anoxia in Chesapeake Bay." Geochim. Cosmochim. Acta (in prep.):

Sholkovitz, E.R. (1976). " Flocculation of dissolved organic and inorganic matter during mixing of riverwater and seawater." Geochim. Cosmochim. Acta, **40**: 831-845.

Stallard, R. F. (1980). Major element geochemistry of the Amazon River System. Woods Hole Oceanographic Institution - Massachusetts Institute of Technology.

Stallard, R. F. and J. M. Edmond (1983). "Geochemistry of the Amazon 2. The influence of geology and weathering environment on the dissolved load." J. Geophys. Res. **88**: 9671-9688.

Sutulov, A. (1965). Molybdenum Extractive Metallurgy. Concepcion, Chile, University of Concepcion.

Tolmazin, D. (1985). "Changing coastal oceanography of the Black Sea. I: northwestern shelf." Prog. Oceanog. **15**: 217-276.

Torrey, S. (1978). Trace contaminants from coal. Pollution Technology Rev., Park Ridge, N.J., Noyes Data Corp., 50, 294pp.

Tribovillard, N.-P., J.-F. Stephan, H. Minivit, V. Reyre, P. Cotillon and E. Jautee (1991). "Cretaceous black shales of Venezuelan Andes: preliminary results on stratigraphy and paleoenvironmental interpretations." Paleo., Paleo., Paleo. **81**: 313-321.

Turekian, K.K. and L.H. Chan. (1971). The marine geochemistry of the uranium isotopes,  $^{230}\text{Th}$  and  $^{231}\text{Pa}$ . In: Activation analysis in geochemistry and cosmochemistry, A.O. Brunfeldt and E. Steinnes, eds., p.311-320. Universitetsforlaget, Oslo.

UN Report. (1989) COAL - Annual Bull. of Coal Statistics for Europe. UN Economic Commission for Europe, 1980-1988. Vol. XXIII.

Vine, J.D. and E.B. Tourtelot. (1970). "The geochemistry of black shale deposits, a summary report", Econ. Geol., **65**: 253-272

Yee, H. S., C. I. Measures, et al. (1987). "Selenium in the tributaries of the Orinoco in Venezuela." Nature **326**(6114): 686-689.

## **Chapter 6:**

### **The marine geochemistry of rhenium: 2. Sinks**

---

#### **6.1 Abstract**

Re is highly enriched in anoxic sediments relative to oxic sediments or average crustal materials, suggesting a number of ways in which its chemistry might be exploited in the study of the oxygen content of ancient environments. In the simplest case, these applications would rely on the assumption that Re is added to anoxic sediments by reduction at or below the sediment-water interface, and that it diffuses in from seawater without interference by adsorption onto and cycling with oxide phases in the oxic portion of the sediment. In an effort to understand the processes by which this enrichment arises, Re concentrations have been determined in sedimentary pore waters from an oxic Pacific site and from the highly anoxic sediments of Chesapeake Bay, as well as in the water column of the Black Sea. Two major questions are posed: 1. Is Re, like Mo cycled with manganese oxides in the upper portion of sediments? and 2. Is Re precipitated or scavenged within the anoxic water column of the Black Sea? The results indicate that the answer to both of these questions is negative, and that Re is added to reducing sediments via diffusion from overlying waters. A comparison of Re, Mo and U in the Black Sea indicates that these elements are characterized by different residence times in the anoxic water column, with the most rapid removal indicated for Mo, followed by Re and U.

#### **6.2 Introduction**

Due to its low concentrations in most crustal materials, Re was one of the last stable elements to be isolated. Its discovery was announced nearly

simultaneously by a number of groups (Noddack et al. 1925; Loring and Druce 1925; and Dolejšek and Heyrovsky 1925). The principal features of the marine geochemistry of Re were first described by Boyko et al. (1986) and Koide et al. (1986), who recognized its relatively high concentrations in seawater (45 pM) and in anoxic sediments. In this regard, its marine geochemistry is similar to that of Mo and U, which are also characterized by high stability in oxic seawater and removal into reducing sediments. Conservative profiles for Re in seawater reported in Chapter 5 indicate that Re is not taken up in great amounts by biogenic material in the water column, and thus is probably added to anoxic sediments at or below the sediment-water interface. By analogy with Mo and U, it is proposed that Re diffuses into sedimentary pore waters along a concentration gradient between overlying waters and the depth at which Re is removed from solution. If this is the case, then its concentration in reducing sediments may be a relatively simple function of sedimentary redox conditions, and comparison with other elements in the sedimentary record may provide a new tool with which to study these conditions in ancient environments.

Re is distinguished from Mo, U and other elements which are accumulated in reducing environments by its extreme enrichment in anoxic relative to oxic sediments, and its apparent lack of enrichment in any other phase. Re concentrations in anoxic sediments are greater than those in oxic pelagic sediments by a factor of approximately 500, whereas this factor for U and Mo is 10-50 (Koide et al. 1986 and Ravizza 1991). The manganese nodule data of Koide et al. (1986) indicate that Re is not enriched in manganese phases in marine sediments (unlike Mo, V, Cu and Cr). If generally true, this would remove a complicating aspect of the interpretation of Re concentrations in the sedimentary record. For example, Mo is scavenged by ferromanganese oxides which form near the sediment-water interface under oxic bottom waters. As

these oxides are buried and dissolved as the sediments become anoxic, Mo is released and re-fixed deeper in the reducing section. Thus the amount and rate of release of Mo from the oxide-rich layer partly controls the accumulation of Mo in the reducing zone (Pedersen et al. 1988). In this case, the concentration of Mo in the reducing sediment is not simply the result of diffusion in from overlying water.

If Re is to be useful in environmental reconstructions, the means by which it is added to anoxic sediments must be clarified. If Re is cycled with ferromanganese oxides at the sediment-water interface, or if it is scavenged in the water column by sinking organic matter, then its concentration in sediments is not strictly diffusion-controlled. This chapter will present Re data from pore waters from an oxic Pacific site, and from anoxic Chesapeake Bay sediments, as well as water column data from the Black Sea. These will allow preliminary assessment of the mechanism of Re enrichment in anoxic sediments.

### **6.3 Methods**

#### *Sample collection*

Sedimentary pore waters were collected in the north eastern Pacific ocean and in Chesapeake Bay. The Pacific samples were from two gravity cores raised from 4400 m water depth at approximately 34°48'N and 122°58'W aboard the R.V. New Horizon in February, 1990. Upon recovery on deck, the sediment core was capped and placed in a refrigerated room to cool to bottom water temperatures (~1°C). Sectioning was carried out in a nitrogen filled glove bag. One centimeter sections were extruded and placed in centrifuge tubes using apparatus illustrated in figure 6.1. Sediments were then centrifuged for 20 minutes at 14000 rpm in a gimble-mounted centrifuge. Pore waters were

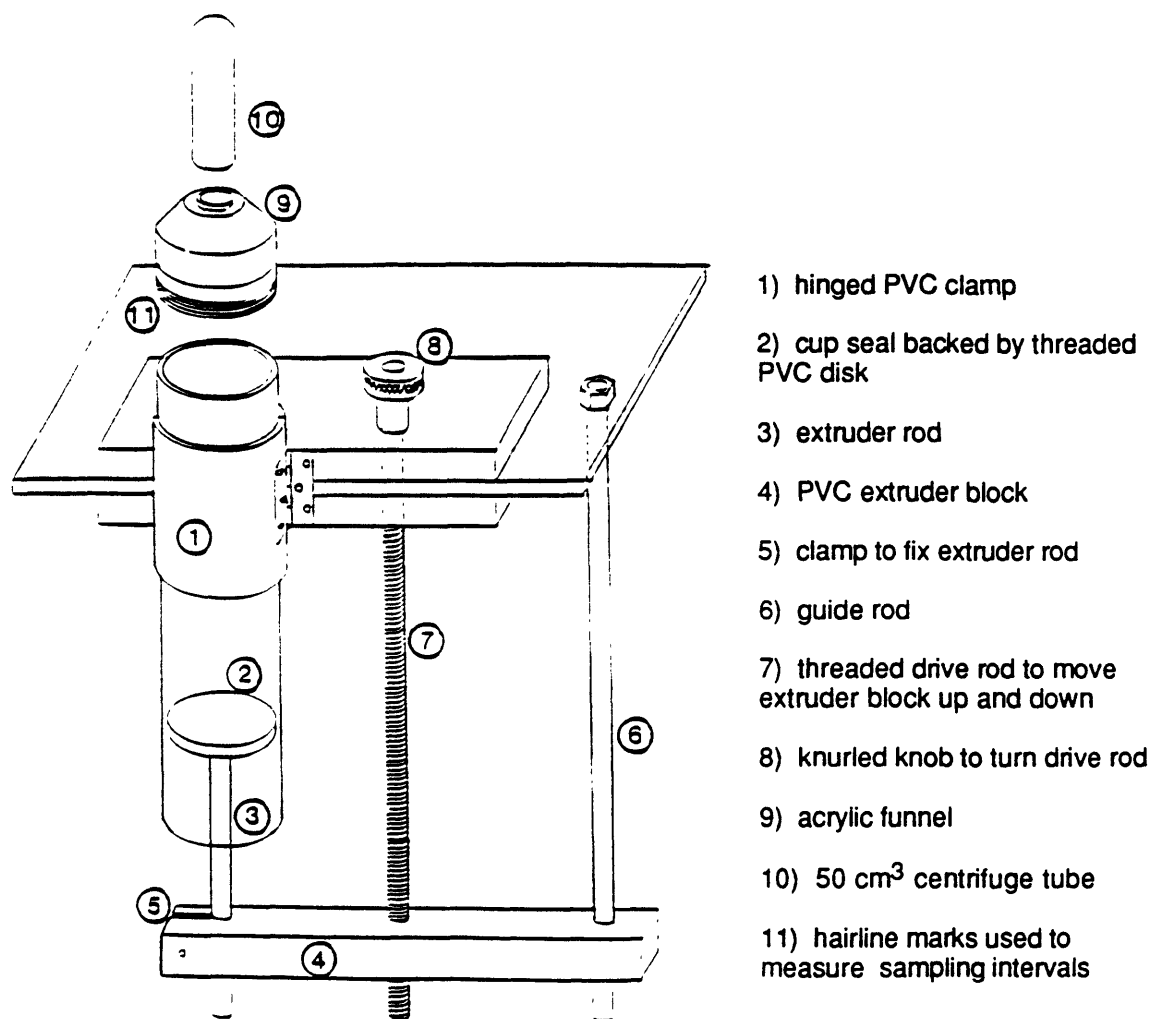


Figure 6.1 Sediment core extruder, from Shaw 1988.

then quickly poured into a syringe and forced through 0.2  $\mu\text{m}$  syringe filters in a laboratory flow bench under filtered air (not under  $\text{N}_2$ ). Two Chesapeake Bay cores were collected aboard the R.V. Ridgely Warfield in July, 1990 (map, figure 6.3); one was a gravity core and the other a subsection of a box core.

Sediments were sectioned as above, although at ship laboratory temperatures. The samples were stored in an incubator set at ambient bottom water temperature (22-23°C) before centrifuging. For these anoxic sediments, sectioning and filtration were carried out in a nitrogen-filled glove bag. Filtered pore water samples (10-20 mL) were acidified with 100  $\mu\text{L}$  triply distilled 16N  $\text{HNO}_3$ .

Black Sea samples were collected during the 1988 joint U.S./Turkish Black Sea Expedition on the RV Knorr. The data reported here are from stations BS3-2 and BS3-6, with the most complete coverage at BS3-2.

### *Analyses*

Sulfide determinations were performed using the colorimetric method of Cline (1969). Re determinations were accomplished using anion exchange preconcentration followed by isotope-dilution, flow-injection ICP-MS, as described previously. Mo measurements were performed on a dilution of 25 $\mu\text{L}$  pore water with 1 mL distilled, deionized water, and the appropriate amount of spike, also by ID-FIA-ICP-MS. Mo data were corrected for interference on the spiked isotope ( $^{95}\text{Mo}$ ) by  $^{79}\text{BrO}$  by monitoring  $^{79}\text{Br}$  and using the  $^{79}\text{BrO}/^{79}\text{Br}$  ratio measured in a Br standard. This limits the precision of the data to  $\pm 10\%$ . Because of the limited pore water volumes available, samples were not run in duplicate, and uncertainties were estimated from several runs of similar volumes of seawater to be  $\pm 6\%$  for Re. Duplicate Re measurements in Black Sea samples from the same bottles were reproducible to  $\pm 1.1\%$ , whereas Re

measurements from the same depths at the same station, collected in different bottles in separate casts, and run on different days were reproducible to  $\pm 4.5\%$ . Detection limits were  $10 \mu\text{M H}_2\text{S}$  for a sample size of  $100 \mu\text{L}$ ,  $\sim 1\text{pM Re}$  for a 10-20 mL sample and  $1\text{nM Mo}$  for a  $25 \mu\text{L}$  sample.

## 6.4 Results

### *North Pacific sediment porewaters*

The two cores analyzed were taken from close to the same location ( $34^\circ 47.67'\text{N}$ ,  $122^\circ 59.55'\text{W}$  and  $34^\circ 47.17'\text{N}$ ,  $122^\circ 59.38'\text{W}$ ). This is a site of an ongoing study of seasonal variations in carbon flux and benthic activity (Smith 1989). Primary productivity varies by a factor of three annually in the overlying waters of the California Current, with a chlorophyll maximum in late spring. This gives rise to variations in the deep water flux of particulate organic matter of a factor of ten or more, with a maximum in June (Smith 1989; Smith 1987). In February, when these samples were collected, the sediment was capped by a 2-3 cm oxic (red-brown) layer, overlying sub-oxic grey-green mud.

Re concentrations are reported in Table 6.1 and plotted in figure 6.2, with accompanying Mo and  $\text{NO}_3^-$  data. In general, there is no unidirectional trend in Re concentrations over the depth interval sampled in both cores, whereas some structure may be discerned in the Mo profile in core F. This release of Mo to the pore waters a few centimeters below the interface was noted at other sites in the California borderlands by Shaw et al. (1990) and was interpreted as the result of cycling of Mo between pore waters and manganese oxide phases. The pore water Re profile does not show any inflection at this depth.

There is more scatter in the data for both elements than can be accounted for by analytical variability, based on analyses of similar volumes of seawater.



Table 6.1 Re and Mo pore water data for an open Pacific site, 34°47'N, 122°59'W

Depth (cm)	Re (pmol/kg)	Mo (nmol/kg)	NO <sub>3</sub> (μM)
<b>Core F</b>			
OW	44	109.1	
0.5	54	116.2	32.2
1.5	44	88.4	35.9
2.5	45	91.9	23.3
3.5	32	114.1	6.8
4.5	34	181.4	6.8
5.5	25	217.0	
7.0	20	157.4	
9.0	20	154.0	3.8
13.0	11	144.0	
17.0	9	125.0	2.2
21.0	42	138.2	
25.0	16	128.2	1.5
30.0	43	154.3	2.2
<b>Core D</b>			
OW	47	106.7	
0.5	32	153.1	
1.5	47	115.1	
2.5	32	132.1	
3.5	33	91.3	
4.5	30	98.7	
5.5	28	121.8	
8.5	25	99.8	
11.5	91*	138.7	
14.5	35	161.6	
17.5	20	103.1	
20.5	21	159.7	
23.5	34	154.9	

OW = overlying water, \* not plotted

SD Re analysis = 6%

SD Mo analysis = 8%

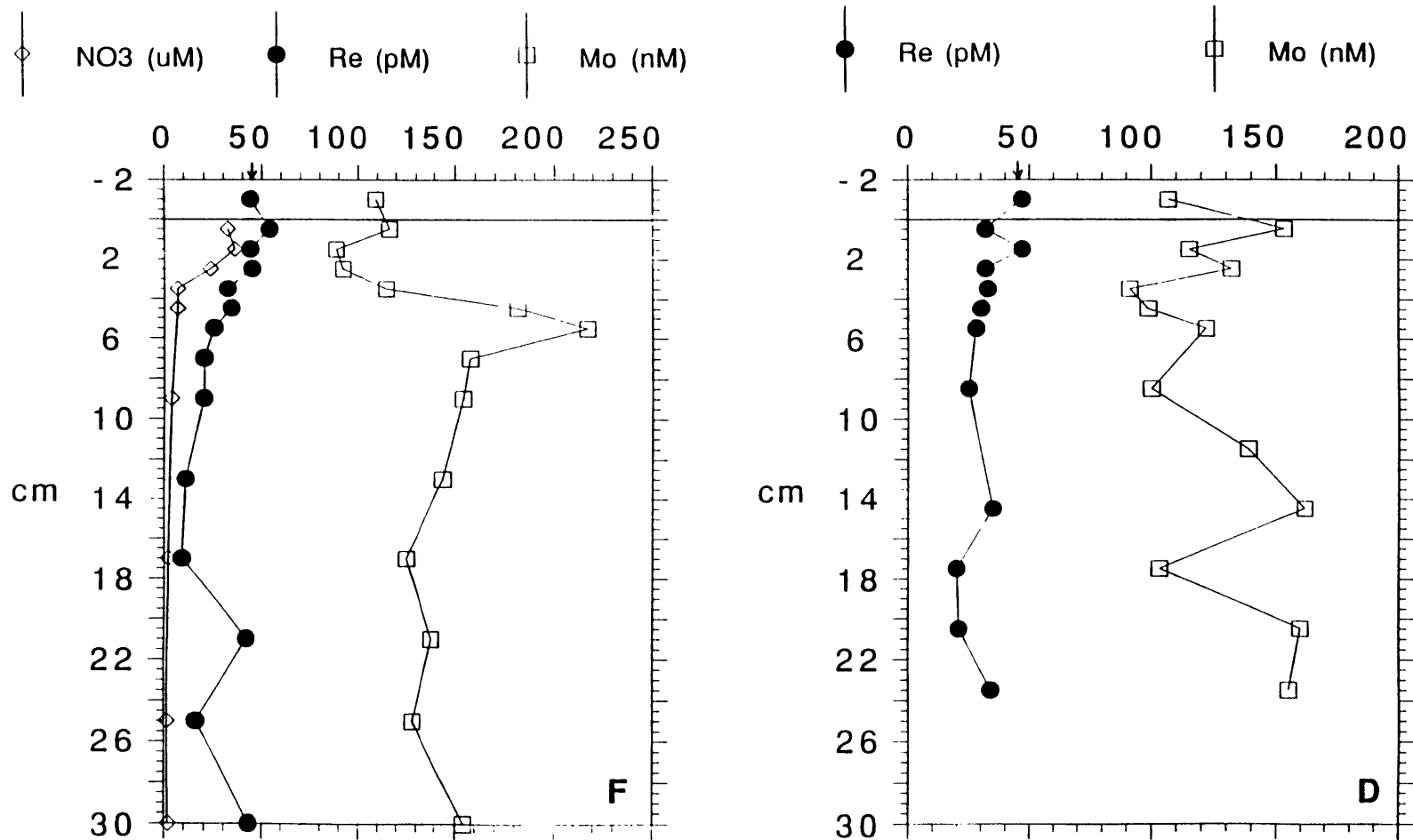


Figure 6.2 Re, Mo and NO<sub>3</sub> results for pore waters from an oxic Pacific site. The uppermost point shows the concentration in water recovered with the core, overlying the sediment. The arrows show the Re concentration in bottom water a) core F: Mo results show evidence for recycling with manganese oxides, whereas Re results do not. b) core D.

The possibility that high values near the bottom of the core were an artifact of oxidation of reduced Re was investigated with sediments from Chesapeake Bay, as described below. It is also possible that Re was strongly complexed by dissolved organic matter in the pore waters and that isotopic exchange between sample and spike was inhibited, leading to low values for some samples. This seems unlikely, however, given the acidity of the samples (0.16N HNO<sub>3</sub>), and the time elapsed between the spiking and anion exchange steps (>4wks). Additionally, UV oxidation had no effect on the measured Re concentration in Woods Hole seawater, although this experiment was not performed with pore waters.

#### *Chesapeake Bay sediment porewaters*

Two cores were collected in Chesapeake Bay (figure 6.3). The Bay is the seasonally anoxic estuary of the Susquehanna, Potomac and several smaller rivers. In July, when these samples were taken, the bottom waters were devoid of oxygen from about 15 m to the bottom at 29 m. The first (Sta.2) was a gravity core taken in sediment that was relatively coherent and had the characteristic grey color of finely disseminated pyrite. Sulfide increases smoothly with depth in the pore waters below 8 cm (figure 6.4 and Table 6.2). Molybdenum is removed from the dissolved phase within the first centimeter, whereas Re decreases more gradually through the top three centimeters. Between four and eight centimeters Re is nearly completely removed, but then reappears in the pore waters below this depth and remain at a nearly constant value (~10 pM). There is currently no explanation for the two high points at 4.5 and 27.5 cm, although possibilities include physical disturbance of the sediment during sampling, contamination, or oxidation before separation of pore waters from solids.

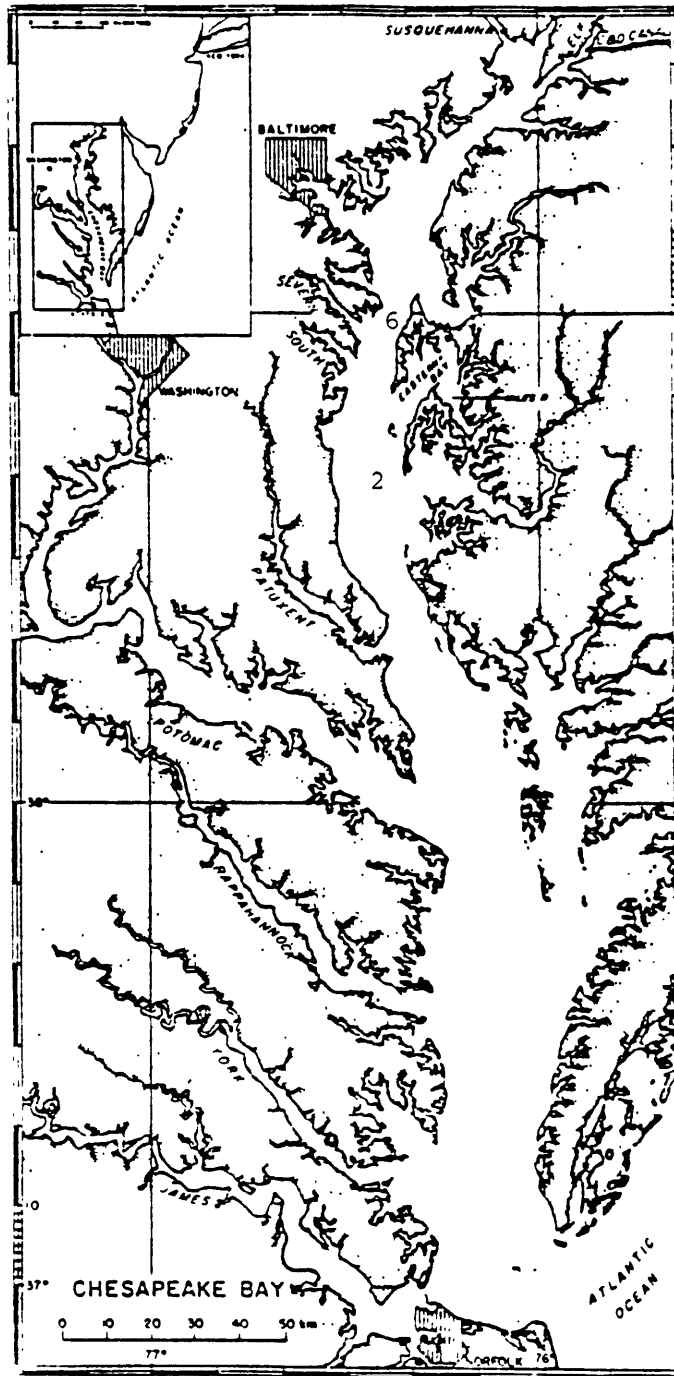


Figure 6.3 Chesapeake Bay and the locations of Stations 2 and 6.

Table 6.2 Re and Mo pore water data from Chesapeake Bay, July 1990

Depth (cm)	Re (pmol/kg)	Mo (nmol/kg)	H <sub>2</sub> S ( $\mu$ M)	PO <sub>4</sub> ( $\mu$ M)	NH <sub>4</sub> ( $\mu$ M)
<u>Station 6</u>					
OW	26.1	25.3	bd		
0.5	24.8	72.3	bd		
1.5	21.0	6.8	8		
2.5	17.8	bd	622		
3.5	14.9	bd	762		
4.5	12.2	bd	790		
5.5	12.1	bd	888		
6.5	4.1	bd	919		
7.5	12.3	bd	727		
9.5	7.7	bd	342		
11.5	12.0	bd	101		
13.5	6.4	bd	32		
16.5	7.6	bd	bd		
17.5	7.9	bd	bd		
18.5	3.8	bd	bd		
19.5	29.2	bd	bd		
<u>Station 2</u>					
OW	20.6	52			
0.5	14.1	1.7	bd	20	55
1.5	3.1	bd	bd	30	55
2.5	3.9	bd	bd	38	55
3.5	bd	bd	bd	45	55
4.5	11.7	bd	bd	51	60
5.5	bd		bd	53	80
7.5	bd	bd	bd	60	175
8.5	8.9		15	63	85
9.5	11.0		45	72	165
10.5	11.5	bd		75	225
11.5	8.0		52	80	175
12.5	10.3	bd		82	200
13.5	8.5		165	88	300
16.5	10.4		315	102	400
18.5	9.4		331	102	410
20.5	12.3		308	110	435
21.5	11.5	bd		113	520
23.5	11.7		376	121	650
24.5	11.2			128	665
27.5	22.2		496	138	800
30.5	8.8		582	140	980
33.5	16.3		751	138	1000

OW = overlying water; PO<sub>4</sub> and NH<sub>4</sub> analyses by Dr. K. Ruttenberg  
 bd = below detection (1nmol/kg Mo), SD Re =  $\pm$ 6%, SD Mo =  $\pm$ 8%

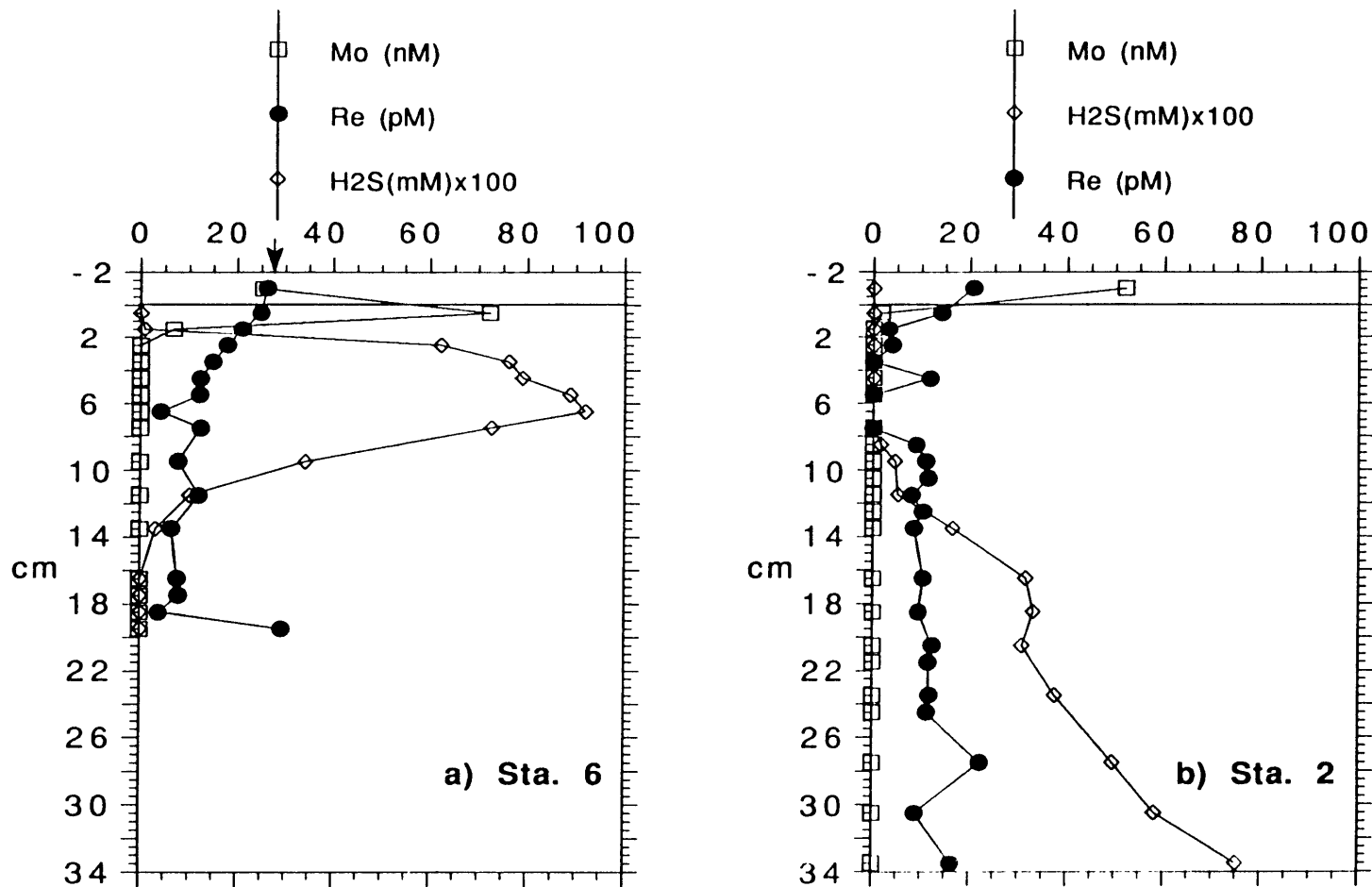


Figure 6.4 Re, Mo and H<sub>2</sub>S pore water data from two cores in Chesapeake Bay. The arrow shows Re concentrations 1m off the bottom at Station 6. The uppermost point represents overlying water. Station locations shown in figure 6.3.

The second core (Sta.6), a subcore of a box core, was taken in more highly reducing sediment. The pore waters were homogenized to some extent by the evolution of methane within the core, and the sediment texture was more gel-like than at Sta 2. Sulfide was detected in pore waters between 1 and 14 cm, with a maximum at 6-7 cm. The rapid removal of sulfide toward the base of the core is the result of depletion of pore water sulfate at these depths. Mo is removed from the pore waters within the first two centimeters and was not detected below this depth. Re concentrations decrease smoothly through the first four centimeters and then stabilize at a lower, but non zero value between 4 and 12 pM. A high value is observed in the deepest section, which may have been the result of inadvertent exposure to air.

In order to test the effect of inadvertent exposure to oxygen, a few samples from the Station 2 core were exposed to air for varying amounts of time before centrifuging. The samples were injected with air several times using a disposable pipet, and were allowed to sit uncapped in centrifuge tubes for 20 to 80 minutes. Sulfide values decreased in all cases, whereas Mo increased only in the uppermost sample and Re did not change at all (figure 6.5, Table 6.3). Even longer times must be necessary to oxidize Re, or the phase which controls its speciation. It is therefore unlikely that the anomalously high values observed were the result of oxidative mobilization of Re. During storage and sectioning, individual sections were not exposed to air long enough to have created these high concentrations. It is possible, however, that a poor seal at the bottom of the core could have led to high values in the bottom section, as the core bottoms were not enclosed in the glove bag during sectioning (3-4 hours).

The origin of the scatter in the data at both sites and the occasional high measurements is not clear. Although higher levels found at the base of the

Table 6.3 Oxidation experiments, Station 2, Chesapeake Bay

Depth (cm)	oxidation time	Re (pmol/kg)	Mo (nmol/kg)	H <sub>2</sub> S (mM)
0.5	0	14	1.7	bd
1.5	0	3	bd	bd
2.5	0	4	bd	bd
3.5	0	bd	bd	bd
4.5	0	12	bd	bd
5.5	0	bd	bd	bd
7.5	0	bd	bd	bd
8.5	20 min	9	4.2	0.015
9.5	0	11	bd	0.045
10.5	20 min	12	bd	
11.5	0	8	bd	0.052
12.5	40 min	10	bd	0.022
13.5	0	8	bd	0.165
16.5	0	10	bd	0.315
18.5	0	9	bd	0.331
20.5	0	12	bd	0.308
21.5	60 min	12	bd	0.037
23.5	0	12	bd	0.376
24.5	80 min	11	bd	0.067
27.5	0	22	bd	0.496
30.5	0	9	bd	0.582
33.5	0	16	bd	0.751



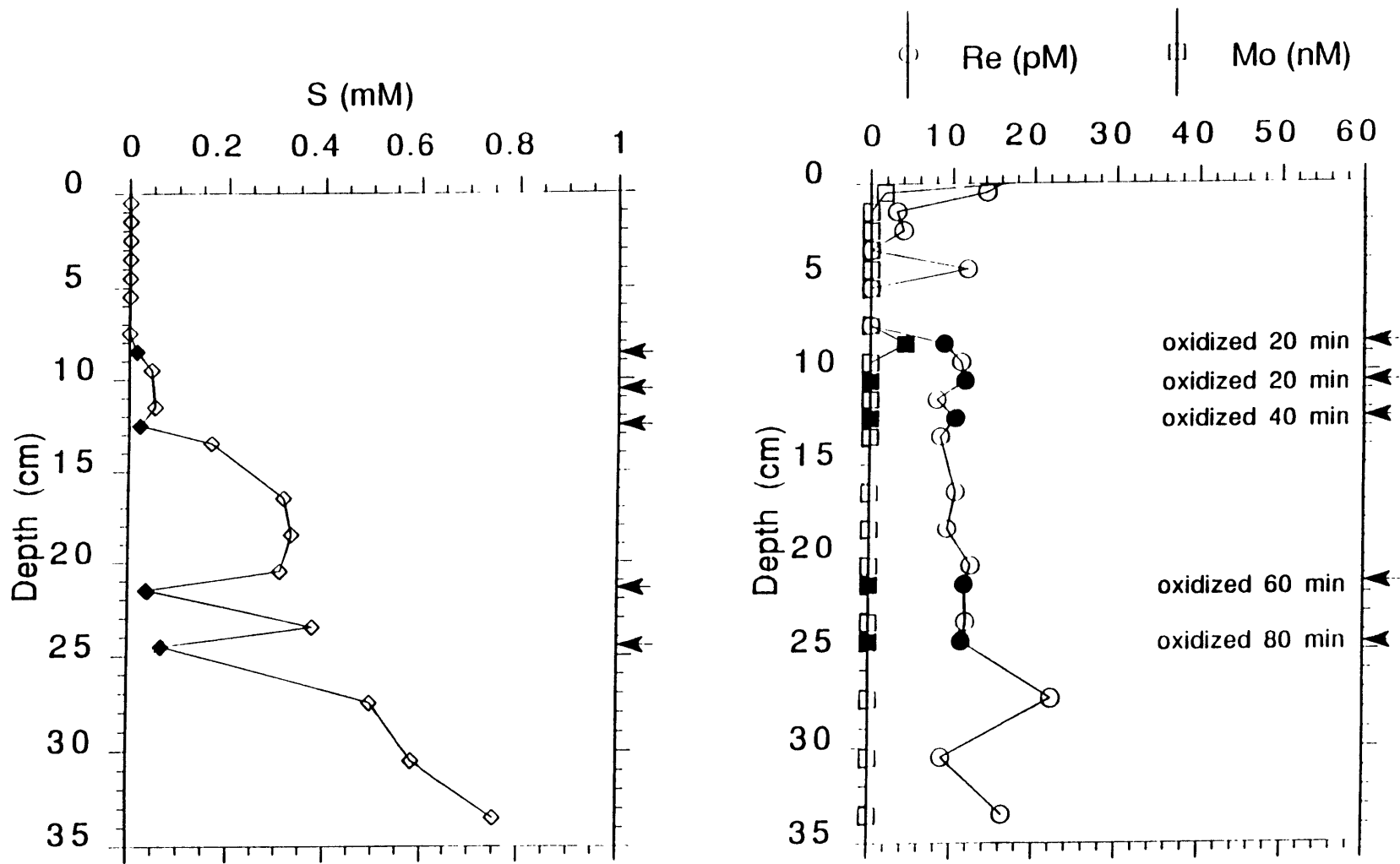


Figure 6.5 Results of oxidation experiment with Chesapeake Bay Station 2 pore waters. Arrows point to samples which were exposed to air for the indicated times before centrifuging; darkened symbols represent these samples.

Chesapeake Bay cores may be due to air leaking through the seal at the base of the core, it is unlikely that this is the explanation for high values found in the middle of the cores. Contamination cannot be ruled out, although procedural blanks were run accompanying every five to ten samples. Possible contaminants include insufficiently cleaned resin (see Chapter 2), or fossil fuel exhaust (? , see Chapter 5); only the former has been proven to contain high Re concentrations.

### *Black Sea and Sea of Marmara*

The Black Sea is the largest body of anoxic water in the world. Its waters are permanently devoid of oxygen below about 100 m due to sluggish renewal of the deep waters. Stable density stratification arises from the excess of fresh water inputs over evaporation, and the inflow of saline waters from the Mediterranean. Exchange with Mediterranean waters occurs via the Sea of Marmara, restricted by the narrow Dardanelles and Bosphorus Straits. Warm, saline waters (~38 ppt) from the Sea of Marmara spill over the Bosphorus sill and entrain colder, less saline waters from intermediate depths of the Black Sea to create Black Sea deep waters with a salinity of about 22 ppt (Murray et al. 1991). The water replacement time of the deep Black Sea has been estimated to be between 500 and 1000 years (Murray et al. 1991; Falkner, O'Neill et al. 1991). The surface waters of the Black Sea are fed by river waters which appear to have been contaminated for Re by anthropogenic sources (see Chapter 5), and surface water renewal times are thought to be rapid (Murray et al. 1991).

Water column profiles were collected at two stations in the central Black Sea and one in the Sea of Marmara. Station locations are shown in figure 6.6. Data for the Black Sea stations, BS3-2 and BS3-6, are listed in Table 6.4, and

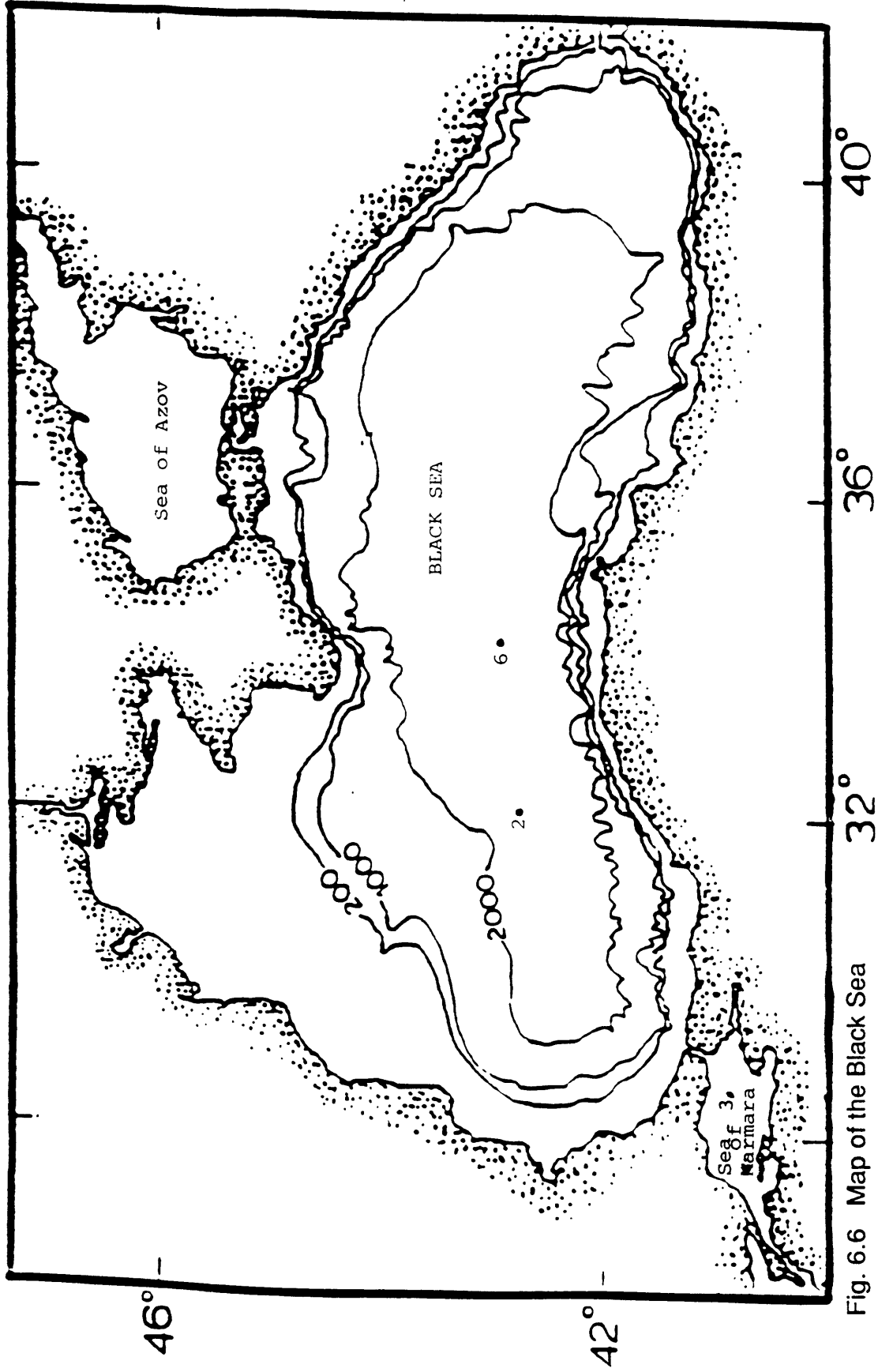


Fig. 6.6 Map of the Black Sea

Table 6.4 Re in the Black Sea, June 1988

Sta.	Sample	Depth (m)	$\sigma_t$	Re (SD) ( $\mu\text{mol/kg}$ )	Salinity (ppt)	O <sub>2</sub> ( $\mu\text{M}$ )	H <sub>2</sub> S ( $\mu\text{M}$ )
2	DH2	20	13.752	29.2	18.465	309	
2	DH1	30	14.348	30.7	18.675	285	
2	DH4	40	14.671	30.3	19.189	253	
2	DH6	50	14.912	28.7	19.992	111	
2	DH8	60	15.452	27.9	20.479	3.4	
2	DH7	70	15.880	27.6 (0.2)	20.727	2.1	
2	DH11	80	16.030	22.5 (0.4)	20.887	1.4	
2	DH13	90	16.108	25.9	21.031		0.6
2	DH15	100	16.257	25.3	21.130		4.9
2	DH16	105	16.281	25.0 (0.04)	21.164		9.8
2	DH17	110	16.276	23.9	21.200		12.9
2	DH18	115	16.355	23.6	21.248		14.4
2	DH19	120	16.391	24.9	21.290		16.9
2	DH20	130	16.440	23.2	21.384		21.0
2	DH21	140	16.490	21.7	21.422		25.4
2	DH22	170	16.598	20.3	21.556		49.1
2	DH23	200	16.690	18.0	21.652		71.0
2	DH24	400	16.972	13.1	22.003		
2	DH25	600	17.104	9.0	22.162		
2	DH26	800	17.171	8.8	22.250		
2	DH27	1200	17.212	8.5	22.310		
2	DH28	1600	17.222	(17.6)	22.318		
2	DH29	2100	17.223	(18.1)	22.330		
2	G1115	2086	17.223	8.4	22.330		
6	DH35	150	16.432	23.4	21.321		
6	DH36	180	16.546	23.8	21.416		
6	DH32	500	17.023	13.0	21.962		
6	DH33	800	17.157	10.0	22.222		
6	G1092	800	17.157	12.3	22.222		
6	DH34	1500	17.219	9.9	22.313		
6	G1093	1500	17.219	9.0	22.313		
6	DH30	2153	17.221	9.1	22.320		
6	G1116	2153	17.221	9.7	22.320		
6	DH31	2174	17.221	9.1	22.320		
6	G1089	2174	17.221	10.1	22.320		
6	G1090	2185	17.221	9.6	22.320		

DH samples were collected by Bill Landing

G samples were collected by P. Froelich and R. Mortlock

SD = difference from the mean of duplicate samples

() = not included in plots

Pooled standard deviation = 1.1% from three duplicate samples, or 4.5% from different samples from the same depths

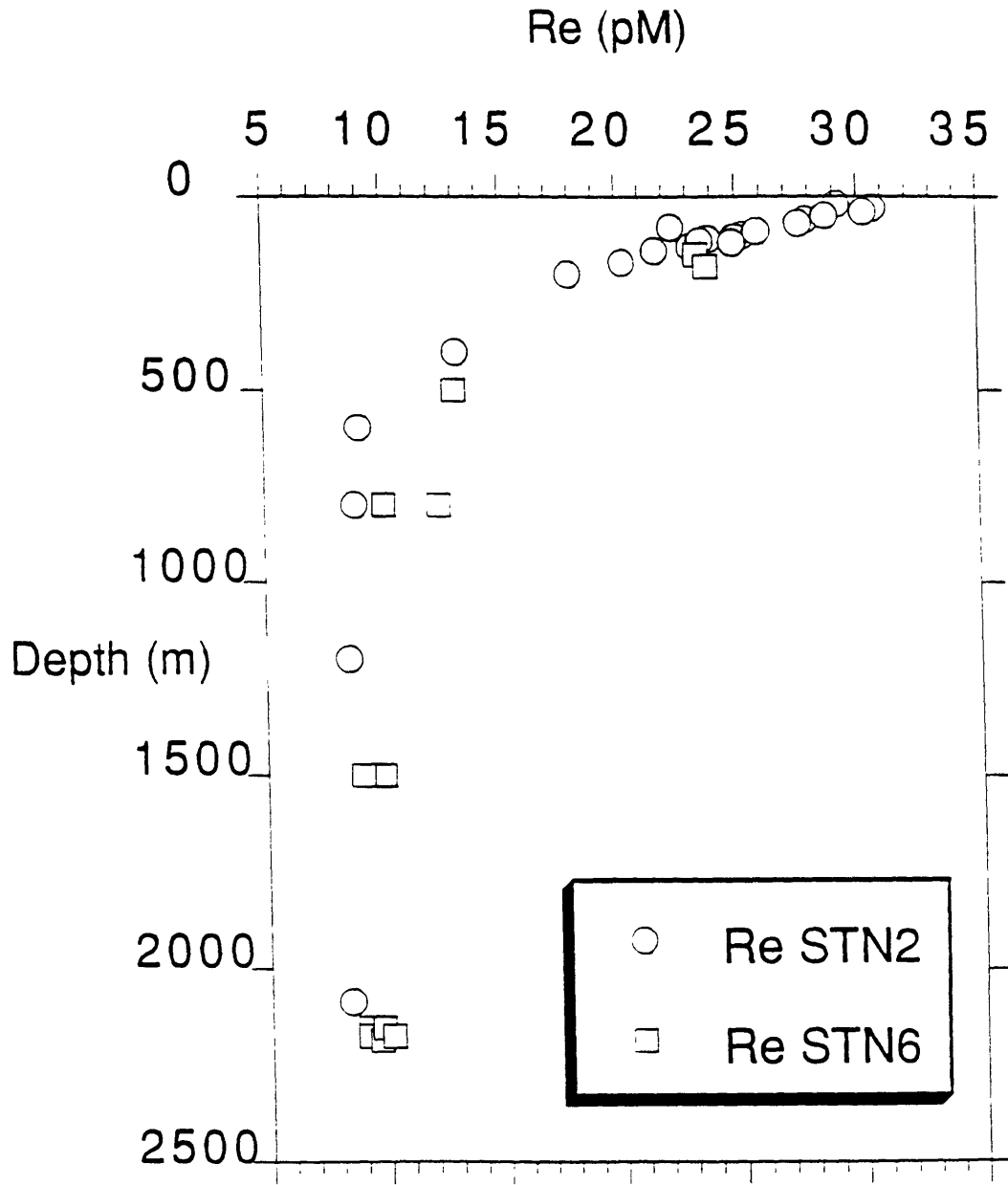


Figure 6.7 Re in the Black Sea water column

plotted against sample depth in figure 6.7. The offset between the two data sets is less apparent when Re is viewed against potential density ( $\sigma_\theta$ ) (figure 6.8). In the summer of 1988, when these samples were collected, the oxic/anoxic interface was marked by a transition zone of low oxygen and sulfide from 60 to 100 m at Station 2 (Table 6.4). Re concentrations decrease smoothly through the upper water column, with the exception of one point at 80 m (figure 6.9). This point is also lower in Mo and V (Emerson and Husted 1991), and occurs at the Mn particulate maximum (Lewis and Landing 1991). This may indicate uptake of the three elements onto manganese oxides which form above the redox boundary. If so, this is the first evidence that Re may be scavenged by manganese oxides. The depletion for Mo and Re represents about 15% of the value expected from the adjacent points with a 22% depletion for V.

When plotted against salinity, Re decreases with depth according to two trends with different slopes, separated by the  $O_2/H_2S$  interface at 21 ppt (figure 6.10). In both the oxic and anoxic regions, Re concentrations covary with salinity, with no evidence for removal or addition of Re within the water column (with exception of the point mentioned above).

Within the Sea of Marmara, Black Sea surface waters flow southward above more saline Mediterranean waters which flow toward the Black Sea. Re concentrations in Marmara surface waters are slightly enriched compared to Black Sea surface waters, but maintain a constant relationship to salinity (Re/sal. = 1.6 pM/ppt in surface waters of both basins) (Table 6.5). Re concentrations in Marmara deep waters reflect the evaporative concentration of seawater as it passes through the Mediterranean. The Re/salinity ratio in Marmara deep waters is identical to that of open ocean seawater (1.3). The higher ratio in Marmara and Black Sea surface waters is the result of high dissolved Re loads carried by rivers draining into the Black Sea.

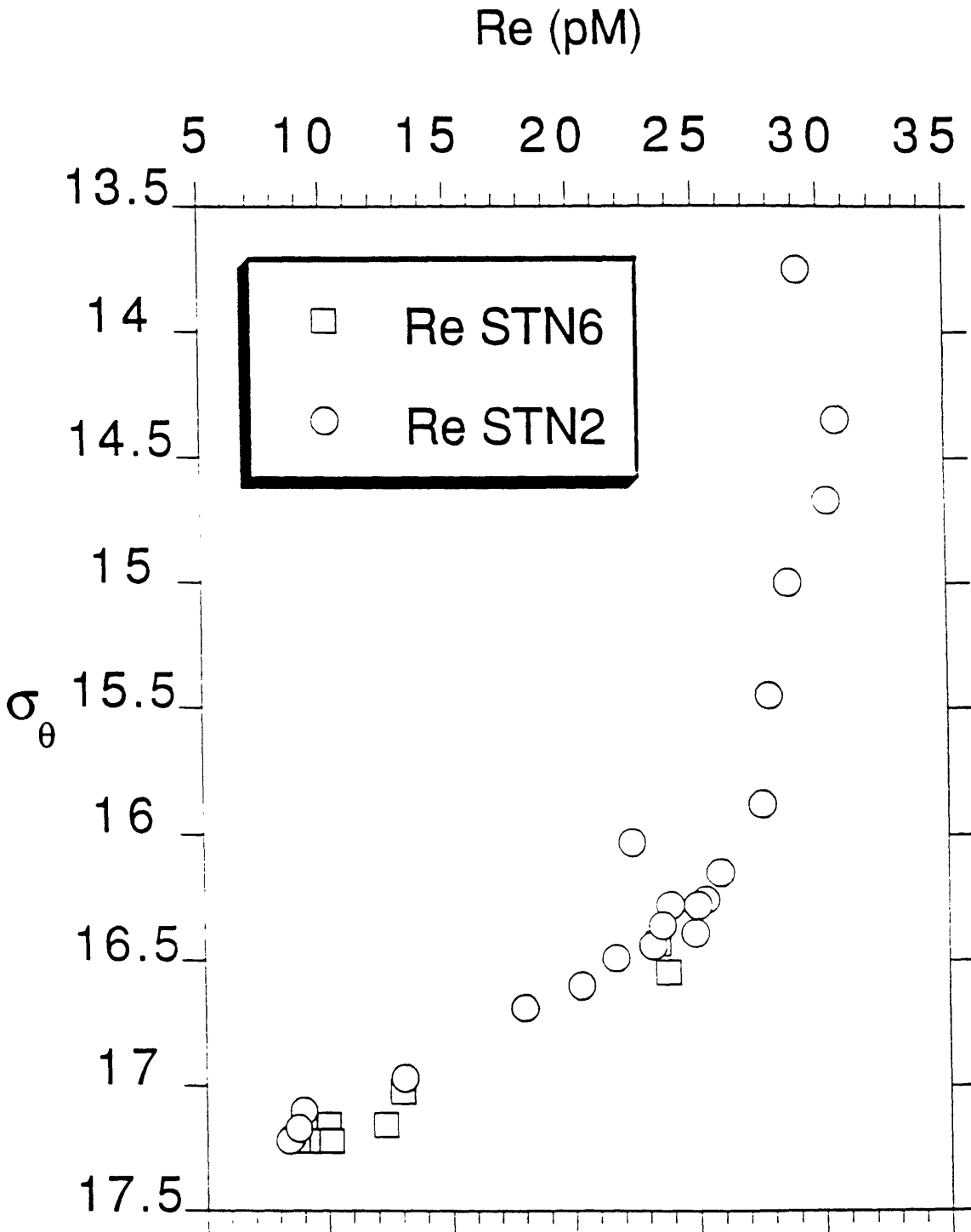


Figure 6.8 Re in the Black Sea vs. potential density

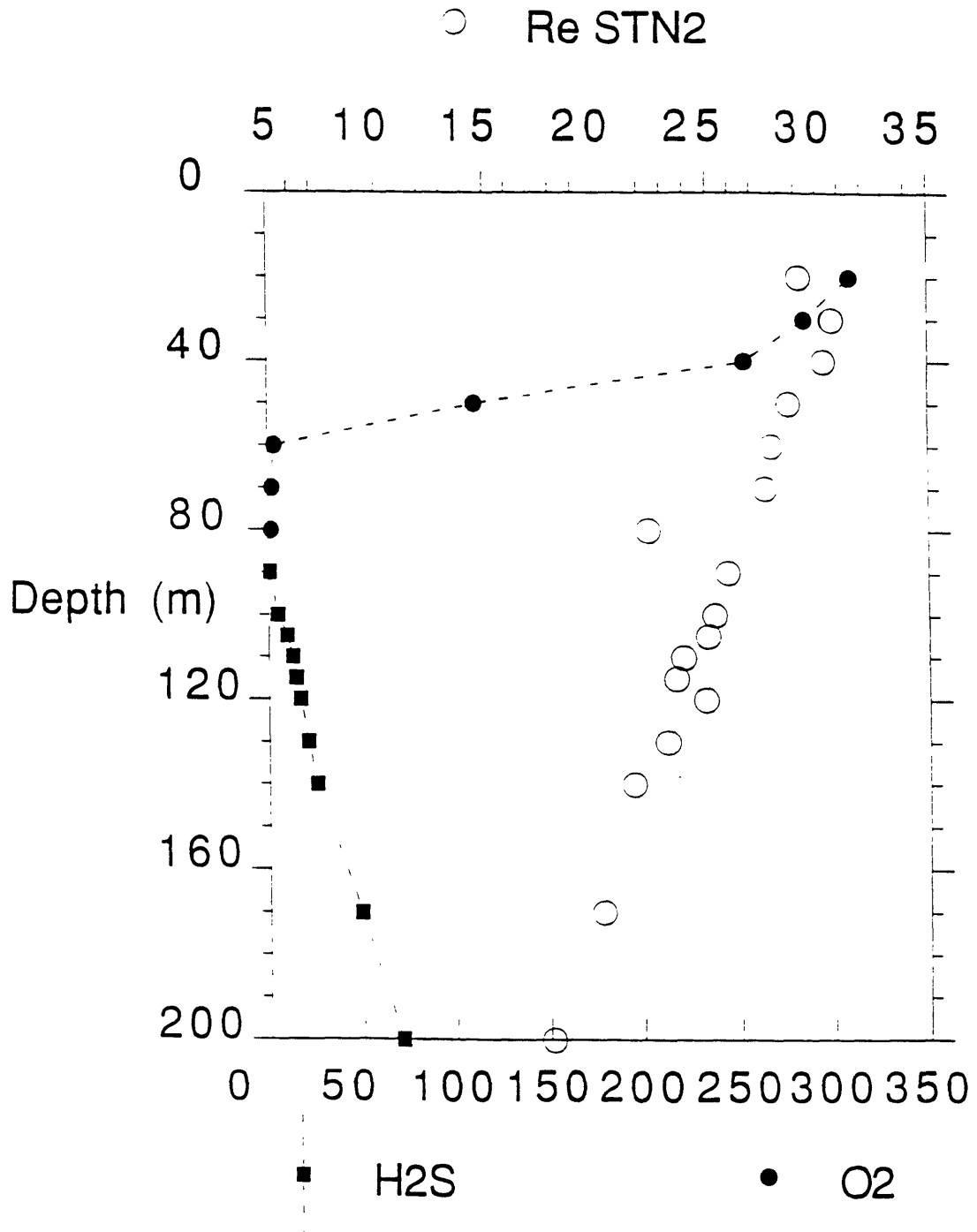


Figure 6.9 Re, O<sub>2</sub> and H<sub>2</sub>S in the top 200 m of the Black Sea, Station 2



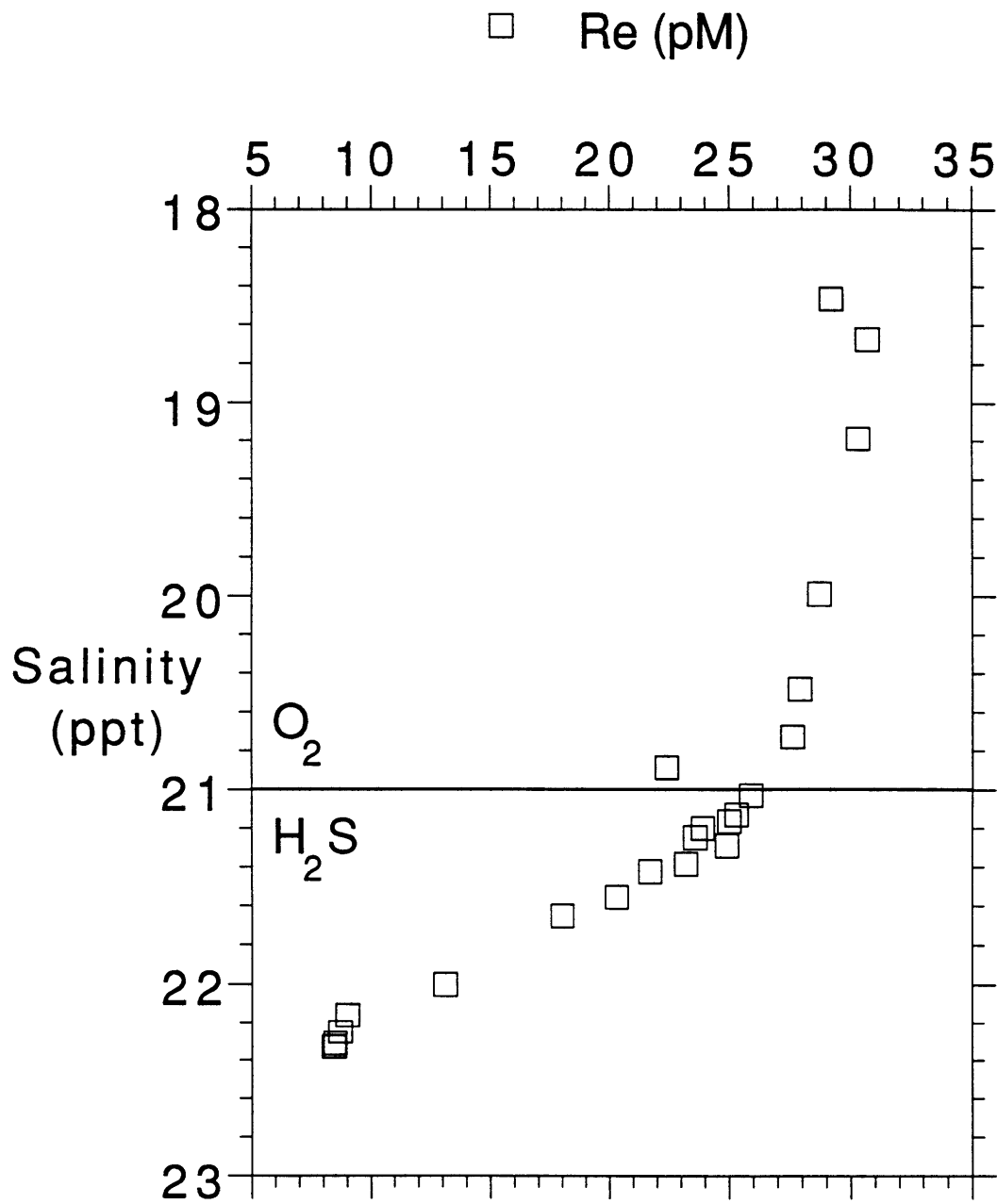


Figure 6.10 Re vs salinity in the Black Sea. The line marks the salinity at the oxic-anoxic interface.

Table 6.5 Re in the Sea of Marmara (Station 3, August 1988)

Depth (m)	Re(pmol/kg)	Salinity
5	34.7	21.5
30	49.3	38.6
100	50.2	38.6
450	48.2	38.6
750	49.4	38.6
1200	48.9	38.6

(Re  $\pm$  2%)

## 6.5 Discussion

### *Pore waters*

Previous work indicated that Re, unlike Mo, is not scavenged or coprecipitated with ferromanganese oxides in manganese nodules (Koide et al., 1986). In order to determine if this is true within the sediment column as well, it is important to show that manganese oxides do not act as a barrier or a "diagenetic pump" (*sensu* Pedersen et al. 1988) for Re, as they do for Mo. The North Pacific sediment pore waters sampled here offer preliminary evidence that Re is not scavenged by manganese oxides within the sediment. Within the resolution of the data, Re pore water concentrations remain constant in the two cores sampled. In contrast, the Mo profile in core F is indicative of uptake onto manganese oxides around 2 cm, and release around 5 cm, as oxides are reduced. This is consistent with previous measurements of Re in manganese nodules (Koide et al. 1986), which showed that although Mo concentrations range up to hundreds of ppm in nodules, Re concentrations in the three nodules analyzed were all less than 0.1 ppb.

In the anoxic sediments of Chesapeake Bay, Re diffusion into the sediments can be inferred from the pore water profiles at both sites. At Station

2, Re is nearly completely removed from pore waters between 3 and 8 cm, but reappears below this depth at nearly constant concentrations of about half that in overlying waters. Its reappearance coincides with the depth at which H<sub>2</sub>S is first observed in the pore waters. In the second core (Sta.6), Re never reaches the low (<1pM) values observed in Station 2 pore waters, and decreases smoothly through the top 5 cm to the same deep value of approximately 10 pM. If H<sub>2</sub>S is responsible for partially stabilizing Re in solution, then one would not expect to see complete removal of Re from the pore waters at this site, as sulfide is elevated through most of the core length. The amount of Re which is stable in solution in the deeper pore waters of these two cores probably represents a small fraction of the total Re present. Assuming that Re diffuses in to the sediment along the gradient established in the top of the Station 2 core, and given the parameters listed in Table 6.6, the Re concentration of the sediment is calculated to be approximately 10 ppb. Based on the pore water gradient in the Station 6 core, the sedimentary concentration is predicted to be about 6 ppb. These concentrations are similar to that in sediments of Saanich Inlet (a seasonally anoxic fjord on the coast of Vancouver Island, British Columbia) where Koide et al. (1986) measured 6 ppb Re. The fraction of the total sedimentary Re content that is contained in the pore waters is therefore approximately 0.1%.

The mechanism by which Re is partially removed from reducing pore waters is not known. Possibilities include the reduction of ReO<sub>4</sub><sup>-</sup> to ReO<sub>2</sub>, ReS<sub>2</sub>, or the formation of Re<sub>2</sub>S<sub>7</sub>, which are all relatively insoluble, or the formation of Re-organic complexes. In early experimental work, Muller and La Lande (1933) (and others summarized in Druce 1948) bubbled solutions containing ReO<sub>4</sub><sup>-</sup> with H<sub>2</sub>S and precipitated a Re-sulfide which they identified as Re<sub>2</sub>S<sub>7</sub>. Re was not quantitatively removed from solution, however, and it was suggested that

Table 6.6 Parameters used in calculating the flux of Re into Chesapeake Bay sediments

**Station 2**

Re concentration in bottom water: $(Re)_{bw} =$	20 pM
Re concentration at minimum: $(Re)_m =$	0 pM
Depth at which Re goes to min.: $z_m =$	3 cm
Porosity: $\phi =$	0.9
Density: $\rho =$	2 g dry sed/cm <sup>3</sup> dry sed
Effective sediment diffusion coefficient: $D_{eff} =$	$5 \times 10^{-6}$ cm <sup>2</sup> /sec <sup>a</sup>
Sedimentation rate: $S =$	0.1 cm/y <sup>b</sup>

Re predicted in sediments =	10 ppb
-----------------------------	--------

**Station 6**

Re concentration in bottom water: $(Re)_{bw} =$	27 pM
Re concentration at minimum: $(Re)_m =$	10 pM
Depth at which Re goes to min.: $z_m =$	4 cm
Porosity: $\phi =$	0.9
Density: $\rho =$	2 g dry sed/cm <sup>3</sup> dry sed
Effective sediment diffusion coefficient: $D_{eff} =$	$5 \times 10^{-6}$ cm <sup>2</sup> /sec <sup>a</sup>
Sedimentation rate: $S =$	0.1 cm/y <sup>b</sup>

Re predicted in sediments =	6 ppb
-----------------------------	-------

- a. (Li and Gregory 1974) - based on tracer and self-diffusion coefficients for  $MoO_4^{2-}$ , corrected for temperature, and tortuosity  
 b. (Nixon 1987)

Re flux into sediments (J, moles cm<sup>-2</sup> sec<sup>-2</sup>) =

$$D_{eff} \times \frac{(Re)_{bw} - (Re)_m}{1000z_m}$$

Re concentration in sediments =

$$\frac{J/S}{(1-\phi)\rho} \times 186 \text{ g/mol}$$

the soluble phase was the thioperrhenate,  $\text{ReO}_3\text{S}^-$ . In basic solution, Re could only be completely precipitated over several days of treatment with  $\text{H}_2\text{S}$ . The precipitation was more rapid under acidic conditions. Solubility of a Re sulfide phase does not appear to be controlling Re concentrations, however, as Re does not correlate with sulfide in the pore solutions.

### *The Black Sea*

Re concentrations decrease from the surface through the deep Black Sea, due to removal of Re to the highly reducing bottom sediments. High Re values in Black Sea surface waters are the result of elevated concentrations in rivers flowing into the Black Sea, presumably as the result of anthropogenic contamination (see Chapter 5). As illustrated by the linear relationship between Re and salinity (figure 6.10), Re does not appear to be removed within the anoxic water column. The observed distribution can be explained by the conservative mixing of low-Re bottom waters with high Re surface waters. The break in slope in the Re-salinity relationship at the oxic-anoxic boundary is due to its coincidence with the pycnocline which restricts mixing between the surface and deep water masses. Thus the Re distribution may be viewed as two conservative mixing lines describing the surface and deep layers.

Re is not removed within the anoxic water column, although sedimentary pore waters are not significantly more reducing than the bottom waters of the Black Sea. This was also noted for U (Anderson et al. 1989) and Mo (Emerson and Husted 1991) in the Black Sea water column. This suggests that the reduction or complexation which is required for Re precipitation is kinetically hindered. The relatively long residence time (400-2000 y) of Re in Black Sea deep waters (calculated below) indicates that its enrichment in sediments is not merely a matter of time allowed, as Re is enriched even at the surface of

sediments (Ravizza 1991) which accumulate at about 20 cm/ky (Calvert et al., 1991). It is possible that the precipitation of Re from anoxic waters requires the presence of mineral surfaces, as suggested for U (Anderson et al. 1989).

Analysis of sediment trap samples from the Black Sea or other anoxic basins will be necessary to confirm the inert behavior of Re in the water column.

In order to compare the Re distribution and removal processes in the Black Sea to those of Mo and U, a simple two box model (figure 6.11) was constructed using the water flux and exchange parameters of Falkner et al. (1991).

Although hydrographic data indicate that water, heat and salt exchange in the Black Sea are more accurately modeled with the inclusion of a third, intermediate-depth box, the dynamics of this intermediate layer are not presently well-constrained (Falkner et al., in prep.). Additionally, the conclusions drawn below are the same whether one employs three boxes, using the parameters given in Murray et al. (in press), or two boxes, as described below. The model assumes steady-state concentrations, so that where model predictions and observations diverge, non-steady state behavior is indicated. It also assumes that exchange of all three elements between the surface and the deep boxes of the Black Sea occurs in constant proportion to salinity, that is, that there are no processes at the interface that fractionate the elements from each other or from major ions. Re concentrations in the deep Sea of Marmara were taken as representative of Bosphorus inflow water, and seawater values (corrected for higher salinity) were used for Mo and U levels in this source. The riverine concentrations were taken to be the water flux weighted average of the riverine concentrations reported in Chapter 5 (Re = 80 pM, Mo = 20 nM and U = 4 nM). It was assumed that Re, Mo and U levels in the Sea of Azov were the same as this average river water. Comparison of the behaviors of the three elements is complicated by the probable anthropogenic

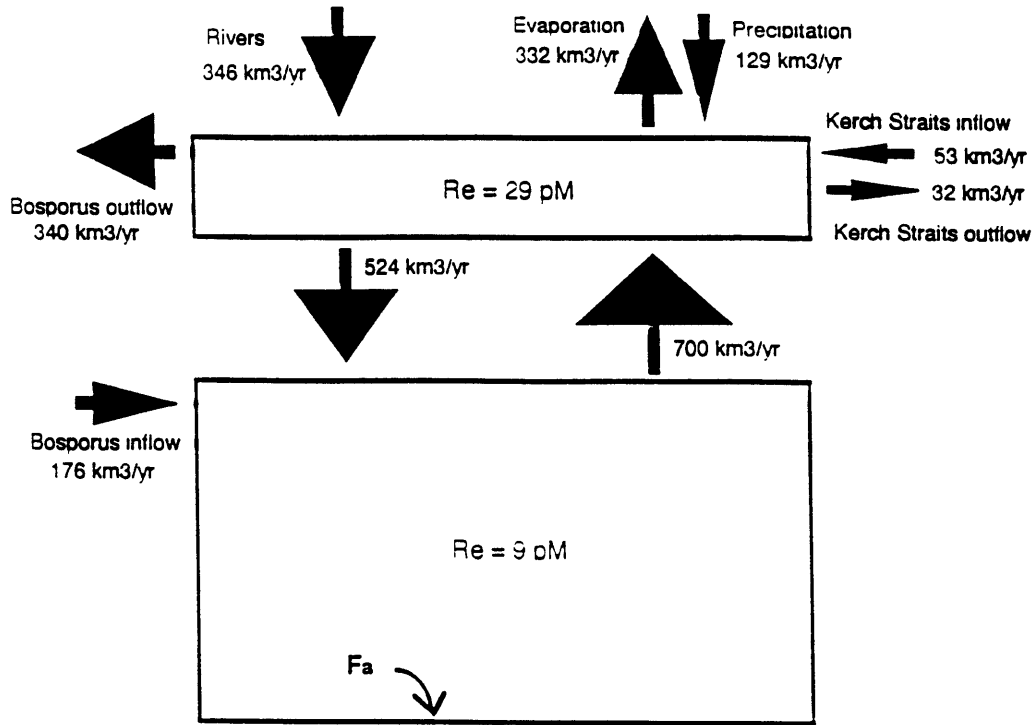


Figure 6.11 Schematic of Black Sea box model with water fluxes as given by Falkner et al., 1991

Surface box:  $F_r C_r + F_{ki} C_a + F_u C_d = F_{ko} C_s + F_{bo} C_s + F_d C_s$

Deep box:  $F_u C_d + F_a = F_{bi} C_b + F_d C_s$

Authigenic flux:  $F_a = k C_d$

Simplified equations:

$$700 C_d - 896 C_s = -346 C_r - 53 C_{az}$$

$$(700+k) C_d - 524 C_s = 192 C_b$$

where,

$F_r$  = river flux into Black Sea

$C_r$  = concentration of Re (or Mo or U) in rivers

$F_{ki}$  = flux through Kerch Straits from the Sea of Azov into Black Sea

$C_{az}$  = concentration in the Sea of Azov

$F_u$  = upward flux of Black Sea deep water

$C_d$  = concentration in deep Black Sea

$F_{ko}$  = flux through Kerch Straits from Black Sea to Sea of Azov

$C_s$  = concentration in surface Black Sea

$F_{bo}$  = flux out of the Black Sea at the Bosporus

$F_d$  = downward flux of Black Sea surface water

$F_{bi}$  = flux into the Black Sea at the Bosporus

$C_b$  = concentration in Bosporus overflow water

$F_a$  = authigenic flux of element into sediments

enrichment of Re in rivers draining into the Black Sea. Although Re, Mo and U behave coherently in many environments, the enrichment of Re in these rivers relative to world average river waters is an order of magnitude higher than that seen for Mo and U (Table 6.7). This may be due to the greater volatility of Re, and its preferential loss to the environment during high temperature combustion processes (Chapter 5).

The authigenic flux ( $F_a$ , mol/y over the whole Black Sea) of the elements into sediments was assumed to be controlled by diffusion, and therefore to be proportional to the concentration of the element in Black Sea deep water ( $M_d$ ). A first order rate constant ( $k$ ) relating deep water concentrations to  $F_a$  was calculated by assuming that current deep waters were relatively unperturbed by any recent increase in riverine inputs. The constant,  $k$  (L/y), could then be calculated from:

$$k = F_a / M_d.$$

$F_a$  was determined from Re, Mo and U sediment concentrations (Ravizza 1991; Emerson and Husted 1991; Anderson et al. 1989) and recent estimates of sedimentation rates (Calvert et al. 1991; Crusius and Anderson 1991) as outlined in Table 6.8. The aluminum content of the sediments and an estimate of the M/Al ratio in average shales were used to correct for the detrital component of the M flux, where M is Re, Mo or U. This was less than 0.4% of the total Re, less than 6% of the Mo and less than 9% of the U in the sediments. A range of  $k$ 's was calculated from the range of authigenic fluxes, as listed in Table 6.8. The values of  $k$  for Re and U are identical (220-780), whereas those for Mo are about a factor of seven higher (1700-5300) where  $k$  is in units of  $10^{12}$  L/y.

With current river inputs and values of  $k$  within the range calculated from sediments, the predicted surface and deep water Re values are substantially



Table 6.7. Sources and sinks of Re, Mo and U to the Black Sea

	<b>Re</b> ( $10^3$ mol/y)	<b>Mo</b> ( $10^6$ mol/y)	<b>U</b> ( $10^6$ mol/y)
Bosporus inflow ( $F_{bi}$ ) ( $176 \times 10^{12}$ L/y) <sup>a</sup>	8.8	19	2.5
River flux ( $F_r$ ) contaminated ( $346 \times 10^{12}$ L/y) <sup>a</sup>	28	7	1.3
River flux ( $F_r^o$ ) uncontaminated ( $346 \times 10^{12}$ L/y) <sup>a</sup>	0.7	1.7	0.7
Authigenic flux ( $F_a$ ) (intermediate value calculated from sed)	4.5	10	2.6
River Concentrations	<b>Re</b> (pM)	<b>Mo</b> (nM)	<b>U</b> (nM)
Danube	80 <sup>b</sup>	20 <sup>b</sup>	4 <sup>c</sup>
Average rivers	2 <sup>b</sup>	5 <sup>d</sup>	2 <sup>e</sup>

a. Falkner et al. 1991; b. Chapter 5; c. Falkner, unpublished and Nikolayev et al. 1977; d. Bertine, 1970; e. Bertine et al., 1970; Sackett et al., 1973

Table 6.8 Authigenic flux of Re, Mo and U into Black Sea sediments

	Sed'n rate (cm/ky)	$\phi^a$	$\rho^a$ (g/cm <sup>3</sup> )	Re <sub>sed</sub> <sup>b</sup> ppb	Mo <sub>sed</sub> <sup>c</sup> ppm	U <sub>sed</sub> <sup>d</sup> ppm
min	16 <sup>a</sup>	0.90	2.42	24	33	20
max	25 <sup>e</sup>	0.91	2.48	48	66	40

a. Calvert et al. 1991, b. Ravizza 1991, c. Emerson and Husted 1991, d. Anderson et al. 1989, e. Crusius and Anderson 1991

$$F_a = A \times S \times \{M_{sed} - Al_{sed} \times (M/Al)_{shale}\}$$

where,

A = Area of the Black Sea =  $3.95 \times 10^{15}$  cm<sup>2</sup> (Falkner et al. 1991).

S = sedimentation rate in cm/y

M<sub>sed</sub> = Re, Mo or U concentration in sediments in mol/cm<sup>3</sup>

Al<sub>sed</sub> = Al concentration in Black Sea sediments =  $5.5 \times 10^{-4}$  mol/cm<sup>3</sup>  
(Emerson and Husted 1991 and Ravizza 1991)

(M/Al)<sub>shale</sub> = Re/Al, Mo/Al or U/Al ratio in average shale (=  $2.4 \times 10^{-10}$ ,  $9 \times 10^{-6}$   
and  $3.8 \times 10^{-6}$ , respectively) (Wedepohl 1978)

	Re	Mo	U
Authigenic Flux F <sub>a</sub> (mol/y)	$2-7 \times 10^3$	$5-16 \times 10^6$	$1-4 \times 10^6$
Deep water concentration (M <sub>d</sub> )	9 pM	3 nM	5 nM
Rate constant: k (10 <sup>12</sup> L/y)	220 - 780	1700-5300	230-780

where,

$$F_a = kM_d$$

higher than observed (figure 6.12a). This conclusion is unchanged whether one allows the authigenic flux to respond to deep water concentrations through the constant  $k$ , or if the authigenic flux is held constant at the value estimated from recent sediments. Thus it appears that  $Re$  is not in steady state in the Black Sea and its concentrations will continue to increase, accompanied by an increased flux into sediments, until a new steady state is approached. The equilibrium deep water concentration predicted depends upon the value of  $k$  chosen, and ranges from 26 to 55 pM. The current deep water concentration (9 pM) is consistent with a preanthropogenic  $Re$  riverine value of 2 pM (average river value as in previous chapter) and  $k \sim 800$ . This value of  $k$  is only slightly higher than that estimated from sediments.

Similar calculations can be made for Mo and U distributions in the Black Sea. Mo concentrations in Black Sea surface and deep waters (Emerson and Husted 1991) are shown in figure 6.12b. Adopting the upper and lower limits of  $k$  calculated from sediments and current riverine inputs ( $Mo_r = 20$  nM), deep water concentrations are predicted to be a factor of 2 - 5 higher than observed. Steady state surface water values are predicted to be lower than measured levels. Using a value for  $Mo_r$  representative of average rivers (5 nM, Martin and Meybeck 1979), the  $F_a$  necessary to produce the deep water concentration of 3nM is  $22 \times 10^6$  mol/y ( $k=6500$ ), which (like the case for  $Re$ ) is somewhat greater than the maximum  $k$  calculated from sediments ( $k=5300$ ). Unlike  $Re$  and Mo, it appears that present U concentrations (Anderson et al. 1989) can be balanced by current inputs and outputs (figure 6.12c). Taking recent river concentrations (4 nM) the observed U distribution can be reproduced with  $F_a=3.5 \times 10^6$  mol/y, or  $k=700$ , which is within the range calculated from the modern sediments.

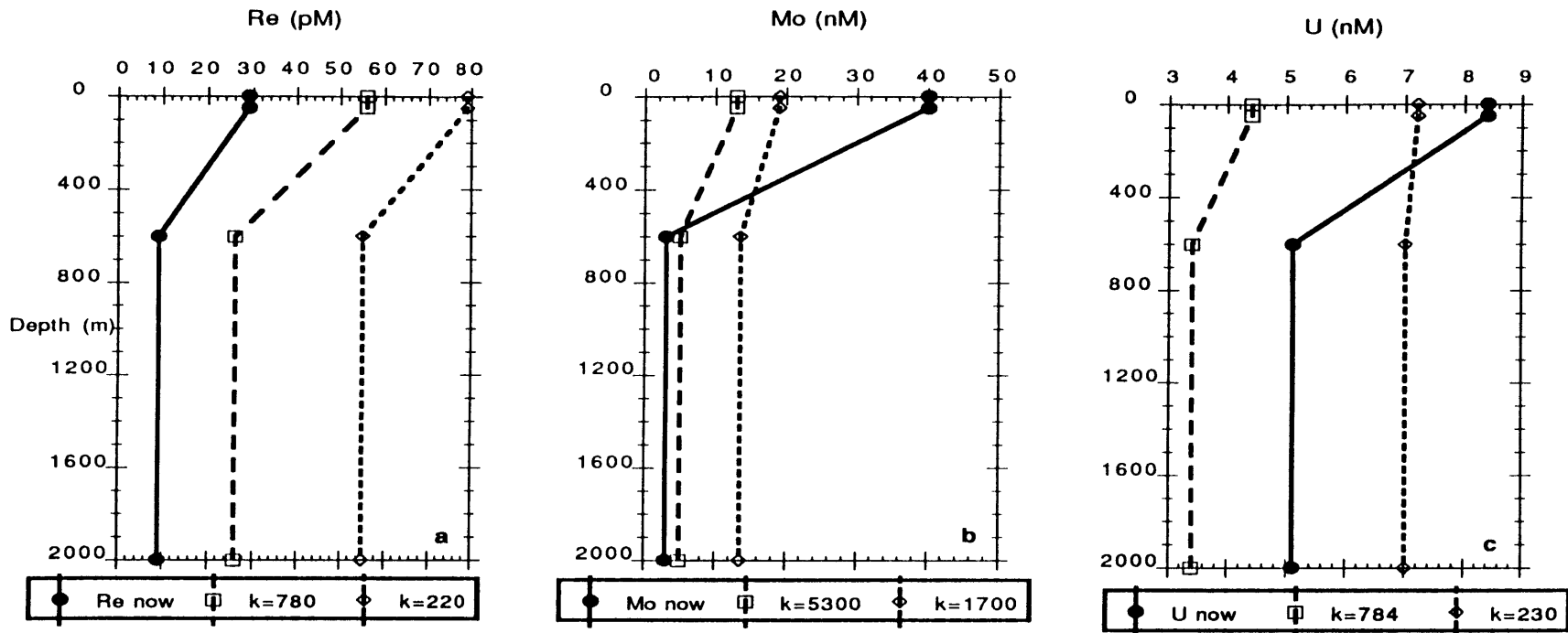


Figure 6.12 Predicted and present Re, Mo and U concentrations in the Black Sea. The solid lines approximate the current distributions of the three elements. The short dashed lines represent the concentrations predicted with current riverine inputs and an authigenic flux rate constant ( $k$ ) at the lower end of the range estimated from sediments. The longer dashed lines represent the concentrations predicted with current riverine inputs and  $k$  at the higher end of its estimated range.  $k$  in units of  $10^{12}$  L/y.

The rate at which the Black Sea responds to changes in riverine inputs depends on the residence times of the elements in the water column, which in the case of Re, Mo and U, depends on the rates of removal to sediments. The higher value of k calculated for Mo suggests that its residence time in Black Sea deep waters is shorter than that of either Re or U. Assuming that the authigenic flux which can be deduced from recent sediments is in equilibrium with Black Sea deep waters, a residence time can be calculated for each of the three elements from the ratio of the water column inventory to the authigenic removal rate:

$$\tau_m = \frac{(M) \times 200000 \text{cm} \times 0.001 \text{L/cm}^3}{F_a} \quad \text{method 1}$$

for a 2000 m water column 1 cm<sup>2</sup> in area, where (M) = Re, Mo or U concentration in mol/L, and F<sub>a</sub> = authigenic flux in mol/cm<sup>2</sup>y.

Residence times of 1000 - 3500 years are determined for Re and U by this method, depending on the authigenic flux chosen, whereas the residence time estimated for Mo is only 150 - 500 years (Table 6.9).

Residence times of the elements may also be computed from the water column depletion from their predicted conservative (ie., no authigenic removal) distributions. By setting the river inputs at uncontaminated values and setting k=0, conservative concentrations (M<sub>i</sub>) in the deep Black Sea may be calculated. Since uncontaminated river values are not well known, M<sub>i</sub> may also be derived using the salinity at each depth to give the mixing ratio of Bosphorus and surface waters there. This requires an estimate of (M) in surface waters, which may be taken as the measured concentration, or as a mixture of uncontaminated river water and seawater in the correct proportions to give the measured salinity. The elemental residence time (τ<sub>m</sub>) may then be estimated as follows:

Table 6.9 Residence times of Re, Mo and U in Black Sea deep waters

	<u>Re</u>	<u>Mo</u>	<u>U</u>
Deep water conc. (M <sub>d</sub> ), (pM)	9	3000 <sup>a</sup>	5100 <sup>b</sup>
F <sub>a</sub> (pmol/cm <sup>2</sup> /y)	0.5-1.6	1200-4000	290-1000
$\tau_m$ (y) method 1 <sup>c</sup>	1000-3200	150-500	1000-3500
Deep conc. calc. with box model and F <sub>a</sub> =0 (M <sub>i0</sub> )	35	73000	10000
Surf. conc. now (M <sub>S1</sub> ), (pM)	29	40000	8000
Surf. conc. calc. (M <sub>S2</sub> ), (pM) <sup>d</sup>	26	55000	7600
Deep conc. (M <sub>i1</sub> ) calc. with M <sub>S1</sub> <sup>e</sup>	34	56000	9400
Deep conc. (M <sub>i2</sub> ) calc. with M <sub>S2</sub> <sup>f</sup>	32	68000	9400
$\tau_m$ (y) method 2 <sup>g</sup>	350-400	41-57	1000-1200

a. Emerson and Husted 1991

b. Ravizza 1991

c. calculated from inventory of the element in a 2000 m x 1cm<sup>2</sup> water column and authigenic flux (see text)

d. The surface concentration that would result from a mixture of seawater and uncontaminated fresh water, with no authigenic removal. The proportions of the two endmembers are determined by the salinity of surface water.

e. The deep concentration that would result from a mixture of Bosphorus water and current surface waters with no authigenic flux. The proportions of the two endmembers are determined by salinity.

f. Same as e, but using M<sub>S2</sub> as the surface value.

g. calculated from depletion of deep water concentrations below initial conservative values: M<sub>i</sub> 0, 1 or 2 (see text).

$$\tau_m = \tau_w \left( \frac{M_d}{M_i - M_d} \right) \quad \text{method 2}$$

where  $\tau_w$  is the renewal time of Black Sea deep water,  $M_d$  is the current deep water concentration of the element and  $M_i$  is the initial concentration assuming no authigenic removal (Anderson et al. 1989). A comparison of  $M_i$  and  $M_d$  for the three elements is shown in figure 6.13. This approach leads to residence times of 350-400 years for Re, 40-60 years for Mo and 1200 years for U, as summarized in Table 6.9. Average values for Mo and U estimated by the two methods are similar to those reported by Emerson and Husted (1991) and Anderson et al. (1989):  $\tau_{Mo} = 150$  y and  $\tau_U = 1350$  y.

Using either method of calculation, U appears to have a relatively long residence time in the Black Sea. The agreement between the two estimates again suggests that the U budget of the Black Sea is near balanced. Mo has the shortest residence time, with Re either intermediate between the two, or similar to U. The higher  $\tau_m$  predicted for Re and Mo with the first method suggests that the authigenic flux has been underestimated, or that current deep water values are higher than those in equilibrium with sediments. Both of these factors may combine to produce the discrepancy between the two methods.

### *Applications*

The general description of Re geochemistry offered at the beginning of this chapter suggests a number of ways in which its concentration in ancient sediments might provide insight into their environment of deposition. Due to its strong enrichment in anoxic sediments, the Re concentration of seawater might be sensitive to changes in the area of the ocean floor on which anoxic sediments are accumulating. If one could find a faithful recorder of the Re

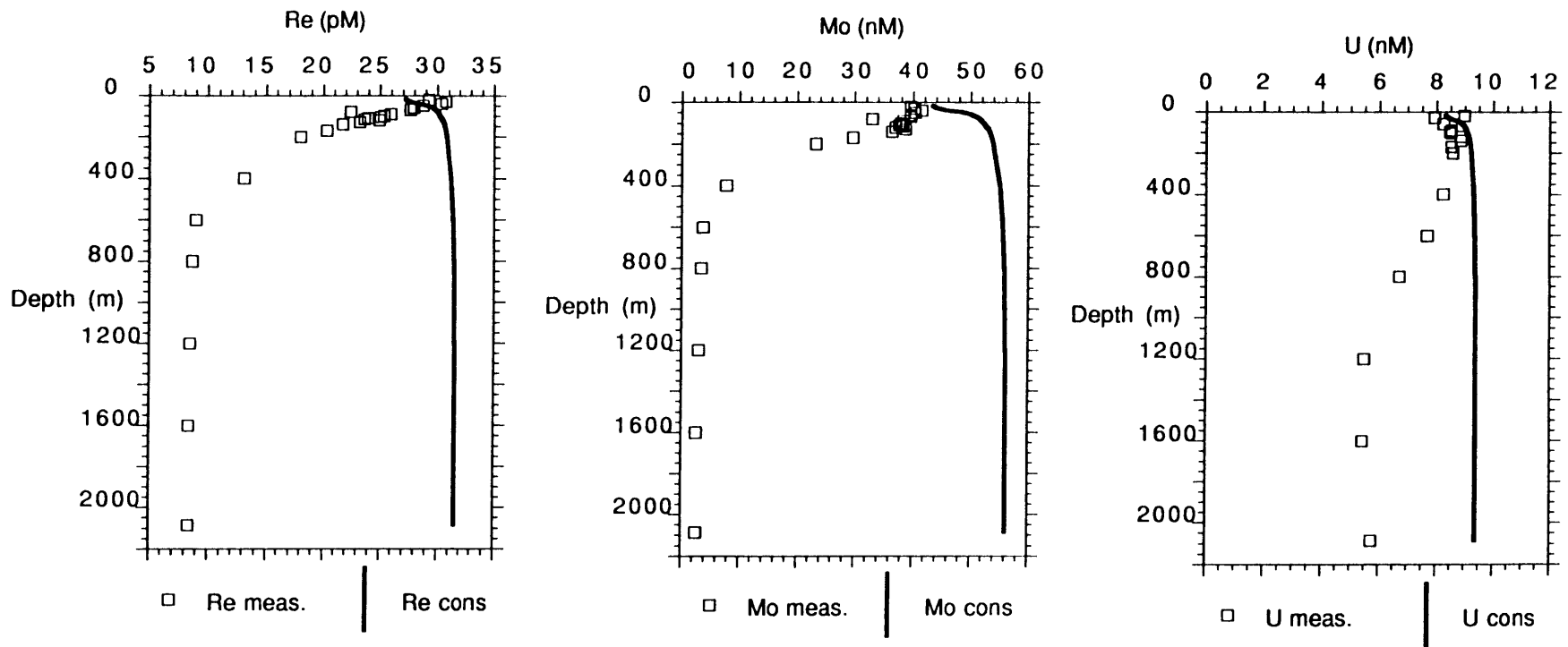


Figure 6.13 Re, Mo and U concentrations (boxes) compared to the concentrations predicted assuming no removal of the elements to the sediments (solid lines). The concentrations with no removal are calculated from a mixture of Marmara water with Black Sea surface waters, using the salinity at each depth to give the mixing ratio, as in Table 6.9.



concentration of seawater, then changes in the Re concentration of the ocean might be used to estimate the extent of anoxic sediments, which in turn could be related to the oxygen content of ancient oceans. This idea was developed and is being pursued for the elements uranium, vanadium and molybdenum by Russell et al. (1990), Hastings et al. (1990), and Emerson and Husted (1991). Russell et al. and Hastings et al. report that foraminiferal calcite appears to record the levels of U and V in seawater, and it has yet to be shown if Re concentrations are reflected as well.

In addition to Re concentrations, ratios of Re to U or Mo in seawater may also be expected to change with the areal extent of anoxic sediments. For example, the Mo/Re ratio of Black Sea deep water (0.3 nmol/pmol) is less than that in seawater (2.3) and in Black Sea surface waters (1.3). Similarly, the Mo/U ratio of Black Sea deep water is 0.6 mol/mol, while it is 7.5 in seawater and 5 in Black Sea surface water. This is due to the preferential removal of Mo to sediments, consistent with the pore water profiles seen in Chesapeake Bay. In the open ocean, the response of elemental ratios to changes in the area of anoxic sediments will be slight due to the large reservoir of the elements in seawater, and to the fact that except for Re, anoxic sediments do not represent the sole sink for the elements. Emerson and Husted (1991) estimate that the current flux of Mo and U into anoxic sediments is 22% and 15% of the present day river flux, respectively. It is not clear what proportion of the riverine Re flux enters oxic sinks and as yet, there is no evidence for an authigenic Re component in oxidized sediments.

Emerson and Husted calculate the expected change in seawater concentrations of Mo and U based on a factor of 10 increase in the area of anoxic or near-anoxic bottom water from its current value, 0.3% of the ocean, to 3% during glacial periods. Their estimates suggest that Mo concentrations may

have been 8% lower and U concentrations 7 % lower during the last glacial maximum (18 ky before present). Taking the extreme assumption that anoxic sediments are the only sink for Re, and following Emerson and Huested, Re concentrations were predicted based on an increase of the area of anoxic sedimentation from 0.3% to 3% for 18,000 years. Running the Emerson and Huested model forward in time, the predicted changes in elemental concentrations are 5% for Mo, 7% for U and 21% for Re, as summarized in Appendix 6.1. The resulting changes in the molar ratios in seawater are as follows: Mo/Re increases from 2300 to 2700 and U/Re increases from 310 to 370. These calculations are intended as a sensitivity test, given assumptions about the behavior of the three elements and oceanic conditions, and are meant only to compare the elements.

Another approach to deciphering redox conditions and/or sediment accumulation rates would utilize bulk sediment concentrations of Re, together with other trace elements. If Re is added to anoxic sediments by diffusion from overlying waters, then the amount of Re which is accumulated will be proportional to the concentration gradient between seawater and pore waters at the depth at which Re is removed from solution (the Re "solubility" boundary). If the concentration in seawater has not varied significantly with time (ie., the area of anoxic sedimentation has not changed dramatically), then the solid phase concentration of Re will be related simply to the depth from the sediment-water interface to the solubility boundary. This depth is in turn a function of many variables, including the oxygen content of overlying waters, the flux of organic matter to the sediments and the overall sedimentation rate. Using multiple tracers, it might be possible to separate some of these factors. For example, the recent work of Klinkhammer and Palmer (1991) suggests that U measurements in rapidly accumulating, organic-rich sediments may be used to estimate recent

sedimentation trends. Re or Mo concentrations would add another constraint to these estimates.

## 6.6 Conclusions

The results of Re measurements in sediment pore waters support the idea that Re is accumulated in anoxic sediments by diffusion, without involvement in manganese oxide cycling in the upper, oxic, portion of sediments. This is consistent with the observed lack of enrichment of Re in Mn nodules (Koide et al., 1986) and in slowly accumulating pelagic sediments (Koide et al., 1986; and results presented in Chapter 4). Re behaves conservatively within the anoxic water column of the Black Sea, with removal to anoxic sediments at or below the sediment water interface. Comparison of Re with Mo and U in the Black Sea suggests that its residence time is intermediate between those of the other elements, with U residing longer, and Mo more briefly, in the deep anoxic water mass. The residence times calculated for Re, Mo and U are approximately 1000 y, 200 y and 1500 y respectively. These estimates are complicated by the likelihood that the elements are not in steady state in the Black Sea due to anthropogenic contamination, and thus carry large uncertainties. Assuming that both Re and Mo values in the deep Black Sea have been perturbed, then the true residence times for these elements should be lower than calculated. The residence times of the three elements in the Black Sea are two to three orders of magnitude lower than their residence times in the open ocean (~500,000 years).

The difference in residence times among the three elements should lead to fractionation of the elements in anoxic basins. For example, the Mo/Re and Mo/U ratios in the deep Black Sea are lower than that in Black Sea surface waters, seawater, or average river waters. Presumably, differences in

authigenic flux rates among the three elements (which give rise to varying residence times) are the result of differences in the depths of the Re, Mo and U redox boundaries within the sediment. The Black Sea results suggest that Mo should be removed from pore waters at shallower depths than Re, consistent with Chesapeake Bay pore water results. If these observations apply to open ocean sediments, then changes in the anoxic area of the ocean have the potential to change the Mo/Re or Mo/U ratios of seawater. This effect on water column concentrations of the three elements is magnified in the Black Sea due to limited supplies of the elements, whereas any change in seawater concentrations will be relatively slight. In addition, oxic sediments are important sinks for U and Mo from seawater, whereas they do not appear to be a significant sink for Re.

## **6.7 Acknowledgements**

Black Sea samples were provided by Dr. S. Emerson (collected by Drs. W. Landing and B. Lewis) and by Dr. P. Froelich. The samples from the Sea of Marmara were collected by Dr. E. Brown on a separate leg of the same expedition.

References for Chapter 6

- Anderson, R. F., M. Q. Fleischer and A.P. LeHuray (1989). "Concentration, oxidation state and particulate flux of uranium in the Black Sea." Geochim. Cosmochim. Acta **53**: 2215-2224.
- Bertine, K.K and K.K Turekian. (1973). "Molybdenum in marine deposits." Geochim. Cosmochim. Acta **37**:1415-1434.
- Bertine, K.K., L.H. Chan and K.K Turekian. (1970). "Uranium determination in deep sea sediments and natural waters using fission tracks." Geochim. Cosmochim. Acta **34**: 641-648
- Boyko, T. F., G. N. Baturin and A.D. Miller. (1986). "Rhenium in recent ocean sediments." Geochem. Int'l **23**: 38-47.
- Buckley, D.E. and R.E Cranston. (1988). "Early diagenesis in deep sea turbidites: The imprint of paleo-oxidation zones." Geochim. Cosmochim. Acta, **52**: 2925-2939.
- Calvert, S. E., R. E. Karlin, L.J. Toolin, D.J. Donohue. J.R. Southon and J.S. Vogel. (1991). "Low organic carbon accumulation rates in Black Sea sediments." Nature **350**: 692-695.
- Cline, J. D. (1969). "Spectrophotometric determination of hydrogen sulfide in natural waters." Limnol. & Oceanog. **14**: 454-458.
- Cochran, J.K. (1982). "The oceanic chemistry of U and Th series nuclides. Uranium Series Disequilibrium: Application to Environmental Problems. Oxford, Clarendon Press.
- Crusius, J. and R. Anderson (1991). Paleoceanog. submitted:
- Dolejšek, V. and J. Heyrovsky (1925). "The occurrence of divi-manganese in manganese salts." Nature **116**: 782.
- Druce, J. G. F. (1948). Rhenium. Cambridge, Cambridge University Press.
- Emerson, S. and S. S. Husted (1991). "Ocean anoxia and the concentrations of molybdenum and vanadium in seawater." in press, Marine Chem.
- Falkner, K. K., D. J. O'Neill, J.F. Todd, W.S. Moore and J.M. Edmond (1991). "Depletion of barium and radium-226 in Black Sea surface waters over the past thirty years." Nature **350**(6318): 491-494.
- Falkner, K.K., G.P. Klinkhammer, T.S. Bowers, J.F. Todd, B.L. Lewis, W.M. Landing and J.M. Edmond. (in prep.) "The behavior of Ba in anoxic marine waters." Earth and Plan. Sci. Lett.

Hastings, D., S. Emerson, A. Mix and B. Nelson. (1990). Vanadium incorporation into planktonic foraminifera as a tracer for the extent of anoxic bottom waters. EOS, Transactions, American Geophysical Union, San Francisco, American Geophysical Union.

Klinkhammer, G.P. and M.R. Palmer. (1991). "Uranium in the oceans: where it goes and why." Geochim. Cosmochim. Acta 55:1799-1806.

Koide, M., V. F. Hodge, J. Yang, M. Stallard, E. Goldberg, J. Calhoun and K. Bertine (1986). "Some comparative marine chemistries of rhenium, gold, silver and molybdenum." Appl. Geochem. 1: 705-714.

Lewis, B. L. and W. B. Landing (1991). "The biogeochemistry of Mn and Fe in the Black Sea." Deep Sea Res., in press.

Li, Y.-H. and S. Gregory. (1974). "Diffusion of ions in seawater and in deep sea sediments." Geochim. Cosmochim. Acta 38: 703-714.

Loring, F. H. and J. G. F. Druce (1925). "Examination of crude divi-manganese." Chem. News (131): 337.

Martin, J. M. and M. Meybeck (1979). "Elemental mass-balance of material carried by major world rivers." Mar. Chem. 7: 173-206.

Muller, J. H. and W. A. La Lande Jr. (1933). "The precipitation of rhenium sulfide from ammoniacal solution. A separation of rhenium from molybdenum." J. Am. Chem. Soc. 55: 2376-2378.

Murray, J. W., Z. Top, and E. Oszoy (1991). "Hydrographic properties and ventilation of the Black Sea." Deep-Sea Res. in press.

Nikolayev, D.S. and K.F. Lazarev and V.M Drozhzhin. (1977). "Trends in the distribution of U, lo Ra and Th in the Black and Azov Seas." Geochem. Int'l. 14: 141-146.

Nixon, S.W. (1987). "Chesapeake Bay nutrient budgets - a reassessment." Biogeochem. 4: 77-90.

Noddack, W., I. Tacke, and O. Berg (1925). "Zwei neue Elemente der Mangangruppe." Naturwissenschaften. 13: 567.

Pedersen, T. F., M. Pickering, J.S. Vogel, J.N. Southon, D.E. Nelson (1988). "The response of benthic foraminifera to productivity cycles in the Eastern Equatorial Pacific: faunal and geochemical constraints on glacial bottom water oxygen levels." Paleoc. 3(2): 157-168.

Ravizza, G. (1991). Rhenium and Osmium Geochemistry of Modern and Ancient Organic-Rich Sediments. PhD Thesis. Yale University.

Russell, A. D., S. R. Emerson, B.K. Nelson, A. Mix and J. Erez. (1990). Uranium in foraminiferal calcite as a tracer of ocean redox conditions. EOS, Transactions, American Geophysical Union, San Francisco, American Geophysical Union.

Sackett, W., T. Mo, R. Spalding, and M. Exner. (1973). "A reevaluation of the marine geochemistry of uranium" Symp. Interact. Radioact. Contam. Const. Mar. Env., Seattle, WA, IAEA, Vienna.

Shaw, T. J., J. M. Gieskes and R.A. Jahnke. (1990). "Early diagenesis in differing depositional environments: The response of transition metals in pore water." Geochim. Cosmochim. Acta **54**: 1233-1246.

Shaw, T.J. (1988) PhD Thesis. The early diagenesis of transition metals in nearshore sediments. Univ. of Calif., San Diego

Smith, K. L., Jr. (1987). "Food energy supply and demand: A discrepancy between particulate organic carbon flux and sediment community oxygen consumption in the deep ocean." Limnol. Oceanogr. **32**: 201-220.

Smith, K. L. Jr. (1989). "Short time series measurements of particulate organic carbon flux and sediment community oxygen consumption in the North Pacific." Deep Sea Res. **36**: 1111-1119.

Appendix 6.1

The sensitivity of Re, Mo and U and their relative concentrations in seawater to changes in the area of anoxic sedimentation was explored with the simplified relationships given below (after Emerson and Husted, 1991).

$$\Delta C_{sw} = \frac{F_r - A_a F_a - (A - A_a) F_o}{V_o} \Delta t \quad (1)$$

$$F_o = \beta C_{sw} \quad (2)$$

$$F_a = \gamma C_{sw} \quad (3)$$

$$\beta = \frac{x_o F_r}{C_{sw}^o (A - A_a^o)} \quad (4)$$

$$\gamma = \frac{x_a F_r}{C_{sw}^o A_a^o} \quad (5)$$

where,

$V_o$  = volume of the ocean ( $1.37 \times 10^{18} \text{ m}^3$ )

$A$  = area of the ocean ( $3.6 \times 10^{14} \text{ m}^2$ )

$A_a$  = area of anoxic ocean ( $\text{m}^2$ )

$C_{sw}$  = concentration of element in seawater

$F_r$  = riverine flux ( $\text{mol/yr}$ )

$F_a$  = flux into anoxic sediments ( $\text{mol/m}^2 \cdot \text{yr}$ )

$F_o$  = flux into oxic sediments ( $\text{mol/m}^2 \cdot \text{yr}$ )

$\gamma$  = rate constant for anoxic sediment uptake ( $\text{m/yr}$ )

$\beta$  = rate constant for oxic sediment uptake ( $\text{m/yr}$ )

$x_a$  = fraction of present river inflow entering sediments of anoxic regions

$x_o$  = fraction of present river inflow entering sediments of oxic regions

$^o$  = superscript indicating present day.



Equation 1 states that the change in seawater concentrations of the elements ( $C_{sw}$ ) is equal to the difference between the river flux and the sedimentary fluxes to oxic and anoxic sediments. The fractions of riverine Mo and U going into oxic and anoxic sediments were taken from Emerson and Husted and are shown in the table below. It was assumed that the only sink for Re in the oceans was in anoxic sediments ( $x_a = 1$ ,  $x_o = 0$ ). The uptake of the elements from seawater was modeled as first order with respect to their oceanic concentrations. The rate constants were calculated based on estimates of present day concentrations and fluxes. The simple situation of a step change in anoxic area from 0.3% to 3% of the ocean, and accumulation of the elements in the expanded sedimentary area for 18,000 years was explored. Because this calculation is not intended to predict real changes, but only relative sensitivities of the elements, calculations were done with a single time-step and the present seawater concentrations were used in equations 2 and 3.

	$F_r$ (mol/y)	$C_{sw}^0$ (mol/m <sup>3</sup> )	$x_a$	$x_o$	$C_{sw}^{18k}$ (mol/m <sup>3</sup> )
Re	$0.08 \times 10^6$	$45 \times 10^{-9}$	1	0	$35.5 \times 10^{-9}$
Mo	$185 \times 10^6$	$105 \times 10^{-6}$	0.22	0.4	$100 \times 10^{-6}$
U	$60 \times 10^6$	$14 \times 10^{-6}$	0.15	0.9	$13 \times 10^{-6}$